

Durham E-Theses

Chemical genetic dissection of efferent IRE1 signalling

LOUISE KATHLEEN SUTCLIFFE

How to cite:

SUTCLIFFE, LOUISE KATHLEEN (2012) Chemical genetic dissection of efferent IRE1 signalling. Doctoral thesis, Durham University.

Use policy

The full-text may be used and/or reproduced, and given to third parties in any format or medium, without prior permission or charge, for personal research or study, educational, or not-for-profit purposes provided that:

- a full bibliographic reference is made to the original source
- a <https://etheses.durham.ac.uk/id/eprint/5943/> is made to the metadata record in Durham E-Theses
- the full-text is not changed in any way

The full-text must not be sold in any format or medium without the formal permission of the copyright holders.

Please consult the [full Durham E-Theses policy](#) for further details.

Author: Louise Kathleen Sutcliffe

Title: Chemical genetic dissection of efferent IRE1 α signalling.

ABSTRACT

The Endoplasmic Reticulum is the cellular organelle primarily responsible for producing proteins on the secretory pathway, a pathway important in the production of biopharmaceuticals. One of the requirements for the successful production of a functional protein is correct folding of the polypeptide sequence. During conditions such as viral infection, mutant protein expression and cell differentiation the endoplasmic reticulum is placed under conditions of stress. IRE1 is a protein kinase and endoribonuclease, which along with PERK and ATF6, forms part of the Unfolded Protein Response, the system by which the cell deals with the stress caused by a high protein load. IRE1 is capable of increasing the protein folding capacity of the ER, by upregulating chaperone proteins and reducing the load by attenuating translation, (protective response). This action is mediated by splicing of the mRNA coding for the bZIP transcription factor XBP-1. IRE1 is also capable of causing apoptotic responses via TRAF2 (cell injuring response) resulting in the activation of JNK and NF κ B. In this study, using site directed mutagenesis a panel of IRE1 mutants was produced and screened for alterations to the protective and cell injuring responses. Of these the D711A mutant was shown in mouse embryonic fibroblasts to retain endoribonuclease activity, and to display an attenuated cell injuring response. When this mutant was applied to an industrial CHO cell line it appeared to exhibit an increase in biopharmaceutical productivity over the wild type IRE1, indicating its potential for use in the biopharmaceutical cell lines.

This work was funded by the Biotechnology and Biological Sciences Research Council and Lonza Biologics Inc.

Chemical genetic dissection of efferent IRE1 α signalling.

By Louise Kathleen Sutcliffe

Submitted for the qualification of Doctor of Philosophy in Molecular Biology

School of Biological and Biomedical Sciences

Durham University

2012

Contents	
Tables.....	10
Illustrations	12
Abbreviations.....	15
Statement of Copyright.....	23
Acknowledgements.....	24
1. INTRODUCTION.....	26
1.1. Industrial Protein Biomanufacture: Selection, Synthesis and Secretion.....	28
1.1.1 Transfection.....	30
1.1.2 Selection and Characterisation of High Producers	31
1.1.3 Culture Media and Nutrients	33
1.1.4 Controlling Apoptosis.....	34
1.1.5 Post-Translational Modifications	37
1.1.6 Exit from the Endoplasmic Reticulum	38
1.2. The Unfolded Protein Response: Adapting Protein Production.....	40
1.2.1. Structure of the Unfolded Protein Response	41
1.3. IRE1: Structure and Function.....	51
1.3.1 Isoforms	52
1.3.2 Domain Structures	53
1.3.3 Clustering and Activation Mechanisms.....	59
1.3.4 Downstream Effects	63
1.4. The IRE1 Kinase Pocket: Application of chemical genetics to a protein kinase.....	67
1.4.1 Protein kinases and the IRE1 Kinase Pocket.....	67
1.4.2 Application of an ATP Analogue to IRE1.....	70
1.5. Project Aims.....	72
2. MATERIALS.....	74
2.1 Chemicals and solutions.....	74

2.2 Oligodeoxynucleotide Primers	88
2.3 Plasmids	99
2.4 Antibodies	111
2.5 Chemically Competent <i>E. coli</i> Cells	113
2.6 Cell Lines	114
2.7 Commercially Available Kits	114
2.8 Specialist Equipment.....	117
3. METHODS	119
3.1 Cell Culture	119
3.1.1 Revival	119
3.1.2 Cryopreservation.....	119
3.1.3 Trypsinisation	120
3.1.4 MEF Culture	120
3.1.5 CHO Culture	120
3.1.6 HEK293 Culture	121
3.1.7 Stable Cell Line Production	121
3.1.8 Transfection - Electroporation	122
3.1.9 Transfection – Jetprime.....	123
3.1.10 Transfection - Lipofectamine.....	123
3.1.11 Induction of endoplasmic reticulum stress with tunicamycin, thapsigargin or DTT	123
3.1.12 Assessment of Transfection Efficiency/Cell Death	124
3.1.13 Limited dilution cloning	124
3.2 Bacterial culture	125
3.2.1 Chemical transformation of <i>E. coli</i>	125
3.2.2 Revival of <i>E. coli</i> cultures.....	126
3.2.3 Growth of <i>E. coli</i> cultures	126

3.2.4	Production of frozen <i>E. coli</i> stocks.....	127
3.2.5	Preparation of chemically competent <i>E. coli</i>	127
3.3	Protocols for preparation/use of DNA	127
3.3.1	Preparation of DNA from <i>E.coli</i> culture by mini/midi/maxi/gigaprep and ethanol precipitation of nucleic acids	127
3.3.2	DNA agarose gel electrophoresis	129
3.3.3	Polymerase chain reaction (PCR) for insert construction	129
3.3.4	Cloning of PCR products with cloning vectors pGEM Easy T and TOPO TA cloning kit.....	130
3.3.5	Restriction enzyme digestion.....	132
3.3.6	10µl reaction (Small volume, for test digests).....	132
3.3.7	50µl Reaction (Large volume for harvesting digest products)	132
3.3.8	Dephosphorylation of DNA 5' termini with calf intestinal alkaline phosphatase (CIAP). 133	
3.3.9	DNA ligation with T4 DNA ligase	133
3.3.9.1	Standard method.....	133
3.3.9.2	High yield method (provided by A. Mohamed).....	134
3.3.10	Mutagenesis	134
3.3.11	Sequencing.....	134
3.4	Protocols for preparation/use of RNA.....	134
3.4.1	RNA isolation	135
3.4.2	RNA agarose gel electrophoresis.....	135
3.4.3	cDNA production from RNA.....	135
3.4.4	Reverse transcription (RT)-PCR Assays for Actin/XBP-1 splicing/IRE1α. Standard Reaction Mixture.....	136
3.4.5	PCR for Sequencing using the FirstChoice® RLM-RACE Kit.....	138
3.4.6	PCR for Sequencing using T-RACE PCR.....	139
3.4.7	qPCR assay for XBP-1/IRE1α /Actin	142

3.5	Western Blotting	143
3.5.1	Protein isolation	143
3.5.2	Production of Poly-acrylamide Gel	143
3.5.3	SDS-PAGE	144
3.5.4	Electrotransfer by Wet Transfer.....	144
3.5.5	Electrotransfer by Semi-Dry Transfer	145
3.5.6	Electrotransfer by Dry Transfer	146
3.5.7	Antibody Immunoblotting	146
3.5.8	Visualisation	146
3.5.9	Dephosphorylation of samples.....	147
3.6	Southern Blotting	147
3.6.1	Transfer.....	147
3.6.2	Hybridisation.....	148
3.7	Spectrophotometric assays	149
3.7.1	Sandwich ELISA for assembled IgG cB72.3	149
3.7.2	β -Gal Assay for pcDNA integration.....	151
4.	RESULTS.....	152
4.1	Cloning of IRE1 α and IRE1 β mutant plasmids	152
4.1.1	Rationale	152
4.1.2	Mutagenesis Strategy: IRE1 α constructs	153
4.1.3	Screening of Transformants for Insertion of Mutation.....	154
4.1.4	Recloning into pED Δ c-hIRE1 α Plasmid	155
4.1.5	Mutagenesis and Cloning Strategy: IRE1 β	157
4.1.6	Screening of Transformants for Mutagenesis	159
4.1.7	Requirement and Strategy for Cloning into puc18	160
4.1.9	Recloning of IRE1 β constructs into pCAG Plasmids.....	162
4.1.10	Cloning Strategy for Addition of HA Tag into pCAG Plasmids.....	164

4.1.11	Summary	166
4.2	Optimisation of IRE1 α and IRE1 β expression in <i>ire1α^{-/-}</i> cells	167
4.2.1	Rationale for Optimisation.....	167
4.2.2	Transfection Efficiency Assessment with GFP	167
4.2.3	Transfection of pED Δ c/pCAG plasmids to assess effect of IRE1 protein on viability of MEFs	168
4.2.4	Strategies for overcoming viability loss – reduced DNA in transfection	171
4.2.5	Strategies for overcoming viability loss – Time Course for Expression	173
4.2.6	Strategies for overcoming viability loss – transfection of <i>traf2^{-/-}</i> cells to eliminate IRE1-induced cell death by the TRAF2 Pathway.....	175
4.2.7	Strategies for overcoming viability loss – weak promoter	177
4.2.8	Cloning of thymidine kinase promoter	177
4.2.9	Strategies for overcoming viability loss – use of alternative transfection buffers	179
4.2.10	Summary	186
4.3	Testing of IRE1 α constructs in IRE1 α ^{-/-} MEFs by transient transfection.....	186
4.3.1	Rationale	186
4.3.2	D711A mutant exhibits XBP-1 Splicing In MEFs Transiently Transfected with Mutant IRE1 α	186
4.3.3	Conclusion	191
4.4	Construction of stable <i>ire1α^{-/-}</i> MEF lines with FRT-IRE1	193
4.4.1	Rationale	193
4.4.2	Flp-In™ System.....	193
4.4.3	Construction of pcDNA5/FRT/TO-hIRE1 α and Mutants Thereof.....	194
4.4.4	Testing of pcDNA5-FRT-TO-hIRE1 α for successful IRE1 α expression in T-Rex HEK293 Cells	194
4.4.5	Stable Transfection with pFRT/lac/Zeo.....	195
4.4.6	Stable Transfection with Tet Repressor Plasmid pcDNA6/TR.....	198

4.4.7	Stable Transfection/Replacement with pcDNA5-FRT-TO-hIRE1 α	199
4.4.8	Summary	200
4.5	Viability and unfolded protein response activation of stably transfected <i>ire1α^{-/-}</i> MEF lines with FRT-IRE1 α	201
4.5.1	Rationale	201
4.5.2	Verification of IRE1 α expression in Stably Transfected IRE1 Reconstituted MEFS	201
4.5.3	D711A Mutant exhibits <i>XBP-1</i> splicing in Stably Transfected <i>ire1α^{-/-}</i> MEFS	202
4.5.4	D711A mutant exhibits similar growth characteristics to wild type IRE1 α in stably transfected <i>ire1α^{-/-}</i> mouse embryonic fibroblasts.	204
4.5.5	D711A mutant improves survival of tunicamycin/thapsigargin-induced unfolded protein stress in stably transfected <i>ire1α^{-/-}</i> MEFS	205
4.5.6	K599A and D711A mutants exhibit increased PARP cleavage in Stably Transfected <i>ire1α^{-/-}</i> MEFS	207
4.5.7	D711A Mutant appears to exhibit decreased JNK expression in Stably Transfected <i>ire1α^{-/-}</i> MEFS	209
4.5.8	IRE1 α phosphorylation in Stably Transfected <i>ire1α^{-/-}</i> MEFS	210
4.5.9	Summary	210
4.6	Cloning of CHO IRE1 α	211
4.6.1	Rationale	211
4.6.2	Degenerate primer design for CHO IRE1 α	211
4.6.3	Harvesting of RNA from CHOK1SV Host Cells	212
4.6.4	Cloning Methods and RACE	212
4.6.5	T-RACE Methodology.....	213
4.6.6	Primers Designed using provided Assembly Sequences	214
4.6.7	Final CHO IRE1 α assembly	215
4.6.8	Summary	229
4.7	Production of Lonza vector pEE12.4-derived silencing vectors.....	230

4.7.1	Rationale	230
4.7.2	Cloning Strategy – shRNA Polylinker.....	231
4.7.3	Cloning Strategy – U6 Promoter vector.....	233
4.7.4	Dilution of T4 Ligase in reaction to ensure a single copy of the polylinker was produced for cloning.....	234
4.7.5	Ligation and Screening of vector with polylinker	235
4.7.6	Summary	236
4.8	Production of shRNA against CHO IRE1 α	237
4.8.1	Rationale	237
4.8.2	Design of shRNAs against choIRE1 α	238
4.8.3	Cloning of shRNAs into U6 Vector.....	239
4.8.4	Cloning into pEE12.4-U6	240
4.8.5	Transient Transfection of shRNA Sequences into Cell Line 42 (High Producer) to produce cDNA for RT-PCR and qPCR knockdown analysis	241
4.8.6	qPCR for XBP-1, Actin	241
4.8.7	Summary	244
4.9	Characterisation of the UPR and its correlation with mAb Production in CHOK1SV 245	
4.9.1	Rationale	245
4.9.2	Spliced and unspliced XBP-1 levels are not significantly different between cell lines of differing mAb production capacity.....	245
4.9.3	Addition of serum to culture medium alters mAb Production and XBP-1 splicing in different levels of mAb Producer.....	247
4.9.4	Summary	249
4.10	Effect of IRE1 α mutant constructs on viability and productivity in CHOK1SV industrial cell lines.	251
4.10.1	Rationale	251

4.10.1	Transient Transfection of kinase deficient IRE1 α plasmids reduces viability in CHOK1SV cells.....	251
4.10.2	Transient transfection with D711A mutant improves mAb yield in CHOK1SV cells	253
4.10.3	Construction of stable CHO cell line	256
4.10.4	Summary	257
5.	DISCUSSION	259
5.1	IRE1 α mechanisms and outputs	259
5.2	Observed effects of IRE1 α mutants	261
5.3	Improvements in industrial biopharmaceutical synthesis.	263
5.4	Effects of IRE1 α mutants on monoclonal antibody productivity of CHOK1SV cells	264
5.5	Methodologies.....	265
6.	CONTINUATION OF WORK.....	266
	REFERENCES	267
	APPENDIX 1 – iCODEHOP Results for mammalian IRE1 α alignments	280
	Luminal Domain.....	282
	Cytoplasmic Domain.....	285
	APPENDIX 2: Sequences obtained by PCR and their position relative to the M. Musculus sequence NM_023913.2	289
	APPENDIX 3 – Sequencing results from mutagenesis of IRE1 α/β constructs.....	297

Tables

Chapter 1 – No tables.

Chapter 2 - Materials

Table 2.1- Solutions for Microbiology	74
Table 2.2 - Solutions for DNA Work.....	77
Table 2.3 - Solutions for RNA Work (all preparation equipment baked to remove RNases or purchased clean).....	78

Table 2.4 - Solutions for Protein Work.....	79
Table 2.5 - Solutions for Tissue Culture.....	83
Table 2.6 - Cell Culture Media and Reagents.....	84
Table 2.7 – Restriction Enzymes	85
Table 2.8 – Other Enzymes.....	87
Table 2.9 - Codes for Degenerate Primers.....	88
Table 2.10 - Restriction enzymes used to screen for mutated clones.....	89
Table 2.11 – Oligodeoxynucleotide Primers	89
Table 2.12 – Plasmids.....	100
Table 2.13 - Antibodies.....	111
Table 2.14 - Cell Lines.....	114
Table 2.15 - Commercially Available Kits	114

Chapter 3 - Methods

Table 3. 1- Cryopreservation media.....	119
Table 3. 2 - Probability that wells showing growth have arisen from one (1/R), two (2/R), three (3/R), four (4/R) or five (5/R) stably transfected cells.	125
Table 3. 3 – Protocol Details for Chemical Transformation.....	125
Table 3. 4 - Thermocycler conditions for PCR for insert construction	130
Table 3. 5 - Thermocycler conditions for cloning vector PCR.....	131
Table 3. 6 - Thermocycler conditions for (RT)-PCR for mouse XBP-1/Actin	137
Table 3. 7 - Thermocycler conditions for touchdown (RT)-PCR for mouse XBP-1/Actin... 137	
Table 3. 8 - Thermocycler conditions for (RT)-PCR for CHO XBP-1/Actin/IRE1 α	138
Table 3. 9 - Thermocycler conditions for 3' RACE PCR.....	139
Table 3. 10 - Thermocycler conditions for T-RACE second strand synthesis	140
Table 3. 11 - Thermocycler conditions for T-RACE asymmetric PCR.....	141
Table 3. 12 - Thermocycler conditions for T-RACE PCR	142
Table 3. 13 - β -galactosidase Assay Standards.....	151

Chapter 4 - Results

Table 4.1. 1 - Mutagenesis schemes, IRE1 α – [<i>EcoRV</i>]: Restriction enzyme sites. Substitutions in italics mark mutagenesis codon changes, those in bold mark conservative substitutions which add a restriction enzyme site for screening.....	153
Table 4.1. 2 - Mutagenesis schemes, IRE1 β – [<i>NaeI</i>]: Restriction enzyme sites. Substitutions in italic mark mutagenesis codon changes, those in bold mark conservative substitutions which add a restriction enzyme site for screening.	158
Table 4.2. 1 – Viable cell counts (cells in one 1mm ² square of haemocytometer, five replicates).....	170
Table 4.2. 2 – Viable cell counts/Transfection efficiency in viability assessments.	172
Table 4.2. 3 – Viability comparison after transfection with weak/strong promoter plasmids.	179
Table 4.2. 4 - Transfection Buffer Recipes (from (Rubio and Terefe 2008)) and the Digital Biotech (Seoul, Korea)/Invitrogen Microporator protocol (Protocol Reference: MP-100 Rev.M.03.51-11/07).....	180
Table 4.2. 5 - Conductivities of Electrotransfection Buffers	181
Table 4.2. 6 - Optimisation of Electrotransfection Buffer	184

Table 4.4. 1 – Beta-galactosidase activity in <i>ire1</i> <i>-/-</i> MEF clones stably transfected with pFRT/lac/Zeo	196
Table 4.6. 1 – Final CHO IRE1 α assembly.	215
Table 4.8. 1 – Anti-CHO IRE1 α shRNAs	239
Table 4.8. 2 – CT values from qPCR Analysis	244
Table 4.9. 1 - Cell line specific productivities of lines used in this thesis (donated by Lonza)	245
Table 4.10. 1 – Viabilities of Mutant Transfected CHOK1SV (by ViCell count)	252
Chapter 5/6 – No tables	

Illustrations

Chapter 1 - Introduction

Figure 1.1 – Timeline for biopharmaceutical production.	28
Figure 1.2 – Pathways of the unfolded protein response (from (Schroder 2008)).	43
Figure 1.3 – One potential ribbon structure of the N-luminal/N-terminal and cytosolic/C-terminal domains of human IRE1, from Zhou et al (Zhou, Liu et al. 2006) and Lee et al (Lee 2008) respectively showing two monomers interfaced together. The C-terminal ends of the two monomers of the N-luminal domains (top) would connect to the transmembrane sections of the monomers (red lines). From this point they would connect with the top of the cytosolic domains (bottom). ADP is shown bound to the kinase domain.....	54
Figure 1.4 – Oligomerised IRE1 multimer structure from (Korenykh, Egea et al. 2009). In this structure, rather than spanning the membrane, multiple IRE1 units assemble with their RNase domains facing outwards.....	54
Figure 1.5 – A) Simplified protein kinase structure (after (Huse and Kuriyan 2002)) B) Structure of IRE1 kinase domain from PDB entry for (Lee, Scapa et al. 2008), IRE1 with ADP situated in nucleotide pocket. N-terminal lobe (upper section), C-terminal lobe (lower section), Activation loop (circled).	57
Figure 1.6 - RNase domain of IRE1 showing C-terminal nuclease/mRNA binding surface (Lee, Scapa et al. 2008).....	58
Figure 1.7 – IRE1 interactions and resultant downstream effects. Outcomes to the left of the diagram are survival oriented, to the right favour apoptosis.	63
Figure 1.8 - Schematic of IRE1 showing kinase pocket with ATP molecule. Dashed lines indicate the order in which the relevant sections fall in the sequence of the protein. Residues marked (e.g. K907/K855) of interest to this study are shown with both alpha and beta isoforms, where the first (K907) is the alpha isoform and the second (K855) the beta isoform. Black arrows indicate donation of phosphates to phosphorylate serine and threonine residues on the activation loop.....	67
Figure 1.9- ATP and 1-NM-PP1.....	71

Chapter 2 – Materials

Figure 2. 1 - pEDΔc-hIRE1α	105
Figure 2. 2 – pCAG-hIRE1β	105
Figure 2. 3 - pCAG-hIRE1β-HA	106
Figure 2. 4 – pTK-HSV-BP2-hIRE1α	106
Figure 2. 5 – p TKRG-hIRE1β	107
Figure 2. 6 – pEE12.4	107
Figure 2. 7 – pEE12.4-U6	108
Figure 2. 8 – pUC18.....	108
Figure 2. 9- pUC18-hIRE1β	109
Figure 2. 10 – pDJB134	109
Figure 2. 11 – pcDNA5/FRT/TO-hIRE1α.....	110

Chapter 3 – Methods

Figure 3. 1 - Semi-Dry Transfer Stack Setup	145
Figure 3. 2 - Southern Blot Transfer Setup.....	148

Chapter 4 – Results

Figure 4.1. 1 - Mutagenesis of pEDΔC-hIRE1α. Mutagenesis primers anneal to site of mutation on denatured plasmid. Proof-reading <i>PfuTurbo</i> polymerase polymerises in direction of arrows around the plasmid.....	154
Figure 4.1. 2 - Subcloning of pEDΔc-hIRE1α mutants into original plasmid.....	156
Figure 4.1. 3 – Example of digests of pEDΔc-hIRE1α with <i>BstZ17I</i> and <i>SnaBI</i> to ensure correct religation and re-insertion of mutated hIRE1α sequence. Ladder – DNA Ladder. Un-Dig./Digested – religated pEDΔc-hIRE1α plasmid.	157
Figure 4.1. 4 - Mutagenesis of pCAG-hIRE1β. Mutagenesis primers anneal to site of mutation on denatured plasmid. Proof-reading <i>PfuTurbo</i> polymerase polymerises in direction of arrows around the plasmid to form mutagenised form.....	159
Figure 4.1. 5 – Unsuccessful mutagenesis of pCAG-hIRE1β.	160
Figure 4.1. 6- Cloning strategy for puc18-hIRE1β. The constructed plasmid comprises the entirety of the pUC18 vector (left-hand arrows) and the IRE1β gene (right-hand arrows). .	161
Figure 4.1. 7 – Digests of pUC18-hIRE1β. A) Restriction sites. B) Test digest of pUC18-hIRE1β-L590A with <i>EcoRI</i> and <i>DraI</i> 1-Ladder, 2-Undigested, 3- Digested.	163
Figure 4.1. 8 – Screening of pCAG-hIRE1β. A) Digestion sites for screening enzyme (<i>SnaBI</i>) B) Correct orientation of insert. C) Screening of pCAG-hIRE1β with <i>SnaBI</i>	164
Figure 4.1. 9 - HA Tag Cloning into pCAG vectors.....	165
Figure 4.1. 10 - Successful and unsuccessful pCAG-hIRE1β HA-tag clones. Representative examples of digests, each pair of lanes LH lane undigested, RH lane digested with <i>EcoRI</i> . Mutants in lanes A-C- D659A/L590A, D-D659A/L590G, E-F – K547A/L590A, G-K547A/L590G.	166
Figure 4.2. 1 – Transfection efficiency of <i>ire1α^{-/-}</i> mouse embryonic fibroblasts with pMAX-GFP. LH panel transfected cells with visible light, RH panel GFP fluorescence of same transfected cells with UV light.	168
Figure 4.2. 2 – Preliminary IRE1 transfections, percentage viability and example of micrograph showing non-adherent cells after transfection with pEDΔC-hIRE1α.	169
Figure 4.2. 3 – Viability of cells transfected with pEDΔc constructs.....	171
Figure 4.2. 4 - Viability of <i>ire1α^{-/-}</i> MEFs with varying concentrations of IRE1 plasmids and GFP expression plasmids.....	172

Figure 4.2. 5 - Expression of GFP Timecourse in <i>ire1α</i> ^{-/-} MEFs. Bright field microscopy with fluorescence microscopy overlay where required.	174
Figure 4.2. 6 – Effect of pEDΔC-hIRE1α on <i>traf2</i> ^{-/-} mouse embryonic fibroblasts. A) Live/Dead cell counts per haemocytometer square. B) Light microscopy of cells 24 hours after transfection. C) % Viability of transfections/untransfected.	176
Figure 4.2. 7 – Cloning strategy for pTK-HSV-BP2-hIRE1α.	178
Figure 4.2. 8 - Transfection efficiency with electrotransfection buffers. Left-hand panels show visible light microscopy and right-hand GFP fluorescence with UV light. DPBS-based buffers exhibit high efficiency of transfection, as opposed to experimental buffers.	182
Figure 4.2. 9 - Buffer 5 Optimisation. Left-hand panels show visible light microscopy and right-hand GFP fluorescence with UV light. Upper panels represent previous optimized transfection conditions with Buffer R. Middle panels show a low voltage with low transfection efficiency. Lowest panels represent optimum conditions for Buffer 5, indicating this buffer requires a higher voltage.	185
Figure 4.3. 1 - Sequence section from murine XBP-1. Red box – Forward primer flanking splicing excision site. Black box – 26 base pairs excised in spliced XBP-1. Blue box – Reverse primer flanking splicing excision site.	188
Figure 4.3. 2 – <i>XBP-1</i> splicing in IRE1-construct expressing cells with/without ER stress induction/1NM-PP1 treatment. XBP1u – unspliced bands, XBP1s – spliced bands.....	190
Figure 4.4. 1 – Plasmid map of pcDNA5/FRT/TO-hIRE1α. Plasmid contains the human IRE1 gene in a vector competent for transfer to a stable cell line using the FRT site.	194
Figure 4.4. 2 – Western blot for IRE1α in HEK293 Cells transiently transfected with pcDNA5-FRT-TO-hIRE1α construct and induced with tetracycline.	195
Figure 4.4. 3 – Phosphoimage of Southern Blot for pFRT/lac/Zeo site. Lanes represent radioactive signal from Clones 1-8.	197
Figure 4.4. 4 – Potential multiple insertions of the pFRT/lac/Zeo	197
Figure 4.4. 5 - PCR for multiple insertions of pcDNA site	197
Figure 4.4. 6 - Transient transfection with FV2e-IRE1 for tetracycline induction.....	199
Figure 4.5. 1 - IRE1 expression in Stably Transfected IRE1Reconstituted MEFs	202
Figure 4.5. 2 – Tetracycline induction of <i>XBP-1</i> splicing in IRE1 stably transfected <i>ire1α</i> ^{-/-} MEFs.....	203
Figure 4.5. 3 – Viability of <i>ire1α</i> ^{-/-} cells stably transfected with IRE1 constructs after 0-48 h tetracycline induction.....	205
Figure 4.5. 4 - Viability of <i>ire1α</i> ^{-/-} cells stably transfected with IRE1α constructs and treated with 100ng/ml tunicamycin – longer timecourse.....	206
Figure 4.5. 5 – PARP Cleavage in IRE1α stably transfected <i>ire1α</i> ^{-/-} MEFs.....	208
Figure 4.5. 6 – JNK Activation in IRE1α stably transfected <i>ire1α</i> ^{-/-} MEFs	209
Figure 4.6. 1 - RNA from CHOK1SV host cell line.....	212
Figure 4.6. 2 - T-RACE Synthesis	214
Figure 4.6. 3 – Conserved domain analysis of H. sapiens ERN1/IRE1α.	229
Figure 4.7. 1 – Lonza pEE12.4 vector backbone.....	232
Figure 4.7. 2 - Multicloning site insert.....	233
Figure 4.7. 3 - U6 Promoter Sequence (from Lin2004).....	234

Figure 4.7. 4 - U6 Polylinker Annealing.....	235
Figure 4.7. 5 – U6 Promoter Vector (pEE12.4-U6).....	236
Figure 4.8. 1 – miRNA scaffold – after (Chang, Elledge et al. 2006)	237
Figure 4.8. 2 - Cloning of shRNAs into U6 Promoter Vector	240
Figure 4.8. 3 - Splice junction primer test.	242
Figure 4.8. 4 - Actin qPCR Efficiency.....	243
Figure 4.8. 5 – Spliced XBP-1 qPCR Efficiency.....	243
Figure 4.8. 6 - qPCR for IRE1 α knockdown	244
Table 4.9. 1 - Cell line specific productivities of lines used in this thesis (donated by Lonza)	245
Figure 4.10. 1 - Viability of CHOK1 cells after transient transfection with IRE1 α plasmids	253
Figure 4.10. 2 - Monoclonal Antibody Production in High Producer Cell transiently.....	254
Figure 4.10. 3 - Monoclonal Antibody Production in High Producer Cell transiently transfected with human IRE1 α mutants at timecourse after transfection.....	255
Figure 4.10. 4 – IRE1 α expression after transient transfection. Each marked lane is three biological replicates.	256
Figure 4.10. 5- Transient transfection of FV2e-IRE1 α to verify presence of tet repressor...	257
Figure 5. 1 – IRE1 kinase pocket, see Fig 1.8 for original.	260

Chapter 6 – No Figures

Abbreviations

1NM-PP1	1-tertbutyl-3-naphthalen-1-ylmethyl-1H-pyrazolo[3,4-d]pyrimidin-4-ylemine
ADP	Adenosine diphosphate
AKT1	V-akt murine thymoma viral oncogene homolog 1
Apaf-1	Apoptotic protease activating factor 1
ASK1	Apoptosis signal-regulating kinase 1
ATP	Adenosine triphosphate

ATF4	Activating transcription factor 4
ATF6	Activating transcription factor 6
Aux1p	Auxin transport protein 1
BAK	Bcl-2 homologous antagonist killer
BAX	Bcl-2 associated X-protein
BBF2H7	BBF2 human homologue on chromosome 7
Bcl-2	B-cell lymphoma 2
BiP/GRP78	Immunoglobulin heavy chain binding protein/Glucose-regulated protein, 78-kDa
BID	BH3 interacting-domain death agonist
BI-1	Bax-Inhibitor 1
BH1, BH3	Bovine spongiform encephalopathy
Blos1	Biogenesis of lysosome-related organelles complex-1, subunit 1
BSE	Bovine spongiform encephalopathy
bZIP	Basic leucine zipper domain
C3	Caspase 3
C9	Caspase 9

C12	Caspase 12
cAMP	Cyclic adenosine mono-phosphate
CMV	Cytomegalovirus
CHO	Chinese hamster ovary
CHOP	CCAAT/enhancer-binding protein homologous protein
CREB3	cAMP response element-binding protein 3
CREB4	cAMP response element-binding protein 4
CREB-H	cAMP response element-binding protein H
CrmA	Cytokine response modifier A
Der1p	Degradation in the ER 1 protein
DHFR	Dihydrofolate reductase
DMEM	Dulbecco's Modified Eagle's Medium
DMSO	Dimethyl sulfoxide
DNA	Deoxyribonucleic acid.
DPBS	Dulbecco's phosphate buffered saline
DTT	Dithiothreitol

eIF2 α	Eukarotic translation initiation factor 2 α
ELISA	Enzyme-linked immunosorbent assay
ER	Endoplasmic reticulum
ERAD	Endoplasmic reticulum associated degradation
ERK2	Extracellular signal-regulated kinase 2
Ero1	ER oxidoreductin 1
ERP72	Endoplasmic reticulum protein of 72 kDa
EPO	Erythropoietin
FACS	Fluorescence-activated cell sorting
FADD	Fas-Associated protein with Death Domain
FRT	Flippase Recognition Target
GAPDH	Glyceraldehyde 3-phosphate dehydrogenase
GDP	Guanosine diphosphate
GFP	Green fluorescent protein
GLUT4	Glucose transporter 4
GRP94	Glucose-regulated protein, 94-kDa
GS	Glutamine synthase

GTP	Guanosine triphosphate
HA	Haemagglutinin
Hac1	H3/H4 histone acetyltransferase/transcription cofactor
HEK	Human embryonic kidney
Herp	Homocysteine-induced ER protein
HIV-1	Human immunodeficiency virus -1
HPLC	High performance liquid chromatography
HRI	heme-regulated eIF-2 α kinase
Hsp1,3, 40	Heat Shock Protein 1,3, 40
HSV	Herpes simplex virus
IKK	Inhibitor of kappa B complex kinase
IRE1 α /ERN1	Inositol requiring enzyme 1 alpha/Endoplasmic reticulum to nucleus signaling 1
IRES	Internal ribosome entry site
IRS	Insulin receptor substrate
JNK	c-Jun N-terminal kinase
LCMS	Liquid chromatography-mass spectrometry

MAP3	Mitogen-activated protein 3
MAPK	Mitogen-activated protein kinase
MEF	Mouse embryonic fibroblast
MHC	Mitogen-activated protein kinase kinase 3,4,7
MKK3,4,7	Major histocompatibility complex
MTX	Methotrexate
mRNA	Messenger ribonucleic acid
MSX	Methionine sulfoximine
NFκB	Nuclear factor kappa B
NF-Y	Nuclear transcription factor Y
NRF2	NF-E2-related factor-2
OASIS	Old astrocyte specifically-induced substance
P38	P38 mitogen activated protein kinase
PARP	Poly ADP ribose polymerase
PCR	Polymerase chain reaction
PDI	Protein disulphide-isomerase

PEI	Polyethyleneimines
Pek-1	Pancreatic eIF-2 α kinase
PI3K	Phosphoinositide 3-kinase
PERK	Protein kinase R-like endoplasmic reticulum kinase
RACE/T- RACE/RLM- RACE	Rapid amplification of cDNA ends/Targetted rapid amplification of cDNA ends/RNA Ligase Mediated Rapid amplification of cDNA ends
RNA	Ribonucleic acid
RNAi	Ribonucleic acid interference
RING	Really Interesting New Gene
RIPA	Radio-Immunoprecipitation Assay
ROS	Reactive oxygen species
RT-PCR	Reverse transcriptase PCR
S1P	Site 1 protease
S2P	Site 2 protease
SDS	Sodium dodecyl sulphate
SERCA	sarco/endoplasmic reticulum Ca ²⁺ -ATPase
Sec61p	Secretory 61 protein

Si/shRNA	Small interfering/small hairpin RNA
SREBP2	Sterol Regulatory Element Binding Protein 2
TK	Thymidine kinase
TNF α	Tumour necrosis factor α
TRAF2	Tumour necrosis factor receptor associated factor 2
TRB3	Tribbles homologue 3
tRNA	transfer ribonucleic acid
UDG	Uracil DNA glycosylase
UPR	Unfolded protein response
UPRE/ERSE	Unfolded protein response element/endoplasmic reticulum response element
UGGT	UDP–glucose glycoprotein:glucosyltransferase
VDAC	Voltage-dependent anion channel
XIAP	X-linked inhibitor of apoptosis protein
Yos9p	Yeast osteosarcoma 9 protein

Statement of Copyright

The copyright of this thesis rests with the author. No quotation from it should be published without the author's prior written consent and information derived from it should be acknowledged.

Acknowledgements

I would like to express my gratitude to the following people. Anyone who I've missed I hope will forgive me, or at least won't be too upset. Heartfelt thanks are owed;

To my supervisor, Dr Martin Schroeder, for his patience, his attention to detail and his encyclopaedic knowledge of the unfolded protein response. I have lost count of the number of times I have asked something along the lines of "but what evidence is there that (Protein X) does (Y)?" and received a comprehensive e-mail in response. During the conduct of this research there has never been a time when I felt anything less than completely supported.

To everyone in Lab 2 past and present, notably Natalie Strudwick for looking after me through my first year, David Cox for all the help with the FRT system, Siddharth Narayanan for taking my plates out on Saturday mornings, and Max Brown for being absolutely incorrigible on a regular basis.

To those elsewhere at the School of Biological and Biomedical Sciences in Durham, particularly my thesis committee, Dr Adam Benham my auxiliary supervisor, the exceedingly patient technical staff and members of Labs 3-5, 8, 9, and 19 for various forms of support, scientific and moral. Special mention goes to Dr Graeme Watson for some very interesting conversations in the tissue culture room.

To everyone (currently and formerly) at Lonza Biologics in Slough and Cambridge for hosting me for three very scientifically rewarding months, and giving me both the use of their molecular biology labs and the support and confidence to use them away from my usual laboratory environment. In particular the members of the Molecular Biology section headed by Dr Robert Young, and others from elsewhere in the company; Dietmar Lang, John Bainbridge, Fran Kenny, many of the members of the cell culture and analytical sections and the placement students for 2010-2011 who made the hotdesk area very much more welcoming to a fellow student.

To my family, and particularly my mother for continually offering to proofread my thesis. It was a very kind offer, but alas she is excessively fond of the Oxford comma, and so I politely declined.

To my friends with multiple publications in a variety of different fields from mathematics to particle physics who have tactfully not mentioned the fact I don't have any yet.

This research would not have been possible without funding from the BBSRC and Lonza Biologics. I express my thanks to those bodies accordingly.

Lastly, I have to thank my girlfriend Amy, for being who she is in general, but particularly given the few times she came in and helped me passage my cells, and for the many times she listened to me when I came in of an evening and produced a stream of expletives followed by the words "XBP-1 splicing assay".

1. INTRODUCTION

In the decades since the first biopharmaceuticals were produced, demand for protein-based products such as antibodies and clotting factors has increased dramatically. This increase is compounded by the large doses which are required for many recently licensed therapeutic biopharmaceuticals, most notably those of humanised monoclonal antibodies.

Bio-manufacturing capacity has begun to expand to accommodate the shortfall, but demand is already beginning to outstrip production (Butler 2005; Schroder 2008). As opposed to traditional drugs and therapies which often involve inserting a foreign agent into the body with all the potential side effects that can result from upsetting the homeostasis of the organism, biopharmaceuticals often consist of an endogenous protein, and may represent a much less invasive method for restoring homeostasis in a disease state. Many biopharmaceuticals are already licensed by regulatory authorities and more are currently in development or clinical trials.

Output remains one of the greatest challenges in biopharmaceutical research – generally speaking and with some exceptions which will be covered later, cells and organisms did not evolve to produce the levels of secreted protein required for industrial bio-manufacture – indeed, systems exist to prevent just such a situation, often evolved to prevent co-opting of protein production systems by viral agents, for example the RNaseL protein which switches off protein production in virally infected cells (Floyd-Smith, Slattery et al. 1981) Secretory output of the cell is well controlled by complex interactomes of kinases, regulatory proteins and regulatory elements that can either help the cell cope with high loads of protein – by upregulating chaperone systems which guide proteins through the secretory pathway and control degradation of proteins, or which can simply sacrifice the cell which is overproducing - by inducing autophagy, caspase cascades and apoptosis. Collectively, these systems are referred to as the unfolded protein response (UPR).

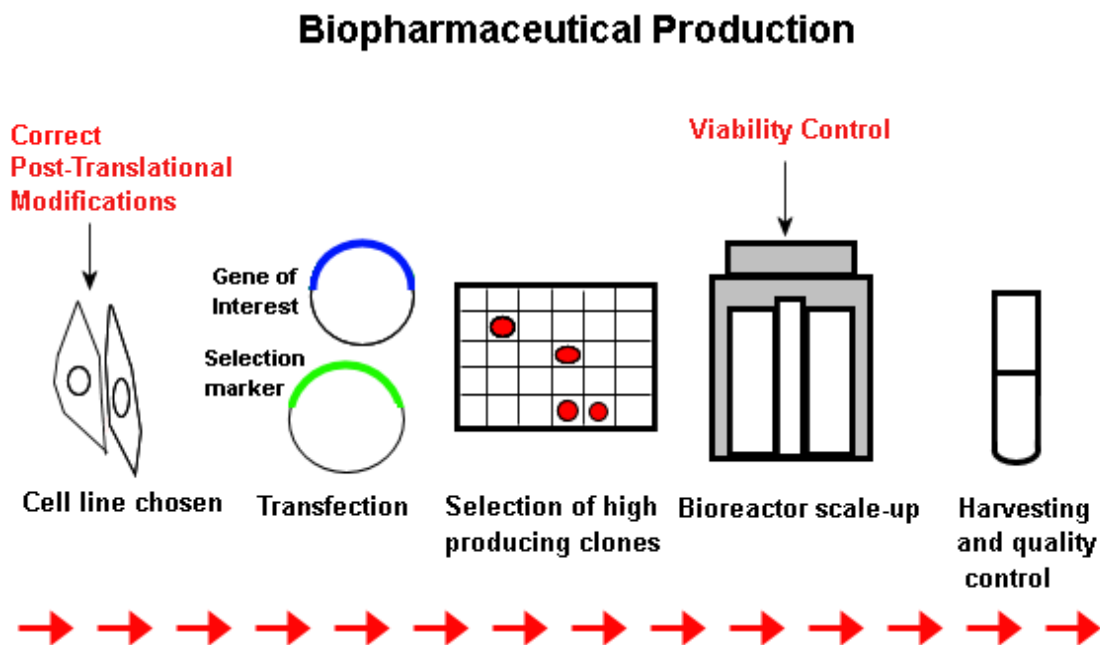
There is potential, therefore in biopharmaceutical research to attempt to circumvent the unfolded protein response or to control its workings and outputs. Indeed, some investigation has already been carried out along these lines (Borth, Mattanovich et al. 2005; Tigges and Fussenegger 2006; Becker, Florin et al. 2008; Ku, Ng et al. 2008). However, these approaches, although effective, often represent simple brute-force overexpression of

chaperones, rather than a more controlled and targeted system, using the UPR's own mechanisms. How could this control potentially be exercised? By using one of the most evolutionarily ancient UPR mechanisms, conserved in eukaryotes from yeast to humans – IRE1.

Part 1.1 of this introductory section will describe the factors involved in industrial biopharmaceutical protein production, covering the stresses, bottlenecks and requirements and some of the cell lines that have been used to produce biopharmaceuticals. It will also make reference to the other great challenge in industrial biopharmaceutical production – cell viability and the control of apoptosis. Part 1.2 will cover the main components and systems of the unfolded protein response in growth, disease and differentiation, with reference to how these workings can affect the cell cycle, development and growth in cells, and some of the endogenous producers of biopharmaceuticals – antibody expressing immune cells. Part 1.3 will focus on IRE1 itself - detailing how the structure and behaviour of this serine-threonine kinase/endoribonuclease is linked to its dual functions of chaperone regulation and apoptosis, both important factors in the production of biopharmaceutical proteins. Part 1.4 will discuss how chemical genetic approaches using the kinase inhibitor 4-Amino-1-tert-butyl-3-(1'-naphthylmethyl)pyrazolo[3,4-d]pyrimidine (1NM-PP1) have both elucidated the structural components of IRE1 and given a potential mechanism for control of its downstream effects. Part five will outline the aims of this project, with reference to the desired scientific and industrially important outcomes.

1.1. Industrial Protein Biomanufacture: Selection, Synthesis and Secretion

Figure 1.1 – Timeline for biopharmaceutical production.



Industrial synthesis of proteins is one of the most useful techniques for the manufacture of medical proteins for clinical treatment, such as clotting factors and insulin. In 2005 there were up to 30 licenced biopharmaceuticals, including recombinant proteins, chimeric or humanised monoclonal antibodies (e.g. Herceptin) and nucleic acid based products. Industrial proteins can be produced in a variety of different host cells, such as bacteria, plants, yeasts and mammalian cells. The earliest licensed biopharmaceutical, human recombinant insulin (Humulin) produced by Genentech in 1982, was originally grown in *E.coli*, however, this organism cannot produce the post-translational modifications required for true eukaryotic cell protein production (Butler 2005). Therefore, mammalian cells are usually the most desirable host, because they are more likely to ensure correct protein folding and to ensure that the correct post-translational modifications are performed on the human protein product. Furthermore, mammalian cells are more suitable for meeting regulatory requirements due to the large knowledge base available on them. As a result, around 60-70% (Wurm 2004) of all recombinant industrial proteins are produced in mammalian cell lines such as Chinese

hamster ovary (CHO) cells and human embryonic kidney (HEK) cells, which are known to produce yields of up to 5g/L of product (Butler 2005). Important requirements for a cell line to be used include – high efficiency of transfection, ability to adapt to serum free medium and ability to adapt to scaling up to bioreactor volumes (Baldi, Hacker et al. 2007). Over the past decades, a number of different cell lines have been employed by the biopharmaceutical industry in production: The most commonly used are HEK293, CHO and NS0 – with the most frequent being CHO cells.

CHO

The CHO cell line was originally studied because its lower chromosome number allowed for easy examination of chromosomal and genetic changes (Tjio and Puck 1958), a fact that is still useful today in examining apoptotic changes in the industrial cell lines. A variant of the CHOK1 cell line from the Puck lab was then produced in 1980 by Urlaub and Chasin with a mutant in the DHFR gene, which codes for a protein that reduces folic acid to tetrahydrofolic acid. This mutant rendered it unable to survive without supplementation of derivatives of tetrahydrofolic acid such as glycine, purine nucleotides and thymidylate (Urlaub and Chasin 1980). Even at this early stage, however, some of the mutants were found to be able to revert to a DHFR producing state (Urlaub and Chasin 1980). CHO cell lines used in transient gene expression include K1 and DHFR mutant DG44 as they are well adapted for both laboratory and industrial production, and well studied. They are therefore useful for drug development and are the cell line of choice for industrial production. Several monoclonal antibody lines are produced using CHO cells, as they are particularly able to produce high protein titres (de la Cruz Edmonds, Tellers et al. 2006).

The Biopharmaceutical Process

Once the most suitable cell line has been selected, a considerable amount of effort goes into the selection and production of this product before the biopharmaceutical product can be harvested. Development of a medical biopharmaceutical protein product usually requires the following:

- 1) The gene of interest, along with the appropriate promoter and transcription sequences, are stably transferred into the cell line, along with another gene, such as dihydrofolate reductase,

which allows the cell line to be selected for, often with the use of a metabolite which prevents growth of the cells which do not have the additional genes.

2) After selection, those cells which have the required genes are moved to larger cultures to scale up production of the clones.

3) The clones are examined to ascertain which are the best producers of the protein. These clones are selected for cultivation, seeking the one cell line with the best production and growth characteristics (Wurm 2004).

Each stage of this process has its own issues and areas for improvement, and the biopharmaceuticals industry has developed and is in the process of developing strategies for overcoming them. The following sections will deal with these issues and strategies in more detail, addressing where in each area genetic and process modifications have been used to help improve product yield. Finally, this section will deal with recent advances in modifying the unfolded protein response in industrial cell lines and the potential for further work in this field.

1.1.1 Transfection

In order to induce an industrial cell line to produce a biopharmaceutical, the gene coding for the product is normally transfected into the cell, usually in order that it may stably integrate into the host cell genome. Integration usually occurs at a random point in the host cell genome, and selection procedures are required to find a clone which is producing the biopharmaceutical at commercially viable levels (see later section on selection of high producers). Improvements can be made to the yield of the recombinant protein by: increasing the strength of the promoter associated with the gene; adding introns to the coding sequence, or modifying it; using a weak promoter for the selection gene as opposed to a strong promoter for the gene of interest to augment gene amplification (although this may reduce the efficiency of selection); linearisation of plasmids; altering the sequence to assure the gene is not affected by the position of its site of integration, such as by the insertion of boundary elements around the gene of interest to negate the transcriptional influences of nearby sequences (Wurm 2004). For most, large scale production of biopharmaceuticals where the cell line is to be used over a long period of time to produce a large amount of product for commercial and medical use, a stable cell line is the most suitable system. However, stable

integration into the host cell genome often takes months of production and characterisation, a large investment of time and resources – for some applications is it possible to use large-scale transient transfection. Transient transfection of biopharmaceuticals is particularly useful to identify proteins for clinical trials or academic research, where a wide range of lead compounds, such as secretory, membrane or intracellular recombinant proteins, or variants of the same protein, must be produced quickly in mammalian cells, in order to enter screening and to identify the best candidate, or where a non-commercial, but still substantial level of protein (10-100 mgs) is required to be produced. This approach may take days or weeks, rather than months and therefore is suitable for these requirements. Productivity of stable transfections, however, still remains at five times that of transient transfections, and cell densities at 3-5 times greater (Wurm 2004). Transgenic expression also requires a lot of DNA, >1ug of DNA per ml of culture (Baldi, Hacker et al. 2007), making DNA a significant contributor to the cost of this method. Indeed, any significant increase in the efficiency of DNA transfer could reduce the costs involved in transient transfections. DNA preparation therefore requires a high yield of usable DNA without any endotoxin, LPS, RNA or other contaminants from bacterial preparation removed (Stadler, Lemmens et al. 2004).

Transfection with recombinant protein DNA usually involves chemical methods of inserting DNA into the cell, as physical methods such as electroporation or microinjection do not work well with large scale transfection. Frequently used chemical methods include polyethyleneimines (PEI), cationic lipids and calcium phosphate. PEIs produce high yields of IgG, but have cytotoxic effects and are not biodegradable. Cationic lipids are expensive to produce and have therefore been little used in large scale transfection (Baldi, Hacker et al. 2007). Calcium phosphate gives high transfection efficiencies and is inexpensive, but the methodology is time-sensitive, reducing the scale upon which it can be performed (Meissner, Pick et al. 2001).

1.1.2 Selection and Characterisation of High Producers

Once the host cell has been transfected with recombinant DNA, the selection process begins to find the transfected clone with the highest production of the recombinant DNA. Why is it necessary to select for the highest producers of biopharmaceuticals? Obviously a higher yield of any product, biopharmaceutical or otherwise is economically and medically desirable, but in the case of one biopharmaceutical, monoclonal antibody (mAb), this is

particularly important – the medical efficacy of this product is dependent upon very high doses (Dinnis and James 2005). Direct modifications to the antibody itself can improve the affinity of the molecule, for example, producing chimeric antibodies, antibodies containing the variable region, containing the murine complementarity defining regions, from mouse to retain specificity and the human constant region to reduce immunogenicity, and increase the half life of the product *in vivo* (Butler 2005). However, it is still necessary to select for the highest producing clone – this is done with a selectable marker, usually something which allows the host cell to grow where it would not otherwise do so, such as an antibiotic resistance gene to allow growth in an antibiotic supplemented medium, or where the host cell is deficient in a gene for a nutrient, such as the DG4 DHFR deficient CHO mutant mentioned above, growth in a medium which is not supplemented with the required nutrient. The biopharmaceutical production gene, driven by a strong viral promoter (Butler 2005), is transfected into the host cell in the form of a linearised plasmid along with a gene such as dihydrofolate reductase (DHFR) or glutamine synthase (GS). Selection pressure is then applied with an inhibitor of the enzyme (methotrexate (MTX) in the case of DHFR, methionine sulfoximine (MSX) in the case of GS). This selects for those cells into the genomes of which the plasmid has stably integrated, producing higher copy numbers of the inserted plasmid (Gasser, Simonsen et al. 1982; Bebbington, Renner et al. 1992). The GS system (de la Cruz Edmonds, Tellers et al. 2006) combines both inhibitor and metabolite approaches – the transfected plasmid contains the glutamine synthase gene which produces glutamine, allowing the host cell to be grown in glutamine free medium. Selection is then further applied by addition of MSX, producing clones with a stronger expression both of GS and the biopharmaceutical product. It also does not require mutant host cells as the DHFR system does, is faster, and produces less toxic ammonia as a byproduct (de la Cruz Edmonds, Tellers et al. 2006). This system also functions well in NS0 cells, as these do not have endogenous glutamine synthase. Site of integration is particularly important with stable cell lines, and can affect gene silencing during repeated cultures. This is thought to be due to the heterochromatin structure in the area in which the gene is integrated (see later sections on the UPR and epigenetics). Positional effects can cause differences in stability and expression. These differences may be offset by vector design, incorporating flanking areas/boundary elements which can insulate genes from positional effects. Matrix or Scaffold elements can also be included that force the chromatin to remain open and transcribable and resist silencing, regardless of location within the chromosome (Kim, Kim et al. 2004).

Once the selection marker has been applied, the cell line goes through many passages to mimick production culture generation numbers. To assess the stability of transfection, this is performed with and without selectable markers, or with variable selection marker concentration and seeding density as yields may reduce when high copy number is not selected for (de la Cruz Edmonds, Tellers et al. 2006). Regular assessments are made of the transfected clones, including viability counts and doubling times. Biopharmaceutical production can be directly assessed by methods such as ELISA, HPLC and glycosylation forms (see later) by LCMS. FACS analysis can be performed where a cell surface marker will indicate transfection(de la Cruz Edmonds, Tellers et al. 2006).

1.1.3 Culture Media and Nutrients

Most biopharmaceutical media have been adapted from those developed for research cell culture, e.g. Eagle's Minimum Essential Medium and Dulbecco's Modified Eagle's Medium (DMEM) which were developed in 1959-1969 for mammalian cell culture (Eagle 1959; Morton 1970). Media also exist that have been specially formulated for particular cell lines, such as CD-CHO (Invitrogen) (Gorfien, Dzimian et al. 1998; Fike, Dadey et al. 2001). Certain media types can also be used for transfection of DNA into cells (Baldi, Hacker et al. 2007). Medium is perhaps one of the simplest factors in biopharmaceutical production to control and optimise as nutrients and cofactors, and selective agents such as drugs, chemicals and growth factors can be added or removed. It is also possible to optimise media by using different media at each manufacturing phase (Wurm 2004). It can take 3-4 days to maximise production at 10^6 cells per ml, during which time the medium in the culture vessel may have accumulated toxic byproducts such as ammonia or vital nutrients may have been depleted, therefore medium is regularly supplemented by batch feeding of predicted concentrations of nutrients. pH is controlled, and carbon substrates are kept to stable levels in order to control production of toxic byproducts, such as lactate, prolonging the production phase (Butler 2005). In research cell culture, medium is usually supplemented with animal serum, for example foetal calf serum. Animal-derived serum is well supplied with hormones, growth factors and thus an excellent supplement for cell growth. Furthermore, serum albumin acts as a buffer against pH and shearing effects in shaken cultures. However, the constituents of animal derived media may vary greatly, making it difficult to maintain the consistency required for biopharmaceutical manufacture, potential contamination, by agents such as the

prion responsible for bovine spongiform encephalopathy (BSE), and possible interference with protein processing, it is necessary to reduce or remove all animal derived materials in production medium. Serum-free medium is therefore usually used in protein biomanufacture and effective substitutes for the growth factors in serum must be produced. Producer cell lines have specific requirements for these nutrients and even different CHO clones can vary, and therefore variations on a basic medium recipe tend to be used to optimise cell lines, and metabolic analysis on the resulting depletions used to build up a picture of what supplements are required, such as protein hydrolysates (Sung, Lim et al. 2004). Microarray analysis can also be used to assess what expression changes are occurring in response to deficiencies in medium and predict what nutrients and ligands are required at a genetic level (Butler 2005).

The production of proteins is important at all stages of nutrient processing – proteins to transport nutrients into the cell, proteins to transport and adjust the lipids that build the cell membranes themselves, protein enzymes to convert and metabolise nutrients into useful forms. Therefore the unfolded protein response plays a role in feeding these proteins into these systems. The cells of eukaryotic organisms are protected to some extent from the stressful environmental changes that single-celled yeasts are exposed to, with the circulatory systems of large multicellular organisms ensuring suitable levels of carbon and nitrogen sources, and no requirements for controlling meiosis in response to nutrient levels, although the control of cell membrane composition and phosphoinositides is still a requirement. The unfolded protein response remains part of nutrient regulation in these cells, taking on other specialized roles, such as control of lipid membrane formation, and although it may not regulate responses to carbon sources, in humans, the UPR is involved in the regulation of glucose levels via insulin secretion.

1.1.4 Controlling Apoptosis

A high cell density and long term cell viability is necessary for high protein output, and therefore control of apoptosis is necessary to preserve this viability. In cell culture, apoptosis can be caused by nutrient depletion, toxic metabolite production, shear forces from mixing, or hypoxia due to insufficient gas distribution. However, it is only of any use to alter apoptosis when this is the limiting factor in the cell culture and product titre, and therefore reducing apoptosis is of most use over long cultures where medium may be depleted and cells are more likely to go into death phase, or for cells under many apoptotically insulting conditions (Arden and Betenbaugh 2004). It is particularly necessary to inhibit apoptosis if

adding cytotoxic increasers of cell productivity (Dinnis and James 2005). Cell death in culture may occur by apoptosis or necrosis. Necrosis results from physical damage to cells, for example as may occur due to shear forces in a stirred-tank bioreactor, and causes swelling and rupture – as a result, careful control of the shear forces applied during growth in a bioreactor can reduce this effect. Apoptosis results from a stimulus, either internal or external, that causes a cellular cascade resulting in programmed cell death. Apoptotic bodies form containing the packaged cellular material, which are absorbed by the surrounding cells in an organism. Unfortunately, this apoptotic material may build up in cultured cells, having a detrimental effect (Mastrangelo and Betenbaugh 1998). Apoptosis can be detected in a variety of ways. DNA fragmentation assays can be used to assess the integrity of the genome. Western blots for caspase 3 and other apoptosis related proteases will indicate the level of apoptotic cascades. Cell integrity can be assessed by labelling cell membranes with annexin V or staining DNA with propidium iodide or ethidium bromide to indicate where the DNA is located and show chromatin condensation. Flow cytometry can be used to detect changes to the plasma membrane, cell size and shape, and propidium iodide/annexin V staining. However, these assays are sensitive but not specific as they may not differentiate between apoptosis and necrosis (Arden and Betenbaugh 2004). There are three main pathways by which a cell can undergo the induction of apoptosis – mitochondrially mediated, cell surface receptor mediated and ER stress mediated (Arden and Betenbaugh 2004).

The mitochondrial pathway is based on the membrane potential of the mitochondria, and is associated with the Bcl-2 family of proteins which control the balance of mitochondrial apoptosis. Bcl proteins come in three forms – antiapoptotic Bcl proteins, which are homologous to Bcl-2, apoptotic proteins which have BH1 homology domains, and apoptotic proteins only containing the BH3 domain. Pro apoptotic proteins such as Bak and Bax, in response to apoptotic stimuli, such as toxin exposure or DNA damage, move into the mitochondrial membrane, and their structure is altered so as to compromise the mitochondrial membrane potential (Harris and Thompson 2000). This causes the release of cytochrome C from the mitochondria, which is pro-apoptotic and promotes the conversion of procaspase 9, which is formed into the apoptosome with Apaf-1, and is proteolysed into caspase 9. Bcl proteins counteract apoptosis by binding to proapoptotic proteins, by retaining the balance of the mitochondrial membrane and by preventing release of the apoptotic factors from the mitochondria (Adams and Cory 2002).

The receptor mediated pathway is mediated via TNF (tumour necrosis factor)-type receptors. When activated, these receptors recruit a death protein, FADD (Fas-Associated

protein with Death Domain) to their cytoplasmic tails - FADD activates pro-caspase 8 into caspase 8, which activates Bak and Bax via Bid and causes mitochondrial apoptosis, and caspase activation. Caspase 8,9 and 12 are initiators from the cell surface, mitochondrial and ER pathway, which trigger effector caspases 3,6, and 7 which finalise the cell death programme (Chandler, Cohen et al. 1998; Ashkenazi 2002).

The ER related pathway is triggered by blocking of glycosylation and disulphide bond formation and by release of calcium from the ER as well as defects in protein secretory transport to the golgi (Oyadomari, Koizumi et al. 2002).

Large buildups of unfolded protein can cause oxidative stress, with all the associated damage caused by reactive oxygen species, such as DNA damage. Around 25% of all ROS is formed during disulphide bond formation and protein folding in the ER controlled by the Ero1-PDI (protein disulphide isomerase) oxidation chain (Tu and Weissman 2004). Apoptotic effects of CHOP induced by cigarette-smoke in bronchial cells can be counteracted by overexpression of BiP/GRP78 and by antioxidant free-radical scavengers, indicating the role of the unfolded protein response in dealing with oxidative stress (Tagawa, Hiramatsu et al. 2008).

Once apoptosis has been assessed and found to be a limiting factor, control can be attempted. Apoptosis can be controlled extracellularly, by adjusting the environment the producer cells are in, particularly the culture medium and intracellularly, by making genetic changes to the cell line itself. One of the issues with removing serum from the culture medium is that serum contributes anti-apoptotic factors to culture medium, making serum free-medium apoptotic (Zanghi, Fussenegger et al. 1999). Expensive anti-apoptotic supplements such as growth factors like insulin, IGF and transferrin (Sunstrom, Gay et al. 2000; Jones, Nivitchanyong et al. 2005), caspase inhibitors (although these only block certain apoptosis pathways, and still leave cells vulnerable to mitochondrial induced cell death, see later) or the anti-apoptotic peptide Suramin (Zanghi, Renner et al. 2000) must then be added to counteract this. Unfortunately Suramin can only protect cells from apoptosis during the death phase, indicating the need for further research on the anti-apoptotic components of serum. Control of nutrients can also be control of apoptosis – glutamine, which is usually supplemented into cell culture medium, suppresses the DNA damage inducible gene *gadd153* (Abcouwer, Schwarz et al. 1999). Galactose is important for post-translational modification, but will also reduce apoptosis if fed in to the culture medium. Some amino acids (e.g. glycine, asparagine, threonine) can also act as a buffer against damage from carbon dioxide, osmolarity and

nutrient depletion (Mendonca, Arrozio et al. 2002) (Sanfeliu and Stephanopoulos 1999; deZengotita, Abston et al. 2002; Lengwehasatit and Dickson 2002). Intracellular control of apoptosis usually involves genetic strategies either using endogenous cell mechanisms or hijacking viral methods for preventing apoptosis during infection. Bcl family proteins are anti-apoptotic, therefore, unsurprisingly, transfection with these reduces apoptosis in cell culture (Mastrangelo, Hardwick et al. 2000). Bcl family proteins can also be engineered so as to remove their ability to be cleaved by caspases during apoptosis and therefore to remove their antiapoptotic activity or trigger their degradation. This results in higher, longer lasting Bcl2 activity. Bcl-X1 can be used in a similar fashion, but this mutant is less stable than the Bcl2 variant (Figueroa, Sauerwald et al. 2003; Arden and Betenbaugh 2004). Caspase inhibitors such as XIAP (X-linked inhibitor of apoptosis protein) and CrmA (cytokine response modifier A) can interrupt the chain of caspase activation that leads to apoptosis. The anti-apoptotic effect of XIAP can be enhanced by removing its RING domain which is proapoptotic. Proapoptotic proteins can be engineered to be dominant negative or ineffective, for example, caspase 9 can be engineered to bind but not cleave its downstream substrates (Sauerwald, Betenbaugh et al. 2002; Sauerwald, Oyler et al. 2003). Caspase mutants cannot inhibit the mitochondrial pathways, however. Instead, the pro-apoptotic protein Bax can be prevented from reaching the mitochondrial membrane by humanin, a short peptide (Guo, Zhai et al. 2003), or cells can be selected with a particularly high mitochondrial membrane which are less susceptible to apoptosis by this pathway (Follstad, Wang et al. 2002). Many types of virus prevent apoptosis of cells they have infected by maintaining mitochondrial membrane integrity and affecting Bcl family members such as VDAC and cyclophilin D. Viral homologues of Bcl2, e.g bhrf-2 from Epstein Barr virus can be used to supplement the cells own Bcl2 and shift the balance away from apoptosis (Jung, Cote et al. 2002; Boya, Roumier et al. 2003).

1.1.5 Post-Translational Modifications

In any review of biopharmaceutical production, particularly one relating to the unfolded protein response, it is necessary to address the optimization of post-translational modifications. In an organism, post-translational modifications such as glycosylation increase the solubility of a protein, act as a shield against other proteins, and can stabilise a protein's conformation, as well as acting as a marker of protein folding status (Schröder 2010). As

already stated, mammalian cells are used for biopharmaceuticals because of their ability to confer the correct post-translational additions to a protein product (Wurm 2004) – these additions can make a crucial difference to the biological activity, bioavailability and immunogenicity of a biopharmaceutical. Biologically active post-translational modifications include glycosylation, galactosylation, sialylation, sulphation, fatty acylation, glycosphosphatidylinositol anchoring, methyl- and acetylation. Galactosylation and sialylation are often incomplete (Butler 2005). The particular glycoforms attached to each site are heterogenous, forming a pool of glycoforms for each product. Expression of glycosylation enzymes in the Golgi affects the level of each glycoform. Sialylation varies in structure across species, CHO forms being closer to human than mouse or ungulate, but still restricted in a manner which affects human EPO production/formation. These affect immunogenicity, with some glycoforms from different species being highly immunogenic in humans (Jenkins, Parekh et al. 1996; Baker, Rendall et al. 2001). Control of glycosylation can potentially also improve consistency and produce more pharmacologically active glycoforms. Proteins can be engineered for longer half lives or greater efficacy by altering the glycan structures or knocking out the enzymes, e.g. altering antibodies for greater affinity for their target (Shinkawa, Nakamura et al. 2003). Glycosylation will also vary according to cell cycle stage and amount of protein throughput. It is difficult to control the exact glycoforms obtained in animal cell cultures, and because a consistent glycosylation profile is required for recombinant protein products, this represents a significant issue. Depletion of glucose and glutamine may reduce the amount of glycosylation and sialylation, altering the profile as these nutrients run out in the medium, and alterations in pH, temperature, oxygen, ammonia can affect the glycosylation profile by changing enzyme activity and glycan branching. It is possible to control the conditions which lead to the glycosylation profile of a product, as levels of nutrients such as glutamine and albumin, levels of dissolved CO₂ and enzymes such as sialidase and glycosidase have been shown to affect type and number of post-translational modifications (Borys, Linzer et al. 1993; Andersen and Goochee 1994; Yang and Butler 2000).

1.1.6 Exit from the Endoplasmic Reticulum

Once the conditions of the bioreactor are controlled appropriately and the correct medium and supplements added to the cell culture medium for growth, production and post-translational modification, one more thing limits the production of a biopharmaceutical - exit

from the secretory pathway from translation at the endoplasmic reticulum, through the Golgi, to secretion into the medium for harvesting (Schroeder 2008).

The size and capacity of the endoplasmic reticulum can be a limiting factor upon the protein production. Therefore, there is a requirement for cellular control systems to regulate this. In yeast, there are two forms of ER, perinuclear and cortical, which are passed on to daughter cells by slightly differing mechanisms. Perinuclear, as its name suggests, is transferred along with the nucleus, whereas cortical ER is attached at the bud site and passed on during budding. Inheritance of cortical ER is dependent upon an ER associated chaperone-like protein, Aux1p possessing an Hsp40-type J- Domain, although this domain does not appear to be required for the localization of the ER (Du, Pypaert et al. 2001; Barr 2002). The unfolded protein response is generally thought to be a controlling factor in the expansion and accommodation of ER capacity by membrane control (Menzel, Vogel et al. 1997) and vesicular budding of the ER in yeast (Sato, Sato et al. 2002), although it may not be necessary for initial formation of the ER (Koning, Larson et al. 2002), and the fact that membrane expansion alone can deal with unfolded protein stress (Schuck, Prinz et al. 2009) indicates that increase in the capacity of the ER may be an independent means for the cell to deal with unfolded protein stress without activating the more detrimental areas of the UPR, such as the apoptotic responses of the IRE1 arm. However, in mammals silencing of the ATF6 arm of the UPR almost completely removes ER proliferation in response to unfolded protein stress, indicating the necessity at least for the transcriptional arm of the UPR (Maiuolo, Bulotta et al. 2011).

Spliced XBP-1 is not only capable of regulating antibody production - expansion of the capacity of the ER by a ectopic expression of XBP-1 improved expression of a number of secreted proteins in CHO cells (Tigges and Fussenegger 2006). Overexpression of the active (spliced), as opposed to the inactive (unspliced) form of XBP-1 in CHO cells was able to increase the production of recombinant monoclonal erythropoetin transiently transfected into a cell line which the secretory capacity of the cell line was the limiting factor in the protein yields. Addition of this transcription factor to erythropoetin producing CHO cell lines caused an 2.5-fold increase in titres of the protein, and approximately 2-fold in NS0 cells (Ku, Ng et al. 2008). Similar experiments with monoclonal antibodies and interferon γ did not yield an increase, however. This was thought to be due to the rate limiting step of these products occurring before the secretory pathway, for example during translation. When CHOKI cells which had reached maximal erythropoetin production capacity, overexpressed spliced XBP-1 allowed them to produce a greater yield, indicating the secretory capacity of host cells must

be at its maximum before addition of spliced XBP-1 can help alleviate it. Similar results were observed in NS0 cells (Ku, Ng et al. 2008). CHO cells seem to downregulate their XBP-1 as they are selected for monoclonal antibody overexpression, as analysis of XBP-1 protein and XBP-1 mRNA indicated a reduction in expression. Thus, lower expression of XBP-1 may be an indicator of well adapted cell line to monoclonal antibody production over a long period of time in cell culture (Becker, Florin et al. 2009). That simple overexpression of chaperones may not necessarily be the best approach, as overexpression of BiP was not successful at increasing monoclonal antibody yields in mammalian cells (Borth, Mattanovich et al. 2005). Indeed, tissue plasminogen activator (TPA) yields were actually increased by a reduction in BiP levels (Dorner, Krane et al. 1988). Furthermore, high levels of spliced XBP-1 decreases CHO cell survival over time after transfection, and thus clones overexpressing XBP-1 are likely to be unsuitable for use in selection procedures and unstable over many passages (Becker, Florin et al. 2008). XBP-1 spliced stable clones had lower productivities and lower survival, and therefore were selected against in clonal selection procedures. XBP-1 spliced transfected cells had seven times lower colony counts as opposed to mock transfected cells and prolonged XBP-1 induction showed apoptotic effects in annexin V stain assay. This can be counteracted by co-expressing the anti-apoptotic protein X-Linked inhibitor of apoptosis (XIAP), which alleviated the effects of XBP-1 alone on colony counts in CHO cells. Indeed, coexpression of XIAP and XBP-1 increased colony counts further, rescuing the XBP-1 reduction, and reducing apoptosis. XBP-1 expression increased the yields of monoclonal IgG 40%, but XBP-1 + XIAP increased it further, by 100% (Becker, Florin et al. 2009). By this, it can be seen that combining overexpression of XBP-1 with an anti-apoptotic protein not only alleviates the effects of XBP-1, but actually increases yields. One of the proteins involved in the unfolded protein response is capable of both of these actions – IRE1.

1.2. The Unfolded Protein Response: Adapting Protein Production

The ER is involved in translocating, manufacturing, storing, folding, and post-translational modification of proteins (Mellman and Warren 2000). Saturation of the protein processing mechanisms of the ER and build-up of unfolded, misfolded and non-functional proteins, and over-expression of proteins puts the endoplasmic reticulum under stress, causing perturbations of ER homeostasis, difficulties in membrane assembly and integrity, loss of secretory proteins due to insufficient processing and release, and the induction of apoptotic

pathways and responses, as well as a build-up of reactive oxygen species generated during the formation of disulphide bonds. This saturation can be induced by a range of conditions. Metabolic imbalances such as a lack of glucose may cause it via signalling cascades. Mutations in genes which code for secretory or transmembrane proteins which fold in the endoplasmic reticulum may prevent proper folding from occurring, thus saturating the folding machinery. Certain pathogens, such as Hepatitis C, may, by hijacking the protein production machinery overload it and cause buildup. Saturation can also be induced experimentally, by blocking of the SERCA calcium pump to perturb calcium homeostasis, preventing proper glycosylation occurring, or by inducing reductive stress which prevents disulphide bonds forming properly (Kaufman 2002). ER homeostasis may be perturbed as part of the physiological process whereby a cell specialises into competency for secretion, for example in the cases of antibody-secreting plasma cells, or insulin-secreting pancreatic cells (Rutkowski and Kaufman 2004).

In the previous section, 1.1.6 Exit from the Endoplasmic Reticulum, brief reference was made to the unfolded protein response and its role in protein secretion. This section will aim to elaborate upon the information given so far in greater detail, illustrating how the control mechanisms in the endoplasmic reticulum affect not only protein throughput, but the whole function of the cell, from early development through to apoptosis.

1.2.1. Structure of the Unfolded Protein Response

Quality control and folding pathways must function in tandem to ensure cell surface and secreted proteins can be kept at functional levels, as minor problems in protein folding may cause rejection of the nascent protein. This control is achieved by a number of signalling pathways and feedback loops, referred to as the unfolded protein response (UPR). The existence of the unfolded protein response was indicated when it was discovered that some pharmacological agents and mutations could change the levels of chaperones that reside in the ER (Kozutsumi, Segal et al. 1988).

1.2.1.2 Detection of Endoplasmic Reticulum Stress

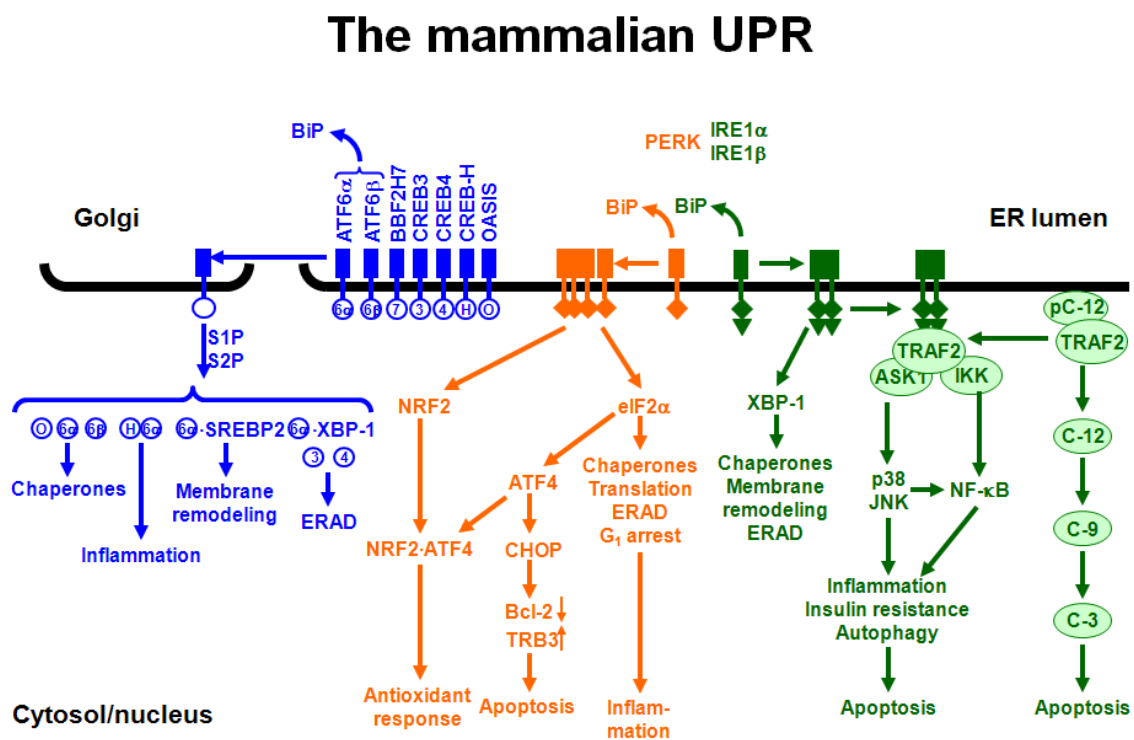
The eukaryotic UPR reduces ER stress caused by a high protein load by three methods, the first two of which seek to rectify the imbalances caused by ER stress. The first

involves reducing the amount of protein load being produced and entering the ER by transiently inhibiting translation of proteins and their transfer into the ER to reduce the amount of proteins that require folding; The second is a longer term adaptation – increasing the cell's ability to fold the excess of polypeptides, by activating UPR genes which make up protein folding machinery, such as chaperones and oxidating and reducing enzymes, thus increasing the protein folding capacity; (Ron and Walter 2007) and increasing the production of proteins which degrade misfolded polypeptide, which may be stalling the folding machinery (Mori 2000) and by increasing phospholipid production and expanding the ER volume (Cox, Chapman et al. 1997). The third mechanism is not rectifying – it involves inducing cell death, usually by apoptotically shutting down persistently ER stressed cells, which may be malfunctioning due to genetic errors, or infected by a virus which is co-opting the protein production machinery (Ron and Walter 2007). However, before these systems can be activated, the presence of a high load of protein must be detected. This detection is achieved by sensors facing the ER lumen wherein the load will first form, which can then send signals to effectors which transfer the unfolded protein signal to other parts of the cell. All eukaryotes have some kind of basic unfolded protein response, ranging from yeast with the most simple to the expanded systems of the higher eukaryotes.

Current opinion differs as to the mechanism by which these signals are detected and to the transmembrane effectors which transduce the signal into a response in eukaryotes. One model (Bertolotti 2000; Oikawa, Kimata et al. 2009) suggests that in an unstressed state where protein load is non-detrimental, BiP exists constitutively bound to the effector proteins. When the ER receives a high load of unfolded protein, as described earlier, these unfolded proteins will present many exposed hydrophobic residues to the ER lumen, some of which will sequester BiP from the effectors by competing for BiP's hydrophobic binding pocket with the sensors. This sequestering leaves areas of these proteins exposed, allowing them to aggregate and form oligomers, and be modified into their active forms. Artificial overexpression of BiP ensures there are sufficient levels to occupy all sites on the effectors and the unfolded protein load, and reverses this activation (Bertolotti 2000) However, a BiP dissociation-incompetent mutant was still capable of dimerising in yeast (Oikawa, Kimata et al. 2005; Ron and Walter 2007), indicating that this model may not completely account for the detection mechanisms. Another model (Credle, Finer-Moore et al. 2005) suggests that at least one of the transducers possesses an area in the ER facing domain which forms a structure similar to the peptide binding groove of the major histocompatibility complexes, (MHC) and therefore may be capable of directly binding unfolded protein peptides, and

sensing unfolded proteins in this manner, as mutations of residues facing into this domain impairs proper function of the transducer. However, this binding groove may not necessarily be accessible in all eukaryotes, and the residues in question may simply be necessary for oligomerisation (Zhou, Liu et al. 2006). It is also possible that a hybrid mechanism of the two systems may exist in yeast, with BiP dissociation as a primary response to low levels of ER stress followed by oligomerisation as a secondary and more consequential reaction in terms of downstream gene expression and apoptotic effects, to prolonged and severe unfolded protein loads (Pincus, Chevalier et al. 2010).

Figure 1.2 – Pathways of the unfolded protein response (from (Schroder 2008)).



1.2.1.3 Activation of the Unfolded Protein Response

The ER contains proteins whose primary function is to sense misfolding and instigate the expression of genes which alter the folding ability of the cell. It is these proteins which are responsible for the downstream effects that interference with ER homeostasis has upon gene expression, metabolism, apoptosis and intracellular signalling (Rutkowski and Kaufman 2004). The more complex the eukaryotic organism, the more complex the unfolded protein response it activates. Simple unicellular organisms such as the yeasts only express the most

highly conserved sensor, Ire1 (Nikawa and Yamashita 1992; Cox, Shamu et al. 1993; Mori, Ma et al. 1993; Tirasophon, Welihinda et al. 1998; Saloheimo, Valkonen et al. 2003; Guerfal, Ryckaert et al. 2010) and some of the salient points of its activation also appear to be conserved across eukaryotes, such as apparent clustering or formation of multimers for the second stage of activation (Korennykh, Egea et al. 2009; Li, Korennykh et al.). The simple multicellular organism *C. elegans* expresses a single isoform of each of three sensors, *ire-1*, *pek-1* and *atf-6* (Shen, Ellis et al. 2001; Calfon, Zeng et al. 2002; Shen, Ellis et al. 2005). Higher eukaryotes such as mammals diverge further, expressing distinct isoforms of IRE1, PERK and ATF6 with apparently differing expression patterns and roles, such as IRE1 α and β and ATF6 α and β (Bertolotti 2001). All three sensors share BiP as a negative regulator, which prevents oligomerisation in IRE1 (Bertolotti 2000; Okamura, Kimata et al. 2000), and translocation to the Golgi in ATF6 by masking the localization signals (Shen, Chen et al. 2002). Furthermore, IRE1 and PERK have interchangeable ER luminal domains, indicating they share a common mechanism of activation (Bertolotti 2000; Kohno). Each sensor induces a set of specific downstream cascades that together reduce the protein load upon, and increase the folding capacity of, the ER.

ATF6

ATF6 (activating transcription factor 6) in higher eukaryotes exists in two isoforms, α and β . ATF6 exists as an ER-localised glycosylated type II transmembrane protein 90kDa long (Haze, Yoshida et al. 1999). This precursor is retained in the ER lumen by interaction with BiP (Shen, Chen et al. 2002) until activation by contact with unfolded protein, or experimental overexpression, but not heat shock, (Yoshida, Haze et al. 1998) causes it to translocate to the Golgi complex. In the Golgi it is cleaved into a 50kDa proteolysed cytoplasmic active bZIP transcription factor by site 1 protease (S1P) and site 2 protease (S2P), proteases previously known to be involved in response to cholesterol deprivation (Sakai, Duncan et al. 1996). Of the two proteases, the cleavage event is dependent upon S2P but can proceed partially without S1P and requires the two processing motifs, RxxL and asparagine/proline (Ye, Rawson et al. 2000). The 50kDa domain is released by proteolysis which reveals a basic region which may function as a nuclear localization sequence (Haze, Okada et al. 2001). 50kDa ATF6 accumulates in the nucleus where it binds, with the general transcription factor NF-Y as a cofactor (Roy, Li et al. 1996) to the CCAAT and CCACG

sections of a CCAAT-N₉-CCACG element and a similar motif on its complementary sequence, the motif TGACGTG(G/A) (Wang, Shen et al. 2000), in the promoters of ER targets such as BiP/GRP78, GRP94, XBP-1 and calreticulin. This upregulates these genes to allow transcriptional alleviation of ER stress (Yoshida, Haze et al. 1998; Li, Baumeister et al. 2000). Via XBP-1, ATF6 and IRE1 activation are linked together to form a co-ordinated transcriptional response to ER stress (Lee, Tirasophon et al. 2002). ATF6 β is a similar glycosylated type II transmembrane protein, related to the cAMP response binding element, and with significant homology to, but slightly longer, than the α isoform at 110 kDa (Haze, Okada et al. 2001). It is cleaved in the same manner as the α isoform, into a 60kDa active form and may act in concert with it to activate ER stress response genes (Haze, Okada et al. 2001). However, it has a lower transcriptional activity than the α isoform and opinion differs as to whether this places it functionally in opposition to it, as the β isoform competes for binding sites may act as a repressor for ATF6 transcriptional induction of the α isoform either as a homodimer or heterodimerically (Thuerauf, Morrison et al. 2004). However, Yoshida et al find no alteration of ATF6 α responses in ATF6 β ^{-/-} mouse cells, contraindicating this (Yoshida, Okada et al. 2000). ATF6 turnover is approximately two hours, allowing it to quickly replenish itself after ER insult, although insult with tunicamycin logically results in an unglycosylated form (Haze, Yoshida et al. 1999). Glycosylation is particularly important to the function of ATF6 β , which possesses five N-linked glycosylation sites upon which its cleavage, activation and repressor effects depend. Unglycosylated β loses repressor effect, whereas unglycosylated α has enhanced activity, suggesting a role for ATF6 in sensing an overload of the post-translational modification systems of the endoplasmic reticulum (Guan, Wang et al. 2009).

PERK

PERK (PKR-like endoplasmic reticulum kinase) is an ER localised type I transmembrane ER-resident protein encoded for by the EIF2AK3 gene involved in translational control via phosphorylation of eIF-2 α (eukarotic initiation factor 2 α) (Shi, An et al. 1999). eIF-2 α facilitates translation in a GTP-dependent manner, by transferring Met-tRNA to the 40S ribosomal subunit, initiating translation, and hydrolyzing GTP to GDP, which causes the release of the eIF-2 α -GDP complex from the ribosome. eIF-2 α -GDP must then be reconverted to eIF-2 α -GTP, a function which is performed by eIF-2B.

Phosphorylation at serine 51, contained within a sequence highly conserved across eukaryotes, produces a non-functional form of eIF-2 α with a higher affinity for eIF-2B than the unphosphorylated. As peIF-2 α increases, it sequesters away the pool of available eIF-2B, preventing the resynthesis of eIF-2 α -GTP, and the formation of eIF-2 complexes which can initiate translation and induce the assembly of the 80s ribosome (de Haro, Mendez et al. 1996; Kimball 1999; Shi, An et al. 1999). Various eIF-2 α kinases exist which respond to cellular stresses by prevent translation in response to stimuli such as PKR (protein kinase R) which responds to viral double-stranded RNA by preventing translation (Thomis and Samuel 1992; Barber, Wambach et al. 1993) and HRI (heme-regulated eIF-2 α kinase) which reduces translation in response to heme to control protein production in developing erythroid cells (Chen and London 1995). PERK functions to couple this translational attenuation response with unfolded protein stress and to allow a direct shutoff of the causative protein load. PERK's different method of activation to that of the other eIF2 α kinases is marked by a divergent 550-residue flanking sequence (Shi, Vattem et al. 1998). PERK dimerises (Liu, Schroder et al. 2000) and becomes autophosphorylated in its kinase domain (Harding, Zhang et al. 1999) in response to unfolded protein. This activation is most likely triggered by dissociation of the GRP78/BiP chaperone from PERK's ER luminal domain, and this detection mechanism is so similar to that of IRE1a that their two luminal domains can be interchanged whilst retaining function, indicating conservation of endoplasmic reticulum detection function (Liu, Schroder et al. 2000). Once active, it phosphorylates eIF-2 α at serine 51 as described above. Downregulation of protein synthesis is a pro-survival response to unfolded protein stress, as it reduces the load of protein which requires processing by the ER. Therefore, PERK fulfils the function of an ER-resident mechanism for controlling protein synthesis, and its long half life (~13h) (Bertolotti 2000) allows continuous functioning. This is consistent with a translational response to long-lived ER stress as opposed to the transcriptional response to short-lived stress induced by ATF6. PERK is also capable of responding to hypoxic stress which can be induced by high loads of unfolded protein via activating transcription factor 4 (ATF4), a regulator of the unfolded protein response and nuclear factor 2 (Nrf2), an important factor in cellular response to hypoxia. In hypoxic conditions, PERK induces more efficient translation of mRNA coding for ATF4, which, like BiP and other genes necessary for hypoxic responses, does not suffer hypoxic downregulation. (Harding, Novoa et al. 2000; He, Gong et al. 2001; Koumenis, Naczki et al. 2002; Blais, Filipenko et al. 2004). ATF4 is then thought to form a leucine zipper dimer with Nrf2 to induce a host of cytoprotective proteins such as NAD(P)H quinone oxidoreductase 1

and glutathione S-transferases (Venugopal and Jaiswal 1996; Hayes, Chanas et al. 2000). Nrf2 deletion mutants exhibit decreased survival following ER stress insult, and *perk*^{-/-} cells have impaired Nrf2 nuclear import, indicating PERK's importance in this signalling pathway (Cullinan, Zhang et al. 2003). After ER stress has caused shutoff of general protein synthesis via eIF-2 α phosphorylation, it must be restarted again to begin coping with protein loads – this function is thought to be performed by Growth arrest and DNA damage-inducible protein 34 (GADD34), which appears to upregulate BiP and CHOP expression in a eIF-2 α independent manner in response to ER stress stimuli (Kojima, Takeuchi et al. 2003).

IRE1

Inositol requiring 1 (IRE1), like PERK is an ER localized transmembrane protein first discovered in yeast to be required for growth in the absence of inositol (Cox, Shamu et al. 1993; Mori, Ma et al. 1993) and possessing both a serine/threonine kinase domain and an RNase domain resembling that of RNase L (Tirasophon, Welihinda et al. 1998). It is the evolutionarily oldest endoplasmic reticulum stress sensor, existing in most eukaryotes from yeast to humans (but not some protozoans), and the only ER stress sensor in yeast. In eukaryotes, there are two IRE1 homologues, IRE1 α (Tirasophon, Welihinda et al. 1998), which is ubiquitous and required for embryogenesis (*irea*^{-/-} embryos die during gestation (Urano, Bertolotti et al. 2000)) required for protection against unfolded protein stress, and IRE1 β (Wang, Harding et al. 1998) which is localized to the gastrointestinal tract and protective against inflammatory bowel disease (Bertolotti 2000). The ER luminal domain of IRE1, thought to be responsible for detection of unfolded protein levels, possesses two specialized areas, a dimerisation domain (Zhou, Liu et al. 2006) and a peptide binding groove similar to that of the major histocompatibility complex (Credle, Finer-Moore et al. 2005). As with PERK, the kinase domain of IRE1 becomes autophosphorylated (Shamu and Walter 1996) after di- or oligomerisation (Korennykh, Egea et al. 2009). This activity may be responsible for IRE1's ability to induce apoptosis, as the cytoplasmic domain of IRE1 was found to bind to the TRAF domain of TRAF2. Once this binding has occurred TRAF2 then induces phosphorylation of c-Jun N-terminal kinase (JNK), resulting in the activation of this apoptotic pathway by an indirect mechanism involving coupling of plasma membrane receptors to JNK (Urano 2000). In mammals, the RNase domain of IRE1 is responsible for non-spliceosomal removal of a 26 base conserved intron from the mRNA of the bZip

transcription factor XBP-1, whose active protein product XBP-1(s) then induces the transcription of a variety of endoplasmic reticulum stress-related targets (see “XBP-1”, later) (Calton, Zeng et al. 2002). In yeast, this splicing is performed instead on the mRNA of the transcription factor Hac1p (Gonzalez, Sidrauski et al. 1999). The structure and function of IRE1 will be covered in more detail in section 1.3 of this introduction.

1.2.1.4 Alleviation of Endoplasmic Reticulum Stress

Once the high load of unfolded proteins has been detected and has caused the activation of one of the sensors PERK, IRE1 or ATF6, the message is then transduced by the downstream activities of these sensors. This response may be translational control, general suppression of translation by phosphorylation of eIF-2 α or increase of the translational targets of PERK such as ATF4, or it may be transcriptional, involving the upregulation of ER stress response genes by ATF6 and XBP-1 in response to IRE1 activation. These responses are protective, helping the cell deal with or at least reducing the unfolded protein load, but both PERK and IRE1 are also capable of inducing apoptotic responses via CHOP and JNK respectively – this inflammatory activity will be covered below in the section on the detrimental effects of the unfolded protein response. As opposed to yeast in which all unfolded protein responses are controlled by Ire1p, mammalian systems with their multiple sensors IRE1, PERK and ATF6 appear to have more redundancy. This may indicate in mammalian cells the IRE1 arm is specialised for protein output, (for example, in plasma cells) indicating the importance of this for industrial protein synthesis. Protective alleviation of endoplasmic reticulum stress can be performed using several mechanisms – activation of ERSE promoter-driven genes to increase the folding capacity of the cell, and endoplasmic reticulum associated degradation (ERAD) which targets excess proteins for degradation.

ERSE Promoters

ATF6 and XBP-1 are bZip transcription factors activated by the unfolded protein response to upregulate endoplasmic reticulum stress-induced genes. These make up the transcriptional response component of the unfolded protein response by binding to ERSE/URPE promoters, which are *cis*-acting elements located in the promoter regions upstream of UPR target genes, including chaperones such as BiP and ERAD components. In yeast, the unfolded protein response element (UPRE) is required for induction of the KAR2 gene which codes for Kar2p, the yeast homologue of the chaperone BiP (Mori, Sant et al. 1992; Kohno, Normington et al.

1993). The UPRE contains the consensus sequence (CAGCGTG), which is required for its function (Mori, Kawahara et al. 1996). In mammalian DNA multiple response elements (Wooden, Li et al. 1991) control the unfolded protein response; endoplasmic reticulum response element (ERSE) I and II, and the unfolded protein response element UPRE (Yamamoto, Sato et al. 2007). ERSE I and II function as binding sites for the bZIP domain of spliced XBP-1, causing transcription of genes involved in the response to ER stress, such as *GRP78*, *GRP94*, and *ERP72*. The ERSE element contains a consensus sequence CCAATN₉-CCACG, which is present in the promoters of and sufficient for the induction of GRP78/BiP, GRP94 and calreticulin, with the CCAAT component binding the general transcription factor NF-Y and the CCACG ATF6/XBP-1 and conferring specificity for the UPR (Roy and Lee 1995; Roy, Li et al. 1996; Yoshida, Haze et al. 1998). The UPRE element has a longer consensus sequence - TGACGTGG/A, and binds XBP-1 more strongly than ATF6. (Wang, Shen et al. 2000; Yoshida, Matsui et al. 2001; Yoshida, Matsui et al. 2003). The ERSE II element has the consensus sequence ATTGG-N-CCACG and was found in the *Herp* gene, (Kokame, Kato et al. 2001) and can bind both ATF6 in an NF-Y dependent manner and XBP-1 [Yamamoto2004].

XBP-1

XBP-1 (X-box binding protein 1) is a basic leucine zipper transcription factor first characterised in B cells (Liou, Boothby et al. 1990), which is a functional homologue of the yeast transcription factor Hac1p. In yeast, Hac1p mRNA is cleaved at two particular splice junctions by Ire1p and splices both sites independently, thus excising an intron. tRNA ligase then joins the 5' and 3' exon ends to form the spliced mRNA (Gonzalez, Sidrauski et al. 1999). The unspliced form of Hac1p mRNA cannot be translated due to internal base pairing (Ruegsegger, Leber et al. 2001), whereas the spliced form of Hac1p mRNA is translated more efficiently and may produce a more stable protein which is resistant to ubiquitin-dependent degradation (Cox and Walter 1996). Hac1p activation is required for activation of UPR target genes in yeast (Casagrande, Stern et al. 2000)

In mammalian cells, IRE1 performs a similar cleavage and intron removal upon the *XBP-1* mRNA, upon which activation of the UPR is dependent. A 26 nucleotide sequence is excised from the *XBP-1* mRNA (Calfon, Zeng et al. 2002). The predicted structure of the areas at the boundaries of the excised section forms two stem loops of seven base pairs, much

like the stem loop in the sequence which is cleaved in HAC1 (Calfon, Zeng et al. 2002). The sequences left when the 26bp are excised are predicted to form interactions with each other, thus closing the gap left by the excision. Removal of the intron causes a shift in the reading frame into the 3' UTR thus giving a protein 54KDa long instead of 33KDa (Calfon, Zeng et al. 2002). Both the spliced and unspliced variants of the mRNA are capable of producing a protein, the two proteins having differing C-termini, and the new terminus conferred upon the spliced variant allowing it to function as a transcription factor (Lee, Tirasophon et al. 2002). The basic leucine zipper domain and the transactivation domain of the spliced form are close enough to each other to allow functioning, without reducing the stability of the protein (Lee, Iwakoshi et al. 2003). Spliced XBP-1 is capable of activating a series of genes under the control of the endoplasmic reticulum response element with a far greater effect than the unspliced form (Iwakoshi, Lee et al. 2003; Yoshida, Matsui et al. 2003). Unlike in yeast, where the unspliced form of Hac1p mRNA is unable to produce a protein due to its secondary structure, (Ruegsegger, Leber et al. 2001) the unspliced form of *XBP-1* mRNA can be translated, but its protein product is expressed only at low levels in a cell undergoing ER stress (Lee, Iwakoshi et al. 2003). The unspliced isoform negatively regulates the spliced form by binding to it and sequestering it away from the nucleus and targeting it for degradation. (Yoshida, Oku et al. 2006). Induction by ATF6 (a similar basic leucine zipper protein with a transmembrane domain which is also required for the UPR) is also required to produce sufficient levels of the *XBP-1* mRNA to activate the unfolded protein response (Wang, Shen et al. 2000). These functions are conserved across eukaryotes – in *C. elegans*, where the excised intron from *xbp-1* mRNA is 23 bases long, silencing of the *xbp-1* gene abolishes the UPR [Shen2001] and the use of an interfering RNAi against the *xbp-1* gene, as with the *ire1* gene blocks expression and tunicamycin-induced upregulation of the *C. elegans* homologues of BiP, *hsp-3* and *hsp-4* (Calfon, Zeng et al. 2002).

ERAD

Another method in addition to the upregulation of chaperone foldases, which the cell can use to deal with ER stress due to a high protein load is ER-associated degradation (ERAD). This pathway utilises many of the same chaperone and ubiquitin conjugating, proteins, but instead of increasing the folding capacity of the endoplasmic reticulum, it aims to reduce the burden of unfolded or misfolded proteins by recognising these proteins and causing them to be targeted for degradation (Vashist and Ng 2004). Lectins such as Yos9p and lectin-like

chaperones such as calnexin and calreticulin play a role in this recognition, as does BiP. Proteins such as Der1p and Sec61p may remove misfolded proteins from the ER by forming pores, and target them for destruction by polyubiquitylation of their lysine residues (Kincaid and Cooper 2007). A third model suggests that a transcription factor, CREB-H can gauge the functioning of the unfolded protein degradation machinery by acting as a suicide probe, being cleaved during ER stress into a form which can affect transcription (Bailey, Barreca et al. 2007). EDEM, an ER mannosidase causes proteasomal degradation of misfolded proteins (Yoshida, Matsui et al. 2003).

1.3. IRE1: Structure and Function

Having illustrated the roles and significance of the arms of the unfolded protein response, and their relation to industrial protein biosynthesis, particularly in the areas of secretion, protein throughput and apoptosis, this introduction will now focus on one particular area of the unfolded protein response, the most evolutionarily ancient one – the IRE1 axis, in particular how its structure, component parts, macromolecular behaviour, and function relate to its downstream effects.

Mammalian IRE1 is a type 1 transmembrane serine/threonine protein kinase (Tirasophon, Welihinda et al. 1998). The yeast orthologue, Ire1p was sequenced by Nikawa and Yamashita in 1992 (Nikawa and Yamashita 1992), who discovered the gene for a membrane spanning protein with similarity to protein kinases (Hanks, Quinn et al. 1988) while studying myo-inositol yeast auxotrophs, and found that it was required for inositol prototrophy. Cox and Shamu (Cox, Shamu et al. 1993) elucidated its function and link to the unfolded protein response whilst screening for the effector that triggered the activation of the unfolded protein response element to upregulate BiP and PDI. They found that rapid cell death occurred on treatment with β -mercaptoethanol or tunicamycin, both ER-stress inducers in *ire1 Δ* mutants. Ire1p is a necessary component of the unfolded protein response in this organism, sensing the levels of unfolded protein induced stress in the lumen of the endoplasmic reticulum and transmitting this information to the nucleus in a kinase activity-dependent manner, by way of the cleavage of an intron from the mRNA encoding the protein Hac1p (Mori, Sant et al. 1992; Cox and Walter 1996) in a unusual non-spliceosomal fashion similar to pre t-RNA splicing (Gonzalez, Sidrauski et al. 1999). This increases the levels of Hac1p, a transcription factor

which binds to a regulatory sequence in the promoters of genes coding for ER resident proteins known as the UPRE (unfolded protein response element). Human IRE1 was cloned using degenerate oligonucleotide primers based upon the highly conserved kinase VII subdomain from *S. cerevisiae* to screen for a human homolog of the Ire1p gene (Tirasophon, Welihinda et al. 1998). This homolog was found by Northern blot to be ubiquitously expressed in many human tissues and by generation of mutants in the putative kinase domain and mRNA studies using *S. cerevisiae* derived Hac1p mRNA, to have both kinase and endonuclease activity, in common with its *S. cerevisiae* homolog. Loss of kinase activity was found to result in a blocking or reduction in the unfolded protein response, however a loss of endonuclease activity induced by point mutation in the RNAase domain was not found to induce a concurrent loss of kinase activity (Tirasophon, Welihinda et al. 1998).

1.3.1 Isoforms

Two genes coding for two human IRE1 proteins exist, IRE1 α which is expressed ubiquitously, and IRE1 β , which is localised to the highly secreting epithelial cells of the gastro-intestinal tract. *ire1 β ^{-/-}* mice were found to be more susceptible to inflammatory bowel disease induced by dextran sodium sulphate (Bertolotti 2001) indicating a role for IRE1 β in inflammatory signalling. IRE1 β 's cleavage effects on RNAs appear to overlap, but not match with IRE1 α 's. Both isoforms are capable of splicing *XBP-1* mRNA, and both are capable of upregulating BiP (Tirasophon 2000; Bertolotti 2001) but IRE1 α 's other targets include particular endoplasmic reticulum-located mRNAs such as biogenesis of lysosome-related organelles complex-1, subunit 1 (Blos1), and scavenger receptor class A, member 3 (Scara3) (Hollien and Weissman 2006; Hollien, Lin et al. 2009) indicating that IRE1 α 's activities appear to remain firmly associated directly with the endoplasmic reticulum stress responses. IRE1 β however, is a little more promiscuous in function – among its effects are translational repression of by cleaving the 28s ribosomal RNA (Iwawaki, Hosoda et al. 2001) and although IRE1 β shares an ability to downregulate expression levels of some ER-localised mRNAs, this function does not appear to be dependent upon 28s ribosome cleavage (Nakamura, Tsuru et al. 2010). Logically given IRE1 β 's localisation in gastrointestinal tract cells, and given the effect of lipotoxicity and overnutrition on IRE1 signalling, it also appears to play some role in regulating fat transport by decreasing levels of microsomal triglyceride transfer protein mRNA, which contributes to the assembly of dietary-fat transporting chylomicrons. These divergent functions may account for some of the two IRE1 isoforms apparently opposing

effects – in *Xenopus laevis* embryos loss of IRE1 β was detrimental to mesoderm formation, whereas loss of the IRE1 α -XBP-1 pathway appears to promote it (Yuan, Cao et al. 2008).

1.3.2 Domain Structures

IRE1 is an unusual protein in that it has both functional kinase and endoribonuclease activities within the same cytosolic effector domain, and it is this compartmentalised structure that contributes to its divergent effects and therefore its usefulness as the target of investigation into the possibility of using the endoplasmic reticulum stress responses to improve biopharmaceutical production levels. The structure of IRE1 comprises the following: an ER luminal domain on the N-terminus, responsible for sensing ER stress (Credle, Finer-Moore et al. 2005; Zhou, Liu et al. 2006); a transmembrane domain, and a protein kinase/endoribonuclease domain thought to be located in the cytosol (Lee 2008). This section will discuss the particular structures of each part of the IRE1 protein and how they contribute to the functions of the protein as a whole.

Figure 1.3 – One potential ribbon structure of the N-luminal/N-terminal and cytosolic/C-terminal domains of human IRE1, from Zhou et al (Zhou, Liu et al. 2006) and Lee et al (Lee 2008) respectively showing two monomers interfaced together. The C-terminal ends of the two monomers of the N-luminal domains (top) would connect to the transmembrane sections of the monomers (red lines). From this point they would connect with the top of the cytosolic domains (bottom). ADP is shown bound to the kinase domain.

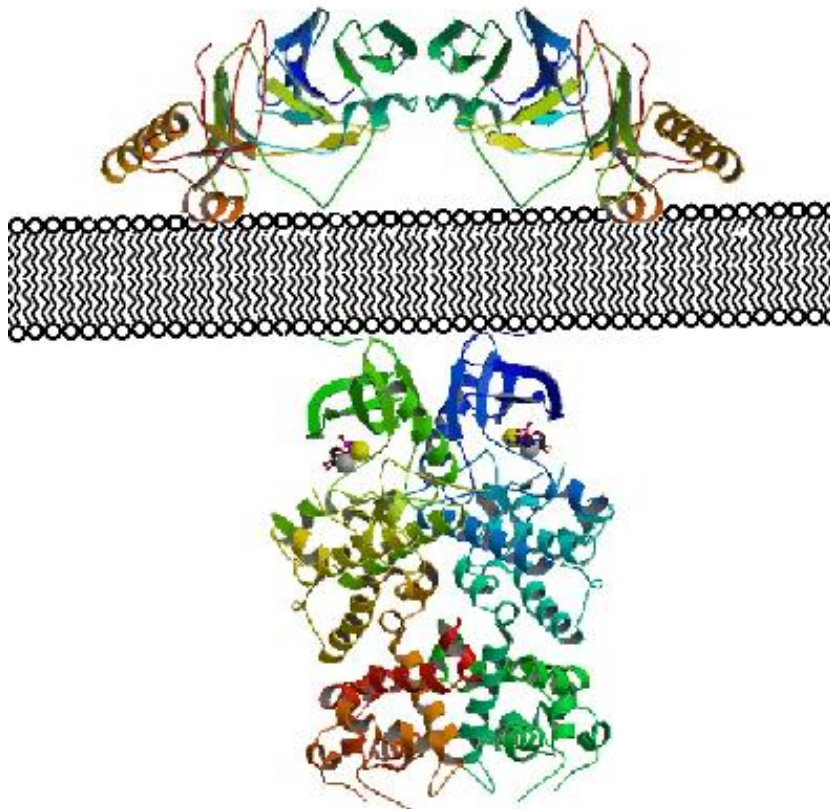
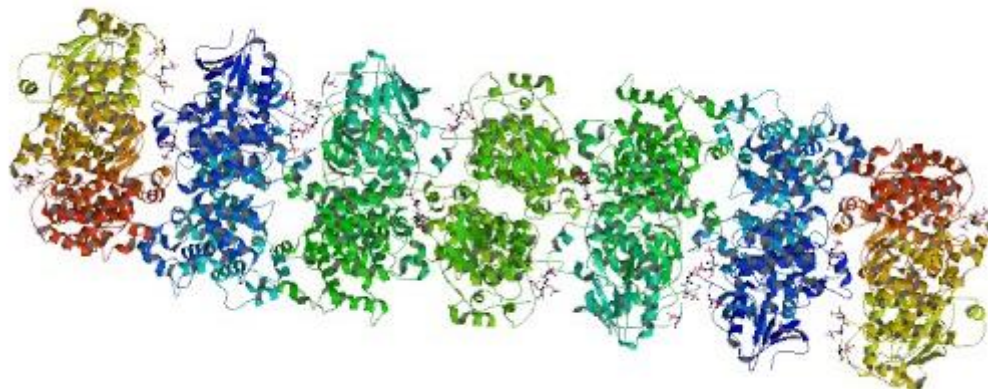


Figure 1.4 – Oligomerised IRE1 multimer structure from (Korennykh, Egea et al. 2009). In this structure, rather than spanning the membrane, multiple IRE1 units assemble with their RNase domains facing outwards.



1.3.2.1 Luminal Domain

The luminal domain of IRE1 functions as its sensor of the presence of unfolded proteins – the precise mechanisms by which the luminal domain transmits a signal to the effector cytoplasmic domains is uncertain – this will be covered in more detail in the following section 1.3.3 “Clustering and Activation Mechanisms”. The luminal domains of IRE1 α and β bear structural resemblance to the Activin/TGF- β serine-threonine kinases (Hanks and Hunter 1995) and functional resemblance to receptor tyrosine kinases, although unlike tyrosine kinases they have no known endogenous small molecule ligand. There appears to be considerable function conservation cross-species in the luminal domains of the of the IRE1 – domains from *C. elegans ire1*, human IRE1 α and murine IRE1 β can each be combined in chimera with the yeast cytoplasmic domain to produce functional unfolded protein response signalling transducers (Liu, Li et al. 2005). The structures of the luminal domain give indications as to how it detects unfolded proteins, but no clear answer as to how, or to what extent these structure contribute to function. Di/oligomerisation of the luminal domains appears to occur in response to dissociation of BiP (Bertolotti 2000) and at a dimerisation interface whose structure, hydrogen bonding and hydrophobic interactions are shared by PERK. A conserved area in the luminal domain of IRE1 is required for this di/oligomerisation, particularly lysine and aspartate residues (K121 and D123 in IRE1-alpha) which if mutated, will disrupt hydrogen bonding within the beta sheets which form the interface (Zhou, Liu et al. 2006). At the dimerisation interface, a central groove is formed roughly resembling that of the antigen binding domains of the major histocompatibility complexes. The groove is formed of α -helices mounted on a triangular β -sheet floor (Credle, Finer-Moore et al. 2005; Zhou, Liu et al. 2006) and contains conserved amino acid side-chains required to contribute to induction of the UPR – binding of unfolded protein to this groove was proposed to cause an alteration in the orientation of the IRE1 dimer which activates its cytoplasmic functions (Credle, Finer-Moore et al. 2005; Zhou, Liu et al. 2006). However, the association of unfolded protein is unlikely to be the sole activator in human IRE1, for several reasons:

- 1) Purified luminal domain forms dimers *in vitro* in the absence of unfolded protein.
- 2) The MHC-like groove is narrower in the human IRE1 isoform than in the yeast, reducing the likelihood of peptide binding. α -helices in the groove contain glutamine residues which span the groove stabilising the dimerisation interface to the detriment of peptide access to it.

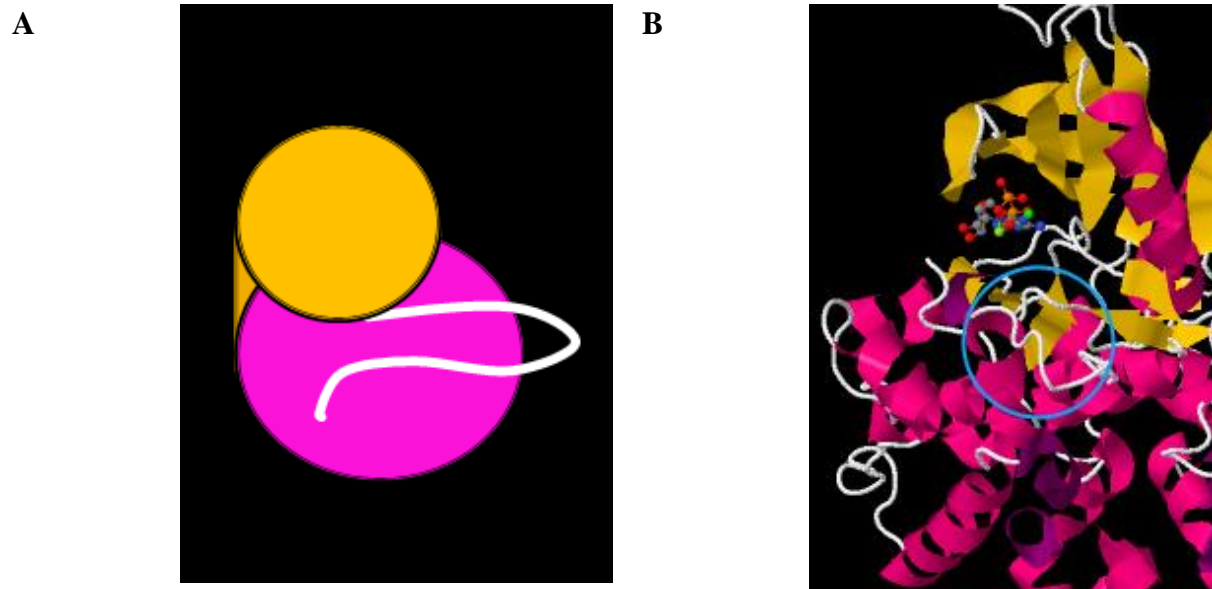
- 3) The orientation of the dimer in the ER membrane is unsuitable for the formation of peptide-IRE1 oligomers (Zhou, Liu et al. 2006).

Given the complex kinetics of interaction between BiP and IRE1 (Pincus, Chevalier et al. 2010) it is more likely that a complex interaction of unfolded protein, BiP association and disassociation with both unfolded protein and IRE1, and auto-dimerisation/ oligomerisation of IRE1 contribute to the picture of mammalian unfolded protein detection under different conditions, and that yeast mechanisms may differ from those of higher eukaryotes.

1.3.2.2 Kinase Domain

The kinase domain of IRE1 is thought to be both a direct functional effector, activating its downstream apoptotic functions, (Urano 2000) and a facilitator for the conformational changes that induce activity of the RNase domain (Sidrauski and Walter 1997). IRE1's activation loop and structural features conform to those of a transmembrane serine/threonine kinase, but it has no known close relatives among the kinases (Hanks, Quinn et al. 1988; Hanks and Hunter 1995). Ire1 is an atypical kinase in more than structure. Currently the only known target of IRE1's phosphorylation is itself. Activation of the kinase domain is dependent upon autophosphorylation of associated IRE1 multimers (Shamu and Walter 1996; Papa, C. et al. 2003). Single IRE1 kinase domains consist of a bilobal fold typical of the protein kinases comprised of an N-terminal lobe and a larger C-terminal lobe with the activation loop flexibly sited in the groove between the two (See Figure 1.5). The N-terminal lobe of IRE1 comprises a twisted 5-strand anti-parallel beta sheet (orange, top of panel B) flanked by a single alpha helix (pink, top right of panel B). The C-lobe consists of two paired beta strands and eleven alpha helices (Lee, Scapa et al. 2008).

Figure 1.5 – A) Simplified protein kinase structure (after (Huse and Kuriyan 2002)) B) Structure of IRE1 kinase domain from PDB entry for (Lee, Scapa et al. 2008), IRE1 with ADP situated in nucleotide pocket. N-terminal lobe (upper section), C-terminal lobe (lower section), Activation loop (circled).

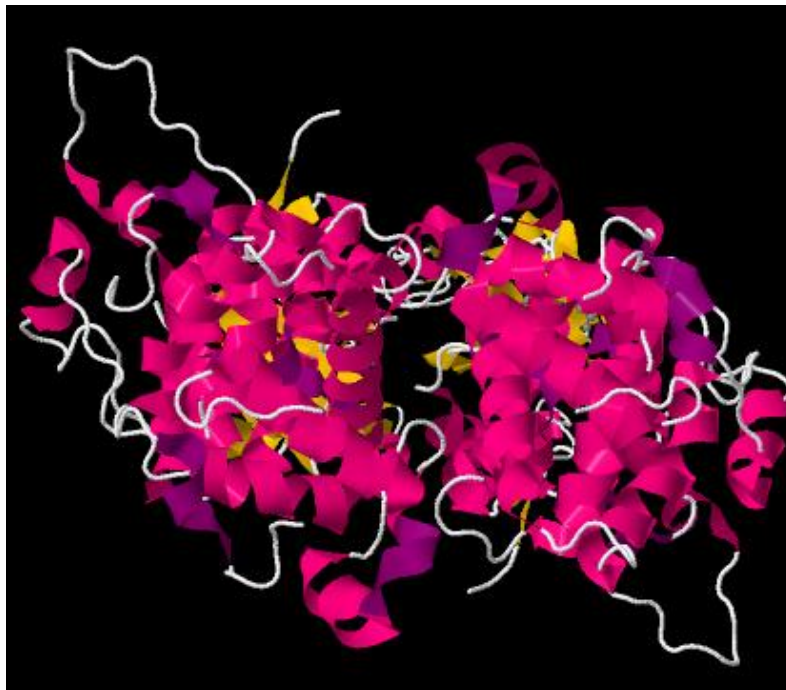


Dimerisation of IRE1 is thought to be induced by bound adenine nucleotides causing a conformational change which activates the RNase domain (Sidrauski and Walter 1997; Lee 2008). The precise nature of the conformational changes is as yet unknown. Crystal structures have been produced indicating at least two conformations, an early “face to face” dephosphorylated conformation of kinase domains that would permit trans-autophosphorylation (Ali, Bagratuni et al. 2011) and a “back to back” conformation in which dimerisation interfaces are aligned forming an active dimeric RNase domain capable of binding XBP-1 mRNA (Lee, Scapa et al. 2008). The fine structure of the IRE1 kinase pocket itself will be covered in more detail in the section below “The IRE1 Kinase Pocket”

1.3.2.3 RNase Domain

The RNase domain of IRE1 confers upon the protein its main marker of function – XBP-1 splicing (Calfon, Zeng et al. 2002). It is a 132 residue globular domain located C-terminally from the kinase domain (Lee, Scapa et al. 2008) and thought to be located in the cytosol in order to access the *XBP-1* mRNAs which preferentially locate there (Uemura, Oku et al. 2009). The RNase domain consists of eight alpha helices, and is highly ordered in crystal structure apart from a short sequence (residue 1036-1041 in (Lee, Scapa et al. 2008)) between helices 3 and 4. The domain is held in a set orientation against the C-lobe of the kinase domain by a set of hydrophobic residues, and a dimerisation interface permits the formation of dimers forming a surface suitable for mRNA binding.

Figure 1.6 - RNase domain of IRE1 showing C-terminal nuclease/mRNA binding surface (Lee, Scapa et al. 2008).



The RNase domain of IRE1 (Figure 1.6) shares close homology with RNaseL, a component of the interferon response to viral infection which degrades single-stranded RNA in response to viral infection at UU and UA nucleotides and inhibits viral protein synthesis (Tirasophon 2000). Like IRE1's change in response to unfolded protein/kinase activation, RNase L undergoes a conformational change in response to activation by the antiviral 2',5'-

oligoadenylate (2-5A) system, which permits interaction with eukaryotic polypeptide chain release factor 3 (eRF3) and localises RNaseL to the mRNA target (Floyd-Smith, Slattery et al. 1981; Bisbal and Silverman 2007). Both proteins also require dimerisation to be activated (Dong and Silverman 1995; Shamu and Walter 1996), but RNaseL has no protein kinase activity (Floyd-Smith, Slattery et al. 1981), however, like IRE1, its RNase function is dependent upon the structural support of the kinase domain between its N-terminal ligand sensor and effector domain (Dong, Xu et al. 1994; Lee 2008). An analysis of the protein sequence of human IRE1 α using the NCBI conserved domains database also reveals similarity of its RNase domain to the PUB/PUG domain (<http://www.ncbi.nlm.nih.gov/Structure/cdd/cdd.shtml>). The PUB/PUG domain is a sequence motif in the N-terminal region of the yeast protein Png1p, a cytoplasmic peptide:N-glycanase which may be involved in proteasomal degradation of misfolded glycoproteins exported to the cytoplasm. The proteasomal domain is predicted to have four alpha helices and be highly conserved, and contain a UBA or UBX domain, present in many enzymes within the ubiquitin degradation pathway (Doerks, Copley et al. 2002; Suzuki and Lennarz 2003). This homology may indicate common ancestral proteins involved in several arms of the unfolded protein response. Although IRE1 has no endogenous small molecule ligand activator, pharmacological agents have been found which modify its activity. The flavonol quercetin can bind in the dimer interface of the RNase domain to act as an agonist and a cofactor for ADP binding on activation (Wiseman, Zhang et al. 2010). Antagonists of IRE1 activation include a range of salicylaldehyde analogs such as 3-ethoxy-5,6-dibromosalicylaldehyde which inhibited cleavage of XBP-1 stem-loop RNase. The salicylaldehyde analogues were selective for IRE1 with no effect on RNaseL, indicating the diversity of activation between the two related proteins (Volkman, Lucas et al. 2011).

1.3.3 Clustering and Activation Mechanisms

The precise nature of activation of IRE1 and the nature of the relationship between domain structures, conformational changes, and interactions with other effectors is still uncertain – this section will deal with current knowledge regarding the mechanisms of IRE1 activation in response to unfolded protein.

Interaction with BiP

The interaction between IRE1 and BiP is known to be a major contributory factor to the induction of response to unfolded protein stress (Bertolotti 2000), as upregulation of BiP is one of the earliest responses to ER stress. GRP78, also known as BiP (heavy chain binding protein), an Hsp70-like chaperone, was identified early on as being upregulated in response to the presence of unfolded protein (Kohno, Normington et al. 1993). In its ADP bound state it has a high affinity for unfolded protein and a low affinity when bound to ATP. ATP hydrolysis therefore results in a switch to the high affinity state. BiP then binds to unfolded or misfolded proteins, stabilising and helping them achieve the correct conformation (Wei and Hendershot 1995). The BiP binding/dissociation does not appear to be an absolute requirement for IRE1 activation in yeast – the BiP binding site is not located in the regions of the luminal domain of yeast IRE1 upon which activation is dependent. Deletion of the BiP binding site hypersensitised yeast IRE1 to ethanol and temperature stress whilst leaving its ER stress responses inactive (Kimata, Oikawa et al. 2004). Mammalian IRE1, however, becomes “leaky”, displaying increased basal activation and overexpression, with its BiP binding site deleted (Oikawa, Kimata et al. 2009). It is likely therefore that the activation of mammalian IRE1 requires a complex dynamic interaction between BiP, and the different states of the IRE1 monomer/multimer complexes, with BiP binding to IRE1 providing a buffer insulating IRE1 from activating immediately in the presence of unfolded protein, and deactivating it rapidly when unfolded protein levels fall again, thus modulating the activity of IRE1 to when unfolded protein levels are high enough to require it (Pincus, Chevalier et al. 2010).

Interaction with Unfolded Protein

Based upon the dynamics of interaction and response of IRE1 to the removal of BiP binding sites activation of mammalian IRE1 could therefore be considered mainly BiP-dependent and activation of yeast unfolded protein/ligand dependent (Liu, Schroder et al. 2000). The differences between the protein accessible (yeast) and glutamine-blocked (mammalian) (Zhou, Liu et al. 2006). MHC-like peptide binding groove would also indicate a greater role for direct activation by unfolded protein. Binding studies using the ER luminal domain of yeast IRE1 appear to confirm this, indicating preferential binding of the luminal area to

peptides with basic and hydrophobic residues, activation upon peptide binding, and loss of activation when amino acids within the peptide binding groove were mutated (Gardner and Walter 2011).

Clustering

Trans-autophosphorylation of IRE1 is required for activation (Shamu and Walter 1996), indicating that some degree of interaction between IRE1 monomers is a requirement for triggering the unfolded protein response via IRE1. Elucidation of the crystal structure and mutational analyses revealed the following characteristics of the N-terminus: IRE1 must at least dimerise, if not oligomerise, (Kimata, Ishiwata-Kimata et al. 2007; Korennykh, Egea et al. 2009) Dimerisation then may site the opposing kinase sites of each IRE1 monomer in a position suitable for trans-autophosphorylation, causing a conformational change whose mechanism is not yet fully understood in the enzyme which shifts the position of the C-terminal lobe and places the nucleotide binding loop in a position to allow mRNA binding. However, the extent and complexity of the interactions required appears to go beyond simple dimerisation. In a radiolabelled *XBPI*-like substrate assay on mammalian IRE1, cleavage of the substrate mRNA displayed a Hill co-efficient of 3.4, indicating the formation of tetramers or larger species to initiate XBP-1 splicing, and ultracentrifugation of activated IRE1 indicates multimers of a size consistent with formation of oct- and decamers (Li, Korennykh et al. 2010). Under conditions of ER stress in association with unfolded protein, yeast IRE1 can be visualised by immunofluorescence microscopy forming visible puncta, which associate and disassociate quickly in wild-type IRE1, a phenomenon that would not be detectable with simple dimerisation. These puncta occur even in kinase-dead (K702A) mutants, indicating clustering occurs pre- or during autophosphorylation, and post-BiP dissociation, placing the clustering shortly after initial ER stress detection (Kimata, Ishiwata-Kimata et al. 2007). Preventing of this clustering by altering the IRE1 dimerisation interface, for example by mutation of a lysine (K121) to a larger tyrosine residue in the luminal interface attenuates splicing and also prevents foci clustering after two hours of ER stress induction with tunicamycin (Li, Korennykh et al. 2010) and reduces UPR signalling at the centres formed by the clustering, preventing recruitment of Hac1 to Ire1 (Aragon, van Anken et al. 2009). The crystal structure of clustered yeast IRE1 indicates the formation of a helical rod comprised of 14 molecules of IRE1 per helical turn. This structure exhibits outward-facing RNase domains competent for Hac1 binding (Korennykh, Egea et al. 2009). An alternative

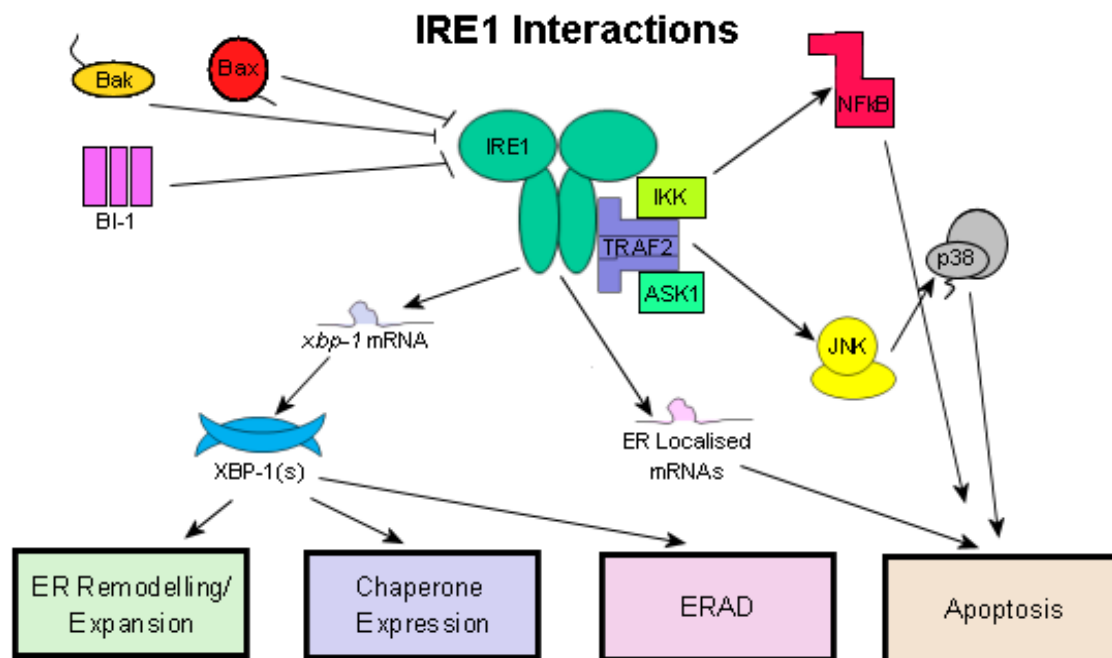
crystal structure of human IRE1 (Figure 1.4) bound to ADP exhibits a potential earlier intermediate form of the multimer – a “face-to-face” orientation where the activation loop of kinase domains are in proximity to each other potentially permitting autophosphorylation – when the nucleotide binds, the interaction between the monomers of IRE1 is strengthened, allowing the activation loops to be accessed for phosphorylation. Conformational changes forming a β -sheet within the helices of the kinase domain then allow shift to the “back-to-back” conformation which permits RNase domains to be sited in a manner competent for splicing (Ali, Bagratuni et al. 2011).

Activation/Deactivation

If activation mechanisms differ between yeast and mammalian systems, then it appears that the mechanisms of activation downstream of this are similar across the eukaryotes : ER stress causes oligomerisation of IRE1, mediated by the peptide-binding structures of the luminal domain in yeast, in the plane of the ER membrane which sites IRE1 in a manner that permits trans-autophosphorylation and the onset of RNase activity. In conditions of prolonged stress in HEK293 cells, however, IRE1 appears to become incapacitated, possibly to bias against the activation of apoptotic cascades(Lin, Li et al. 2007; Li, Korennykh et al. 2010), even if the stress has not been relieved. This incapacitation is characterized by dissociation of clustering over the 6-8 hours after stress induction, dephosphorylation beginning at four hours and declining at six and reductions in *XBP-1* splicing correlating with the de-clustering(Li, Korennykh et al. 2010). This deactivation could be considered a natural consequence of the formation of multimers - once free IRE1 molecules have been trapped within the higher-order structures, they lose the steric freedom to activate and de-activate – as the structures increase in size, so the number of IRE1 monomers that are removed from the free pool increases(Pincus, Chevalier et al. 2010). The deactivation mechanism may be mediated by a fully functioning kinase domain. In yeast, a kinase defective IRE1 mutant showed an inability to properly deactivate in a reporter assay, accumulating the reporter product long after the wild type had deactivated , causing continuous ER stress and impairing cell survival(Rubio, Pincus et al. 2011). Phosphorylation and de-phosphorylation then are likely to be required for both assembly and disassembly of the IRE1 multimer and therefore homeostatic adaptation to ER stress.

1.3.4 Downstream Effects

Figure 1.7 – IRE1 interactions and resultant downstream effects. Outcomes to the left of the diagram are survival oriented, to the right favour apoptosis.



Under normal levels of ER stress, IRE1 protects the cell and ensures survival by halting transcription, upregulating the expression of proteins which will help it deal with the increased protein load and the ER stress that follows, activating the genes that increase its capacity to fold proteins, or to remove misfolded proteins and thus preventing the build-up of toxic reactive oxygen species produced during disulphide bond formation and reducing unfolded proteins with exposed residues and other harmful side effects of high unprocessed protein levels (Figure 1.7, left-hand side). Since ER stress occurs within the compartment of the ER membrane and upregulating of the necessary genes must occur in the nucleus, IRE1 is required to transduce the signal of ER stress from one to the other. Human IRE1 performs this function via downstream signalling and the upregulation of XBP-1, which then triggers activation of the endoplasmic reticulum stress response element (ERSE) promoter, which alters the expression of folding machinery such as foldases and chaperone proteins. However, under extended ER stress, IRE1's signalling activity switches to more detrimental downstream effects – effecting a general translational downregulation by degrading ER-

located mRNAs, and triggering apoptosis via the JNK pathways (Figure 1.7, right-hand side).

IRE1 Dependent mRNA Decay

Part of the unfolded protein response involves the control of translational throughput in order to alleviate the protein load upon the ER. Although in higher eukaryotes the PERK pathway can regulate translation via control of phospho-eIF2 α , this results in a generalised downregulation of translation, rather than a targeted ER downregulation. There is a potential role then for an ER targeted translational downregulation. Both IRE1 α and beta isoforms have been seen to exhibit effects on targets other than the classic XBP-1 splicing pathway – IRE1 α controls its own mRNA levels in response to overexpression (Tirasophon 2000), can reduce levels of protectin/complement defense 59 (Oikawa, Tokuda et al. 2007) and regulate levels of insulin mRNA (Lipson, Ghosh et al. 2008). IRE1 β also controls levels of the microsomal triglyceride transfer protein (Iqbal, Dai et al. 2008). Furthermore, in insect cells IRE1 was found to degrade particular ER localised mRNAs associated with particularly complex folding products (Hollien and Weissman 2006), results which were then confirmed in mammalian fibroblasts. This IRE1 dependent mRNA decay may clear ribosomes ready to produce UPR proteins to alleviate stress, and appears to be more pronounced in the insect over mammalian cell (Hollien, Lin et al. 2009). It is dependent upon the presence of the RNase domain, and kinase activity independent suggesting a similar mechanism to that of XBP-1 splicing via the dimerised RNase surface (Hollien, Lin et al. 2009). Conversely, Han et al suggest that pharmacological activation of XBP-1 splicing by kinase inhibitors that prevent autophosphorylation could push the activity of IRE1 towards the XBP-1 splicing rather than the mRNA decay pathway, indicating that there is a role of kinase activity in regulating the switch between these two outcomes (Han, Lerner et al. 2009).

IRE1 Dependent Apoptosis

As has been shown, IRE1 is capable of activating the protective arm of the unfolded protein response and increasing the ER output of proteins. When the levels of unfolded and misfolded protein and the damage from reactive oxygen species generated during the formation of disulphide bonds become too high for the cell to safely deal with, components of the UPR can respond appropriately; IRE1 may bring about cell injuring and cell death responses via pro-apoptotic proteins such as JNK and CHOP, (Schroeder 2008) a 19 kDa,

pro-apoptotic transcription factor normally induced under conditions of stress such as glucose starvation (Carlson, Fawcett et al. 1993). Within the unfolded protein response, CHOP initiates cell death responses to overloading of the endoplasmic reticulum, (Wang, Harding et al. 1998). One of the earliest proteins in the apoptotic pathway of IRE1 is TRAF2 (TNF Receptor Associated Factor 2), normally associated with the transduction of cytokine signals from membranes to the activation of JNK. TRAF2 consists of an N-terminal ring finger domain, a section of five zinc finger domains (the central intermediate domain), and a highly conserved TRAF domain at the C-terminal end, common to all TRAF proteins. JNK activation by TRAF2 can be induced by IRE1 when TRAF2 interacts with IRE1. TRAF2 binds to the cytosolic domain of IRE1 (Urano 2000). This allows TRAF2 to form a signalling complex with IKK, (I- κ B kinase complex) a complex consisting of a heteromer of IKK1 and IKK2; and ASK1 (apoptosis signal-regulating kinase), a MAP3 kinase, leading to MKK4 and 7 phosphorylating JNK and MKK3 and 6 to activate the p38 signalling cascade. JNK (c-Jun N-terminal kinase), is activated by phosphorylation of tyrosine and threonine residues in its activation loop, which allows it to activate transcription factors by phosphorylation of their activation domains. This action allows the upregulation of genes involved in apoptosis. JNK also causes the release of apoptotic proteins such as BIM from the cytoskeleton (Lei and Davis 2003). The Bax/Bak type pro- apoptotic proteins have a both a direct effect upon IRE1 function, and an indirect one via their regulatory effect on intracellular calcium. The pro-apoptotic proteins BAX and BAK control ER calcium levels which will induce the unfolded protein response when perturbed (Wajant 2003). These proteins have been shown to associate directly with IRE1 to modulate the UPR – mice lacking both BAX and BAK were particularly vulnerable to tunicamycin treatment and had reduced XBP-1 levels/expression of XBP-1 target genes. (Hetz 2006). Bax Inhibitor -1 (BI-1) (Xu and Reed 1998) , an inhibitor of Bax-induced apoptosis also inhibits XBP-1 splicing by suppressing IRE1 activity (Lisbona, Rojas-Rivera et al. 2009).

In addition to its apoptotic effects, JNK is capable of mediating insulin resistance via phosphorylation of IRS-1 (insulin reception substrate) at serine 307, which prevents tyrosine phosphorylation by the activated insulin receptor of this protein (Hirosumi, Tuncman et al. 2002). Phosphorylated IRS initiates the phosphatidylinositol 3-kinase pathway (PI3K), which activates Akt and causes PI3K to be translocated to the plasma membrane, where it increases glucose transport and levels of the glucose transporting protein GLUT4 (Chang, Chiang et al. 2004). Glucose transport stimulates glucose metabolism and glycogen synthesis. p38 is a mitogen activated protein kinase (MAPK) which is activated by the phosphorylation of

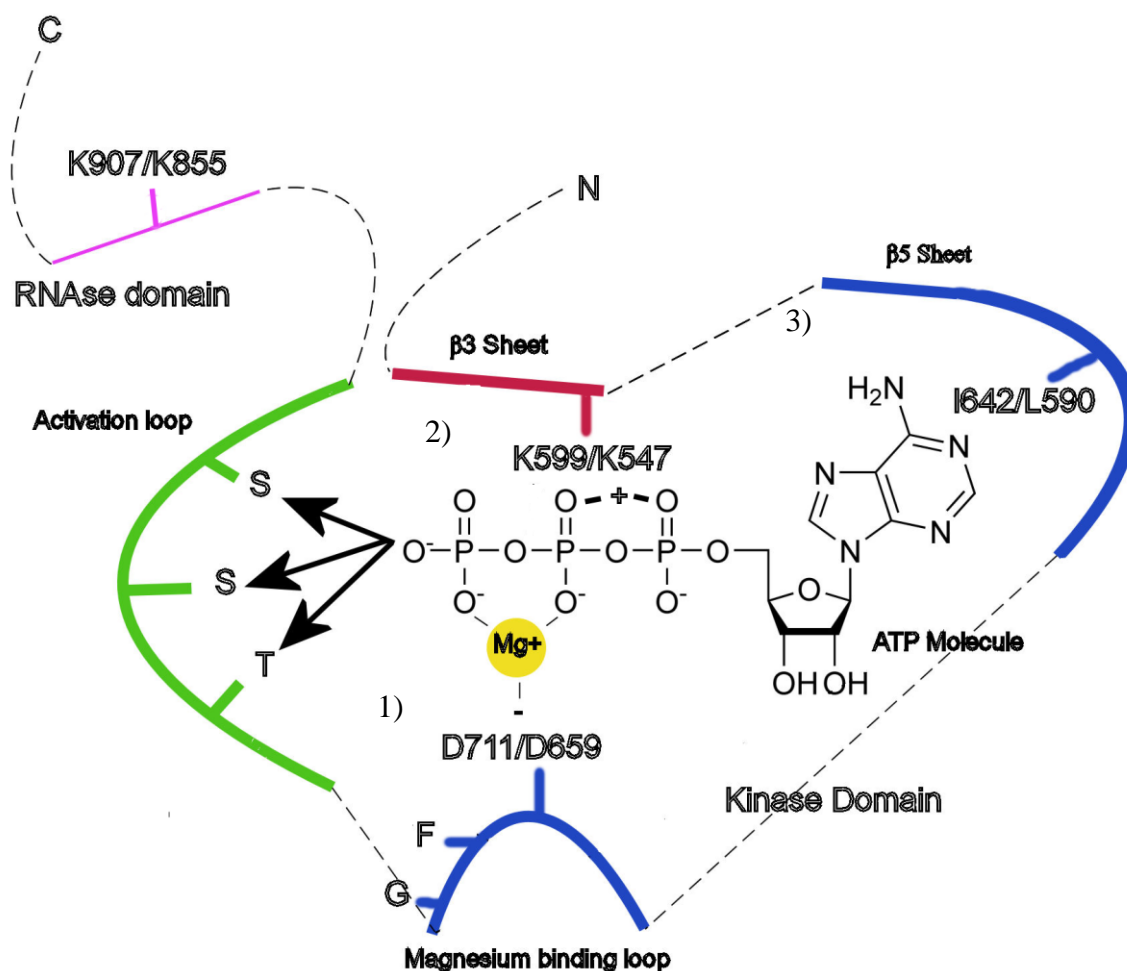
tyrosine and threonine residues and induces the transcription of apoptotic genes in a similar way to JNK. The TRAF2-ASK1-IKK complex also induces serine phosphorylation, ubiquitinylation and degradation by the proteasome of I κ B releasing Nuclear factor kappa B (NF- κ B), which is then capable of translocating to the nucleus and inducing apoptosis and inflammation. This pathway can also be activated by PERK via eIF2 α . IRE1-induced JNK signalling is also involved in insulin resistance and type II diabetes. Changes in glucose uptake and lipidaemia associated with overnutrition, obesity and a lack of exercise result in ER stress which then causes JNK to mediate insulin resistance, resulting in impaired glucose homeostasis and insulin signalling. Furthermore, the IRE1 JNK axis was found to be the transducer of ER-stress induced autophagy in neuroblastoma cells, and cells with impaired autophagic responses were more vulnerable to ER stress, indicating a role for autophagy upregulation in response to a requirement for degradation of unfolded protein (Ogata, Hino et al. 2006). In mammalian cells, the very presence of IRE1 appears to be cytoprotective – artificially extended IRE1 signalling prolonged survival of cells, counteracting the detrimental effect of PERK signalling that normally persists after IRE1 has been inactivated (Lin, Li et al. 2007). However, this role of a counterpoint to PERK-dependent translational arrest is already performed by GADD34, as detailed above in the section on PERK. Ligand- rather than protein-activated investigations used to separate IRE1 signalling from PERK signalling showed that extended PERK signalling was anti-proliferative and pro-apoptotic, whereas IRE1 signalling encouraged proliferation, indicating differential contributions to the apoptotic decision (Lin, Li et al. 2009).

Although increasing of the protective responses may not necessarily help in diseases where the problem lies in the loss of function of a protein not reaching its intended destination, upregulation of the chaperones required for proper folding can help deal with the load. Dissection of the apoptotic, inflammatory and insulin-resistance causing pathways of the UPR from the protective pathways could also offer insight into the mechanisms involved, and possibly help treat some of the diseases where the majority of the damage is caused by cell death and inflammatory responses (Ozcan, Cao et al. 2004). The following section will examine the functional components of the IRE1 kinase pocket in greater detail and propose a method whereby this dissection could be carried out.

1.4. The IRE1 Kinase Pocket: Application of chemical genetics to a protein kinase.

1.4.1 Protein kinases and the IRE1 Kinase Pocket

Figure 1.8 - Schematic of IRE1 showing kinase pocket with ATP molecule. Dashed lines indicate the order in which the relevant sections fall in the sequence of the protein. Residues marked (e.g. K907/K855) of interest to this study are shown with both alpha and beta isoforms, where the first (K907) is the alpha isoform and the second (K855) the beta isoform. Black arrows indicate donation of phosphates to phosphorylate serine and threonine residues on the activation loop.



Phosphorylation of proteins is a major modification that controls many cellular processes (Adams 2001) – it is performed by protein kinases in an ATP, and usually a magnesium or other divalent metal ion dependent manner, transferring a phosphoryl group from ATP to the hydroxyl group of tyrosine, serine or threonine, dependent upon the type, tyrosine kinase or serine/threonine kinase. Rare kinases exist which can phosphorylate both. (Ben-David,

Letwin et al. 1991; Rossomando, Wu et al. 1992). In the case of kinases such as IRE1, serine residues in the activation loop are phosphorylated by ATP, causing the activation loop to refold into connection with positively charged residues in the RD pocket. Phosphorylatable regions are recognized by residue motifs around the phosphorylation site (Adams 2001). Protein kinases share a conserved 200-250 amino-acid core (Hanks, Quinn et al. 1988) and kinase domains are present in 2% of eukaryotic genes (Rubin, Yandell et al. 2000). The structure of protein kinases is highly conserved across the proteome, and a functional kinase enzyme will consist of a number of conserved functional residues and motifs. Of these motifs, the following are to be examined during this project (see Figure 1.8 above for locations):

1) The magnesium binding loop: This motif marks the N-terminal anchor end of the activation segment of the protein kinase and forms part of the $\beta 9$ sheet which joins the magnesium binding loop to the activation segment. It consists of a short tripeptide sequence, DFG. The aspartate residue in this motif chelates a positively charged magnesium ion which then positions the phosphates of ATP correctly for cleavage. (Zhou and Adams 1997) which appears in the conserved DFG motif (Huse and Kuriyan 2002). Yeast with this residue mutated do not survive (Gibbs and Zoller 1991). Protein kinases also possess an activation loop which alters in conformation when phosphorylated and may allow access to substrate pockets (Hubbard, Wei et al. 1994; Hubbard 1997; Mohammadi, McMahon et al. 1997) In insulin receptor kinase (IRK) this results in a conformational change that positions the DFG motif in the active site (Hubbard, Mohammadi et al. 1998). In human IRE1 α/β D711A/D659A forms the beginning of the conserved Asp-Phe-Gly motif (D711A α /D659A β) and prevents chelation of the magnesium ion for MgATP (Hubbard, Mohammadi et al. 1998). In yeast this mutant is reduced to 4% of activity (Mori, Ma et al. 1993) and suffers viability loss without losing nucleotide binding (Chawla, Chakrabarti et al.). As of the time of writing, it has not as yet been studied in a mammalian system.

2) A positively charged lysine in the $\beta 3$ helix, which orientates the α and β phosphates of the ATP molecule and may also stabilise the α and β phosphates, helping with phosphotransfer without reacting itself or altering binding of ATP. This lysine residue is situated on the smaller, N-lobe of the kinase and deep inside the ATP binding cleft. K \rightarrow R substitution of this residue in ERK2 produces an impaired protein with no changes to ATP binding (Carrera, Alexandrov et al. 1993; Robinson, Harkins et al. 1996). In human IRE1 α

/β, the K599A/K547A where the lysine residue has been altered to the smaller, uncharged residue alanine, is thought to produce a kinase-defective and RNase defective IRE1 incapable of splicing XBP-1 or activating the unfolded protein response (Tirasophon, Welihinda et al. 1998; Tirasophon 2000; Iwawaki, Hosoda et al. 2001; Lee, Tirasophon et al. 2002; Urano, Calton et al. 2002; Kaneko, Niinuma et al. 2003; Imagawa, Hosoda et al. 2008; Han, Lerner et al. 2009; Lin, Li et al. 2009; Oikawa, Kimata et al. 2009; Uemura, Oku et al. 2009; Nakamura, Tsuru et al. 2010; Mao, Shao et al. 2011; Kato, Nakajima et al.). Mutation to arginine (K599R /K547R) which is a mutation conserving the positive charge of the amino acid resulted in an incomplete loss of function (Mori, Ma et al. 1993; Shamu and Walter 1996).

3) A large hydrophobic residue in the β5 sheet which forms a pocket accepting the adenine of ATP (Huse and Kuriyan 2002; Nolen, Taylor et al. 2004; Lee 2008). This conserved residue is known as the “gatekeeper” (Bishop, Ubersax et al. 2000), is usually large and hydrophobic or polar aligns with the nucleotide portion of ATP masks a hydrophobic pocket next to the ATP binding area. Mutations of this residue reduce affinity for ATP, but not in a manner than significantly affects binding given normal cellular ATP concentrations (Shah, Liu et al. 1997). Alteration of the site to admit a larger ATP analogue produces an analogue sensitized kinase (as-Kinase). These can be used to investigate the role of the kinase by rendering them activable by the pharmacological agent of the analogue, however, this methodology is limited by issues such as potential reduction or removal of kinase activity due to removal of the gatekeeper residue, an unsuitable gatekeeper residue, competition with ATP or the properties of the enlarged analogue itself (Zhang, Kenski et al. 2005; Hodgson and Schroder). I642A/G and L590A/G are the equivalent mutations of the hydrophobic “gatekeeper” residue in human IRE1 α and β that analogue sensitise the IRE1 protein into which an enlarged ATP analogue such as 1NM-PP1, which was used in (Papa, C. et al. 2003) (see below) can fit. K907A, like K599A has been used as a RNase defective control, as it cannot bind the XBP-1 mRNA and has no splicing activity, although it can cross-phosphorylate the K599A mutant (Tirasophon 2000). K855A also does not splice in mammalian cells (Imagawa, Hosoda et al. 2008)

A combination of a kinase dead/reduced mutations and an analogue sensitised mutant should result in a variant of IRE1 whose RNase domain can be activated by an ATP analogue whilst its kinase domain cannot. In order to fully characterise the possible combinations and increase the chances of producing a variant which splices XBP-1 mRNA

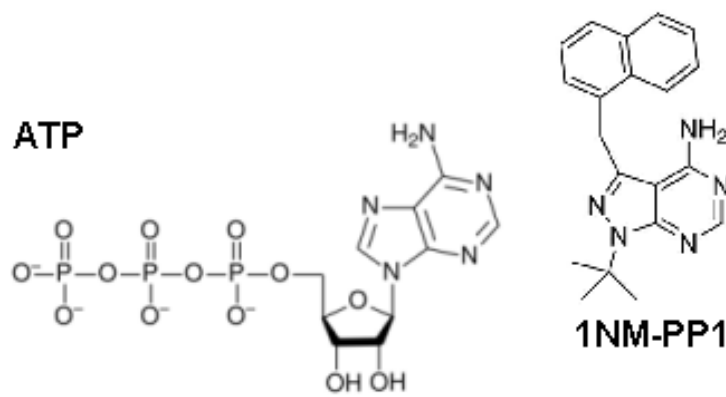
but does not cause JNK phosphorylation via TRAF 2, a range of kinase dead and analogue sensitised mutants in combination were produced. Given the mutations exhibiting dissective effects upon IRE1 function, a screen of kinase pocket mutants can be performed in a model mammalian system to predict their effect upon industrial cell line productivity, and to allow the selection of a suitable mutant to be tested in an industrial cell line – therefore, the mutants detailed above will be produced in this study and screened for their effect on markers of IRE1 function such as XBP-1 splicing and JNK activation, and upon viability and resistance to ER stress. Should a suitable mutant be found, this mutant will be progressed onto examination in a suitable producer cell line as provided by our industrial collaborator, Lonza Biologics.

1.4.2 Application of an ATP Analogue to IRE1

In the case of IRE1, it has been demonstrated that alteration of the kinase site in combination with small molecule chemical genetics (Elphick, Lee et al. 2007) can provide insight into how its kinase function activates its RNase function. In yeast, mutation of Leu⁷⁴⁵, a highly conserved residue located in the ATP binding site of Ire1p to alanine or glycine was predicted to be able to sensitise this site to binding of 1NM-PP1. The large leucine residue normally extends into the ATP binding site allowing binding of the substrate. Replacement with an amino acid with a smaller side chain is thought to produce a pocket into which the large side chain of 1NM-PP1 can fit [Bishop1998]. The L-> A mutation shows a 40% decrease in activity, the L-> G a >90% decrease. Addition of 1NM-PP1 to the L->A mutant did not inhibit, but rather partially rescued the RNase activity. In the case of the L->G mutant, activity was restored almost to wild type levels. These effects were specific for 1NM-PP1, and did not require the kinase activity of Ire1p to be functional, as the effect of 1NM-PP1 remained even when a further mutation (K599A) which normally renders IRE1 kinase-dead was introduced. The requirement for serine trans-phosphorylation can also be bypassed by 1NM-PP1. Splicing of Hac1 mRNA and upregulation of UPR associated genes does still occur in the sensitised mutants, but requires 1NM-PP1 as a cofactor. This indicates that RNase activity is being regulated independently of phosphorylation (Papa, C. et al. 2003). IRE1 mutants in which phosphorylation has been bypassed whilst retaining kinase pocket occupancy in this way exhibit altered characteristics - this modulation of IRE1 activity by 1NM-PP1 appears to be pro-survival(Han, Upton et al. 2008). Furthermore, 1NM-PP1 activated IRE1 with the I642G mutant did not induce IRE1 dependent mRNA degradation,

unless ER stress was applied (Hollien, Lin et al. 2009). These characteristics indicate the potential usefulness of this system, either using 1NM-PP1, or by producing mutants that mimick this ability without the ATP analogue to improve viability in industrial cell growth, and indicate the possibility of dissecting other individual components of IRE1 function one from the other in manner which is useful for improving viability and cell mass in industrial biopharmaceutical manufacture.

Figure 1.9- ATP and 1-NM-PP1.



1.5. Project Aims

1. To dissect the activities of IRE1 involved in protective signalling pathways via XBP-1 from the activities involved in inflammatory and apoptotic responses.

Since XBP-1 splicing is dependent upon the RNase function of IRE1 and JNK activation has been hypothesised to be dependent upon its kinase function (Urano 2000), a mutant such as the one described above sensitised to 1NM-PP1, which is able to bypass the kinase function of IRE1 could be capable of splicing XBP-1 in the presence of a small molecule activator, but unable to trigger the apoptotic pathways.

- Mutations will be made in residues which evidence suggests are involved in ATP binding, binding of magnesium ions and RNase activity in an attempt to produce an analogue-sensitised human mutant which can be induced by 1NM-PP1.
- Where possible, both the alpha and beta isoforms of human IRE1 will be used as the two forms differ in distribution and effects.
- Plasmids containing mutated IRE1 will be re-introduced into *ire1 α ^{-/-}* mouse embryonic fibroblasts.
- Expression of the mutant IRE1 will be assessed to ensure levels are similar to that of the wild type.
- Splicing of XBP-1 RNA will be assessed by RT-PCR, and JNK activation via TRAF2 will be assessed by Western blot.
- Kinase activity will be assessed by the most appropriate method, e.g. Western blot, phosphorylation assays.
- Viability will be assessed by cell counts or photography.

2. Ascertain whether industrial protein yields in an industrial cell line can be increased by addition of these mutants.

- These cell lines will need their own endogenous IRE1 to be knocked down, possibly by siRNAs, to eliminate the confounding effects of endogenous wild-type IRE1 on the mutant IRE1 forms.
- If it is possible to produce a mutant with increased protective and reduced or inactive apoptotic activity, it will be attempted to repeat the analyses used in the MEF system in CHO cell lines used for industrial protein synthesis.
- The effect of these mutants on cell productivities will be assessed by the appropriate industrial method.

2. MATERIALS

2.1 Chemicals and solutions

De-ionised/MilliQ/Sterile Water

Where water, de-ionised or otherwise sterilised water is referred to in these solutions, this was produced by the MilliQ water purifier to a total organic carbon level of less than 3.0 parts per billion.

Autoclaving

Autoclaving was performed at 121°C for 20 min at 1 atmosphere.

Bacto-Tryptone/Yeast Extract/NZ Amine

Where these are used individually, they are as follows:

Tryptone – OXOID, Code: L42

(Bacto-) Yeast Extract – BD, Code: 212750

N-Z Amine A – Fluka, Code: C0626-500G

Where they are used for LB agar plates, a combined LB agar mixture from Formedium was used – LB Agar (Lennox) (Code: LBX0302)

Table 2.1- Solutions for Microbiology

30% (v/v) glycerol	189 g glycerol Add H ₂ O to ~400 ml, mix well by stirring. Add H ₂ O to 500 ml and autoclave.
--------------------	---

LB broth, Lennox	10 g/l tryptone 5 g/l yeast extract 5 g/l NaCl Add 1l H ₂ O.
LB agar, Lennox + 50 µg/ml ampicillin	10 g/l tryptone 5 g/l yeast extract 5 g/l NaCl 15 g/l agar Add 1l H ₂ O. Autoclave. Add 1ml 50 mg/ml ampicillin after cooling to <50°C.
LB agar, Lennox + 50 µg/ml ampicillin + 10µg/ml tetracycline	10 g/l tryptone 5 g/l yeast extract 5 g/l NaCl 15 g/l agar 50 µg/ml ampicillin Add 1l H ₂ O. Autoclave. Add 1ml 50 mg/ml ampicillin
LB agar, Lennox + 50 µg/ml ampicillin + 80µg/ml X-Gal + 500µM IPTG	3.3g/l tryptone 1.6 g/l yeast extract 1.6 g/l NaCl 5 g/l agar 300ml DI H ₂ O 1.5ml 0.1M IPTG 300µl 80mg/ml X-Gal 300µl 50mg/ml Ampicillin after cooling to <50°C.

NZY+ Broth	<p>10g NZ amine 5g yeast extract 5g NaCl Add 950ml H₂O. Adjust to pH7.5 with NaOH. Autoclave. Add 12.5ml filter sterilised 1M MgCl₂, 12.5ml filter sterilised 1M MgSO₄, Make up to 1l with H₂O. Autoclave Add 10ml filter sterilised 2M glucose</p>
S.O.C. Medium	<p>2g bacto-tryptone 0.5g yeast extract 0.05g NaCl 0.0186g KCl Autoclave. Add 90ml H₂O. Add 1ml filter sterilised 1M MgCl₂ Make up to 100ml with H₂O. Autoclave Add 1ml filter sterilised 2M D-glucose</p>
1x TSS	<p>1 g tryptone 5 g yeast extract 0.5 g NaCl 100g polyethylene glycol 3350 5ml DMSO 5ml 1M MgCl₂ Adjust pH to 6.5 with HCl Make up to 100ml Filter sterilise.</p>

Table 2.2 - Solutions for DNA Work

1 x GTE (50 mM D-Glucose, 25 mM Tris·HCl (pH 8.0), 10 mM EDTA)	2.50 ml 1 M D-Glucose 1.25 ml 1 M Tris·HCl (pH 8.0) 1.00 ml 0.5 M EDTA 50 ml H ₂ O
10x DNA gel electrophoresis sample loading buffer	10 g Ficoll 400 125 mg bromophenol blue 10 ml 0.5 M EDTA (pH 8.0) Add H ₂ O to ~ 35 ml. Dissolve. Add H ₂ O to 45 ml. Autoclave. Add 5 ml 10% (w/v) SDS.
2 mM dNTPs	910 µl H ₂ O 10 µl 100 mM Tris·HCl (pH 8.0) 20 µl 100 mM dATP 20 µl 100 mM dCTP 20 µl 100 mM dGTP 20 µl 100 mM dTTP
10 mg/ml ethidium bromide	Supplier: Sigma-Aldrich, Gillingham, UK
Hybridization solution	5 ml 20 x SSC, 2 ml 10% (w/v) SDS 1 ml 100 x Denhardt's solution Prewarm at 42°C. Prewarm 10 ml formamide to 42°C. Immediately before use boil 2 ml 1 mg/ml salmon sperm DNA for 5 min, then place for 30 s on an ice-H ₂ O bath. Add denatured salmon sperm DNA to the aqueous premix, and mix. Mix aqueous premix and formamide for use.
0.2 N NaOH + 1% (w/v) SDS	4 g NaOH 5 g SDS

	Dissolve in ~450 ml H ₂ O, add H ₂ O to 500 ml. Store in a polyethylene bottle.
10mg/ml RNase A	10mg RNase A Dissolve in 1ml of 1xTE
8x SYBR Green	(from Molecular Probes/Invitrogen, Paisley, UK) 10,000 x Stock in DMSO Dilute 1:1250 to 8x
50x TAE	242 g Tris 57.1 ml HOAc 37.2 g Na ₂ EDTA•2H ₂ O Add H ₂ O to 1 l pH ~ 8.5
10x TE (pH 8.0)	400 ml 1 M Tris•HCl (pH 8.0) 80 ml 0.5 M EDTA Add H ₂ O to 4 l Autoclave
0.1M Sodium Citrate /10% Ethanol (v/v)	1.47g Sodium Citrate 45ml H ₂ O 5ml 100% Ethanol
1M Sodium Hydroxide	2g NaOH 50ml H ₂ O
20 x SSC (for southern blot)	175.32 g NaCl 88.23 g Na ₃ •citrate•2 H ₂ O Add H ₂ O to 1 l. Add 1 ml DEPC treated H ₂ O. Autoclave.

Table 2.3 - Solutions for RNA Work (all preparation equipment baked to remove RNases or purchased clean)

DEPC-H ₂ O	1 ml DEPC 1l sterile H ₂ O Autoclave.
-----------------------	--

6 x RNA sample loading buffer	63 g glycerol 250 mg bromophenol blue 10 ml 100 mM Na ₃ PO ₄ (pH 7.0) Add DEPC-H ₂ O to 100 ml. Add 100 µl DEPC treated H ₂ O. Autoclave.
2 mM dNTPs	910 µl DEPC treated H ₂ O 10 µl 100 mM Tris•HCl (pH 8.0) in DEPC treated water. 20 µl 100 mM dATP 20 µl 100 mM dCTP 20 µl 100 mM dGTP 20 µl 100 mM dTTP
dNTP-UTPs	36.5 µl DEPC treated H ₂ O 1 µl 100 mM Tris•HCl (pH 8.0) in DEPC treated water. 10 µl 100 mM dATP 10 µl 100 mM dCTP 10 µl 100 mM dGTP 2.5 µl 100 mM dTTP 20µl 100mM dUTP

Table 2.4 - Solutions for Protein Work

2x Assay Buffer (β - galactosidase assay)	177 ml 0.4 M Na ₂ HPO ₄ 23 ml 0.4 M NaH ₂ PO ₄ 0.8 ml 1 M MgCl ₂ 2.8 ml β-mercaptoethanol 532 mg 2-nitrophenyl-β-D-galactopyranoside Add H ₂ O to 400 ml and mix.
---	--

E. coli Positive Control (Escherichia coli) Whole Cell Lysate (ab5395)	Supplier: Abcam, Cambridge, UK
Electrotransfer buffer	4.20 g NaHCO ₃ 1.59 g Na ₂ CO ₃
ELISA coating buffer (0.05 M sodium carbonate, pH 9.6)	1.59g Na ₂ CO ₃ 2.93g NaHCO ₃ 0.2g NaN ₃ Dissolve in 900ml H ₂ O. Adjust to pH9.6 +/- 0.02 using 10N HCl or NaOH. Make up to 1l with H ₂ O
ELISA wash buffer (pH 7.2)	5.844 g NaCl 1.153 g Na ₂ HPO ₄ 0.258 g NaH ₂ HPO ₄ ·H ₂ O 3.722 g EDTA 0.2 ml Tween 20 10.0 ml butanol Dissolve in 900ml of H ₂ O Adjust pH to 7.2+/- 0.02 H ₂ O to 1 L
ELISA blocking buffer	250.0 ml coating buffer 1.25 g casein (Sigma Aldrich, Gillingham, UK – Code: C3400)
ELISA sample/conjugate buffer	6.05 g Tris 2.92 g NaCl 1.0g casein 0.1 ml Tween 20 H ₂ O to 500 ml
ELISA stop solution	68ml conc. H ₂ SO ₄ Add to 432ml of H ₂ O slowly on ice.

PBS	8.0 g NaCl 0.2 g KCl 14.4 g Na ₂ HPO ₄ 0.2 g KH ₂ PO ₄ Add 1L H ₂ O
PBST	8.0 g NaCl 0.2 g KCl 14.4 g Na ₂ HPO ₄ 0.2 g KH ₂ PO ₄ Add 900ml H ₂ O Add 1ml Tween 20 Add H ₂ O up to 1l
PBST + 5% (w/v) skim milk powder	8.0 g NaCl 0.2 g KCl 14.4 g Na ₂ HPO ₄ 0.2 g KH ₂ PO ₄ Add 900ml H ₂ O Add 1ml Tween 20 Add 50g skimmed milk powder before use Add H ₂ O up to 1l
PBST + 5% (w/v) bovine serum albumin	8.0 g NaCl 0.2 g KCl 14.4 g Na ₂ HPO ₄ 0.2 g KH ₂ PO ₄ Add 900ml H ₂ O Add 1ml Tween 20 Add 50g bovine serum albumin before use Add H ₂ O up to 1l
0.5% (w/v) Ponceau S, 1% (v/v) HOAc	1.25 g Ponceau S Dissolve in 2.5 ml HOAc. Add H ₂ O to 250 ml.

5 x Reporter lysis buffer	From Promega, Southampton, UK. Catalogue number E3971. Dilute 1:5 in water for 1x working solution.
RIPA buffer	0.5 ml 1M Tris-HCl pH 8.0 0.3 ml 5 M NaCl 0.1 ml Triton X-100 0.5 ml 10% (w/v) sodium deoxycholate 0.1 ml 10% (w/v) SDS Add H ₂ O to 10 ml
10x semi-dry transfer buffer	73.19g glycine 60.6 Tris-Base Add DI H ₂ O to 500ml DI
1x semi-dry transfer Buffer	50ml 10x Semi-dry transfer buffer 25ml methanol Add DI H ₂ O to 500ml DI
TBST	24.2 g Tris 80g NaCl 1ml Tween 20 Add H ₂ O to 1l Adjust pH to ~ 7.6 with 10N HCl
10x TBS/casein (Lonza Wash Buffer)	12g Tris 45g NaCl 5g casein Add 450ml H ₂ O. Adjust to pH 8.2+/-0.1 with HCl Make up to 500ml
TBSTriton + Casein (Lonza Blocking Buffer)	2.4g Tris base 9.0g NaCl 0.5ml TritonX 100 5.0g Casein Add 950ml H ₂ O

	Adjust to pH 7.6 with HCl Make up to 1l
6 x SDS-PAGE sample buffer	3.50 ml 1 M Tris·HCl 3.78 g glycerol 1.00 g SDS 500 µl 10 g/l bromophenol blue 200 µl β-mercaptoethanol Add H ₂ O to 10 ml.
10 x SDS-PAGE running buffer	144.13 g glycine 30.03 g Tris 10.00 g SDS Add H ₂ O to ~ 900 ml, stir until completely dissolved, then add H ₂ O to 1l.

Table 2.5 - Solutions for Tissue Culture

20mM 1NM-PP1 (1-(1,1-dimethylethyl)-3-(1-naphthalenylmethyl)-1H-pyrazolo[3,4-d]pyrimidin-4-amine)	6.62g 1NM-PP1 Dissolve in 1ml DMSO
20mM Bn-PP1 (3-Benzyl-1-tert-butyl-1H-pyrazolo[3,4-d]pyrimidin-4-ylamine.)	5.62g Bn-PP1 Dissolve in 1ml DMSO
20mM Ph-PP1	5.34g Ph-PP1 Dissolve in 1ml DMSO

1M DTT	1.54g DTT Dissolve in 10ml of H ₂ O Filter sterilise.
100mM thapsigargin	1mg thapsigargin, dissolve in 1ml of DMSO Dilute into 15ml DMSO. Use at 500nM-1µM
10mg/ml tunicamycin	10mg tunicamycin, dissolve in 1ml DMSO Use at 0.1-2.0 µg/ml
25mM Stock MSX (methionine sulphoximine)	250mg MSX 55ml DMSO Dilute in medium 1:1000 for 25µM working use.
10mg/ml blasticidin	Supplier: Melford Laboratories, Ipswich, UK
50mg/ml hygromycin	Supplier: Merck, Middlesex, UK
20mg/ml zeocin	Supplier: Melford Laboratories, Ipswich, UK
10mg/ml tetracycline.	100 mg tetracycline Dissolve in ~9 ml EtOH. Add EtOH to 10 ml. Filter sterilise.
Trypan blue 0.4% (v/v)	Supplier: Sigma-Aldrich, Gillingham, UK

Table 2.6 - Cell Culture Media and Reagents

Medium	Supplier	Cat No
Dulbecco's Modified Eagle's Medium with Pyruvate (Dulbecco and Freeman 1959)	Sigma-Aldrich, Gillingham, UK	D6546
Dulbecco's Modified Eagle's Medium without pyruvate (Dulbecco and Freeman 1959)	Sigma-Aldrich, Gillingham, UK	D5671
Dulbecco's PBS	Sigma-Aldrich, Gillingham, UK	D5652

Fetal Bovine Serum	Sigma-Aldrich, Gillingham, UK	F7524
L-Glutamine	Sigma-Aldrich, Gillingham, UK	G7513
0.25% Trypsin-EDTA	GIBCO/Invitrogen, Paisley, UK	25200-056
CD-CHO (Gorfien, Dzimian et al. 1998)	Invitrogen, Paisley, UK	10743-029
Opti-Mem	Invitrogen, Paisley, UK	11058021

Table 2.7 – Restriction Enzymes

Enzyme	Source	Enzyme	Source
<i>AflIII</i>	New England Biolabs, Hitchin, UK	<i>NheI</i>	Fermentas, Cambridge, UK
<i>AgeI</i>	New England Biolabs, Hitchin, UK	<i>NruI</i>	Roche Applied Science, Burgess Hill, UK
<i>AvrII</i>	Roche Applied Science, Burgess Hill, UK	<i>PdiI</i>	Fermentas, Cambridge, UK
<i>BglII</i>	Fermentas, Cambridge, UK	<i>PvuI</i>	Roche Applied Science, Burgess Hill, UK
<i>BsiWI</i>	Roche Applied Science, Burgess Hill, UK	<i>PvuII</i>	Roche Applied Science, Burgess Hill, UK
<i>BssHI</i>	Roche Applied Science, Burgess Hill, UK	<i>PstI</i>	New England Biolabs, Hitchin, UK

<i>BstZ17I</i>	New England Biolabs, Hitchin, UK	<i>SacI</i>	New England Biolabs, Hitchin, UK
<i>ClaI</i>	Fermentas, Cambridge, UK	<i>SalI</i>	New England Biolabs, Hitchin, UK
<i>DraI</i>	Fermentas, Cambridge, UK	<i>SbfI</i>	New England Biolabs, Hitchin, UK
<i>EagI</i>	New England Biolabs, Hitchin, UK	<i>Scal</i>	Fermentas, Cambridge, UK
<i>EcoRI</i>	Fermentas, Cambridge, UK	<i>SmaI</i>	Fermentas, Cambridge, UK
<i>EcoRV</i>	Fermentas, Cambridge, UK	<i>SnaBI</i>	New England Biolabs, Hitchin, UK
<i>HindIII</i>	Fermentas, Cambridge, UK	<i>SpeI</i>	New England Biolabs, Hitchin, UK
<i>HpaI</i>	Source: Roche Applied Science, Burgess Hill, UK	<i>SphI</i>	New England Biolabs, Hitchin, UK
<i>KasI</i>	New England Biolabs, Hitchin, UK	<i>StuI</i>	Fermentas, Cambridge, UK
<i>KpnI</i>	Fermentas, Cambridge, UK	<i>XbaI</i>	Fermentas, Cambridge, UK
<i>MluI</i>	Fermentas, Cambridge, UK	<i>XhoI</i>	Roche Applied Science, Burgess Hill, UK
<i>MscI</i>	Fermentas, Cambridge, UK	<i>XmaI</i>	New England Biolabs, Hitchin, UK
<i>NgoMIV</i>	Promega, Southampton, UK.	<i>ZraI</i>	Fermentas, Cambridge, UK

Table 2.8 – Other Enzymes

Enzyme	Source
Accuprime <i>Taq</i>	Invitrogen, Paisley UK
β -galactosidase (1U/ μ l.)	Promega, Southampton, UK
Calf Intestinal Alkaline Phosphatase	Fermentas, Cambridge, UK
<i>GoTaq</i> Polymerase	Promega, Southampton UK.
Hotstar <i>Taq</i> DNA polymerase	Qiagen, Crawley, UK
illustra Hot Start Master Mix (<i>Taq</i>)	GE Healthcare, Chalfont St. Giles, UK
Lambda phosphatase	Sigma-Aldrich, Gillingham, UK
<i>Pfu</i> Polymerase	Promega, Southampton, UK.
<i>Phusion</i> Polymerase	Finnzymes/ New England Biolabs, Hitchin, UK
Superscript III reverse transcriptase	Invitrogen, Paisley UK
T4 DNA Ligase	Promega, Southampton, UK.
T4 DNA Ligase	Roche Applied Science, Burgess Hill, UK
Uracil DNA Glycosylase	New England Biolabs, Hitchin, UK

2.2 Oligodeoxynucleotide Primers

Table 2.9 - Codes for Degenerate Primers

Letter	Includes
R	Either Purine (A or G)
Y	Either Pyrimidine (C or T)
M	Adenine or Cytosine (A or C)
K	Guanine or Thymine (G or T)
S	Guanine or Cytosine (G or C)
W	Adenine or Thymine (A or T)
H	Anything but Guanine (A,T or C)
D	Anything but Cytosine (A,T or G)
B	Anything but Adenine (C,T or G)
V	Anything but Thymine (A,C or G)
N	Any base (A,T,G or C)

Table 2.10 - Restriction enzymes used to screen for mutated clones.

pEDΔC-hIRE1α		pCAG-hIRE1β	
Mutant	Enzyme	Mutant	Enzyme
I642A	<i>EagI</i>	L590A	<i>HindIII</i>
I642G	<i>NgoMIV</i>	L590G	<i>NheI</i>
D711A	<i>EcoRV</i>	D659A	<i>HindIII</i>
K599R	<i>EcoRI</i>	K547R	<i>NgoMIV</i>
		K855A	<i>AflI</i>

Table 2.11 – Oligodeoxynucleotide Primers

Code (where available)	Purpose	Primer
<i>Mutagenesis codon change. Restriction site codon change. Underlining</i> – Restriction site – see Table 2.10 for relevant enzyme and sources.		
H8207	K599R Forward	CAACCGCGACGTGGCCGTGAGGAG <u>AATT</u> TCTCCCCGAGTG
H8227	K599R Reverse	CACTCGGGGAG <u>AATT</u> TCTCCTCACGGCCACGTCGCGGTTG
H8212	K547R Forward	CGGGCAGTGGCTGT <u>CGCC</u> GGCTCCTCCGCGAGTGCT
H8232	K547R Reverse	AGCACTCGCGGAGGAGCC <u>GCGG</u> ACAGCCACTGCCCC
H8204	I642A Forward	GGCAATTCCAGTACATT <u>GCGCC</u> GAGCTGTGTGCAGCCACCC
H8224	I642A Reverse	GGGTGGCTGCACACAGCT <u>CGGCC</u> GCAATGTACTGGAATTGCC

H8208	L590A Forward	CAGTTCCACTACATTGCCGCGGAGCTCTGCCGGGC <u>AAGCTT</u> GCAG
H8228	L590A Reverse	CTGCA <u>AAGCTT</u> GCCCCGGCAGAGCTCCGCGGCAATGTAGTGGAAGCTG
H8205	I642G Forward	GCAATTCCAGTACATTGCC <u>GGCG</u> GAGCTGTGTGCAGCC
H8225	I642G Reverse	GGCTGCACACAGCTC <u>GCCGGCAATGTACTGGAATTGC</u>
H8209	L590G Forward	CAGTTCCACTACATTGCCGGGAGCTCTGCCGGGC <u>AAGCTT</u> GCAG,
H8229	L590G Reverse	CTGCA <u>AAGCTT</u> GCCCCGGCAGAGCTCCCCGGCAATGTAGTGGAAGCTG
H8206	D711A Forward	CAAGGCCATGAT <u>ATCCG</u> CCTTTGGCCTCTGCAAGAAGCTGGC
H8226	D711A Reverse	GCCAGCTTCTTGAGAGGCCAAAGGCG <u>GATATCATGGCCTTG</u>
H8210	D659A Forward	GGTGCTCTCAGCCTTCGGCCTCTGCAAGA <u>AAGCTT</u> CCTGCT
H8230	D659A Reverse	AGCAGG <u>AAGCTT</u> CCTTGAGAGGCCGAAGGCTGAGAGCACC
H8211	K855A Forward	GCGAGACCT <u>CTTAAG</u> AGCTGTGAGGAACGCGAAGCACCCTACAGGGAGC
H8231	K855A Reverse	GCTCCCTGTAGTGGTGCTTCGCGTTCCTCACAGCT <u>CTTAAG</u> AGGTCTCGC
H8341	IRE1a Activation Loop - <i>BstZ17I</i> End	TACGCTTGGAAGCAAGAATAATGAA
H8397	IRE1a Activation Loop - <i>BstZ17I</i> End -2 overhang	CAG CCT GTA TAC GCT TGG AAG CAA GAA TAA TGA A
H8364	IRE1a Activation Loop -Aloop- Reverse	CACCCCAGCTCGGCGGGCCAAAGCGTGTCTGCCCACTGCCAGCTT
H8364	IRE1a Activation Loop -Aloop- Reverse-2	CACCCCAGCTCGGCG GCGAAAGCGTGTCTGCCCACTGCCAGCTT
H8343	IRE1a Activation Loop -Aloop-	AGACACGC TTCGCCCGCCGAGCTGGGGTGCTGGCACAGAAGGC

	Forward	
H8344	IRE1a Activation Loop - <i>SnaBI</i> End	GTAGTAAAAGACGCAGCCTGC
H8398	IRE1a Activation Loop - <i>SnaBI</i> End- 3 overhang	AGA GAT TAC GTA GTA AAA GAC GCA GCC TGC
H8345	IRE1b Activation Loop - <i>KpnI</i> End	CCCCTGGTACCTGCAGACACTGCT
H8347	IRE1b Activation Loop - Aloop-Forward	CGCTGTGCCTTCGCCCTCCACGCCGGCATCCCCGGCACGGAAGGC
H8346	IRE1b Activation Loop - Aloop-Reverse	GATGCCGGCGTGGAGGGCGAAGGCACAGCGGCCAGCAGGCAGCTT
H8348	IRE1b Activation Loop - <i>BglII</i> End	GGA AAA AGA TCT CAG TGG TAT TTG
IRE1 Vector Sequencing		
Code	Name/Purpose	AAGAGGCTGCTCTGTTCTGG
H8033	hIRE1 α sequencing 1	CGTGACCTACAGGGAAGTGG
H8034	hIRE1 α sequencing 2	CGTGGTGAAGATGGACTGG
H8035	hIRE1 α sequencing 3	CTCATATCCATGCCCAATGC
H8036	hIRE1 α sequencing 4	ACCAGCGTGGTGATAGTTGG
H8037	hIRE1 α sequencing 5	CATCGGGAAAATGTGATTCC
H8038	hIRE1 α sequencing 6	TTTGTGTCCAATGGTGATGG

H8039	hIRE1 α sequencing 7	GGACAGGCTCAATCAAATGG
H8040	hIRE1 α sequencing 8	TGCTTCCAAGCGTATACAGG
H8041	hIRE1 α sequencing 9	ATGCCACACAGATGGTCTCC
H8042	hIRE1 β sequencing 1	CAGTGA CTGGCTGGAGAAGG
H8043	hIRE1 β sequencing 2	GAGTGGTGCTCTCAGACTTCG
H8044	hIRE1 β sequencing 3	CAGAGTCCCTCAAAGCAAGC
H8045	hIRE1 β sequencing 4	AGTCTCAGGAGAGCGAGAGG
H8046	hIRE1 β sequencing 5	TCACCTGGGAAATACATGAGC
H8047	hIRE1 β sequencing 6	CACCTTGGATGGAAGTCTCC
H8048	hIRE1 β sequencing 7	TCCAGGAACTGATGATGAACC
H8049	hIRE1 β sequencing 8	GCCCTTCTCATCACACTCC
H8050	hIRE1 β sequencing 9	GTCGAGAGGTTTTCCGATCC
H8155	hIRE1 α -pED Δ c sequencing 1	GGACAGGCTCAATCAAATGG
H8156	hIRE1 α -pED Δ c sequencing 2	GTTCCCTGGAGTCCTCACTGC
H8157	hIRE1 β -pCAG sequencing 1	CAAGGGAGCGCTCTGTCC
H8158	hIRE1 β -pCAG sequencing 2	TGCTGGGTCAGAGAGAAAGG
H8159	hIRE1 β -pCAG sequencing 3	GGAGAAGCAGCAGGAGACC
H8160	hIRE1 β -pCAG sequencing 4	ATAGTCCCGCCCCTAACTCC
H8192	hIRE1 α -pED Δ c sequencing 5	CTCTGCTCCCCTCCTAAAGC
H1893	hIRE1 α -pED Δ c sequencing 6	GCACAGATTTGGGACAAAGG
H8194	hIRE1 β -pCAG sequencing 5	TTGTTATCCGCTCACAATTCC

H8195	hIRE1 β -pCAG sequencing 6	ATTTCGGCTTATCGATTGAGG
H8213	hIRE1 α -pED Δ c sequencing 7	ACTTTTCGGGGAAATGTGC
H8214	hIRE1 α -pED Δ c sequencing 8	TTTTTGGCGAGCTCGAATTA
H8219	hIRE1 β -pCAG sequencing 7	GCCCTCTCGCACGATTACCA
H8220	hIRE1 β -pCAG sequencing 8	CTGCGAGGGGAACAAAGG
H8221	hIRE1 β -pCAG sequencing 9	GCACGCAGCCTTTGTTCC
H8222	hIRE1 β -pCAG sequencing 10	GGAGATGGGGAGAGTGAAGC
H8223	hIRE1 β -pCAG sequencing 11	TCACAGAAAAGCATCTTACGG
H8261	hIRE1 β -pCAG sequencing 12	TCACAGAAAAGCATCTTACGG
H8262	hIRE1 β -pCAG sequencing 13	AGTTCGCCAGTTAATAGTTTGC
H8276	hIRE1 α -pED Δ c sequencing 9	AGGTCGACTCTAGAACCATGC
CHO IRE1a Sequencing		
	A-102	GCCGGTCCGCTTGSWNACNGCRTG
	A-85	CGGACCGGCTCCATHAARTGGAC
	A130	CCCGGGTCTTGGTGTCRTACATNGT
	A49	GACGTGCTGTGGATCCARAAYTAYGC
	A41	CCCCCTCCATGGTGCAYGARGGNGT
	A143	TTGGGGAAGGGGTACTTCCAYTTNGT
	A20	GAAGAGGTCCTTCGAGGARGTNATHAA
	A163	CGGACAGAGGGGTCTCRTGRTGGNCC
	A1	GAAGATCCAGCTGCTGCARCARCARCA

	A173	CGTGGGCCAGCTTCTCYTCNACRTC
	B74	CGTGTACAAGGGCATGTTYGAYAAIMG
	B102	GTCTCCTCGTCCTCGTCRTCENKGYTC
	B61	CACCAGACCACCTCCGGNYTNGCNCA
	B121	GAAGTCCTTCTGCTCCACRTAYTCYTG
	B50	GTGCCCGGCACCGARGGNTGGAT
	B135	TGATCCTGCCGTGGGCRRTNNGGCAT
	B28	AAGCAGCTGCAGTTCTTYCARGAYGT
	B161	CCAGCTGCCTCACGATNGGNCRTC
	B18	CATGCGGAACAAGAAGCAYCAYTAYMG
	B182	TCGTGCCGGCACARYTCCATNGC
H8430	B-186	CTGGGGCTCGGTGGGYTCRTGVMA
H8431	B-168	ATGGCCCGCAGCARRTCNCKNAC
	5'1	TTCCCAACGTACAGGGTAGG
	5'2	TGTGCATCACCTTTCTCAGG
	5'3	CGTACAGGGTAGGCGTTAGC
	5'4	GGGGTGATCACACACTCTCC
	5'5	GTCCAGGGTCAAACCTTGAGG
	3'1	CATCGGGAAAATGTGATTCC
	3'2	GCTAACGCCTACCCTGTACG
	3'3	CTTCATGTCTGGGGAAGTGG

	3'4	GAAGTATCCGTCCCCAAGG
	3'5	GGAGAGATTCCCCAACAACC
	Luminal1	TTCCCCAACGTACAGGGTAGG
	Luminal2	GCTCTTGGCCTCTGTCTCC
	Luminal 3	CCCAACGTACAGGGTAGGC
H8410	347Luminal01	GCTCTTCCACGTGTGTTGG
H8411	407Lumina01	AGGCCTTCGTTGTTTTTGC
H8412	2605Kinase01	AGTTCTTCCAGGACGTGAGC
H8413	2665Kinase01	GATCGTGAGGCAGCTGGA
H8424	372Luminal	GACTGCCATCATTGGGATCT
H8425	317Luminal	CCTGCAGGACTGGATCTTCT
H8426	2627Kinase	AAGCAGCTCCAGTTCTTCCA
H8427	2624Kinase	AGCAGCTCCAGTTCTTCCAG
H8432	2970Kinase	CAGCCACGAGAGACTCTTCC
H8433	2910Kinase	GCTACTTCACGTCTCGCTTCC
H8455	CHOIRE1180bpF	ACTGCCTGAAACCCCTGTTGT
H8456	CHOIRE1180bpR	ACAACAGGGTTTCAGGCAGT
H8457	CHOIRE1500bpF	TGACTGGAGAGAAGCAGCAG
H8458	CHOIRE1500bpR	TCTCCAGTCAGGAGGTCGAT
H8459	CHOIRE12000bpF	CTTCGAGAATCAGACGAGCA
H8460	CHOIRE12000bpR	GATTCTCGAAGCAGCTGGAC

H8461	CHOIRE12500bpF	AGGACGTCATTGCTCGTGA
H8462	CHOIRE12500bpR	TGGGGATCCATAGCAATCAT
H8463	CHOIRE13000bpF	TGGAGCTCTGCAGACATGAG
H8464	CHOIRE13000bpR	TCATGTCTGCAGAGCTCCAT
H8465	CHOIRE13500bpF	AGCAAGAGCACCCCTCTGCT
H8466	CHOIRE13500bpR	TTCTAGCAGAGGGTGCTCTTG
H8467	CHOIRE13900bpF	GTGGAGAGGCTCAGAACCAG
H8468	CHOIRE13900bpR	CTGGTTCTGAGCCTCTCCAC
H8469	CHOIRE13endbpF	AAGGCCCTGGGGGTAGAGAG
H8470	CHOIRE13endbpR	CTCTCTACCCCCAGGGCCTT
T-RACE Primers		
H8414	T-RACE Adapter A (poly-A tail)	AUCUCGAGUUCGCGCCGGAUCCTTTTTTTTTTTTTTTTTTTTTTTTTTTTTTTVN
H8415	T-RACE Adapter B (5' Cap)	AUAUGCACUGCCGCGUCUGAGGGGGGGG
H8416	T-RACE Primer A	CUCGAGUUCGCGCCGGAUC
H8417	T-RACE Primer B	AUAUGCACUGCCGCGUCUGA
H8418	5' T-RACE Primer	ATATGCACTGCCGCGTCTGA
H8419	3' T-RACE Primer	CTCGAGTTCGCGCCGGATC
RT-PCR Primers		
H7961	Mouse Forward	GATCCTGACGAGGTCCAGA
H7962	Mouse Reverse	ACAGGGTCCAACCTGTCCAG

H8395	Mouse Gene Specific Primer	CTAGCAGACTCTGGGGAAGG
H7994	Mouse Actin Forward	AGCCATGTACGTAGCCATCC
H7995	Mouse Actin Reverse	CTCTCAGCTGTGGTGGTGAA
	CHO XBP-1 Forward 1	ACTACTGAAGAGGCTCCAGA
H8420	CHO XBP-1 Forward 2	CTGAAGAGGCTCCAGAGACG
H8421	CHO XBP-1 Forward 3	CCAAGGGAAATGGAGTAAGG
	CHO XBP-1 Reverse 1	ACAGGGTCCAACCTTGTCCAG
H8422	CHO XBP-1 Reverse 2	TCCATGGGAAGATGTTCTGG
H8423	CHO XBP-1 Reverse 3	GTCCAGAATGCCCAAAGG
H8451	CHO Gene Specific Primer 2	ATTGGCAGACTCTGGGGATGGA
	CHO Actin Forward	AGCTGAGAGGGAAATTGTGCG
	CHO Actin Reverse	GCAACGGAACCGCTC
qPCR Primers		
	CHO XBP-1 Splice Junction -1	GCTGAGTCCGCAGCAGGTGC
H8452	CHO XBP-1 Splice Junction -2	CTGAGTCCGCAGCAGGTG
H8453	CHO XBP-1 Splice Junction -3	GCTGAGTCCGCAGCAGGT-
H8454	CHO XBP-1 Splice Junction -4	GTCCGCAGCAGGTGCAGGCC
	CHO XBP-1 Intron	GCACTCAGACTACGTGCACC
	CHO Actin Forward	AGCTGAGAGGGAAATTGTGCG
	CHO Actin Reverse	GCAACGGAACCGCTC
	CHO IRE1 F	AAGGTCCCCAGACAGATGG

	CHO IRE1 R	CCAGATGAATCCAGAAACTCG
H8440	CHOIRE1F3	CTTCATGTCTGGGGAAGTGG
H8441	CHOIRE1R2	GCTCAGGGGGTAAGTGATGA
H8442	CHOIRE1R3	CATGCTCAGGGGGTAAGTGA
H8439	CHOIRE1F2	CGCATCACCAAGTGGAAGTA
Vector Sequencing and Other Primers		
	SacI to Multiclone Site I	CGTGTACGGTGGGAGGTC
	SacI to Multiclone Site II	CAT GACCTTATGGGACTTTCC
H8428	SacI to Multiclone Site III	CAAATCAACGGGACTTTCC
H8429	SacI to Multiclone Site IV	GGATAGCGGTTTGACTCACG
	PvuII to Multiclone Site	TTGCATACTTCTGCCTGCTG
	Avr to Multiclone Site	GTAAATTCCTTGCGGCTTTG
	U6 Promoter + Multiclone Site Short F	CTAGGTTAAAATGGACTATCATATGTCATATGCTTACCGTAACTTGAAAG TATTTTCGATTTCTTGGCTTTATATATCTTG
	U6 Promoter + Multiclone Site Long F	TGGAAAGGACGAACACCGACCGGTCCCGGGGCGCGCTCGCGACGTACGGGAA TTCCCTCGAGGGCGCCGTTAACCAG
	U6 Promoter + Multiclone Site Long R	CTGGTTAACGGCGCCCTCGAGGAATTCCGTACGTGCGGAGCGCGCCCCGGG ACCGGTGCGGCGGTGTTTCGTCTTTCCACAAGA
	U6 Promoter + Multiclone Site Short R	TATATAAAGCCAAGAAATCGAAATACTTTCAAGTTACGGTAAGCATATGACA TATGATAGTCCATTTTAAC
	Multiclone Site for CMV F	AGCTCACCGGTCCCGGGGCGCGCTCGCGACGTACGGAATTCCTCGAGGGCG

		CCGTTAACCAG
	Multicloning Site for CMV R	CTGGTTAACGGCGCCCTCGAGGAATTCCGTACGTCGCGAGCGCGC CCCGGGACCGGTG
H8475	T7 Sequencing Primer for pGEM Vector	TAATACGACTCACTATAGGGCGA
H8476	SP6 Sequencing Primer for pGEM Vector	ATTTAGGTGACACTATAGAATACT
	M13 R	CAGGAAACAGCTATGACC
	M13 F	TGTAAAACGACGGCCAGT
	Random Hexamers	From Promega, Southampton, UK.
	Oligo(dT) ₂₀	From Promega, Southampton, UK.
	lacZ Probe F	GACGTCTCGTTGCTGCATAA
	lacZ Probe R	CAGCAGCAGACCATTTTCAA

2.3 Plasmids

Plasmids were subjected to restriction digest and bioinformatic analysis, and sequenced by DBS Genomics, Durham to produce maps for use in restriction enzyme analyses and site directed mutagenesis.

Table 2.12 – Plasmids

Name	Source	Reference	Origin/Derivation
IRE1 Expression Vectors			
pEDΔC pEDΔC-hIRE1α, pEDΔC-hIRE1α-K599A, pEDΔC-hIRE1α-K907A	R. Kaufman, University of Michigan, USA.	(Kaufman1991)(Kaufman, Davies et al. 1991) (Tirasophon1998, 2000)(Tirasophon, Welihinda et al. 1998; Tirasophon 2000)	pEDΔC-hIRE1α derived from pED plasmid by inserting a 3.5kb hIRE1α <i>XbaI-EcoRI</i> cDNA into the <i>XbaI</i> site. Mutagenesis as described in. pEDΔC-hIRE1α-K599A and pEDΔC-hIRE1α-K907A derived from pEDΔC-hIRE1α.
pEDΔC-hIRE1α- K599A/I642A pEDΔC-hIRE1α- K599A/I642G pEDΔC-hIRE1α-K599R pEDΔC-hIRE1α- K599R/I642A pEDΔC-hIRE1α- K599R/I642G pEDΔC-hIRE1α-D711A pEDΔC-hIRE1α- D711A/I642A	Produced in this study.	None	Produced from pEDΔC-hIRE1α or pEDΔC- hIRE1α-K599A in this study by site-directed mutagenesis using QuikChange® II XL Site- Directed Mutagenesis Kit (see Commercially Available Kits, below) (See Chapter 1)

Name	Source	Reference	Origin/Derivation
pEDΔC-hIRE1α-D711A/I642G			
pCAG pCAG-hIRE1β pCAG-hIRE1β-K547A pCAG-hIRE1β-HA pCAG-hIRE1β-HA-K547A	K. Kohno, Nara Institute of Science and Technology, Japan	(Iwawaki, Hosoda et al. 2001)	Derived from the pCAGGS plasmid by inserting a 2.9kb hIRE1β <i>EcoRI-EcoRI</i> cDNA into the <i>EcoRI</i> site
pCAG-hIRE1β-K547A/L590A pCAG-hIRE1β-HA-K547A/L590A pCAG-hIRE1β-K547A/L590G pCAG-hIRE1β-HA-K547A/L590G pCAG-hIRE1β-K547R pCAG-hIRE1β-HA-K547R pCAG-hIRE1β-K547R/L590A pCAG-hIRE1β-HA-	Produced in this study.	None	Produced from pCAG-hIRE1β or pCAG-hIRE1β-K547A by excising hIRE1β with <i>EcoRI</i> and subcloning into <i>EcoRI</i> site of puc18 and site-directed mutagenesis using QuikChange® II XL Site-Directed Mutagenesis Kit (see Commercially Available Kits, below). HA tags cloned as described in “Cloning of IRE1α and IRE1β mutant plasmids” (See Chapter 1)

Name	Source	Reference	Origin/Derivation
K547R/L590A pCAG-hIRE1 β - K547R/L590G pCAG-hIRE1 β -HA- K547R/L590G pCAG-hIRE1 β -D659A pCAG-hIRE1 β -HA-D659A pCAG-hIRE1 β - D659A/L590A pCAG-hIRE1 β -HA- D659A/L590A pCAG-hIRE1 β - D659A/L590G pCAG-hIRE1 β -HA- D659A/L590G pCAG-hIRE1 β -K855A pCAG-hIRE1 β -HA-K855A			
pTK-HSV-BP2-hIRE1 α	Produced in this study.	None	Derived from pDJB134 by removing the CREB-H gene with <i>SpeI</i> and <i>XbaI</i> and replacing with hIRE1 α cut from pED Δ C-hIRE1 α with <i>SpeI</i> and <i>XbaI</i>

Name	Source	Reference	Origin/Derivation
pTKRG-hIRE1 β	Produced in this study.	None	Derived from pCAG-hIRE1 β by excising the chicken beta actin promoter with <i>Sall</i> and <i>Xbal</i> and cloning in the thymidine kinase promoter and intron cut from pDJB134 with <i>Sall</i> and <i>NheI</i> .
Lonza Plasmids			
pEE12.4-replacement	Donated by Lonza Biologics, Slough, UK		
pEE12.4-U6 pEE12.4-U6-4- pEE12.4-U6-sh01 pEE12.4-U6-egfp	Produced in this study.	None	Derived from pEE12.4 by cutting CMV promoter out with <i>AvrII</i> and <i>PvuII</i> cloning U6 promoter sequence from (Lin, Yang et al. 2004) combined with polylinker sequence (see Chapter 4.7). shRNA sequences were then cloned in with <i>AgeI</i> and <i>NruI</i> (See Chapter 4.8)
Other			
puc18	Standard cloning vector kept in lab	(Yanisch-Perron, Vieira et al. 1985)	
pUC18-hIRE1 β	Produced in this study.	None	Derived from pCAG-hIRE1 β and pUC18 vector by excising hIRE1 β with <i>EcoRI</i> and inserting into the <i>EcoRI</i> site of the multi-cloning site of pUC18
pDJB134	Gift from Marie Curie Research Insitute,	(Bailey, Barreca et al. 2007)	

Name	Source	Reference	Origin/Derivation
	Surrey		
Invitrogen Plasmids for Stable Cell Line Production – T-Rex System (See “Commercially Available Kits”, below)			
pcDNA/lac/Zeo	Purchased from Invitrogen, Paisley UK		
pcDNA6/TR			
pcDNA5-FRT-TO			
pOG44			
pcDNA5-FRT-TO-hIRE1 α pcDNA5-FRT-TO-hIRE1 α -K599A pcDNA5-FRT-TO-hIRE1 α -K599R pcDNA5-FRT-TO-hIRE1 α -D711A pcDNA5-FRT-TO-hIRE1 α -I642G pcDNA5-FRT-TO-hIRE1 α - D711A/I642G pcDNA5-FRT-TO-hIRE1 α - K599A/I642G pcDNA5-FRT-TO-hIRE1 α - K599R/I642G	Produced in this study.	None	Produced by collaborator S. Sestak, Bratislava from pcDNA5-FRT-TO by Cloning the 1,071 bp <i>SalI-PspOMI</i> fragment from pED Δ C-hIRE1 α into <i>XhoI + PspOMI</i> digested pcDNA5/FRT/TO to produce pcDNA5/FRT/TO-hIRE1 α -N'. The 2,679bp <i>PspOMI</i> fragment from pED Δ C-hIR and each mutant pED Δ C plasmid into pcDNA5/FRT/TO-hIRE1 α -N'.

Figure 2. 1 - pEDΔc-hIRE1α

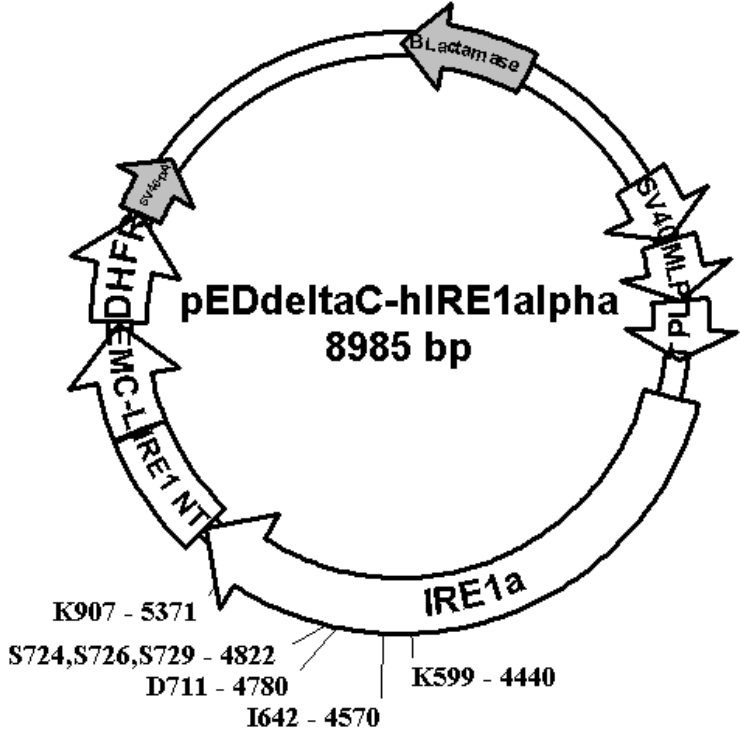


Figure 2. 2 – pCAG-hIRE1β

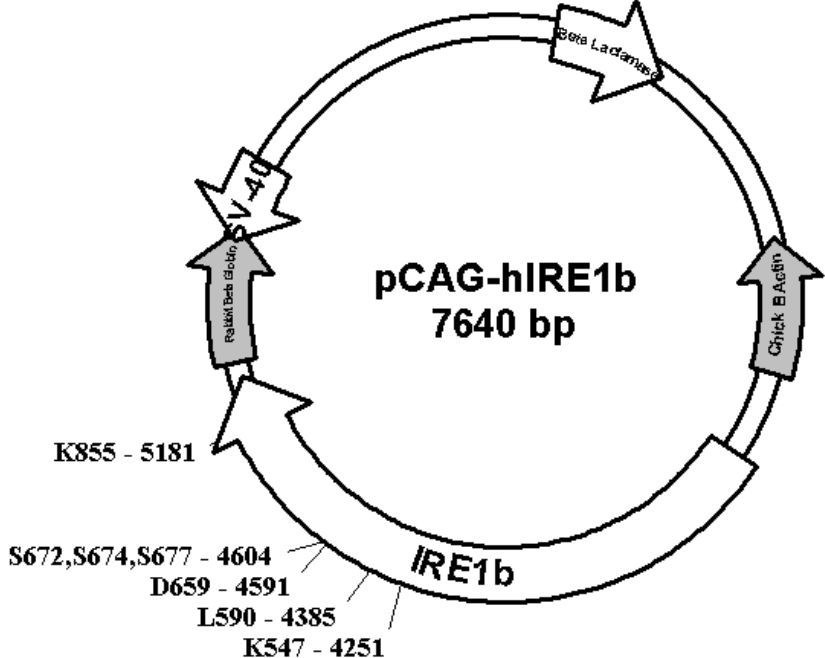


Figure 2. 3 - pCAG-hIRE1β-HA

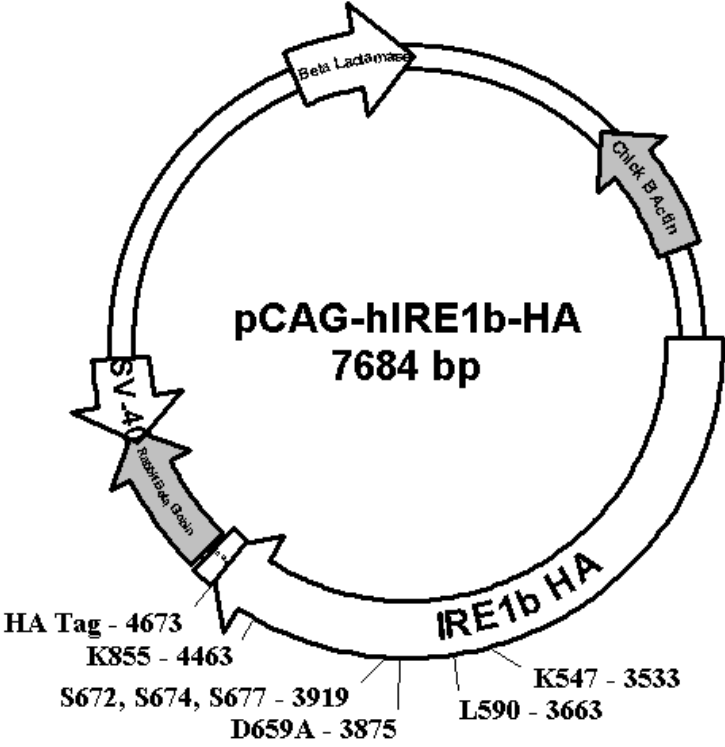


Figure 2. 4 – pTK-HSV-BP2-hIRE1α

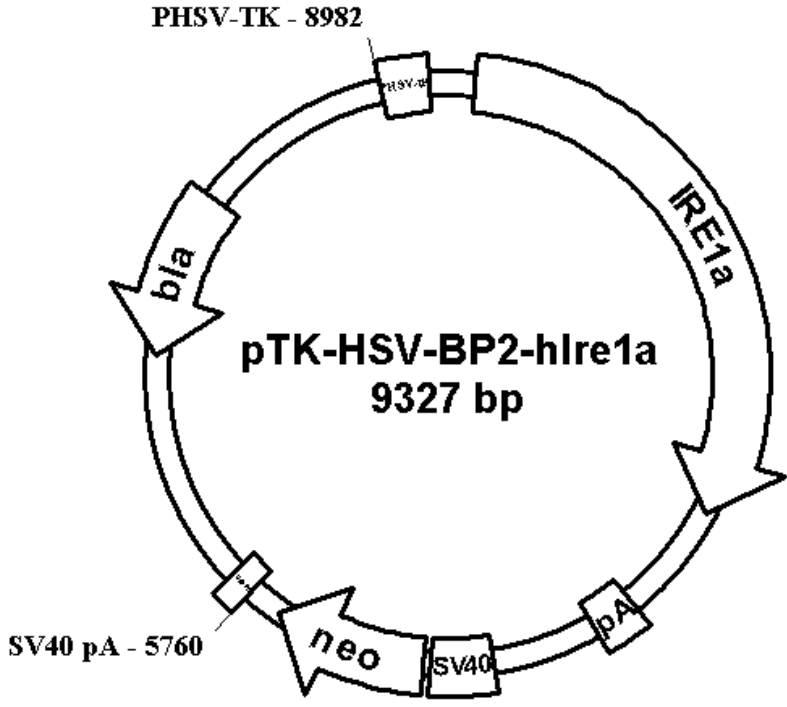


Figure 2. 5 – p TKRG-hIRE1β

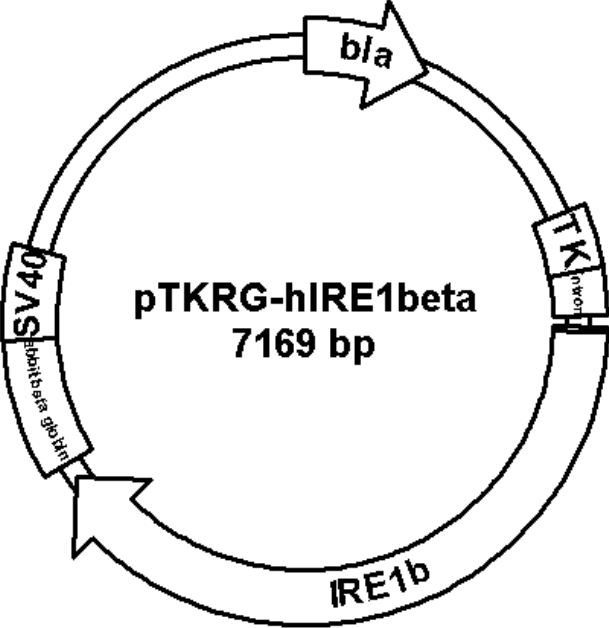


Figure 2. 6 – pEE12.4

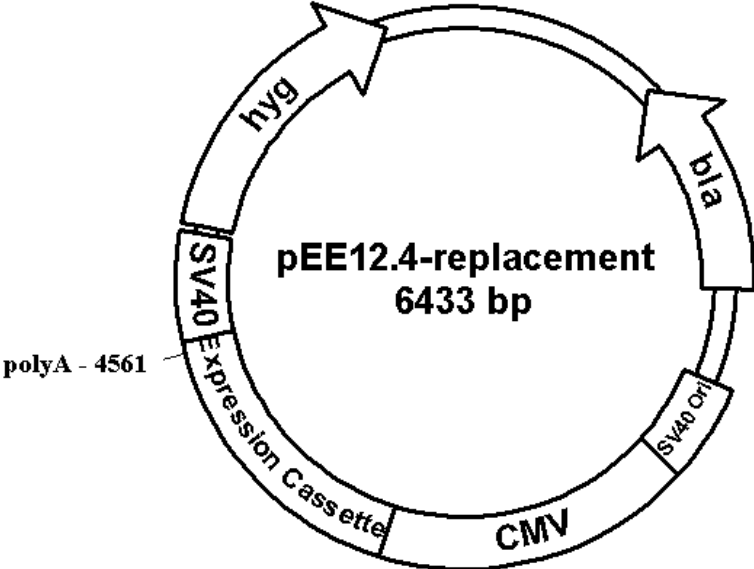


Figure 2. 7 – pEE12.4-U6

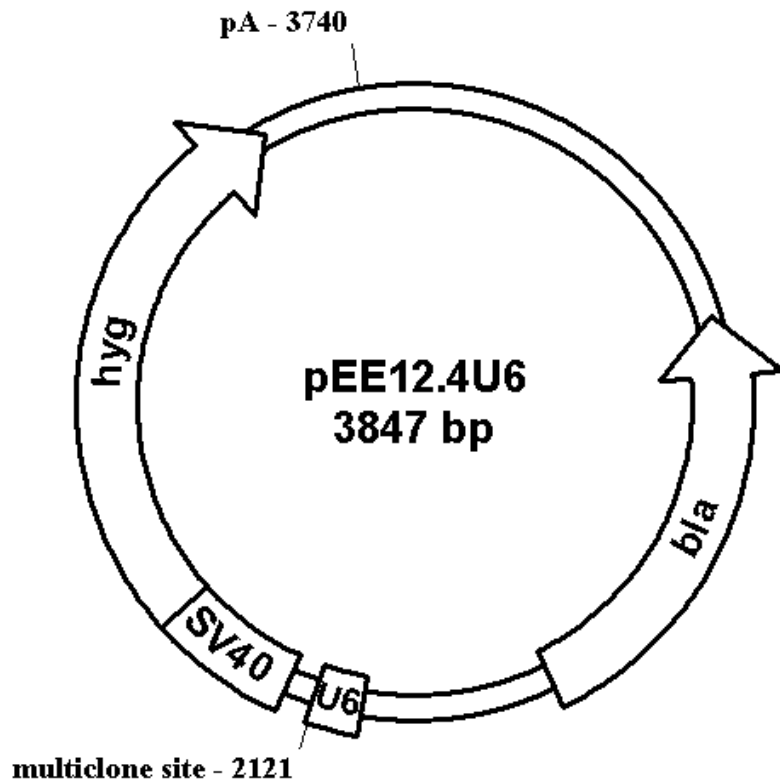


Figure 2. 8 – pUC18

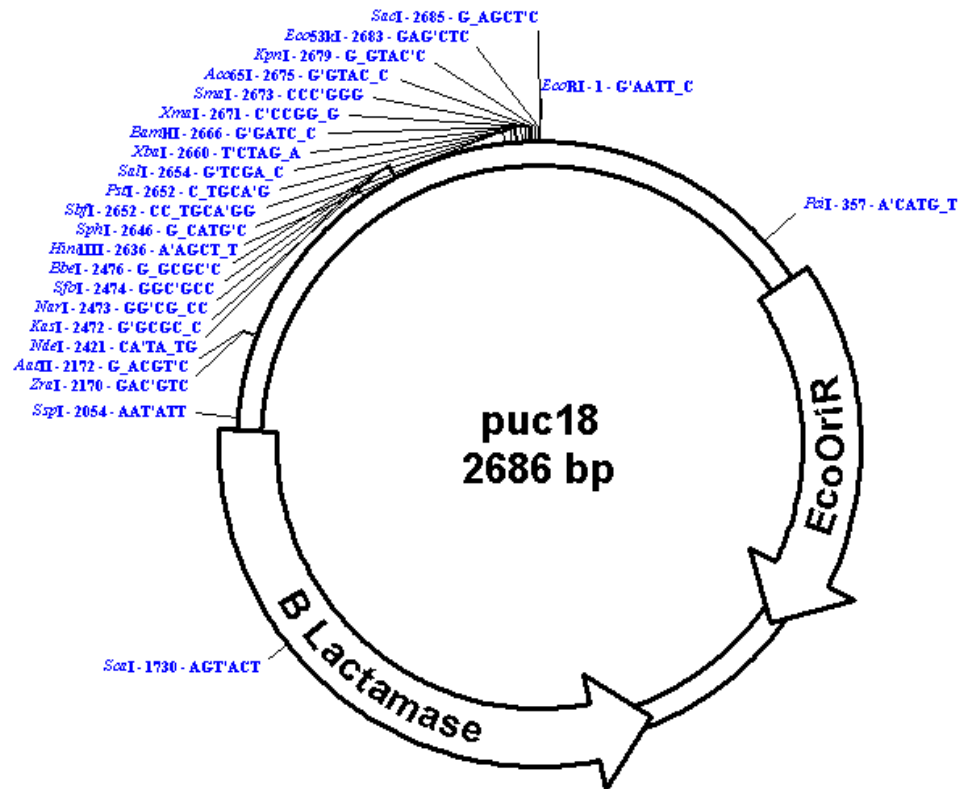


Figure 2. 9- pUC18-hIRE1 β

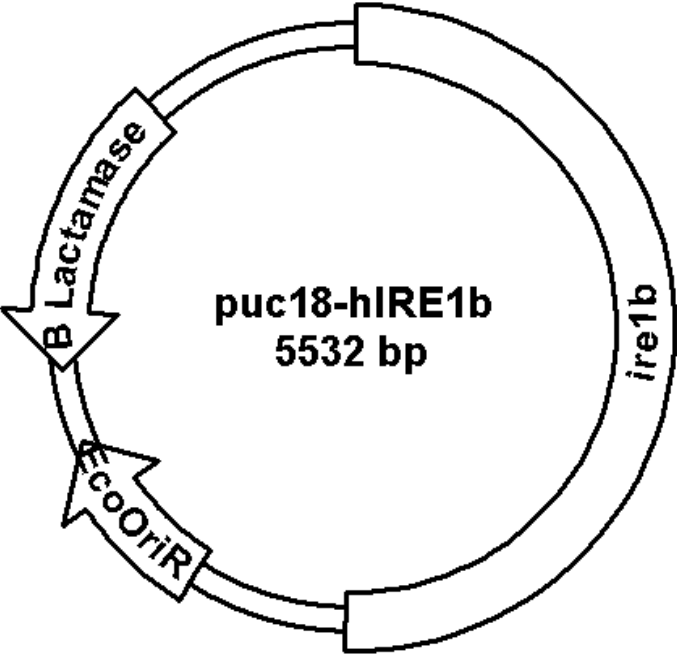


Figure 2. 10 – pDJB134

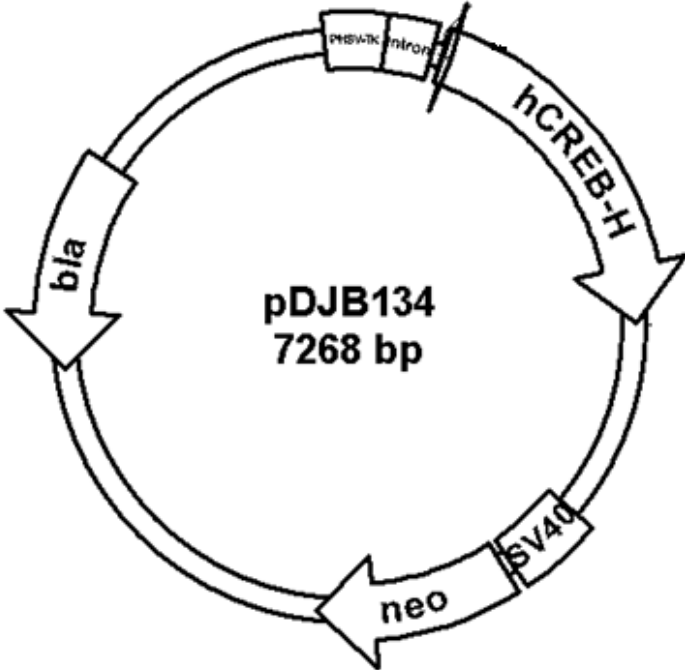
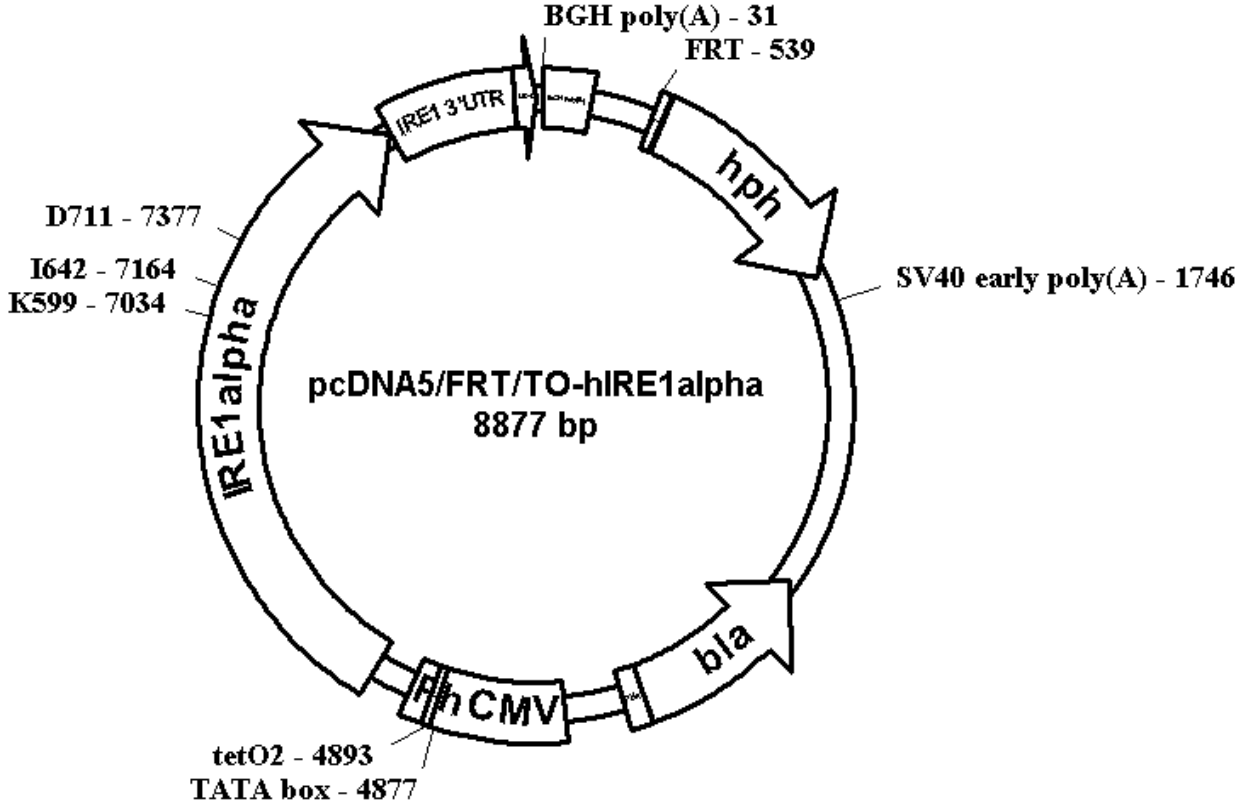


Figure 2. 11 – pcDNA5/FRT/TO-hIRE1 α



2.4 Antibodies

Table 2.13 - Antibodies

Name	Type	Source	Catalogue No.	Lot No.
Anti-eIF2 α	Primary	Santa Cruz Biotechnology Inc/ Insight Biotechnology Ltd, Wembley, UK	sc-11386	G1309
Anti-GAPDH	Primary	Sigma-Aldrich, Gillingham, UK	G8795	028K4859
Anti-HA	Primary	Sigma-Aldrich, Gillingham, UK	H8908-2ml	118K4800
Anti-human IgG kappa HRP conjugate	ELISA Conjugate	US Biological/Stratech Scientific, Newmarket, UK	11903-37P	L10073010
Anti-IRE1 α	Primary	Abcam, Cambridge, UK	ab37073	870410
Anti-IRE1 α	Primary	Cell Signalling Technology/ New England Biolabs, Hitchin, UK	3294S	4
Anti-IRE1 α	Primary	Sigma-Aldrich, Gillingham, UK	I6785	128K4827
Anti-IRE1 α phospho serine 724	Primary	Abcam, Cambridge, UK	ab481187	GR1571-2
Anti-IRE1 α phospho serine 724	Primary	Novus Biologicals, Novus Europe, Cambridge, UK	NB100- 2323H	I

Anti-IRE1 β	Primary	Prestige Antibodies/ Sigma-Aldrich, Gillingham, UK	HPA016558	R06214
Anti-JNK (TJNK)	Primary	Cell Signalling Technology/ New England Biolabs, Hitchin, UK	9258	6
Anti-PARP	Primary	Cell Signalling Technology/ New England Biolabs, Hitchin, UK	9542	9
Anti-peIF2 α	Primary	Cell Signalling Technology/ New England Biolabs, Hitchin, UK	9721	10
Anti-Phospho-JNK (PJNK)	Primary	Cell Signalling Technology/ New England Biolabs, Hitchin, UK	492515	11
Anti-Rabbit IgG	Secondary	Cell Signalling Technology/New England Biolabs, Hitchin, UK	7074	17,18
Donkey Anti-Rabbit	Secondary	ThermoFisher Scientific, Loughborough, UK	31458	117095904
Fab2 goat anti-human IgG Fc (product number).	ELISA Coating	Jackson ImmunoResearch Labs Inc/Strattech Scientific, Newmarket, UK	109 – 006 – 098	97700

Goat Anti-Mouse	Secondary	ThermoFisher Scientific, Loughborough, UK	31432	HF1010102
-----------------	-----------	---	-------	-----------

2.5 Chemically Competent *E. coli* Cells

Name	Source
XL10-Gold (Genotype - <i>TetrD(mcrA)183 D(mcrCB-hsdSMR-mrr)173 endA1 supE44 thi-1 recA1 gyrA96 relA1 lac Hte [F' proAB lacIqZDM15 Tn10 (Tetr) Amy Camr]</i>)	Produced in-lab (see Preparation of Chemically Competent <i>E. coli</i> , below)
XL-2 Blue (Genotype - <i>endA1 gyrA96(nal^R) thi-1 recA1 relA1 lac glnV44 F'[::Tn10 proAB⁺ lacI^q Δ(lacZ)M15 Amy Cm^R] hsdR17(r_K⁻ m_K⁺)</i>)	Stratagene/Agilent Technologies Wokingham, UK – Cat No. #20024
One shot TOP10 chemically competent cells (Genotype - <i>F- mcrA (mrr-hsdRMS-mcrBC) 80lacZM15 lacX74 recA1 ara139 (ara-leu)7697 galU galK rpsL (Str^R) endA1 nupG></i>)	Invitrogen Life Technologies Ltd, Paisley, UK – Cat No. C4040

2.6 Cell Lines

Table 2.14 - Cell Lines

Cell line	Source/Reference
<i>ire1a</i> ^{-/-} mouse embryonic fibroblasts	From R. Kaufman of the University of Michigan (Lee, Tirasophon et al. 2002).
<i>traf2</i> ^{-/-} mouse embryonic fibroblasts	From T. Mak, of the Campbell Family Institute for Breast Cancer Research, (Yeh, Shahinian et al. 1997).
Wild type mouse embryonic fibroblasts	From T. Mak, of the Campbell Family Institute for Breast Cancer Research, (Yeh, Shahinian et al. 1997).
<i>CHO Cell Line 33</i>	From Lonza Biologics, Slough, UK (Porter, Racher et al. 2010)
<i>CHO Cell Line 41</i>	From Lonza Biologics, Slough, UK (Porter, Racher et al. 2010)
<i>CHO Cell Line 42</i>	From Lonza Biologics, Slough, UK (Porter, Racher et al. 2010)
<i>CHO Cell Line 137</i>	From Lonza Biologics, Slough, UK (Porter, Racher et al. 2010)
<i>CHO Cell Line 159</i>	From Lonza Biologics, Slough, UK (Porter, Racher et al. 2010)
<i>CHO Cell Line Null</i>	From Lonza Biologics, Slough, UK (Porter, Racher et al. 2010)
<i>CHO Cell Line Host.</i>	From Lonza Biologics, Slough, UK (Porter, Racher et al. 2010)
<i>T-Rex</i> TM -293	Purchase from Invitrogen, Paisley UK
<i>Flp-In</i> TM 293 - <i>Fv2e-C'hIRE1</i>	Invitrogen, Paisley UK. (Cat no. R75007) Stably transfected with C-Terminal human IRE1 chimerically fused to a Fv2e dimerisation domain by David Cox, Durham University.
<i>Flp-In</i> TM - <i>CHO</i>	Invitrogen, Paisley UK (Cat no. R758-07).

2.7 Commercially Available Kits

Table 2.15 - Commercially Available Kits

Name	Purpose	Source	Protocol Version
DC Protein Assay	Protein	Biorad, Hemel	LIT448 Rev D

	quantification	Hempstead, UK	
ECL Plus Western Blotting Detection Reagents	Western blot luminescence detection	Amersham Biosciences/ GE Healthcare, Chalfont St. Giles, UK	RPN2132PL Rev-B, 2002
EndoFree Plasmid Maxi Kit	Large volume DNA preparation	Qiagen, Crawley, UK	Third Edition, November 2005
EZ-RNA kit	RNA Harvesting	Geneflow Ltd., Fradley, UK.	Dec 2003
RNA Easy Kit	RNA Preparation	Qiagen, Crawley, UK	Fourth Edition, September 2010
Miniprep Kit	Large volume DNA preparation	Qiagen, Crawley, UK	Second Edition, Dec 2006
FirstChoice® RLM-RACE Kit	RACE	Applied Biosystems/Ambion, Foster City, CA, USA	P/N 1700M Revision C, Revision Date: March 21, 2008
First Strand cDNA Synthesis Kit	Reverse transcription of cDNA from RNA	Invitrogen, Paisley, UK	18080400.pps 8-Oct 2004

Flp-In T-REx Core Kit pcDNA™ 5/FRT/TO expression vector	Generating stable cell lines	Invitrogen, Paisley, UK	Version D 111110 25-0366 Version G 11 November 2010 25-0368
GenElute™ Gel Extraction Kit	Purification of DNA from agarose gels.	Sigma-Aldrich, Gillingham, UK	SM/MAM 7/03
GenElute™ HP Plasmid Midiprep Kit	Preparation of Plasmid DNA from E. coli.	Sigma-Aldrich, Gillingham, UK	01911-502620 0019
GenElute™ PCR Clean-Up Kit	Purifying DNA.	Sigma-Aldrich, Gillingham, UK	CP/JWM 8/04
Gigaprep Kit	Large volume DNA preparation	Qiagen, Crawley, UK	May 2002
jetPRIME™	Transfection	Polyplus Transfection, Illkirch, France	4/12 CPT 114 vF May 2011
Lipofectamine 2000	Transfection	Invitrogen, Paisley, UK	Rev Date: 11 July 2006
Neon® Transfection System	Electroporation	Invitrogen, Paisley, UK	MP-100 Rev.M.03.51-11/07
pGEM Easy T Vector	Cloning of PCR products	Promega, Southampton, UK.	Revision 2/09
QIAquick PCR Purification Kit	Purifying DNA.	Qiagen, Crawley, UK	March 2008

QuikChange® II XL Site-Directed Mutagenesis Kit	Mutagenesis	Agilent Technologies, Wokingham, UK	200521-12 Revision B
Rediprime™ II DNA Labeling System	Southern blotting (Probe labelling).	GE Healthcare, Chalfont St. Giles, UK	RPN1633PC Rev C 04-2008
RNasein	RNase inhibitor	Promega, Southampton, UK.	See First Strand Synthesis protocol.
TOPO TA Cloning kit	Cloning of PCR products	Invitrogen, Paisley, UK	Version O 10 April 2006 25-0276
3,3', 5,5' tetramethylbenzidine (TMB) Liquid Substrate System	ELISA	Sigma-Aldrich, Gillingham, UK	alc 10/99

2.8 Specialist Equipment

Item	Code	Manufacturer
Mr Frosty Cryo Freezing	5100-0001	Nalgene/ ThermoFisher Scientific, Loughborough.
6 well plates	83.1839.300	Sarstedt, Leicester, UK
24 well plates	83.1836.300	
96 well plates	83.1835.300	
25cm ² flask (Adherent)	83.1810.002	Sarstedt, Leicester, UK
25cm ² flask (Suspension)	83.1810.500	
75cm ² flask (Adherent)	83.1813.002	
75cm ² flask (Suspension)	83.1813.500	

75cm ² flask (Adherent)	83.1812.002	
75cm ² flask (Suspension)	83.1812.500	
PVDF membrane, pore size 0.45 µm	RPN303F	GE Healthcare, Chalfont St. Giles, UK
Kodak BioMax MS	Z363049	ThermoFisher Scientific, Loughborough, UK
96 well Maxisorp ELISA plates	475094	Nunc/ThermoFisher Scientific, Loughborough, UK
Abgene adhesive plate seals	AB-0580	ThermoFisher Scientific, Loughborough, UK

3. METHODS

3.1 Cell Culture

All cells were incubated at 37°C with 5% (v/v) CO₂ at 95% humidity. Appropriate antibiotics were added to medium as required in stable cell line production.

3.1.1 Revival

Cryovials containing cells were stored either in -140°C freezer or liquid nitrogen cryostorage vessels. The cryovial was removed from storage and incubated at room temperature for approx 1 min and then warmed in a 37° C water bath for 1-2 min, submerging only 2/3 of the vial into the water bath to prevent contamination and shaking continuously, but gently, until the cells were completely thawed. The cryovial was wiped dry with a tissue and then cleaned with 70% (v/v) ethanol before introduction into the tissue culture hood. Using a 2ml pipette, the contents of the cryovial was pipetted drop by drop into a 50ml falcon tube. 10-50ml of the appropriate culture medium, pre-warmed was pipette onto the cells, which were then centrifuged at 110 g, 5 min, RT, to collect them on the bottom of the tube. The supernatant was aspirated and replaced with 5-10ml of appropriate fresh pre-warmed medium and mixed gently. The cell suspension was then transferred to a 25 cm² vented flask and incubated. Cells were checked daily to monitor their growth.

3.1.2 Cryopreservation

Table 3. 1- Cryopreservation media

Cell Types	Medium
<i>ire1a</i> ^{-/-} , <i>traf2</i> ^{-/-} , wild type MEFS, <i>Flp-In</i> TM -293- <i>Fv2e-C'hIRE1</i> HEK293s, <i>Flp-In</i> TM -CHO	90% FBS, 10% DMSO
CHO Cell Lines 33, 41, 42, 137, 159, Null, Host (serum-free adapted lines).	90% CD-CHO, 10% DMSO

1ml of the appropriate cryopreservation medium for the cell type was prepared and placed on ice. A cryovial labeled with the cell line, date and passage number was prepared. Where adherent cells were being frozen, they were removed from the flask surface with Trypsin-EDTA. Cells were counted with an Improved Neubauer haemocytometer, centrifuged and resuspended in the appropriate cryopreservation medium to give a concentration of $2-4 \cdot 10^6$ cells/ml. 1ml of cell suspension was pipetted into each vial. The cells were frozen at a slow cooling rate by placing them in the Mr Frosty Cryo Freezing Container (see “Specialist Equipment”) with 100% isopropyl alcohol (250 ml) added. The Cryo Freezing Container was then placed into a -80°C freezer for a minimum of 4 h and a maximum of 24 h. The individual vials were transferred to either a -140°C freezer or liquid nitrogen for long-term storage.

3.1.3 Trypsinisation

When passage was required, (cell confluence of $>90\%$ in flask) the medium was aspirated and replaced with 5ml of Dulbecco’s PBS and washed. The PBS was then aspirated cells were trypsinised for >1 min with 0.25% with 1ml Trypsin-EDTA (See “Cell Culture Media and Reagents”, above) and incubated for 1 min at 37°C . Trypsinisation was halted with an equal volume of the appropriate medium for the cell line (as above, “Table 2.6 - Cell Culture Media”).

3.1.4 MEF Culture

ire1 α ^{-/-} MEF cell lines were cultured in Dulbecco’s Modified Eagle’s Medium with 110 mg/l pyruvate, and with 10% (v/v) foetal calf serum and 2mM L-glutamine. Wild type and *traf2^{-/-}* MEF cell lines were cultured in Dulbecco’s Modified Eagle’s Medium with 10% (v/v) foetal calf serum and 2mM L-glutamine. Appropriate antibiotics were added to medium as required in stable cell line production.

3.1.5 CHO Culture

CHO cells were cultured in CD-CHO medium supplemented with $25 \mu\text{M}$ MSX . Flp-In™-CHO were cultured in Dulbecco’s Modified Eagle’s Medium without pyruvate, and with 10% foetal calf serum and 2mM L-glutamine added. If suspension CHO cells grown in CD-CHO were required to be made adherent for purposes of transfection, they were transferred to adherent

flasks and cultured in Dulbecco's Modified Eagle's Medium without pyruvate, containing 10% foetal calf serum and 2mM L-glutamine and trypsinisation was as described above.

3.1.6 HEK293 Culture

HEK293 cells were cultured as MEFs, but were grown in Dulbecco's Modified Eagle's Medium with 10%(v/v) foetal calf serum and 2mM L-glutamine.

3.1.7 Stable Cell Line Production

Stable cell lines production was performed according to the protocol in the Invitrogen "Flp-In T-REx Core Kit" Manual.

3.1.7.1 Antibiotic Tolerance

ire1 α ^{-/-} MEFs were exposed to varying concentrations of zeocin, blasticidin or hygromycin by addition to their growth medium and incubated for 14 days and the viable cells counted to ascertain a concentration of antibiotic that was not immediately lethal, but that killed all non-stably transfected cells within 14 days.

3.1.7.2 Transfection with pFRT/lac/Zeo or pcDNA6/TR

As recommended in Flp-In™ manual, the pFRT/lac/Zeo or pcDNA6/TR plasmid was linearised by digestion with the restriction enzyme *ScaI* or *BtZ171/Bst1107I* respectively. The digestion reaction was run on a gel and purified using the GenElute™ Gel Extraction Kit. 2ug of the linearised pFRT/lac/Zeo or pcDNA6/TR plasmid was then transfected into *ire1 α ^{-/-}* cells using an electroporator and the cells were grown for 24 hours to recover from transfection. The medium was then removed, the cells washed, and replaced with medium containing 10µg/ml zeocin or blasticidin respectively. The stably transfected cells were incubated for 14 days with zeocin until colonies of stably transfected cells began to form, and then grown until the colonies approached confluence and would normally have been passaged.

3.1.7.3 Storage of Stable Clones

Frozen stocks of the mixed population of transfectants were made as described in Materials and Methods – “Cell Culture – Cryopreservation” and one passage was continued for limited dilution cloning using 96 well plates (See “Specialist Equipment”) as described in Materials and Methods – “Limited Dilution Cloning”.

3.1.7.4 Co-Transfection with pcDNA5-FRT-TO-hIRE1 α / pOG44

Clone 4,3 was used for the final cell line production and transfection as it exhibited the best response in the tet-repressor function assay above. As recommended by the Flp-In manual, 1×10^6 cells from the line 4,3 were electrotransfected with 2 μ g of the required *pcDNA5-FRT-TO-hIRE1 α* construct and 20 μ g of pOG44 (1:10). Cells were grown for 24 hours to allow recovery from transfection before application of hygromycin medium. A lower dose of 25 μ g/ml was applied for the first 24 hours after recovery to allow the cells to acclimatise to the hygromycin, as during the production of other cell lines in our laboratory by David Cox, it had been found that this increased the likelihood of successfully gaining viable clones. After this period, the full selection concentration of 100 μ g/ml was applied. After six days of this treatment all non-transfected cells and colonies of stably transfected cells were growing. Frozen stocks of the transfectants were made as described in Materials and Methods – “Cell Culture – Cryopreservation” and one passage was continued for characterisation in the following chapter.

3.1.8 Transfection - Electroporation

Mouse embryonic fibroblasts were grown in a 75cm² flask (See “Specialist Equipment”) until confluent at a density of 9×10^6 cells. The cells were washed with PBS and trypsinised with 1ml trypsin-EDTA and incubated for 1 min at 37°C. Trypsinisation was halted with an equal volume of medium (as above, “Cell Culture”) and the solution was aspirated and centrifuged at 110 g for 2 min. The medium was removed and the cells were resuspended in PBS and counted with an Improved Neubauer haemocytometer. 1×10^6 cells were removed per transfection, centrifuged at 110 g for 2 min and the PBS removed. Cells were resuspended in Buffer R and transiently transfected according to the Digital Biotech (Seoul, Korea)/Invitrogen Microporator protocol (Protocol Reference: MP-100 Rev.M.03.51-11/07) with 0.2-8 μ g of plasmid DNA

using the Digital Biotech Microporator MP-100. Transfected cells were immediately transferred into medium and grown at 37°C.

3.1.9 Transfection – Jetprime

HEK293 cells were seeded at $0.05\text{-}0.2 \times 10^6$ cells per 0.5-2ml of appropriate growth medium into either 6-well or 24-well plates (See “Specialist Equipment”) as required and grown for 24 h or until confluent at a density of 60-80% at time of transfection. 0.25-2µg of DNA, 0.5-4µl of jetPRIME™ (DNA:Jetprime ratio 1:2) and 50-200µl of jetPRIME™ buffer per transfection were mixed to produce the reaction mixture and mixed by vortexing, then centrifuged briefly at 14000g. The reaction was incubated for 10 min at room temperature. The reaction mix was added to the cells with growth medium drop by drop and gently rocked from side to side to mix. Cells were incubated at 37°C for 4h and then the medium replaced. Analyses were performed 24h after transfection.

3.1.10 Transfection - Lipofectamine

CHO cells were seeded at 0.15×10^6 per 0.5ml of appropriate growth medium into 24-well plates as required and grown for 24 h at 37°C or until confluent at a density of 60-80% at time of transfection. Before transfection, seeding medium was replaced with 800µl fresh prewarmed medium and incubated at 37°C for at least 30 min. During the incubation, DNA and lipofectamine was prepared. 2µg of DNA per transfection was mixed with 100µl of Optimem (See “Cell Culture Media”, above) and incubated for 5 min. 5µl of Lipofectamine were mixed with 100µl of Optimem and incubated for 5 min. After the 5 min incubations, the two mixtures were combined and the Optimem-DNA-Lipofectamine incubated together for 20 min. The cell culture medium was removed from the cells and replaced with the Lipofectamine mixture and incubated for 2-3 days, or until the appropriate amount of time for the time course conducted had elapsed.

3.1.11 Induction of endoplasmic reticulum stress with tunicamycin, thapsigargin or DTT

Endoplasmic reticulum stress was induced by treatment with 100nM-1µM thapsigargin, 100ng-1µg/ml tunicamycin (Calbiochem/VWR, Lutterworth, UK) or 10mM DTT (Sigma Aldrich, Gillingham, UK). Medium was removed from cells and replaced with medium containing the

ER stressor. Cells were incubated at 37°C for 1-2hr or whichever time was appropriate for the experimental time course.

3.1.12 Assessment of Transfection Efficiency/Cell Death

Transfection efficiency was assessed by GFP fluorescence by eye, and living versus dead cells were stained with trypan blue 0.4% (v/v) (see “Cell Culture Media and Reagents”) and counted with an Improved Neubauer haemocytometer.

3.1.13 Limited dilution cloning

Limited dilution cloning was performed according to the methodologies in papers by Collier and Lefkovits (Lefkovits 1979; Collier and Collier 1986). Cells were transfected with 2ug of the DNA to be stably integrated and grown under the appropriate antibiotic selection conditions for >14 days in order to remove all transiently transfected cells. At least three vials of the mixed transfection were frozen for a back-up stock according to the above protocols. Sufficient cells of the mixed population were grown for the cloning ($\sim 1 \times 10^6$) and trypsinised where required to remove them from culture vessels. Cells were diluted to a concentration of either 10, 3 or 1 cells per 50 μ l of the appropriate growth medium. Three 96 well cloning plates were set up, one for each dilution. 50 μ l of each dilution were dispensed into the appropriate 96-well plate and grown for at least 14 days or until it was clear whether or not cells were growing in each individual well. The percentage of wells with growth was assessed and the probability of their arising from single clones assessed according to Table 3. 2 below. If no plates had <10% of wells containing cells, the experiment was repeated with lower dilutions, 1 cell/well, 0.3 cells/well and 0.1 cells/well. If less than 10% of wells exhibited growth, each well colony was trypsinised and removed from its well and subcultured into a 24 well plate. Once confluence was achieved in a 24 well plate, the cell cultures were scaled up to larger plates as required until sufficient cells had been achieved for freezing stocks. At least three vials of each clone were frozen and those exhibiting the best growth characteristics selected for further testing.

Table 3. 2 - Probability that wells showing growth have arisen from one (1/R), two (2/R), three (3/R), four (4/R) or five (5/R) stably transfected cells.

Wells showing growth [%]	Mean no. of transfected cells/well at inoculation	1/R	2/R	3/R	4/R	5/R
1	0.01	0.995	0.004			
5	0.05	0.975	0.024			
10	0.10	0.950	0.047	0.001		
15	0.16	0.922	0.073	0.003		
20	0.22	0.894	0.099	0.007		
25	0.29	0.861	0.124	0.012		
30	0.35	0.835	0.146	0.017	0.001	
35	0.43	0.800	0.172	0.024	0.002	
40	0.51	0.766	0.195	0.033	0.004	
45	0.61	0.725	0.221	0.044	0.006	
50	0.69	0.694	0.239	0.055	0.009	0.001
55	0.80	0.652	0.261	0.069	0.013	0.002
60	0.91	0.613	0.278	0.084	0.019	0.003
65	1.05	0.565	0.296	0.103	0.027	0.005
70	1.20	0.517	0.310	0.124	0.037	0.008
75	1.39	0.461	0.320	0.148	0.051	0.014
80	1.61	0.402	0.329	0.179	0.069	0.022

3.2 Bacterial culture

3.2.1 Chemical transformation of *E. coli*

Table 3. 3 – Protocol Details for Chemical Transformation

Cell Type	Tube Size	Cell Volume	Heat Shock for	Incubation on ice	Culture Medium
XL-10 Gold	14ml	100 μ l	90s	5min	900 μ l LB with 20 mM D-glucose
XL-2 Blue	1.5ml	50 μ l + 1 μ l of β -	30s	2min	0.9ml of NZY+

Ultracompe -tent Cells		mercaptoethanol			broth preheated to 42°C
TOP10	1.5ml	50 µl	30s	2min	250µl of S.O.C. medium pre-warmed to room temperature

Standard Protocol

Competent cells were removed from a -80°C freezer and immediately put on ice where they were allowed to thaw. Up to 5µl of DNA was added to the appropriate size of tube for the cell type (see Table) and put on ice. Once competent cells were thawed, they were mixed carefully by swirling every 2 min. The appropriate volume (see Table 3. 3 – Protocol Details for Chemical Transformation , above) of competent cells were carefully added to the DNA, pipetting slowly to avoid the production of bubbles/over-agitation of the cells, and mixed briefly by flipping, then incubated on ice for 30 min. At the end of the incubation period tubes were placed into a rack and heat shocked in a 42°C waterbath for the appropriate number of seconds without moving the tubes, and then placed on ice for X mins as listed in the table above. X µl of the appropriate culture medium was added to each tube and incubated at 37°C with shaking at ~250 rpm for 1h. 200 µl cell suspension was plated onto LB-ampicillin 100 µg/ml agar plates. Plates were incubated in a 37°C incubator overnight.

The following solutions were used as controls for transformation: 5 µl water (negative control) to determine if contamination of materials gives rise to undesired colonies and 1 µl pUC18 at 10ng/µl (positive control) to ensure success of transformations.

3.2.2 Revival of *E. coli* cultures

A cryotube containing frozen stock was removed from the -80°C freezer and placed on dry ice. The frozen cell suspension was scraped with a pipette tip to loosen some ice (~10-20 µl) and streaked onto an LB-ampicillin agar (100 µg/ml) plate. The plate was incubated in a 37°C incubator overnight.

3.2.3 Growth of *E. coli* cultures

LB-broth was added to sterile Erlenmeyer flasks at least twice as big as the intended culture volume while working close to the flame of a Bunsen burner. Ampicillin was added to the broth

to a final concentration of 100 µg/ml. The broth was then inoculated with a single *E. coli* colony from a LB-agar plate or a fresh saturated overnight culture was diluted 1:100 into the new medium, after washing three times with 1ml sterile H₂O. Cultures were incubated with shaking at 225 – 250 rpm at 37°C overnight.

3.2.4 Production of frozen *E. coli* stocks.

1ml of 30% (v/v) glycerol was pipetted into each of two labelled cryotubes. *E. coli* cultures grown as described above were resuspended by vortexing and 1ml was added to each cryotube. The cryotubes were then mixed by inverting and flash-frozen by immersion in liquid nitrogen. Cryotubes were stored in a -80°C freezer until required for revival.

3.2.5 Preparation of chemically competent *E. coli*.

4 ml of LB broth was inoculated with one colony of *E. coli* cells from a fresh LB agar plate and grown >16 h at 37°C with shaking at 225 rpm. The overnight culture was diluted 1:100 into LB broth and incubated at 37°C with shaking at 225 rpm. After ~1 h, the absorbance at 600nm of the culture was measured every 15 - 30 min until it reached 0.3 – 0.4 A_{600 nm}. The culture was transferred to a centrifuge tube precooled on ice and centrifuged for 10 min at 1,000 g and 4°C to collect the cells. The supernatant was decanted off, and the cells resuspended by gentle shaking and resuspended in 1/10 of the original culture volume of ice-cold 1 x TSS. Cells were aliquoted at 500µl into ice-cold 1.5 ml microcentrifuge tubes and snap-frozen in liquid nitrogen. Cells were stored at -70°C.

3.3 Protocols for preparation/use of DNA

3.3.1 Preparation of DNA from *E.coli* culture by mini/midi/maxi/gigaprep and ethanol precipitation of nucleic acids

3.3.1.1 Plasmid Miniprep

4ml of LB broth with 100µg/ml ampicillin was inoculated with one colony *E. coli* cells as described in “Growth of *E. coli* cultures”. 1ml of the fresh overnight culture was transferred into a 1.5 ml microcentrifuge tube. The remainder of the culture was stored at 4°C. The cells

were collected by centrifugation for 1 min at 14,000 g at room temperature and the supernatant removed. The cells were centrifuged at 14,000 g again to collect the remaining supernatant which was aspirated. The cell pellet was resuspended in 100 μ l 1xGTE and mixed by pipetting up and down, then incubated at room temperature for 5 min. 200 μ l 0.2 N NaOH, 1% (w/v) SDS was added to lyse the cells. It was then agitated gently by inverting the tubes 4-6 times to prevent nicking of genomic DNA. The solution was then incubated on ice for 3-5 min. Then the reaction was neutralised by addition of 150 μ l ice-cold 5 M KOAc (pH 4.8), and mixed gently by inverting the tube 4-6 times. The solution was incubated 5 min on ice, centrifuged for 5 min at 14,000 g, 4°C and the supernatant transferred into a new microcentrifuge tube, ensuring not to remove any flocculent material with it. The supernatant was centrifuged again at 14,000 g, 4°C to remove any remaining flocculent material. The remaining supernatant was removed and transferred into a new microcentrifuge tube, and mixed with 800 μ l of 100% ethanol by inverting the tube 2-3 times. The mixture was incubated at room temperature for 2 min, then centrifuged for 1 min at 14,000 g. The supernatant was removed and discarded, and replaced with 1 ml of 70%(v/v) EtOH. The solution was centrifuged for 1 min at 14,000 g, RT (18-24°C), and the supernatant removed and discarded. The remaining pellet was centrifuged again for 10-15 s at 14,000 g at room temperature and the remaining ethanol supernatant removed. The DNA pellets were air-dried for no more than 5 min at room temperature to prevent over-drying. Dry pellets were resuspended in 33 μ l of 1x TE (pH8.0), with 0.3 mg/ml RNase A and incubated at 4°C until dissolved for up to 30 min. DNA was quantified on a Molecular Devices Spectramax Spectrophotometer and the concentration confirmed by DNA gel electrophoresis.

3.3.1.2 Plasmid Midi/Maxi/Gigaprep

Preparation of DNA from the appropriate volume of culture in LB-ampicillin medium was performed according to the instructions in the Sigma/Qiagen Kits listed above in “Commercially Available Kits”. If further concentration of DNA was required, the following protocol was followed:

0.1 Volume of 3 M NaOAc (pH 5.2) was added to the nucleic acid sample in a 1.5 ml microcentrifuge tube and mixed well. Based on the new volume of the sample 2.5 volumes of EtOH at -20°C were added to the sample and mixed well. The precipitations were incubated for ≥ 30 min at -70°C or ≥ 1 h at -20°C. Then the nucleic acid precipitate was sedimented by

centrifugation at 15,000 g, 4°C for 30 min. The supernatant was aspirated and 1 ml 70% (v/v) EtOH was added. The nucleic acid precipitate was sedimented again by centrifugation at 15,000 g, 4°C for 10 min and the supernatant aspirated. The solution was centrifuged for 10-20 s at 15,000 g, room temperature and the remaining liquid aspirated. Then the pellet was air-dried by incubating the open tubes for 5 min at room temperature. 10-50 µl of TE (pH 8.0) was added and samples were placed at 4°C to dissolve nucleic acid. DNA was quantified on a Molecular Devices Spectramax Spectrophotometer and confirmed by DNA gel electrophoresis.

3.3.2 DNA agarose gel electrophoresis

An adequate volume of TAE was prepared to fill the electrophoresis tank and to prepare the gel. 0.3-1.5g of electrophoresis-grade agarose, dependent upon gel size was placed into an Erlenmeyer flask and dissolved in 30-150 ml TAE to produce a 0.9%(w/v), 1%(w/v) or 2% (w/v) agarose gel. The agarose was dissolved in a microwave oven at the highest power setting for 1 – 5 min, swirling every ~30 to 60 s to ensure even mixing and to avoid boiling over of the agarose solution. The agarose solution was allowed to cool to below 40°C, and ethidium bromide was added to 0.5 µg/ml to the agarose solution, and mixed. The gel casting platform was sealed at the open ends with masking tape. The dissolved agarose was poured in and a gel comb inserted. After the gel had solidified, walls were removed from the open ends of the gel platform and the gel comb withdrawn. The gel casting platform containing the set gel was placed into the electrophoresis tank. Sufficient electrophoresis buffer to cover the gel to a depth of about 1 mm was added. The required amount of DNA diluted 1:10 in 1:9 DNA loading buffer (1µl DNA, 1µl loading buffer, 9µl water) was added to the wells using a pipette. A DNA ladder marker (1Kbp DNA Ladder, Promega, Southampton, UK Code: G5711) was added to the first well of each gel at the same proportions as the DNA/Buffer/Water mix. Field strengths of 1-1.5V/cm were applied to the gel. Once the DNA had migrated to the required distance (judged by migration of the loading dye), the DNA was visualized under a UV transilluminator using UV light at 302nm for DNA bands.

3.3.3 Polymerase chain reaction (PCR) for insert construction

The following components were combined in a 100 µl PCR tube.

1.25 units of *Pfu* Polymerase

3 μ l 25 mM MgCl₂
 5 μ l 2 mM dNTP
 1 μ M of primer 1
 1 μ M of primer 2
 1 μ l of template DNA at 0.5 μ g
 5 μ l of 10x *Pfu* polymerase buffer.
 H₂O to 50 μ l

and subjected to the following conditions in the thermocycler:

Table 3. 4 - Thermocycler conditions for PCR for insert construction

Temperature	Time	No. of Cycles
95°C	2 min	1
95°C	30 s	35
60.5°C	30 s	
72°C	2 min 39 s	
72°C	5 min	1
4°C	∞	1

3.3.4 Cloning of PCR products with cloning vectors pGEM Easy T and TOPO TA cloning kit

In all cases, see “Oligodeoxynucleotide Primers” for sequences of vector primers

The Promega pGEM Easy-T Vector was used according to the protocol listed above (“Commercially Available Kits”). PCR products requiring cloning were separated on an agarose gel, excised and purified from the gel using the GenElute™ Gel Extraction Kit (ibid.) then DNA concentration was measured using the Molecular Devices Spectramax Spectrophotometer. The DNA was used in the following ligation reaction.

3 μ l PCR Product

5 μ l 2x Rapid ligation buffer

1 μ l pGEM Easy-T Vector (50ng)

1 μ l T4 DNA Ligase (at 1-3u/ μ l)

The reaction was incubated >16h at 4°C. 5 μ l of the reaction mixture was chemically transformed into *E. coli* cells according to the protocol above (3.1.1. “Chemical Transformation of *E. coli*”) and plated on to LB agar + 50 μ g/ml ampicillin + 80 μ g/ml X-Gal + 500 μ M IPTG

plates. Blue/white colonies were counted, and white colonies selected using a pipette tip for colony PCR. The following mix was prepared:

- 10µl 5x Promega GoTaq Buffer
- 5µl 2mM dNTPs
- 0.5µl T7 Sequencing Primer for pGEM Vector at 100µM
- 0.5 µl SP6 Sequencing Primer for pGEM Vector 100µM
- 0.5µl Promega GoTaq Polymerase
- 3µl 25mM MgCl
- Sterile H₂O to 50µl

White colonies selected were briefly dipped in the PCR mix and then placed in 4ml of LB broth + 50 µg/ml ampicillin and grown >16 h at 37°C with shaking at 225 rpm. Inoculated PCR mixtures were subjected to the following PCR protocol.

Table 3. 5 - Thermocycler conditions for cloning vector PCR

Temperature	Time	No. of Cycles
94°C	2 min	1
94°C	15 s	30
55°C	15 s	
72°C	1 min	
4°C	Until required	1

PCR products were run on a 1% (w/v) agarose gel (3.2.2 DNA agarose gel electrophoresis) and those producing a band of a correct length compared the original PCR product were selected for DNA preparation by miniprep (3.2.1 “Preparation from E.coli culture...of nucleic acids”) and sequencing.

The TOPO TA cloning vector was used according to the protocol listed above (“Commercially Available Kits”). PCR products requiring cloning were separated on an agarose gel, excised and purified from the gel using the GenElute™ Gel Extraction Kit (ibid.). The DNA concentration and purity was measured using the Molecular Devices Spectramax

Spectrophotometer (OD at 260nm, OD₂₆₀/OD₂₈₀ ratio). The DNA was used in the following ligation reaction:

4µl PCR Product

1µl Salt solution (1.2 M NaCl, 0.06 M MgCl₂).

1µl TOPO Vector (10 ng/µl plasmid DNA in: 50% glycerol, 50 mM Tris-HCl pH 7.4 (at 25°C),

1 mM EDTA, 1 mM DTT, 0.1% Triton X-100, 100 µg/mL BSA, phenol red)

Chemical transformation, into TOP10 Chemically competent *E. coli* cells, colony selection and colony PCR, and agarose gel run of products was performed as above. Colony PCR used the following PCR mix and PCR conditions as above.

5µl 10x Accuprime PCR BufferI

0.5µl Primer M13 R 100µM

0.5 µl Primer M13 F 100µM

0.2µl (1unit) Accuprime *Taq*

42.µl H₂O (to 50µl)

3.3.5 Restriction enzyme digestion

Restriction enzyme digest was performed according to the appropriate protocols recommended by the manufacturer. If cleanup was required after the enzymatic digest, it was either purified with a GenElute™ PCR Clean-Up Kit or the reaction was run on an agarose gel as described above and purified from the gel using a GenElute™ Gel Extraction Kit.

3.3.6 10µl reaction (Small volume, for test digests)

Xµl 100ng-1µg DNA

1µl 10x restriction enzyme buffer

1µl restriction enzyme at 10units/µl

H₂O to 10µl

3.3.7 50µl Reaction (Large volume for harvesting digest products)

Xµl 10-50ug DNA

5µl 10x restriction enzyme buffer

10units/1µl-50units/5µl Restriction Enzyme (Recommended amounts not exceeded in case of star activity)

H₂O to 50µl

Digestion is 1hr-Overnight depending on whether enzymes suffered from star activity/loss of specificity upon too long a digest.

3.3.8 Dephosphorylation of DNA 5' termini with calf intestinal alkaline phosphatase (CIAP).

The following components were combined in a 100 µl PCR tube:

1-10 µg of DNA

5 µl CIAP reaction buffer

1 µl 0.01U/µl CIAP

H₂O to 50 µl

and mixed well by flipping the tube. Tubes were briefly centrifuged in a microcentrifuge to collect all liquid at the bottom of the tube, and incubated at 37°C for 30 min. After the incubation, an additional 1 µl 0.01U/µl of CIAP was added and the sample was incubated for another 30 min at 37°C.

3.3.9 DNA ligation with T4 DNA ligase

3.3.9.1 Standard method

The following components were combined in a 100 µl PCR tube:

33-50 ng of vector DNA

Insert DNA at a 1:1 or 1:3 molar ratio, calculated as follows:

$((\text{ng vector}) \times (\text{kb size of insert})) / (\text{kb size of vector}) \times (\text{molar ratio of (insert/vector)}) = (\text{ng insert})$

e.g. $((50\text{ng}) \times (0.5\text{kb})) / (6\text{kb}) \times (3/1) = (12.5\text{ng insert})$

2 µl of T4 DNA ligase buffer

1 µl of T4 DNA ligase

H₂O to 20 µl

and mixed well by flipping the tube. Tubes were briefly centrifuged in a microcentrifuge to collect all liquid at the bottom of the tube, and incubated at 16°C for \geq 16 h.

A control reaction only consisting of vector DNA was also performed. Ratio of vector:insert was increased from 1:3 to 1:10 if colonies were found to contain a high proportion of religated vector.

3.3.9.2 High yield method (provided by A. Mohamed)

Where a low number of colonies were obtained, the above reaction was repeated, replacing the incubation at 16°C for \geq 16 h with the following. Vector and insert DNA, and water were incubated at 65°C for 15 min to denature any secondary structure in the DNA, then allowed to cool to 16°C. Ligase buffer and ligase were then added and incubated at 16°C for 30 mins. Then the mixture was incubated at 4°C for >16h.

3.3.10 Mutagenesis

Point mutations were performed using the Stratagene Quik-Change Site-Directed Mutagenesis Kit (See “Commercially Available Kits” for protocol reference and supplier information). Each primer inserted a novel restriction enzyme site into the sequence near to the mutation (see Table: “Restriction enzymes used to screen for mutated clones.” in “Restriction Enzyme” section) to allow screening of clones. Plasmids were then sequenced by DBS Genomics to ensure no point mutations had been produced and the mutated section subcloned back into the original plasmid.

3.3.11 Sequencing

Sequencing was performed by DBS Genomics, Durham University, or Eurofins MWG Operon, London.

3.4 Protocols for preparation/use of RNA

3.4.1 RNA isolation

Cells were washed with PBS, and then scraped from the bottom of the culture dish to remove adherent cells, or directly lysed in the appropriate volume of lysis buffer depending on the kit used. The cells were then resuspended and harvested according to the EZ-RNA protocol or the RNA Easy Kit (see “Commercially available Kits”, above). RNA was quantified and purity was measured using the Molecular Devices Spectramax Spectrophotometer (OD at 260nm, OD₂₆₀/OD₂₈₀ ratio) and concentrations confirmed by intensity of bands visible by RNA gel electrophoresis.

3.4.2 RNA agarose gel electrophoresis

RNA gels were prepared as DNA gels, above. The required amount of RNA was diluted 1:1:4 RNA:RNA loading buffer with 0.5 µg/ml ethidium bromide:DEPC treated water and was added to the wells using a pipette. A DNA ladder marker (1Kbp DNA Ladder, Promega, Southampton, UK Code: G5711) was added to the first well of each gel at the same proportions as the RNA/Buffer/Water mix. Field strengths of 1-1.5V/cm were applied to the gel. Once the RNA had migrated to the required distance (judged by migration of the loading dye), the RNA was visualized under a UV transilluminator (312nm, 0.120 J/cm²) for RNA bands.

3.4.3 cDNA production from RNA

cDNA was reverse transcribed from RNA using the first strand cDNA synthesis kit (Invitrogen, see Commercially available Kits”, above). The following reaction was set up:

1µl of oligo(dT)₂₀ (See “vector sequencing and general primers”) or 1µl of mouse/CHO gene specific primer (See “RT-PCR primers”) or 250ng of random hexamers (See “Vector Sequencing and General Primers”).

Up to 11µl of RNA dissolved in DEPC-treated Water (containing up to 5µg total RNA).

1µl of 100mM RNase-free dNTPs (See “Solutions for RNA work”)

DEPC-treated water to 13µl

The reaction mixture was heated to 65°C for 5 min and then cooled on ice to 4°C for > 1 min.

The following components were then added:

4µl 5x First Strand Buffer

1µl 0.1M DTT

1µl RNaseOUT or RNasein

1µl of Superscript III reverse transcriptase

The reaction mixture was then incubated at 50°C for 50 min and then inactivated at 85°C for 15 min.

3.4.4 Reverse transcription (RT)-PCR Assays for Actin/XBP-1 splicing/IRE1α.

Standard Reaction Mixture

10µl 5x Promega GoTaq Buffer

5µl 2mM dNTPs

0.5µl forward primer at 100µM

0.5 µl reverse primer 100µM

0.5µl Promega GoTaq HotStart Polymerase

3µl 25mM MgCl₂

Xµl cDNA Reaction (from 3.3.3. “cDNA production from RNA”)

Sterile H₂O to 50µl

3.4.4.1 RT-PCR for Mouse XBP-1/Actin

Spliced and unspliced XBP-1 cDNA was amplified using primers covering the splice site (see “Primers”, above) and using conditions given in Table 3. 6, below. Actin cDNA was similarly amplified using primers listed above. Amplified DNA was analysed on 2%(w/v) agarose gel (see above) run for 1h 15min at 100 mV.

The standard reaction mixture was set up, using the Actin or XBP-1 primers as listed in “Primers”, and either 1µl (actin) or 5µl (XBP-1) of cDNA mixture. It was subjected to the following PCR cycles:

Table 3. 6 - Thermocycler conditions for (RT)-PCR for mouse XBP-1/Actin

Temperature	Time	No. of Cycles
95°C	2 min	1
95°C	30 s	35
66°C	30 s	
72°C	15 s	
72°C	7 min	1

3.4.4.2 Touchdown RT-PCR for mouse XBP-1/Actin

The standard reaction mixture was set up, using the Actin or XBP-1 primers as listed in “Primers”, and either 1µl (actin) or 5µl (XBP-1) of cDNA mixture. It was subjected to the following PCR cycles:

The reaction was subjected to the following PCR conditions,

Table 3. 7 - Thermocycler conditions for touchdown (RT)-PCR for mouse XBP-1/Actin.

Temperature	Time	No. of Cycles
95°C	2 min	1
95°C	30 s	22
72-50°C*	15 s	
72°C	15 s	
95°C	30 s	13
50°C	15 s	
72°C	15 s	
72°C	7 min	1

*Step down by one degree per cycle

3.4.4.3 RT-PCR for CHO XBP-1/Actin using Promega Taq

The standard reaction mixture was set up, using the CHO Actin or XBP-1 primers as listed in “Primers”, and either 1µl (actin) or 5µl (XBP-1/IRE1α) of cDNA mixture. It was subjected to the following PCR cycles:

The reaction was subjected to the PCR conditions in Table 3. 8, below.

3.4.4.4 RT-PCR for CHO XBP-1/Actin using GE Illustra HotStart Taq

25µl 2x GE Illustra Hot Start PCR Master Mix
2µl CHO XBP-1/Actin Forward 2 primer at 100µM
2µl CHO XBP-1/Actin Reverse 2 primer at 100µM
5/1-2µl cDNA Reaction
Sterile H2O to 50µl

The reaction was subjected to the following PCR conditions in Table 3. 9, below.

Table 3. 8 - Thermocycler conditions for (RT)-PCR for CHO XBP-1/Actin/IRE1α

Temperature	Time	No. of Cycles
95°C	2 min	1
95°C	30 s	35
59°C XBP-1/Actin 56°C IRE1α	30 s	
72°C	15 s	
72°C	7 min	1

3.4.5 PCR for Sequencing using the FirstChoice® RLM-RACE Kit

The FirstChoice® RLM-RACE Kit was used according to the protocol listed above in “Commercially Available Kits”.

The RACE PCR reaction was performed as listed in the RLM-RACE Kit manual, using the RT reaction from above and the degenerate primers combined with the 3’RACE outer primer from the RLM-RACE kit.

1µl RT Reaction
5µl Accuprime Taq buffer
4µl dNTPs
5µl 100µM Degenerate Primer

2uL 3' RACE outer primer
 1µl/1.25U Accuprime Taq
 Nuclease-free water to 50µl

The following PCR cycles were used:

Temperature	Time	No. of Cycles
94°C	2 min	1
95°C	30 s	18
68-50°C (Touchdown)	30 s	
72°C	2 min	
95°C	30 s	17
50°C	30 s	
72°C	2 min	
72°C	7 min	1

Table 3. 9 - Thermocycler conditions for 3' RACE PCR

3.4.6 PCR for Sequencing using T-RACE PCR

The protocol used for T-RACE (Targetted Rapid Amplification of cDNA ends) was from (Bower and Johnston 2010). T-RACE involves an additional second strand synthesis of cDNA and digestion of original templates, and an asymmetric PCR for cDNA ends.

RNA was extracted as in “RNA Isolation” above. First strand synthesis was performed similar to the cDNA production protocol above, but using the T-Race Adaptor A instead of OligoDT and replacing dNTPs with dNTP-UTPs. The following reaction was set up;

0.5µl 100mM T-Race Adaptor A (1:40 dilution from 100mM stock for 2.5mM)

11.5µl of RNA/DEPC Water (1ug total RNA).

1µl of 10mM dNTP-UTPs (See “Solutions for DNA Work”)

The reaction mixture was heated to 65°C for 5 min and then cooled on ice to 4°C for > 1 min.

The following components were then added:

4µl 5x First Strand Buffer

1µl 0.1M DTT

1µl RNaseOUT or RNasein

1µl of Superscript III reverse transcriptase

The reaction mixture was then incubated at 42°C for 1h and then the following added:

0.4µl of 100mM MnCl₂

1µl of 10µM T-Race Adaptor B (1:10 dilution of 100µM stock)

And the reaction was incubated at 42°C for 15 min. The reaction was then heat inactivated at 70°C for 10 min. The reaction was purified with a QIAquick PCR Purification Kit and eluted in 30µl elution solution. Second strand synthesis was performed in a 50µl reaction containing:

10µl 5x GoTaq Buffer

2.5µl of 10mM dNTP-UTPs

2.5µl of 10mM T-Race Primer A

2.5µl of 10mM T-Race Primer B

5µl of 25mM MgCl₂

1µl (5u) of GoTaq

2µl of purified First Strand Synthesis reaction.

And subjected to the following thermocycler conditions.

Table 3. 10 - Thermocycler conditions for T-RACE second strand synthesis

Temperature	Time	No. of Cycles
95°C	2 min	1
95°C	30 s	21
60°C	30 s	
72°C	6 min	
4°C	As required	1

The reaction was purified with a QIAquick PCR Purification Kit and eluted in 100µl elution solution. Asymmetric PCR was performed using standard dNTPs and a gene specific primer towards the 5' or 3' ends of the required transcript. The following reaction was set up:

0.5µl of Gene Specific Primer (See “CHO IRE1a Sequencing” Primers above)

3.2µl 100mM (NH₄)₂SO₄

1.3µl 1M TrisHCl

2.4µl of 25mM MgCl₂

2.5 µl of 2mM dNTPs

2µl of Second Strand Synthesis Reaction

The reaction was heated to 95°C for 2 min 30s and one unit (0.2µl) GoTaq added. Then the reaction was subjected to the following PCR conditions.

Table 3. 11 - Thermocycler conditions for T-RACE asymmetric PCR

Temperature	Time	No. of Cycles
95°C	30 s	20
60°C	30 s	
72°C	2-7 min*	
4°C	As required	1

*Dependent upon amplicon length, 1kb per min

The reaction was purified with a QIAquick PCR Purification Kit and eluted in 11µl sterile water. The original template was digested with Uracil DNA Glycosylase (UDG) in the following reaction:

2µl GoTaq Buffer

2µl/2 units of UDG

2.4µl 25mM MgCl₂

10µl Asymmetric PCR Product

1µl 10mM Nested Gene Specific Primer (5' or 3' of the primer used in Asymmetric PCR)

1µl 10mM 5' or 3' T-RACE primer

0.6µl Sterile H₂O

The reaction was incubated at 37°C for 30 min then heated to 95°C for 2 min. 2µl of 10mM dNTPs and 0.2µl of GoTaq added and a final T-RACE PCR performed according to the following PCR conditions.

Table 3. 12 - Thermocycler conditions for T-RACE PCR

Temperature	Time	No. of Cycles
95°C	5 min	1
95°C	30 s	35
60°C	30 s	
72°C	2-7 min*	
72°C	7 min	1
4°C	As required	1

*Dependent upon amplicon length, 1kb per min

The final amplified DNA was analysed on 1%(w/v) agarose gel.

3.4.7 qPCR assay for XBP-1/IRE1 α /Actin

qPCR was performed on the Qiagen (Crawley, UK)/Corbett Research Rotorgene 3000 qPCR machine according to the instructions in the manual for that instrument (Manual version 6.1.7.1, 2004). Specifics of the appropriate qPCR run for each gene are listed in the results section. The following mixture was set up for each reaction:

2µl GoTaq Buffer

2µl 2mM dNTPs

1.2µl 25mM MgCl₂

0.3µl 10mM appropriate qPCR forward primer

0.3µl 10mM appropriate qPCR reverse primer

0.4µl (2units) GoTaq
0.3µl 8x Sybr Green
1.0-4.0µl of cDNA template or diluted standard.
Sterile/Nucleotide Free Water to 20µl

Standards used were 500ng, 250ng, 125ng, 62.5ng and 31.25ng of cDNA produced from the appropriate organism's RNA and Sterile/Nucleotide Free Water for no-template control.

3.5 Western Blotting

3.5.1 Protein isolation

Mouse embryonic fibroblasts, HEK293 cells and adherent CHO cells were placed on ice, their growth medium was removed and then washed with PBS. Dependent upon experimental protocol, cells were either then scraped from the bottom of the culture dish to remove adherent cells and resuspended in 0.1-0.5ml of RIPA buffer, or lysed directly using the RIPA buffer. Suspension CHO cells were aspirated and centrifuged at 110 g, 2-5 min, RT, and then lysed directly using RIPA buffer. Protein lysates were centrifuged at 16,000g for 10 min and protein concentration assessed using the DC Protein Assay (See above, "Commercially Available Kits").

3.5.2 Production of Poly-acrylamide Gel

The gel casting unit was assembled according to manufacturer's instructions and appropriately sized plates inserted into the caster, which was sealed. 12% (w/v) SDS Poly-Acrylamide Gel was assembled as below.

Separating Gel:

4.5ml 30% (w/v) acrylamide, 0.8% (w/v) bisacrylamide
2.18 ml 1 M Tris·HCl, pH 8.9
3.9 ml H₂O

75 μ l 10% (w/v) SDS
33.75 μ l 10% (w/v) ammonium persulfate
7.5 μ l TEMED

Stacking Gel:

0.5 ml 30% (w/v) acrylamide, 0.8% (w/v) bisacrylamide
0.94 ml 1 M Tris·HCl, pH 8.9
2.32 ml H₂O
9.4 μ l 10% (w/v) SDS
16.9 μ l 10% (w/v) ammonium persulfate
5.6 μ l TEMED

Components of the separating gel were mixed together and pipetted between the glass plates of the gel caster. H₂O saturated butanol was pipetted on top of the gel to ensure the top level of the gel was even. The gel was left to polymerise for >30 min. Once the separating gel was set, the butanol was removed and the gel washed with water before the stacking gel was pipetted on top of the separating gel and left to polymerise for > 30 min.

3.5.3 SDS-PAGE

An electrophoresis unit (Biorad, Hemel Hempstead, UK) was assembled and buffer reservoirs were filled with 1 x SDS-PAGE running buffer. Samples were mixed on ice with 5 μ l of 6 x SDS-PAGE sample buffer, and centrifuged for ~15 s at 12,000 g at room temperature. Samples were then boiled for 5 min at 100°C and then centrifuged again for ~15 s at 12,000 g at room temperature to collect the whole sample at the bottom of the tube. Samples were loaded onto SDS-Poly-acrylamide Gel using gel loading pipette tips. The SDS-PAGE electrophoresis unit was closed and a voltage of 100mV was applied for >1hr. The gel was run until the bromophenol blue dye front eluted from the gel. The gel was then removed from the electrophoresis unit and the plates disassembled. The stacking gel was removed using a ruler and a scalpel.

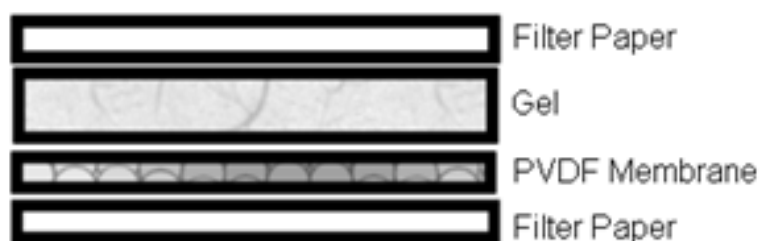
3.5.4 Electrotransfer by Wet Transfer

The gel was transferred into 100 ml of 4°C electrotransfer buffer and incubated with gentle agitation for 1 h at 4°C. PVDF membrane (See “Specialist Equipment”) and two pieces of filter paper were cut to the dimensions of the gel. Filter papers were soaked in ice-cold transfer buffer. PVDF membrane was placed into 50 mL methanol and soaked until completely wetted and then transferred into electrotransfer buffer and soaked for >15 min. Filter papers, gel, and membrane were placed between fibre pads in a Bio-Rad (Biorad, Hemel Hempstead, UK) electrotransfer cassette, which was closed, locked and placed in the Bio-Rad electrotransfer unit with 2.5-3 L electrotransfer buffer. 30 mV was applied to the electrotransfer unit and the assembly was incubated overnight with stirring. After this time, the electrotransfer unit was disassembled and the membrane removed.

3.5.5 Electrotransfer by Semi-Dry Transfer

A pre-run SDS-PAGE gel was removed from its cassette and soaked in a container with sufficient chilled 1x Semi-Dry Transfer Buffer to cover the gel. The gel was measured and a suitable size of PVDF membrane was cut to cover it, along with eight pieces of laboratory filter paper of the same size. The laboratory filter paper was allowed to soak in 1x Semi-Dry Transfer Buffer. The PVDF membrane was wetted in methanol and then rinsed in 1x Semi-Dry Transfer Buffer. The surface of the semi-dry transfer apparatus was cleaned and the gel stack assembled as in Figure 3. 1 - Semi-Dry Transfer Stack Setup below. Bubbles and excess buffer were removed from the stack by rolling a sterile pipette across it.

Figure 3. 1 - Semi-Dry Transfer Stack Setup



Amperage on the Semi-Dry Transfer apparatus (Model AE6675, Atto Corporation, Tokyo, Japan) was set to 2mA/cm² and transfer was set to a duration of 1h 15 min. Once transfer was complete the electrotransfer unit was disassembled and the membrane removed.

3.5.6 Electrotransfer by Dry Transfer

Dry protein transfer was performed according to the iBlot (Invitrogen, Paisley UK) manual, Revision 21 Nov 2010. The iBlot stack was setup up as described in the iBlot manual with gel and PVDF membrane between anode and cathode stack. Protocol 9 (20V for 2 min, 5V for 3 min, 5V for 3 min) was used to transfer the protein to the PVDF membrane.

3.5.7 Antibody Immunoblotting

PVDF membrane with protein samples were stained by incubating 5 min at room temperature in 0.5% (w/v) Ponceau S, 1% (v/v) HOAc to visualise proteins, then destained by washing for 12 min in H₂O. Membranes were transferred into plastic trays containing ≥ 0.75 ml/cm² TBST + 5% (w/v) non-fat dry milk powder or 5% bovine serum albumin (Sigma-Aldrich, Gillingham, UK) and were incubated 1 h at room temperature with shaking (~50-60 rpm) to block. They were then washed three times with TBST. The membranes were transferred into a 50 ml centrifuge tube or hybridization bottle and any air bubbles caught between the tube walls and the membrane removed, then incubated overnight in 5% milk or 5% BSA (w/v) TBST containing the appropriate concentration of primary antibody (see “Antibodies”, above). The membranes were then transferred into plastic trays containing ≥ 0.75 ml/cm² TBST and rinsed twice. The TBST was replaced and the membranes were incubated for 5 min at RT with shaking (~50-60 rpm). This replacement and incubation was repeated three times. The membranes were transferred into a 50 ml centrifuge tube or hybridization bottle and any air bubbles caught between the tube walls and the membrane removed, then incubated for 1 h in TBST containing 50 μ l/cm² TBST + 5% (w/v) solution of non-fat dry milk and the appropriate concentration of secondary antibody (see “Antibodies”, above)

Alternatively TBSTriton (Lonza Wash Buffer) was used for washing steps and TBSTriton with Casein (Lonza Blocking Buffer) was used for blocking and antibody incubation steps.

3.5.8 Visualisation

The membranes were washed again three times in TBST or TBSTriton and chemiluminescence detected with the ECL Plus detection kit (see “Commercially Available Kits”, above) according to the manufacturer’s protocol, by exposing to Kodak BioMax MS film (See

“Specialist Equipment”) in an exposure cassette for 30 seconds – overnight, and developed on an Xograph Compact 4 (Xograph Healthcare, Tetbury, UK).

3.5.9 Dephosphorylation of samples

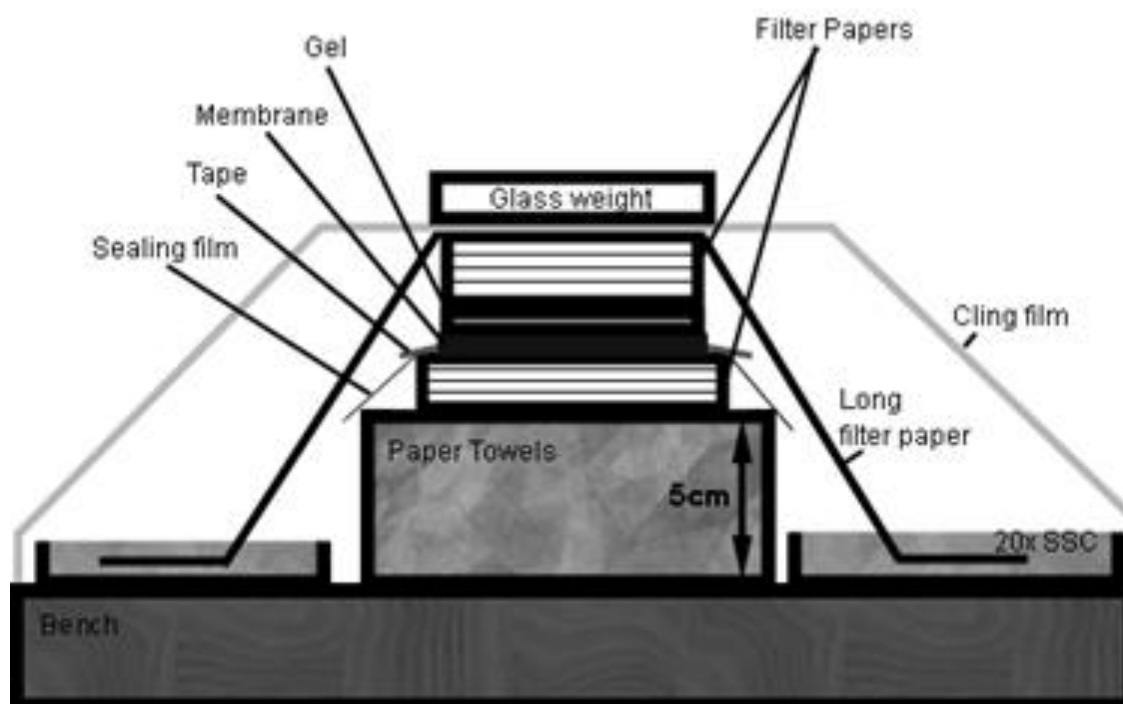
Where required for phosphorylation analysis, a 50µl sample of lysate in RIPA buffer containing 10-50ug of protein was treated with 100 units of lambda phosphatase for 20 min at 30 °C.

3.6 Southern Blotting

3.6.1 Transfer

Genomic DNA extracts were prepared using the DNA component of the EZ RNA kit and digested with the appropriate restriction enzyme chosen for the genomic DNA. The digest was run on a 1%(w/v) agarose DNA gel to separate out the genomic DNA for blotting. The following transfer stack was set up. A stack of paper towels 5cm high was used for a base and two basins of 20x SSC set up either side. Four pieces of filter paper were placed on top of the paper towels and sealed with film to prevent short-circuiting between the gel and filter papers/towels. A fifth filter paper was wetted with 20x SSC and placed on top of the other four. The membrane was wetted with sterile water and placed on top of the filter paper stack then flattened out by rolling a sterile pipette over it. The gel was then placed on top of the membrane, taking care to not extend the gel over the edges of the membrane. Three pieces of filter paper were soaked in 20x SSC and placed on top of the gel, then one long piece of filter paper was soaked in SSC and hung across the top of the filter papers with each end in the basins of 20x SSC so as to retain the 20x SSC in the filter paper. Air bubbles were removed by rolling with a sterile pipette. The apparatus was sealed to prevent evaporation with cling film and weighed down with a glass plate. The DNA was transferred overnight (>16h), then the apparatus was disassembled with forceps. The membrane was placed, nucleic acid side up onto a piece of filter paper and crosslinked to the membrane using the UVP ultraviolet crosslinker (Upland, CA, USA, manual reference 81-0112-01 Rev F) with 120mJ of UV light.

Figure 3. 2 - Southern Blot Transfer Setup



3.6.2 Hybridisation

The membrane was transferred into a hybridisation bottle and wetted with 6 x SSC. The membrane was then prehybridized at 42°C with 20 ml hybridization solution/bottle for ≥ 3 h. During this incubation the DNA probe was prepared using the Rediprime labelling kit (See “Commercially Available Kits”). A PCR product polymerised from the pFRT/lacZeo plasmid using the lacZ probe primers (see “Primers”, above) was diluted to 25ng in 45 μ l of TE then denatured by heating for 5 min at 95-100°C. The probe was then chilled on ice and centrifuged at 13,000 rpm. Denatured DNA was then added to the Rediprime reaction tubes and dissolved by flipping the tube. The solution was collected at the bottom of the tube by briefly centrifuging and then 5 μ l of Redivue [\square - 32 P]-dCTP, 3000 Ci/mmol, ~ 10 μ Ci/ μ l (Amersham Biosciences/GE Healthcare, Chalfont St. Giles, UK) was added and the tube mixed by flipping. The solution was incubated at 37°C for 10 minutes. After this, the reaction was halted by adding 5 μ l of 0.2 M EDTA. A

microspin S300 HR column was prepared by vortexing, and placed in a 1.5ml microcentrifuge tube, then centrifuged at 735g for 1 min. The column was then transferred to a new 1.5ml microcentrifuge tube and the sample carefully added to the top-centre of the resin without disturbing the resin. The tube was recapped loosely and centrifuged at 735g for 2 min. The prepared labeled probe was denatured by boiling for 5 min and then added to the pre-hybridised membrane at 2ng/ml along with 1 mg/ml denatured salmon sperm solution and 5ml hybridisation solution per hybridisation bottle and hybridised overnight. After hybridisation, the membrane was washed three times for 5 min at room temperature with ~ 200 ml 2 x SSC + 0.1% (w/v) SDS. Then the membrane was washed again with 0.2 x SSC + 0.1% (w/v) SDS for 5 min at room temperature. The membrane was transferred into a clean hybridisation bottle and washed again for 15 min at 42°C with ~ 50 ml 0.2 x SSC + 0.1% (w/v) SDS. Finally, the membrane was rinsed in 2x SSC and the excess liquid blotted off. The membrane was then visualised either by placing it in an exposure cassette overnight and imaging the irradiated insert from the cassette on a Typhoon 9400 Variable Mode Imager (GE Healthcare, Chalfont St. Giles, UK) or by exposing the membrane to Kodak BioMax MS film at -80°C in an exposure cassette fitted with intensifying screens overnight and developing the film on an Xograph Compact 4 (Xograph Healthcare, Tetbury, UK).

3.7 Spectrophotometric assays

3.7.1 Sandwich ELISA for assembled IgG cB72.3

The Sandwich ELISA was performed according to a protocol provided by Lonza Biologics, Slough. ELISA plates (See “Specialist Equipment”) were coated with goat anti-human IgG diluted 1:1200 (10µl in 12ml) in ELISA coating buffer by dispensing 100µl of the dilution into each well and incubating overnight at 4°C. Plates were sealed with Abgene adhesive plate seals (See “Specialist Equipment”) during this and every following incubation step. After the incubation period, each well was then washed with 300µl of ELISA wash buffer and excess buffer tapped out onto a paper towel. The plates were then blocked by dispensing 100µl of ELISA blocking buffer into each well and incubating >1 h with shaking. The wash step with 300µl of wash buffer was repeated. The assembled cB72.3 antibody ELISA standard (provided by Lonza Biologics, Slough, UK) was diluted to 200ng/µl from the stock in ELISA sample/conjugate buffer and serial dilutions 1:2 down to 3.91 ng/µl made for a calibration curve. Samples of medium clarified by centrifugation at 110 g, 5 min, room temperature were

diluted 1:100-1:1000 as required by the experiment in ELISA sample/conjugate buffer. ELISA sample/conjugate buffer was used as a negative control and a standard dilution of one standard used as an interassay control. 100µl each of samples, standards and controls were dispensed into wells in duplicate. The plate was incubated at room temperature with shaking for 1h.

After the incubation period, each well was then washed with 300µl of ELISA wash buffer and excess buffer tapped out onto a paper towel. Goat anti-Human IgG (kappa chain specific) HRP conjugate was diluted 1:8000 in ELISA sample/conjugate buffer and 100µl was dispensed into each well, before incubating for 1h with shaking. After the incubation period, each well was then washed twice with 300µl of ELISA wash buffer and excess buffer tapped out onto a paper towel. TMB Liquid Substrate System was allowed to equilibrate to room temperature and then 100µl added to each well of the plate. The plate was shaken at 220 rpm at room temperature for 10-45 min until the 2000ng/µl standard had reached a mid- to dark blue. The reaction was stopped by the addition of 50µl of ELISA stop solution, changing the colour of the wells from blue to yellow. The absorbance of the plate at 450nm was immediately read on a Molecular Devices Spectramax Spectrophotometer.

Optimisation of Goat anti-Human IgG (kappa chain specific) HRP conjugate antibody was performed as recommended by Lonza with concentration ranges of conjugate antibody used from 1:8000 to 1:100,000. The 1:8000 dilution passed the acceptance criteria of $OD\ 1.0 < x > 3.0$ for the 200ng/µl standard and was used for future assays.

3.7.2 β -Gal Assay for pcDNA integration.

β -galactosidase standard was prepared by adding 1 μ l 1 U/ μ l β -galactosidase to 99 μ l ice-cold 1 x RLB, mixed, and the tube placed on ice. The standard was then diluted again 10 μ l in 990 μ l ice-cold 1 x RLB, mix, and the final 0.1 mU/ μ l solution placed on ice. A 96-well plate was set up with the following dilutions in duplicate of the β -galactosidase solution in 1 x RLB buffer for a standard curve.

Table 3. 13 - β -galactosidase Assay Standards

β -galactosidase standard [mU/50 μ l]	volume of 0.1 mU/ μ l β -galactosidase solution (step 2)	volume of 1 x RLB
0.0	0 μ l	50 μ l
1.0	10 μ l	40 μ l
2.0	20 μ l	30 μ l
3.0	30 μ l	20 μ l
4.0	40 μ l	10 μ l
5.0	50 μ l	0 μ l

50 μ l of each sample was added to the 96 well plate in duplicate. If required, 1:50 dilutions were also assayed. 50 μ l of 2x assay buffer was then added to each well and mixed by pipetting up and down. The plate was covered with parafilm (Pechiny Plastic Packaging Company/Camlab, Over, UK) or a plate sealer (ThermoFisher Scientific, Waltham, USA) and incubated at 37°C for 30 min or until a faint yellow colour developed (up to 3 h). The reaction was stopped by adding 150 μ l 1 M Na₂CO₃ and bubbles removed with a pipette tip. Absorbance of samples was read at 405-420 nm on the Molecular Devices Spectramax Spectrophotometer.

4. RESULTS

4.1 Cloning of IRE1 α and IRE1 β mutant plasmids

4.1.1 Rationale

Testing used to isolate the effect of IRE1 α mutant constructs created in this study on mammalian cells required the use of mammalian expression vectors. Vectors used for expression of IRE1 wild type and mutants were gifts from R. Kaufman, University of Michigan, USA (pED Δ C-hIRE1 α) and K. Kohno, Nara Institute of Science and Technology, Japan (pCAG-hIRE1 β). Both vectors had been previously tested and shown to produce functional IRE1 product visible at 110 KDa (Tirasophon, Welihinda et al. 1998; Iwawaki, Hosoda et al. 2001). Both vectors were fully sequenced and the DNA and translated protein sequences compared against those in the Genbank databases (IRE1 α /ERN1 - NM_001433, IRE1 β /ERN2 NM_033266.3). During sequencing of mutated vectors, a point mutation was found in the donated pED Δ C-hIRE1 α –K599A which altered an amino acid (R->L) at the beginning of the open reading frame of hIRE1 α . As a result, the cloning strategy was adjusted to ensure this mutation was removed before the pED Δ C-hIRE1 α plasmid was used for cloning double mutants. Sequencing of the pCAG-hIRE1 β plasmid was impeded by a GC rich region in the rabbit β -globin which appeared to possibly be stalling sequencing polymerases – sequencing across the region was only achieved by designing primers with small gaps between them against the rabbit β -globin gene itself. Bioinformatic sequence alignments were performed using the sequences of yeast Ire1p, and hIRE1 α and β to ascertain the equivalent residues to those used in (Mori, Ma et al. 1993; Tirasophon, Welihinda et al. 1998; Tirasophon 2000; Iwawaki, Hosoda et al. 2001; Papa, C. et al. 2003; Lin, Li et al. 2007; Imagawa, Hosoda et al. 2008) to select for mutagenesis. These residues are K599, I642, D711 and K907A in the α isoform of hIRE1 and K547, L590, D659 and K855 in the β .

4.1.2 Mutagenesis Strategy: IRE1 α constructs

Based upon the predicted restriction enzyme sites in the sequenced pED Δ C-hIRE1 α plasmid, the following restriction enzymes were selected to use to screen for mutagenesis and incorporated into the sequences used: *EcoRI*, *EcoRV*, *EagI*, *NgoMIV*.

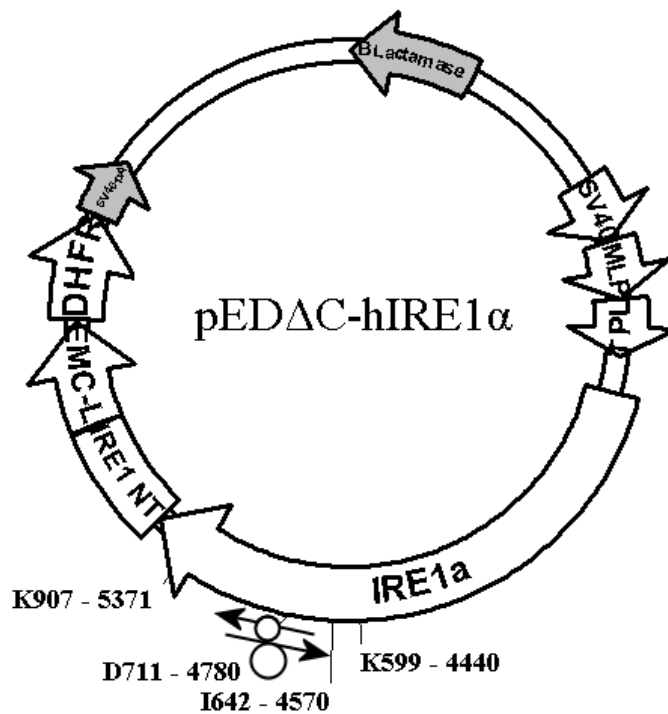
Mutagenesis was performed using the Stratagene QuikChange® II XL Site-Directed Mutagenesis Kit according to the protocol described in the manual for that kit. Primers (listed in Materials and Methods – Primers) were designed to produce the appropriate point-mutation substitutions to give the desired effect and used in the Quik-change reactions with pED Δ C-hIRE1 α as a template. Where mutagenesis had not introduced a new restriction enzyme site for screening, a second point mutation was also included in the primers to aid in later screening for transformants. The kinase-dead mutant K599A and the RNase dead mutant K907A had already been obtained from R. Kaufman, University of Michigan, USA, and the K599A was also used as a template for double mutants, as were D711A and K599R once they had been produced. The alterations to be made using the primers are listed in Table 4.1. 1.

Table 4.1. 1 - Mutagenesis schemes, IRE1 α – [*EcoRV*]: Restriction enzyme sites. Substitutions in italics mark mutagenesis codon changes, those in bold mark conservative substitutions which add a restriction enzyme site for screening.

Mutant	Alterations to Sequence
K599R	ATGTTTGACA ACCGCGACGT GGCCGTGAAG AGGATCCTCC CCGAGTGTTT
	M F D N R D V A V K R I L P E C F
	<i>[EcoRI]</i>
	ATGTTTGACA ACCGCGACGT GGCCGTGAGG AGAATCTCC CCGAGTGTTT
D711A	M F D N R D V A V R R I L P E C F
	GCAAGATCAA GGCCATGATC TCCGACTTTG GCCTCTGCAA GAAGCTGGCA
	K I K A M I S D F G L C K K L A
	<i>[EcoRV]</i>
I642A	GCAAGATCAA GGCCATGATA TCCGCCTTTG GCCTCTGCAA GAAGCTGGCA
	K I K A M I S A F G L C K K L A
	AGGACCGGCA ATTCCAGTAC ATTGCATCG AGCTGTGTGC AGCCACCCTG
	D R Q F Q Y I A I E L C A A T L

	<i>[EagI]</i>
	AGGACCGGCA ATTCCAGTAC ATTGCC G CCG AGCTGTGTGC AGCCACCCTG
	D R Q F Q Y I A A E L C A A T L
I642G	AGGACCGGCA ATTCCAGTAC ATTGCC A T C G AGCTGTGTGC AGCCACCCTG
	D R Q F Q Y I A I E L C A A T L
	<i>[NgoMIV]</i>
	AGGACCGGCA ATTCCAGTAC ATTGCC G GCG AGCTGTGTGC AGCCACCCTG
	D R Q F Q Y I A G E L C A A T L

Figure 4.1. 1 - Mutagenesis of pEDΔC-hIRE1α. Mutagenesis primers anneal to site of mutation on denatured plasmid. Proof-reading *PfuTurbo* polymerase polymerises in direction of arrows around the plasmid.



4.1.3 Screening of Transformants for Insertion of Mutation

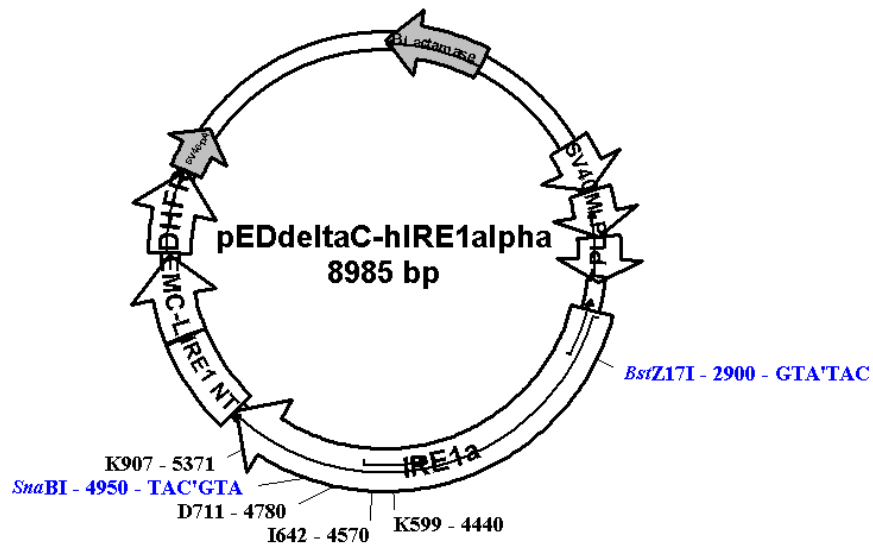
Original methylated and unmethylated template DNA was digested with *DpnI* leaving the mutated plasmid, which was then transformed into XL-Blue supercompetent cells and plated out on LB-ampicillin plates. Transformants plated out on LB-ampicillin plates were counted

for number of colonies. If transformation efficiency/plasmid yield was low and \leq eight colonies had grown on the plate, all colonies were used. If yield was sufficient and >8 colonies were counted, eight transformants were selected from random sites across the plate. Colonies were grown up (see Materials and Methods - “Preparation from E.coli culture by Mini/ Midi/ Maxi/ Gigaprep and Ethanol Precipitation of Nucleic Acids”) overnight and minipreped to harvest the mutated plasmid. 5 μ l of each miniprep was digested overnight with the appropriate restriction enzyme in a 10 μ l reaction (see Materials and Methods - Restriction Enzyme Digestion, 10 μ l Reaction). This digest reaction was run on an agarose gel side by side with the undigested plasmid to ascertain whether the extra restriction enzyme site had been successfully mutagenised. Selected clones that digested correctly were sequenced to check the correct mutations and if these were present, preparations of the clones were frozen in 30% glycerol and stored for recloning (See Appendix 3 – Sequencing results from mutagenesis of IRE1 constructs).

4.1.4 Recloning into pED Δ c-hIRE1 α Plasmid

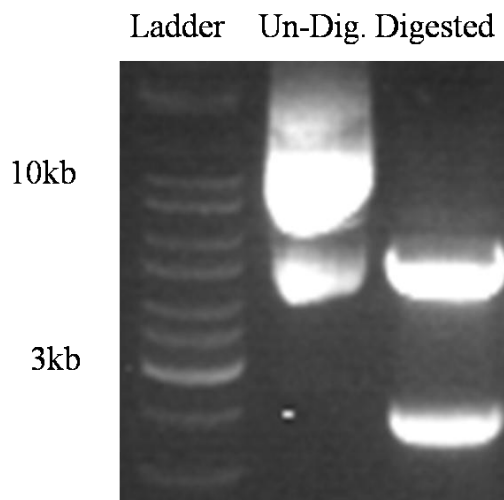
Although proofreading Pfu polymerase was used for mutagenesis cloning, there was a risk of unwanted base-pair substitutions in the plasmid constructs. Therefore, the section between the restriction enzyme sites for *BstZ17I*, and *SnaBI* was sequenced in each plasmid and then excised and subcloned back into the original, fully sequenced plasmid. This was performed for all mutants apart from the K907A which was already fully sequenced. For this reason, the *SnaBI* site was acceptable, despite the desired product of digesting using *BstZ17I*, and *SnaBI* excluding the K907 site.

Figure 4.1. 2 - Subcloning of pEDΔc-hIRE1α mutants into original plasmid.



For each of the clones produced by mutagenesis and for the original pEDΔc-hIRE1α plasmid, 10-50ug of a midiprep were digested in a 50μl double digest enzyme reaction with 1μl each of *BstZ171* and *SnaBI* and using the New England Bioscience Buffer 4. Each reaction was run on a 1% agarose gel and the band for the *BstZ171-SnaBI* fragment (2050bp), or that for the larger -*SnaBI -BstZ171* fragment (6935bp) in the case of the original pEDΔc-hIRE1α vector, excised (see below) and purified using the GenElute™ Gel Extraction Kit. Each mutant's fragment was ligated to the original plasmid's larger fragment using the standard method reaction as described in Materials and Methods "DNA Ligation with T4 DNA ligase" and the resulting ligant chemically transformed into competent *E. coli* and plated out. Resulting colonies were minipreped and screened for completed ligation by redigesting with *BstZ171* and *SnaBI*.

Figure 4.1. 3 – Example of digests of pED Δ c-hIRE1 α with *Bst*Z17I and *Sna*BI to ensure correct religation and re-insertion of mutated hIRE1 α sequence. Ladder – DNA Ladder. Un-Dig./Digested – religated pED Δ c-hIRE1 α plasmid.



Bands appear in digested plasmid at ~6000 (predicted 6935), and ~2400 (predicted 2050). *E. coli* clones with correctly religated plasmids were frozen in 30% glycerol and stored. Large scale preparations were made of each mutant using an endotoxin-free maxiprep kit (EndoFree Plasmid Maxi Kit) to produce plasmid suitable for mammalian transfection.

4.1.5 Mutagenesis and Cloning Strategy: IRE1 β

Based upon the predicted restriction enzyme sites in the sequenced pCAG-hIRE1 β plasmid, the following restriction enzymes were selected to use to screen for mutagenesis and incorporated into the sequences used: *Nae*I, *Hind*III *Nhe*I and *Afl*II.

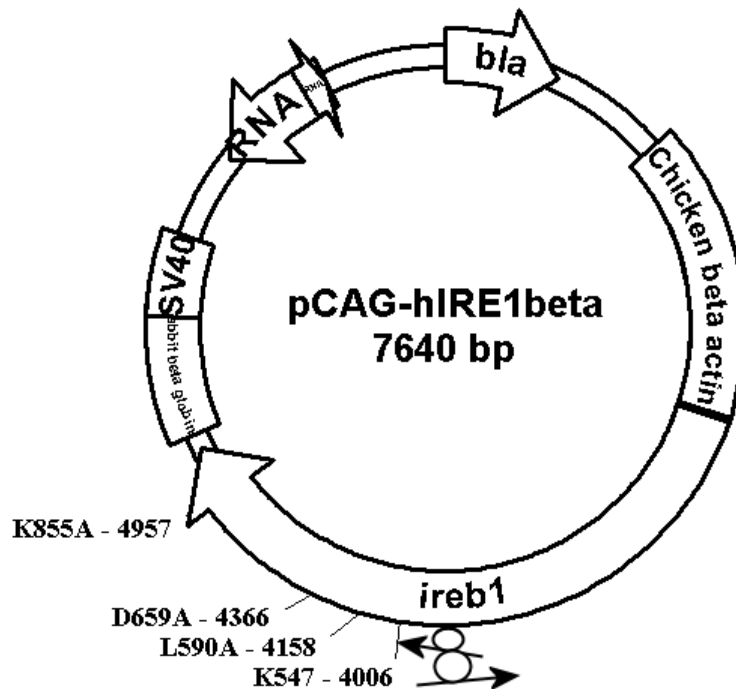
As with the IRE1 α mutants, mutagenesis was performed using the Stratagene QuikChange[®] II XL Site-Directed Mutagenesis Kit according to the protocol described in the manual for that kit. Primers (listed in Materials and Methods – Primers) were designed to produce the appropriate point-mutation substitutions to give the desired effect and used in the Quik-change reactions with pCAG-hIRE1 β as a template. Where mutagenesis had not introduced a new restriction enzyme site for screening, a second point mutation was also included in the primers to aid in later screening for transformants. The kinase-dead mutant K547A had

already been obtained from K. Kohno, NAIST, Japan, and this was also used as a template for double mutants, as were D659A and K547R once they had been produced. The alterations to be made using the primers are listed in Table 4.1. 2.

Mutant	Alterations to Sequence
K547R	<p>TTTGAGGGAC GGGCAGTGGC TGTCAAGCGG CTCCTCCGCG AGTGCTTTGG F E G R A V A V K R L L R E C F G <i>[NaeI]</i></p> <p>TTTGAGGGAC GGGCAGTGGC TGTCCGCCGG CTCCTCCGCG AGTGCTTTGG F E G R A V A V R R L L R E C F G</p>
D659A	<p>TGGGCAGAGT GGTGCTCTCA GACTTCGGCC TCTGCAAGAA GCTGCCTGCT G R V V L S D F G L C K K L P A <i>[HindIII]</i></p> <p>TGGGCAGAGT GGTGCTCTCA GCCTTCGGCC TCTGCAAGAA GCTTCCTGCT G R V V L S A F G L C K K L P A</p>
L590A	<p>GACCCAGTT CCACTACATT GCCCTGGAGC TCTGCCGGGC CTCCCTGCAG P Q F H Y I A L E L C R A S L Q <i>[HindIII]</i></p> <p>GACCCAGTT CCACTACATT GCCGCGGAGC TCTGCCGGGC AAGCCTGCAG P Q F H Y I A A E L C R A S L Q</p>
L590G	<p>GACCCAGTT CCACTACATT GCCCTGGAGC TCTGCCGGGC CTCCCTGCAG P Q F H Y I A L E L C R A S L Q <i>[NheI]</i></p> <p>GACCCAGTT CCACTACATT GCCGGGGAGC TCTGCCGGGC TAGCCTGCAG P Q F H Y I A G E L C R A S L Q</p>
K855A	<p>GCGAGACCTG CTCCGTGCTG TGAGGAACAA GAAGCACCAC TACAGGGAGC R D L L R A V R N K K H H Y R E <i>[AflIII]</i></p> <p>GCGAGACCTC TTAAGAGCTG TGAGGAACGC GAAGCACCAC TACAGGGAGC R D L L R A V R N A K H H Y R E</p>

Table 4.1. 2 - Mutagenesis schemes, IRE1 β – *[NaeI]*: Restriction enzyme sites. Substitutions in italic mark mutagenesis codon changes, those in bold mark conservative substitutions which add a restriction enzyme site for screening.

Figure 4.1. 4 - Mutagenesis of pCAG-hIRE1 β . Mutagenesis primers anneal to site of mutation on denatured plasmid. Proof-reading *PfuTurbo* polymerase polymerises in direction of arrows around the plasmid to form mutagenised form.

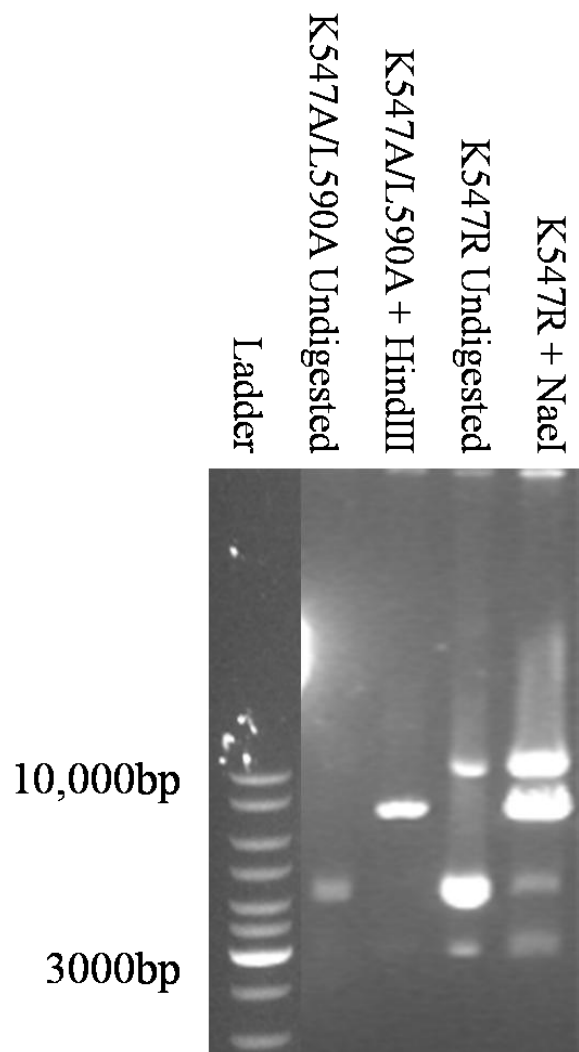


Original methylated and unmutated template was digested with *DpnI* leaving the mutated plasmid, which was then transformed into XL-Blue supercompetent cells and plated out on LB-ampicillin plates.

4.1.6 Screening of Transformants for Mutagenesis

Mutagenesis reactions were attempted as above, but either did not result in colonies on the plates or resulted in very few colonies which did not digest correctly, indicating the mutagenesis was unsuccessful. It is likely that the presence of the GC rich region in the rabbit β -globin gene was stalling the polymerase, as occurred during sequencing of the plasmid. Therefore, the IRE1 β gene required subcloning out of the pCAG plasmid. The pUC18 vector was used for this, as it possessed a suitable cloning site (*EcoRI*) and is a short vector, therefore increasing the likelihood of successful readthrough of the polymerase across its length.

Figure 4.1. 5 – Unsuccessful mutagenesis of pCAG-hIRE1 β .

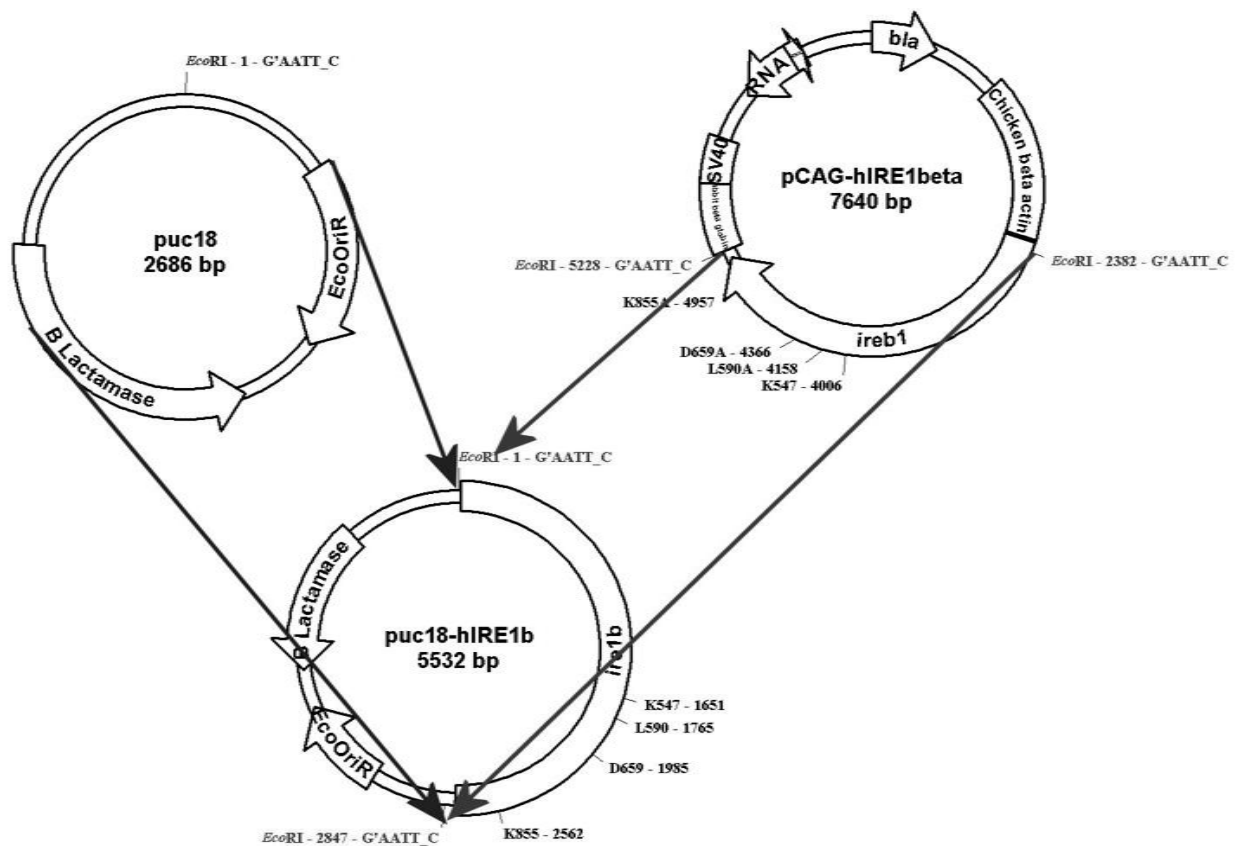


500ng-1ug of minipreped plasmid clone was digested for 1hr with 10 units of the labeled restriction enzyme or no enzyme was used (undigested). Resulting preparations were run on a 1% agarose gel. Digestion of clone from mutagenesis reaction, shows linearised band indicating the second NaeI or HindIII site has not been integrated into the plasmid.

4.1.7 Requirement and Strategy for Cloning into puc18

Mutation of pCAG-hIRE1 β proved difficult due to the aforementioned heavily GC-rich rabbit β -globin gene, which may have been stalling the polymerases used. To overcome this, hIRE1 β was digested with *EcoRI* and the resulting fragment ligated into the *EcoRI* site within the multi-cloning site of the pUC18 plasmid, producing pUC18-hIRE1 β .

Figure 4.1. 6- Cloning strategy for puc18-hIRE1 β . The constructed plasmid comprises the entirety of the pUC18 vector (left-hand arrows) and the IRE1 β gene (right-hand arrows).



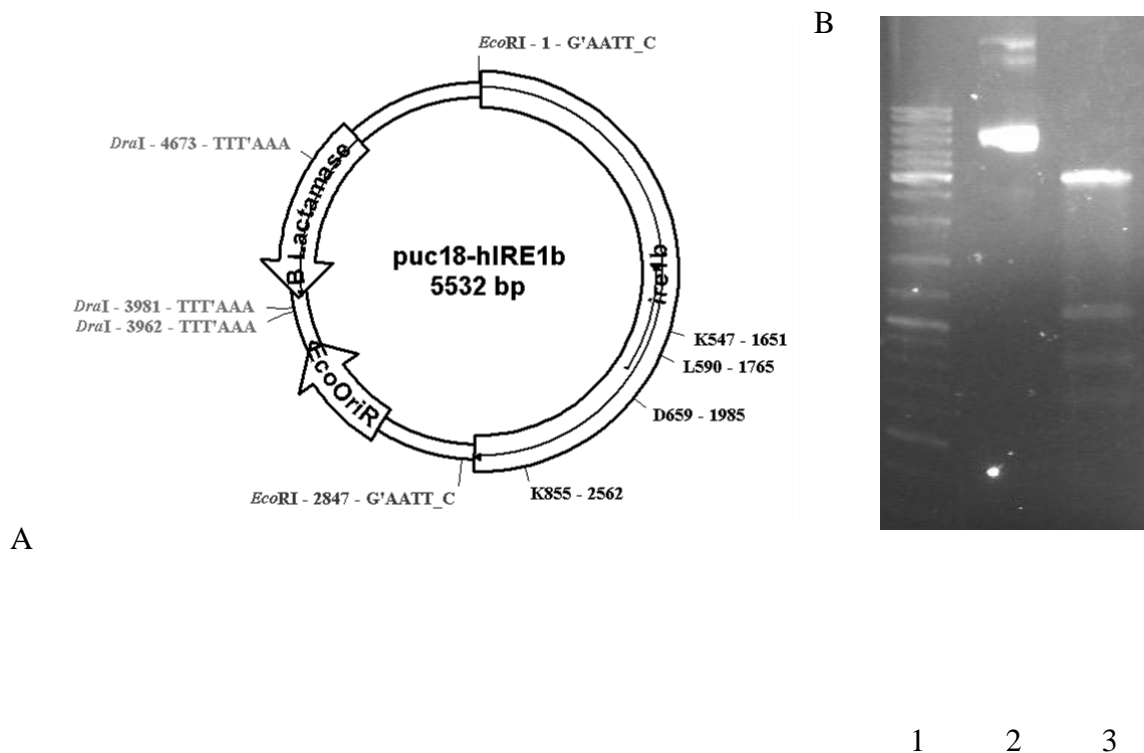
4.1.8 Mutagenesis on pUC18-hIRE1 β

Mutagenesis reactions were attempted as above upon the pUC18-hIRE1 β plasmid, and screened using the same restriction enzymes. This shorter plasmid without the GC rich region of pCAG-hIRE1 β gave a higher number of correct clones, examples of which can be seen in the sequencing results in Appendix 3. Selected clones that digested correctly were sequenced to check the correct mutations and if these were present, preparations of the clones were frozen in 30% glycerol and stored for recloning (See Appendix 3 – Sequencing results from mutagenesis of IRE1 constructs).

4.1.9 Recloning of IRE1 β constructs into pCAG Plasmids

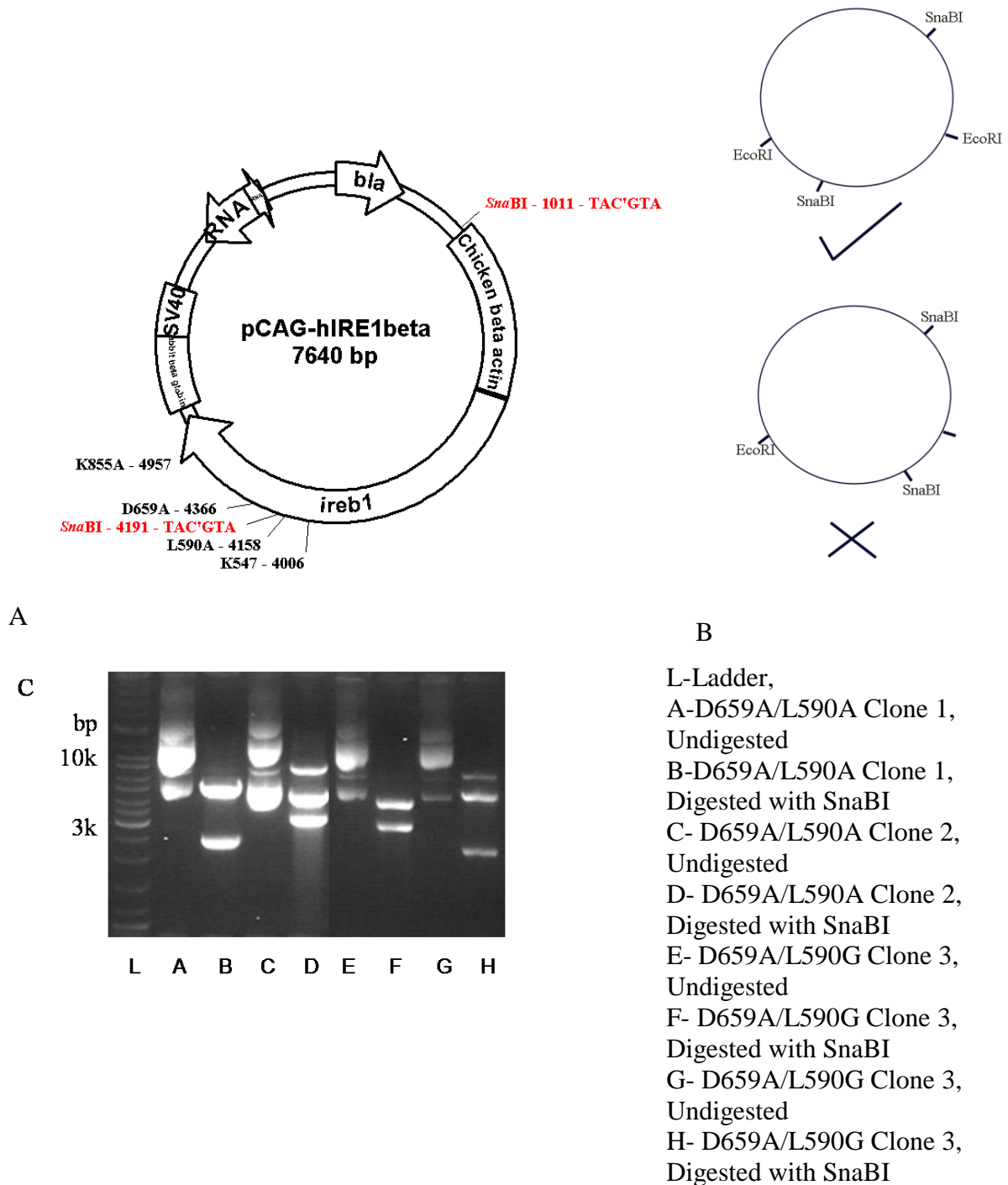
As with the pED Δ c plasmid, although proofreading Pfu polymerase was used for mutagenesis cloning, there was a risk of unwanted base-pair substitutions in the plasmid constructs. Therefore, the section between the two restriction enzyme sites for *EcoRI* was sequenced in each plasmid and then excised and subcloned back into the original, fully sequenced *pCAG* plasmid. For each of the pUC18-hIRE1 β clones produced by mutagenesis and for the original *pCAG* plasmid, 10-50ug of a midprep were digested in a 50 μ l double digest enzyme reaction with 1 μ l(10units) of *EcoRI* and using the Fermentas *EcoRI* buffer. Each reaction was run on a 1% agarose gel and the band for the *IRE1 EcoRI-EcoRI* fragment (2847bp), or that for the larger *EcoRI-EcoRI* fragment from pCAG-hIRE1 β (4794bp) in the case of the original vector, excised from the gel and purified using the GenElute™ Gel Extraction Kit. As the two bands in the pUC18-hIRE1 β were very close to one another in size (2847 and 2685), it was necessary to use an extra restriction site to distinguish between the fragments. Double digests were performed with *EcoRI* and *DraI* in Fermentas Tango buffer with *DraI* in excess at a 1:2 ratio, to divide the 2685 fragment into four fragments, at 1115, 859, 692, 19bp (19bp fragment too small to be visible on gel). Test digest was performed for one hour on 500ng of pUC18-hIRE1 β , large scale digests overnight on 10ug (Figure 4.1.7).

Figure 4.1. 7 – Digests of pUC18-hIRE1 β . A) Restriction sites. B) Test digest of pUC18-hIRE1 β -L590A with *EcoRI* and *DraI* 1-Ladder, 2-Undigested, 3- Digested.



Each mutant's fragment was ligated to the original plasmid's larger fragment using the standard method reaction as described in Materials and Methods "DNA Ligation with T4 DNA ligase" and the resulting ligant chemically transformed into competent *E. coli* and plated out. Resulting colonies were minipreped and screened for completed ligation by redigesting with *SnaBI*, which digests twice, once in the predicted insert, once in the pCAG vector yielding bands at 3180 and 4460 bp. An incorrect alignment of the insert would result in bands at 5232 and 2408.

Figure 4.1. 8 – Screening of pCAG-hIRE1 β . A) Digestion sites for screening enzyme (*Sna*BI) B) Correct orientation of insert. C) Screening of pCAG-hIRE1 β with *Sna*BI.

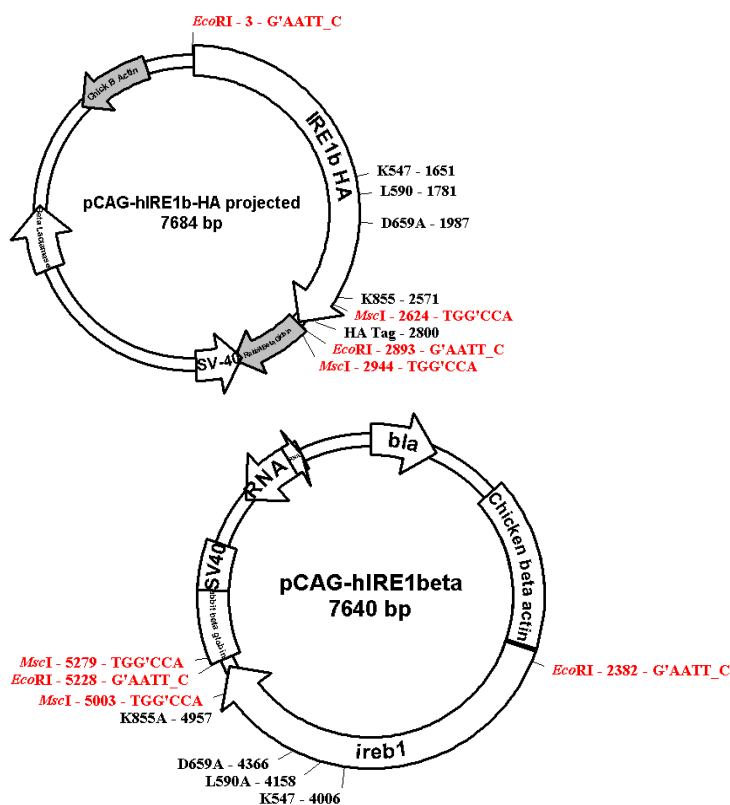


In Figure 4.1. 8 above, Clones 2 and 3 have aligned successfully. *E. coli* clones with correctly religated plasmids were frozen in 30% glycerol and stored. Large scale preparations were made of each mutant using an endotoxin-free maxiprep kit (EndoFree Plasmid Maxi Kit) to produce plasmid suitable for mammalian transfection.

4.1.10 Cloning Strategy for Addition of HA Tag into pCAG Plasmids

As at the time of cloning, no antibody was available to perform a Western blot for the hIRE1 β protein that could detect the product of the pCAG-hIRE1 β , therefore it was determined to use the HA tag in the plasmid provided by K. Kohno, Nara Institute of Science and Technology, Japan to permit detection by Western blot, and clone this tag into all the pCAG-hIRE1 β mutant expressing plasmids. The two *MscI* sites flanking the HA tag end of the pCAG-hIRE1 β -HA plasmid were chosen to clone the HA tag into the pCAG-hIRE1 β mutants, but this required screening of the clones by digest with *EcoRI* to ensure the HA tag had been cloned in the correct orientation. pCAG-hIRE1 β -HA was digested with *MscI* and run on a gel and the 320 bp insert containing the HA tag excised from the gel and purified using the GenElute™ Gel Extraction Kit. pCAG-hIRE1 β mutants were digested with *MscI* and the vector 7364bp similarly purified. The two fragments were religated the standard method reaction as described in Materials and Methods “DNA Ligation with T4 DNA ligase” and the resulting ligant chemically transformed into competent *E. coli* and plated out. Resulting colonies were minipreped and screened for completed ligation by redigesting with *EcoRI*.

Figure 4.1. 9 - HA Tag Cloning into pCAG vectors.

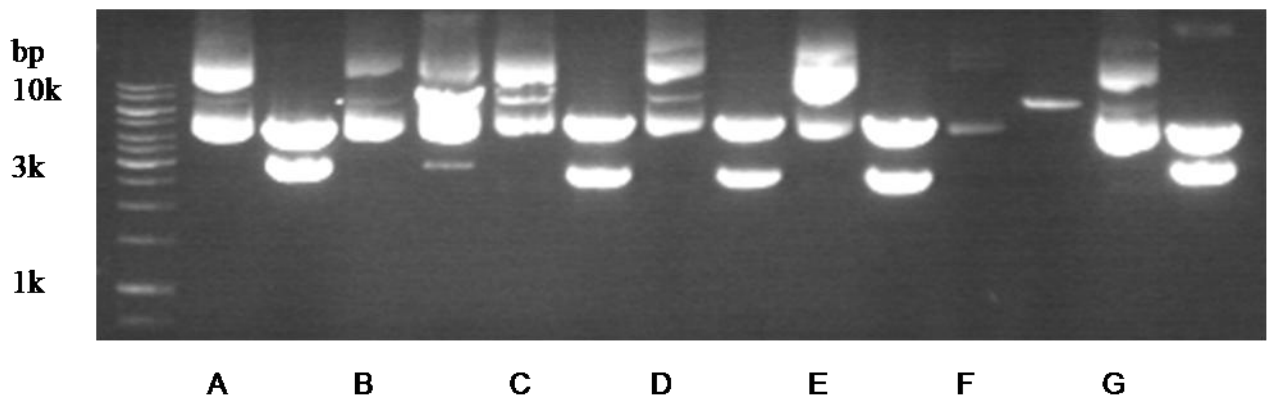


After digest of clones by *EcoRI*, the resulting samples were run on 1% agarose gel. Correctly orientated religated plasmid gave bands at 4794 and 2890bp, reversed insert gave bands at 5063 and 2621 (see

Figure 4.1. 9).

Figure 4.1. 10 - Successful and unsuccessful pCAG-hIRE1 β HA-tag clones. Representative examples of digests, each pair of lanes LH lane undigested, RH lane digested with *EcoRI*.

Mutants in lanes A-C- D659A/L590A, D-D659A/L590G, E-F – K547A/L590A, G- K547A/L590G.



Lanes A and G show bands at 4794 and 2890, correct orientation, Lanes C,D and E are the incorrect 5063 and 2621 orientation, Lanes B and F have not sufficiently digested (linearised).

4.1.11 Summary

After mutagenesis, successful mutant plasmids were produced for all the required mutants of the IRE1 kinase pocket. Enzymes were selected to use to screen for each mutagenesis and mutagenesis primers successfully designed. After mutagenesis the mutated IRE1 sequence was subcloned into the original plasmid to reduce the risk of point mutations produced during mutagenesis affecting the plasmid. Problems encountered included the GC-heavy region of the rabbit β -globin gene which severely impeded sequencing and mutagenesis and forced subcloning into a shorter plasmid – the large size of both plasmids may have contributed to the low number of transformants in most mutagenesis reactions.

Ideally it would have been better to test/check the availability of anti IRE1 β antibody and perform all initial cloning steps in the HA tagged IRE1 β plasmid rather than the untagged. This would have saved multiple cloning steps.

4.2 Optimisation of IRE1 α and IRE1 β expression in *ire1 α ^{-/-}* cells

4.2.1 Rationale for Optimisation

As described in Bertolotti (Bertolotti 2000), the IRE1 β isoform is only expressed in gastrointestinal cells, and therefore an *ire1 α ^{-/-}* mouse embryonic fibroblast cell line was considered adequate for testing putative analogue-sensitised IRE1 mutants, as α is the ubiquitous isoform. In order to isolate the optimum conditions for the expression of mutant constructs in this cell line, the optimum conditions for transfection, concentration of DNA and growth of cells required testing. Previous experiments by N. Strudwick in our laboratory indicated the optimum method for transfection of MEFs was by electroporation, as these cells were difficult to transfect by chemical methods. Transfection was performed using the pre-optimised parameters used by N. Strudwick with the Digital Biotech/Invitrogen Electroporator, set to a single pulse at 1700mV, 20ms. All micrographs in this study are at 10x magnification.

4.2.2 Transfection Efficiency Assessment with GFP

ire1 α ^{-/-} mouse embryonic fibroblasts were grown to 80-90% confluency, trypsinised and centrifuged. 1×10^6 cells per transfection were resuspended in 100 μ l of Neon[®] Transfection System Buffer R (Invitrogen Life Technologies Ltd, Paisley, UK), then electrotransfected using the above conditions and according to the protocol in Materials and Methods - “Transfection – Electroporation” with 2 μ g of pMAX-GFP plasmid. After transfection they were grown in a six well tissue culture plate (Sarstedt, Leicester, UK) for 24 hours in Dulbecco’s modified eagle’s medium with pyruvate and then visualised by UV and visible light confocal microscopy. Transfection efficiency was high, 70-80%, and therefore it was determined this methodology was suitable for transfection. Untransfected cells show no visible background fluorescence under the UV filter.

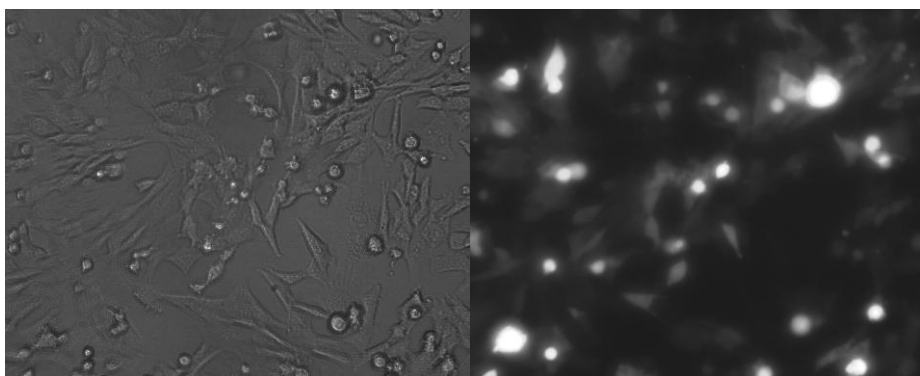


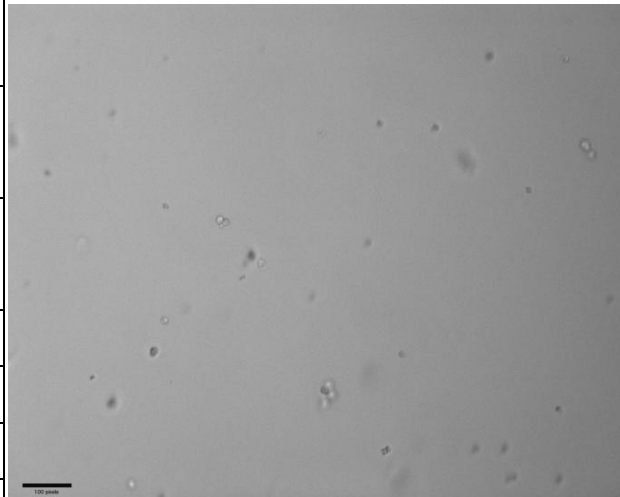
Figure 4.2. 1 – Transfection efficiency of *ire1a*^{-/-} mouse embryonic fibroblasts with pMAX-GFP. LH panel transfected cells with visible light, RH panel GFP fluorescence of same transfected cells with UV light.

4.2.3 Transfection of pEDΔc/pCAG plasmids to assess effect of IRE1 protein on viability of MEFs

Once the efficiency of the transfection method had been established, preliminary transfections were performed with the wild-type and available mutant IRE1 plasmids and the empty pEDΔC and pCAG vectors provided by R. Kaufman, University of Michigan, USA (pEDΔC) and K. Kohno, Nara Institute of Science and Technology, Japan (pCAG) to ascertain their effect on MEF viability. *ire1a*^{-/-} mouse embryonic fibroblasts were grown to 80-90% confluency, trypsinised, centrifuged. 1×10^6 cells per transfection were resuspended in 100μl of Buffer R, then electrotransfected by a single pulse at 1700mV, 20ms with 4ug of the listed plasmid. After transfection cells were seeded into a six well tissue culture plate (Sarstedt, Leicester, UK) and grown for 24 hours in Dulbecco's Modified Eagle's Medium with pyruvate. Cell growth was assessed by eye.

Figure 4.2. 2 – Preliminary IRE1 transfections, percentage viability and example of micrograph showing non-adherent cells after transfection with pEDΔC-hIRE1α.

Transfected Plasmid	% Viability
pMAX-GFP (Positive control)	40-50%
No plasmid (Negative control)	40-50%
pEDΔC-hIRE1α	<5%
pCAG-hIRE1β	<5%
pEDΔC	20-30%
pCAG	10-20%
pEDΔC-hIRE1α-K599A	<10%
pCAG-hIRE1β-K547A	<10%
pEDΔC-hIRE1α-K907A	<5%
No transfection	100%



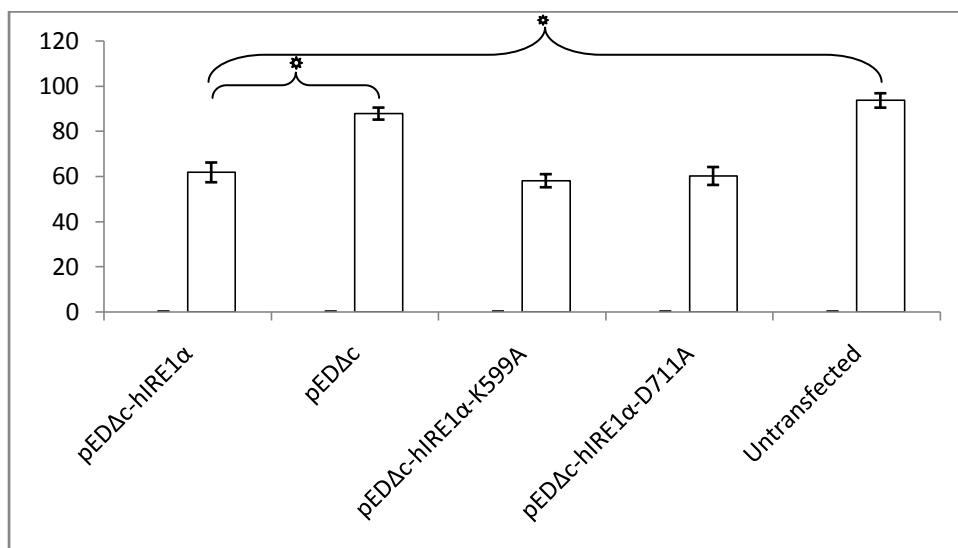
Initially, experiments using 4μg of DNA per transfection resulted in low viability of cells transfected with IRE1 plasmids, possibly due to triggering of apoptosis or ER stress from overexpressing the IRE1 protein. Iwawaki et al report similar problems with viability in HeLa cells overexpressing transiently transfected IRE1 (Iwawaki, Hosoda et al. 2001). Viability was lost both by transfection alone and by transfection with the empty vector but not to the same extent as that by either wild type or mutant IRE1. It was not possible to ascertain whether the loss of viability was due to the presence of IRE1 or due to overexpression of plasmid.

To elucidate the role of the IRE1 plasmid in the loss of viability, further quantitative examination was made into the detrimental effect of transfection of the pEDΔC plasmids into cell death. As above *ireα*^{-/-} mouse embryonic fibroblasts were grown and electrotransfected with 4μg of the listed plasmid in Table 4.2. 1. After transfection cells were grown for 24 hours and cell viability assessed by trypsinising cells, resuspending and staining with trypan blue and then counting live/dead cells with an improved Neubauer haemocytometer

Table 4.2. 1 – Viable cell counts (cells in one 1mm² square of haemocytometer, five replicates).

Plasmid	Dead					Live					% Viability							
	1	2	3	4	5	1	2	3	4	5	1	2	3	4	5	Mean	SE	
pEDΔc-hIRE1α	20	19	14	11	17	33	20	21	29	29	62.3	51.3	60	72.5	63	61.81794	4.37	
pEDΔc (empty vector)	5	7	6	2	5	36	31	35	25	57	87.8	81.6	85.4	92.6	91.9	87.85555	2.66	
pEDΔc-hIRE1α-K599A	15	11	18	16	22	21	14	25	31	24	58.3	56	58.1	66	52.2	58.12085	2.9	
pEDΔc-hIRE1α-D711A	15	19	12	10	20	23	21	27	18	24	60.5	52.5	69.2	64.3	54.5	60.21765	3.97	
Untransfected	1	1	0	2	0	9	10	17	14	9	90	90.9	100	87.5	100	93.68182	3.19	

Figure 4.2. 3 – Viability of cells transfected with pEDΔc constructs.



* P = <0.005

In this experiment viability counts indicated no significant difference between the untransfected cells and the empty vector transfection, but a significant difference between untransfected and empty vector, and IRE1α constructs, demonstrating a role for the IRE1α protein in the loss of viability.

4.2.4 Strategies for overcoming viability loss – reduced DNA in transfection

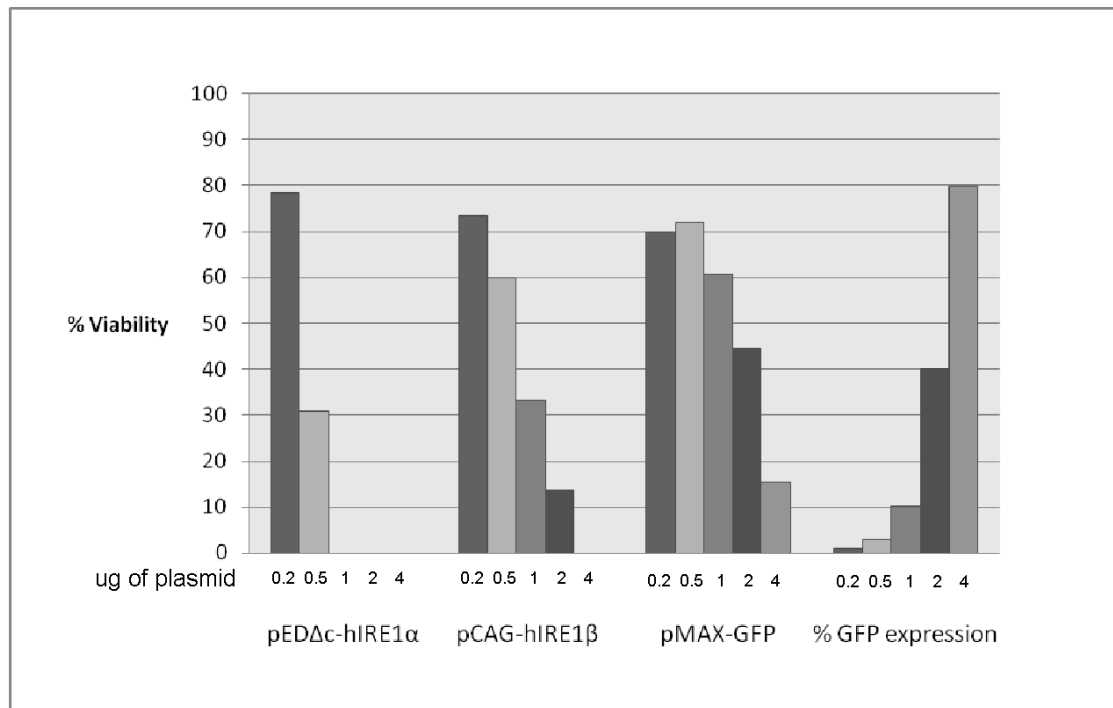
The loss of viability due to the IRE1α construct expression was detrimental to further study of the protein, and was required to be overcome. To attempt to overcome this viability issue, varying concentrations of 0.1, 0.5, 1, 2 and 4 μg of DNA were transfected to ascertain if there was a level at which expression was detectable but cells were sufficiently viable. pMAX-GFP was used to assess plasmid expression. *ire1α*^{-/-} mouse embryonic fibroblasts were grown to 80-90% confluency, trypsinised and centrifuged. 1x10⁶ cells per transfection were resuspended in 100μl of Neon® Transfection System Buffer R, then electrotransfected using the above conditions and according to the protocol in Materials and Methods - “Transfection – Electroporation” with 2μg of either pEDΔc-hIRE1α, pCAG-hIRE1β or pMAX-GFP plasmid. After transfection they were grown in a six well tissue culture plate (Sarstedt, Leicester, UK) for 24 hours in Dulbecco’s Modified Eagle’s Medium with pyruvate and then visualised by UV and visible light confocal microscopy. Viability was measured by

trypsinising cells, resuspending and staining with trypan blue and then counting live/dead cells with an Improved Neubauer haemocytometer. GFP expression was measured by UV fluorescence under confocal microscope.

Table 4.2. 2 – Viable cell counts/Transfection efficiency in viability assessments.

µg of plasmid/ transfection	pEDΔC-hIRE1α			pCAG-hIRE1β			pMAX-GFP			% GFP Fluorescence
	Live	Dead	%	Live	Dead	%	Live	Dead	%	
0.2	18	5	78.3	11	4	73.3	7	3	70	<1%
0.5	18	8	30.5	21	14	60.0	13	5	72	3%
1	26	0	0	5	10	33.3	17	11	60.7	10%
2	21	0	0	3	19	13.6	4	5	44.4	40%
4	20	0	0	0	15	0	2	11	15.3	80%

Figure 4.2. 4 - Viability of *ire1α*^{-/-} MEFs with varying concentrations of IRE1 plasmids and GFP expression plasmids.



As seen in Figure 4.2. 4, viability of MEFs inverse correlation with transfection efficiency/DNA concentration, suggesting that transfection of cells may result in cell death and therefore there was unlikely to be a suitable concentration of plasmid which can be transfected which will produce suitable expression levels of IRE1 without also reducing

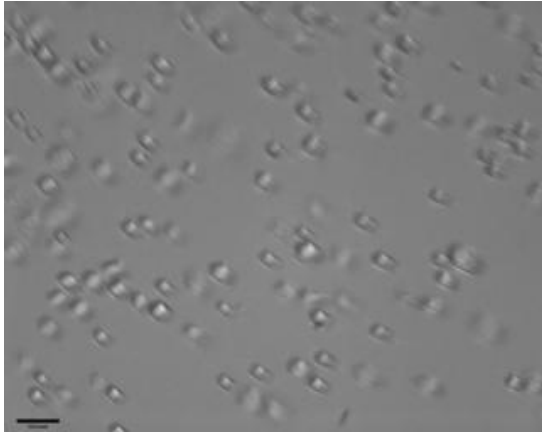
viability so far as to make harvesting of mRNA or protein in high enough concentrations for further analysis possible.

4.2.5 Strategies for overcoming viability loss – Time Course for Expression

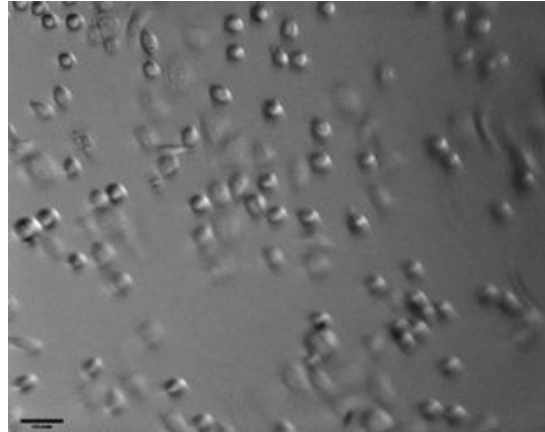
Having eliminated the possibility of reducing the levels of DNA transfected, next the possibility of reducing the amount of time cells were expressing IRE1 was examined, to reduce the stress of constant high expression of the protein. MEFs were transfected with 2 μ g of pMAX-GFP and inspected for expression at 0.5, 1, 2, 4, 8, and 12hrs. Fluorescence due to GFP expression was not found to occur until the 8 hr timepoint when most cells had adhered to the surface of the culture dish (Figure 4.2. 5), indicating a minimum of eight hours before plasmid expression could be detected. Having ascertained when GFP expression was occurring, MEFs were transfected with pED Δ C-hIRE1 α and examined for viability at 4, 6, 8 and 12h. After 4 h, some cells appeared to be adhering and growing, while most floated in the medium, either dead or unable to adhere. It is difficult to ascertain whether adherent cells were untransfected or not. GFP fluorescence was not detectable until at least eight hours, after viability was already being lost in pED Δ C-hIRE1 α transfection.

Figure 4.2. 5 - Expression of GFP Timecourse in *ire1 α* ^{-/-} MEFS. Bright field microscopy with fluorescence microscopy overlay where required.

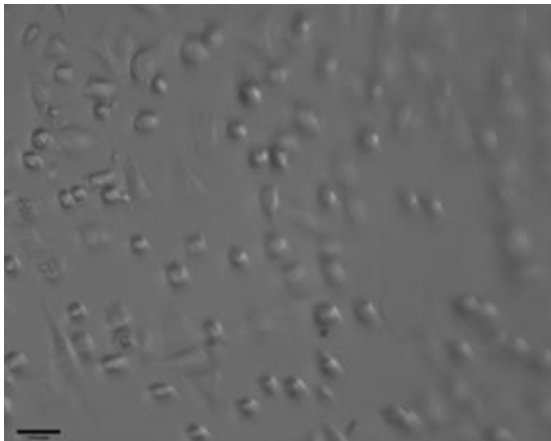
0.5h



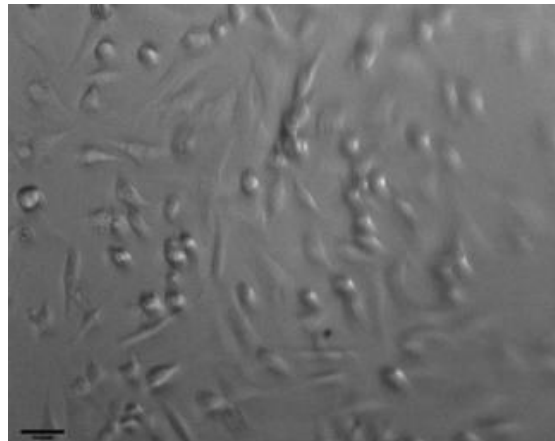
1hr



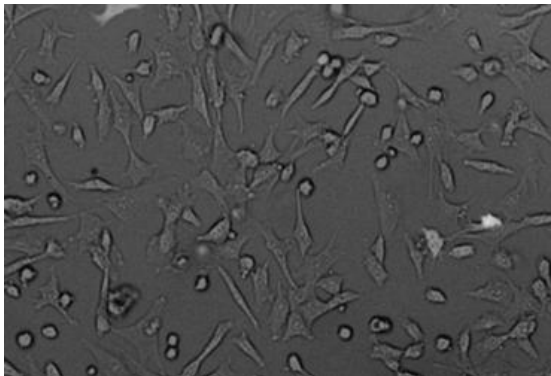
2hrs



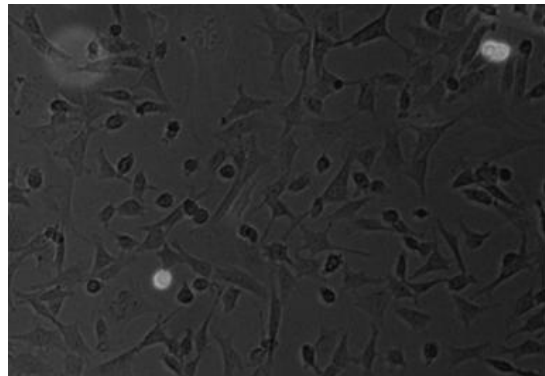
4hrs



8hrs



12hrs



4.2.6 Strategies for overcoming viability loss – transfection of *traf2*^{-/-} cells to eliminate IRE1-induced cell death by the TRAF2 Pathway

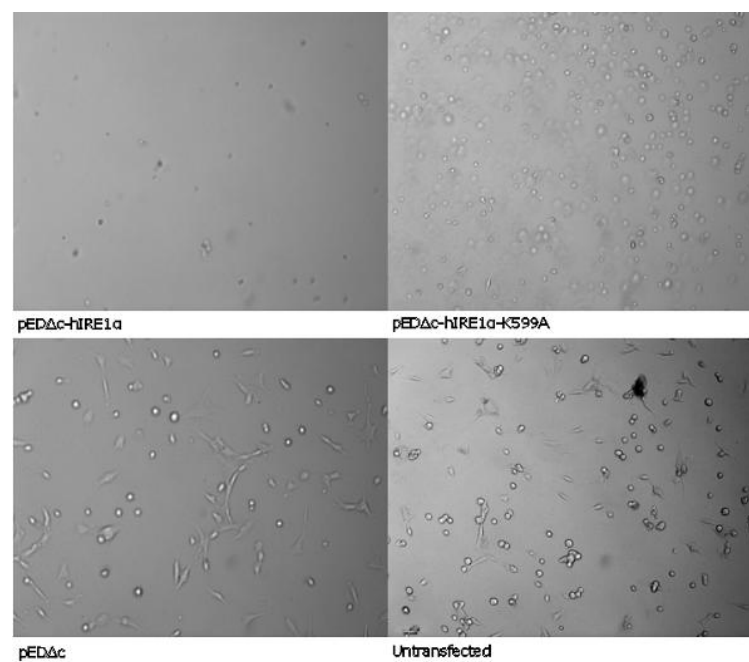
In order to ascertain whether cell death after transfection was via a TRAF2 dependent pathway as would be expected if expression of IRE1 was responsible (Urano, Bertolotti et al. 2000), 1×10^6 *traf2*^{-/-} MEFs (see Materials and Methods “Cell Lines”) were resuspended in 100 μ l of transfection Buffer R and transfected with 4ug of pED Δ C-hIRE1 α , kinase dead pED Δ C-hIRE1 α -K599A, and empty vector pED Δ C. After 24 hrs, the cells were photographed by confocal microscopy and live vs. dead cells counted. Untransfected cells were also assessed as a control.

Both empty vector and untransfected cells again showed similar viability, and both the wild type and the kinase dead IRE1 α (rather than wild-type alone – a kinase-dead IRE1 should not be capable of inducing this pathway were TRAF2 to in fact be present for some reason) suffered loss of viability, suggesting that problems in viability may be due to a general overexpression of a transmembrane protein, which could potentially be overcome using a weaker promoter such as herpes simplex virus (HSV) thymidine kinase (TK) to express the IRE1 protein (Allen 1988; Nakamura, Watanabe et al. 2008). It is also possible that a point mutation in the K599A mutant (see “Cloning of IRE1 α and IRE1 β mutant plasmids”, above) may have been interfering with the results, and a corrected version of this mutant was produced by subcloning.

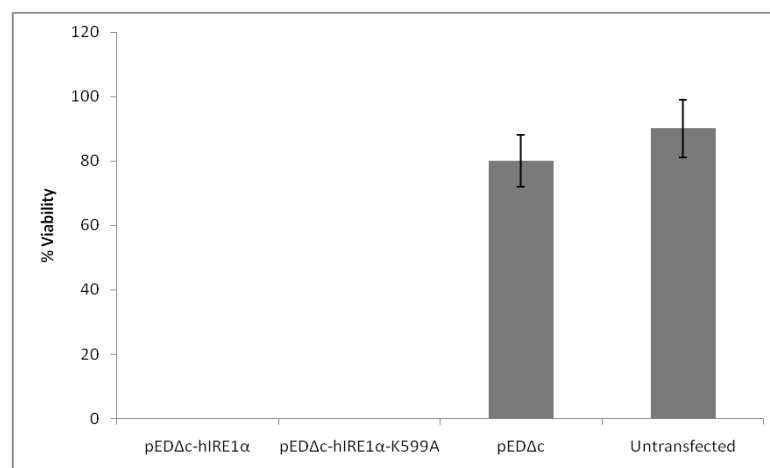
Figure 4.2. 6 – Effect of pEDΔC-hIRE1α on *traf2*^{-/-} mouse embryonic fibroblasts. A) Live/Dead cell counts per haemocytometer square. B) Light microscopy of cells 24 hours after transfection. C) % Viability of transfections/untransfected.

A	Replicate	1			2			3			4			5			Mean	SE
		Live	Dead	%	L	D	%	L	D	%	L	D	%	L	D	%		
pEDΔC-hIRE1α		0	6	0	0	2	0	0	5	0	0	9	0	0	6	0	0	0
pEDΔC-hIRE1α-K599A		0	4	0	0	2	0	0	6	0	0	4	0	0	2	0	0	0.00
pEDΔC		3	3	50	1	0	100	6	0	100	3	1	75	3	1	75	80	9.35
Untransfected		3	4	43	4	0	100	2	0	100	2	0	100	6	0	100	88.57	11.43

B



C



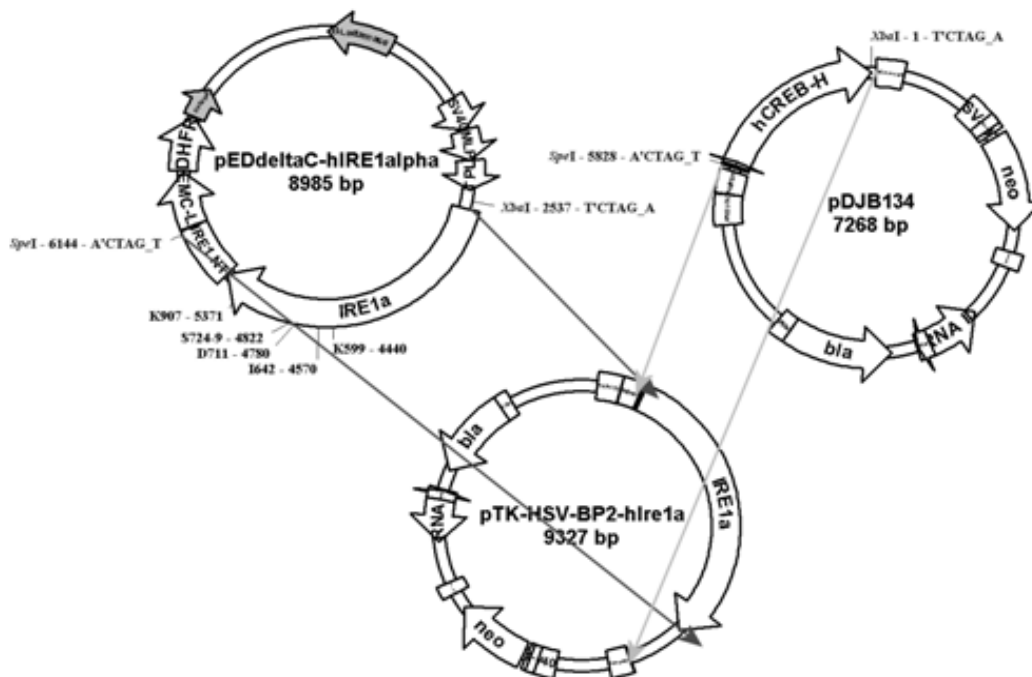
4.2.7 Strategies for overcoming viability loss – weak promoter

As the sequences driving the pEDΔC-hIRE1 α and pCAG-hIRE1 β plasmids were strong, adenoviral/ β -actin promoters, it was determined to ascertain whether the use of a weaker promoter would reduce the expression of IRE1 α to levels suitable to retain viability. The herpes simplex thymidine kinase (an enzyme involved in DNA synthesis) promoter is a weak promoter with no tissue specificity whose sequence contains only 5' flanking sequences associated with an early gene of herpes simplex virus. Its promoter sequences include a C-AT-A-T-T-A-A sequence 31 nucleotides, and a G-G-C-G-A-A-T-T-C sequence frequently conserved in eukaryotic organisms 85 nucleotides upstream of the initiation codon (Wagner, Sharp et al. 1981; Allen 1988; Nakamura, Watanabe et al. 2008). The pDJB134 plasmid containing the HSV thymidine kinase promoter was a gift from the Marie Curie Research Institute, Surrey.

4.2.8 Cloning of thymidine kinase promoter

The IRE1 α sequence was cloned into the thymidine kinase plasmid by digesting pEDΔC-hIRE1 α with the restriction enzymes *SpeI* and *XbaI* to excise the IRE1 sequences and untranslated region. The pDJB134 plasmid was also digested with *SpeI* and *XbaI* to remove the CREB-H sequence. The IRE1 fragment was then ligated into the pDJB134 plasmid to produce pTK-HSV-BP2-hIRE1 α (See Figure 4.2. 7). As *SpeI* and *XbaI* ends are compatible, the IRE1 fragment could ligate in either orientation, therefore transformants were minipreped and screened for the orientation of the plasmid which no longer digested with *SpeI* and *XbaI* as the sites had been destroyed by the cloning.

Figure 4.2. 7 – Cloning strategy for pTK-HSV-BP2-hIRE1 α .



The IRE1 β sequence was cloned into the thymidine kinase plasmid by digesting pCAG-hIRE1 β overnight with the restriction enzymes *Sall* and *XbaI* to excise the strong chicken β -actin promoter. The pDJB134 plasmid was digested with *Sall* and *NheI*, in recommended Fermentas Buffer AarI, to remove the thymidine kinase promoter. The 1162bp thymidine kinase promoter fragment was then ligated at a 1:3 vector:insert ratio into the pCAG-hIRE1 β plasmid to produce pTKRG- hIRE1 β . The hIRE1 β insert contains a single *KpnI* site in the middle of the IRE1 β sequence. This was used to screen miniprep ligants for inserted hIRE1 β .

ire1 α ^{-/-} mouse embryonic fibroblasts were grown to 80-90% confluency, trypsinised and centrifuged. 1x10⁶ cells per transfection were resuspended in 100 μ l of Buffer R, then electrotransfected using the above conditions and according to the protocol in Materials and Methods - “Transfection – Electroporation” with 4 μ g of either pTK-HSV-BP2-hIRE1 α , pTKRG-hIRE1 β (thymidine kinase promoter plasmids) pEDAC-hIRE1 α , pCAG-hIRE1 β (strong promoter plasmids) or the empty vectors pEDAC or pCAG. After transfection they were grown in a six well tissue culture plate (Sarstedt, Leicester,UK) for 24 hours in Dulbecco’s Modified Eagle’s Medium with Pyruvate. After 24 hours there was no visible

difference between the cell death due to the weak promoter thymidine kinase plasmids and the strong promoter plasmids suggesting that the weaker promoter was not sufficient to reduce the loss of viability.

Table 4.2. 3 – Viability comparison after transfection with weak/strong promoter plasmids.

Plasmid	% Viability/Confluence
pTK-HSV-BP2-hIRE1 α	<5%
pTKRG-hIRE1 β	<5%
pED Δ C-hIRE1 α	<5%
pCAG-hIRE1 β	<5%
pED Δ C	60-70%
pCAG	60-70%
No transfection	100%

4.2.9 Strategies for overcoming viability loss – use of alternative transfection buffers

Concomitantly with the production of the thymidine kinase plasmids, it was determined that since a certain amount of viability was lost by the transfection method alone, to attempt to use a transfection buffer which resulted in a higher viability. The transfection Buffer R used for electrotransfection of plasmids is described as a DPBS-based buffer in (Kim2008). Patent WO/2008/134200 (Rubio and Terefe 2008) describes a set of high efficiency transfection buffers containing a number of additional components which could contribute to viability and transfection efficiency – a sugar to match cellular osmolarity, HEPES as a buffering agent, MgCl₂ and EGTA to chelate halide salts, DMSO to render cells permeable, ATP to retain viability, glutathione to neutralise any free radicals, and pH adjustment with potassium salts rather than sodium to more closely mimic the intracellular environment. Additionally, the Eppendorf Multiporator manual (Version 2006) recommends an electrical conductivity of 3.5 mS/cm and not exceeding 10 mS/cm (<http://www.eppendorf.com/script/cms-newspic.php?id=1744&inline=1&col=DOWNLOADFILE>) to be achieved by the addition of myo-inositol to approximately 90mOsmol/kg. One of the buffers listed as most efficient in the patent WO/2008/134200 was prepared and tested under the same transfection conditions as the Invitrogen Buffer R. pMAX-GFP was used to assess plasmid expression. *irea*^{-/-} mouse

embryonic fibroblasts were grown to 80-90% confluency, trypsinised and centrifuged. 1×10^6 cells per transfection were resuspended in 100 μ l of Neon® Transfection System Buffer R (Invitrogen Life Technologies Ltd, Glasgow, UK), or the Buffer to be tested then electrotransfected using the above conditions and according to the protocol in Materials and Methods - “Transfection – Electroporation” with 2 μ g of pMAX-GFP plasmid. After transfection they were grown in a six well tissue culture plate (Sarstedt, Leicester, UK) for 24 hours in Dulbecco’s modified eagle’s medium with pyruvate and then visualised by UV and visible light confocal microscopy.

Table 4.2. 4 - Transfection Buffer Recipes (from (Rubio and Terefe 2008)) and the Digital Biotech (Seoul, Korea)/Invitrogen Microporator protocol (Protocol Reference: MP-100 Rev.M.03.51-11/07)

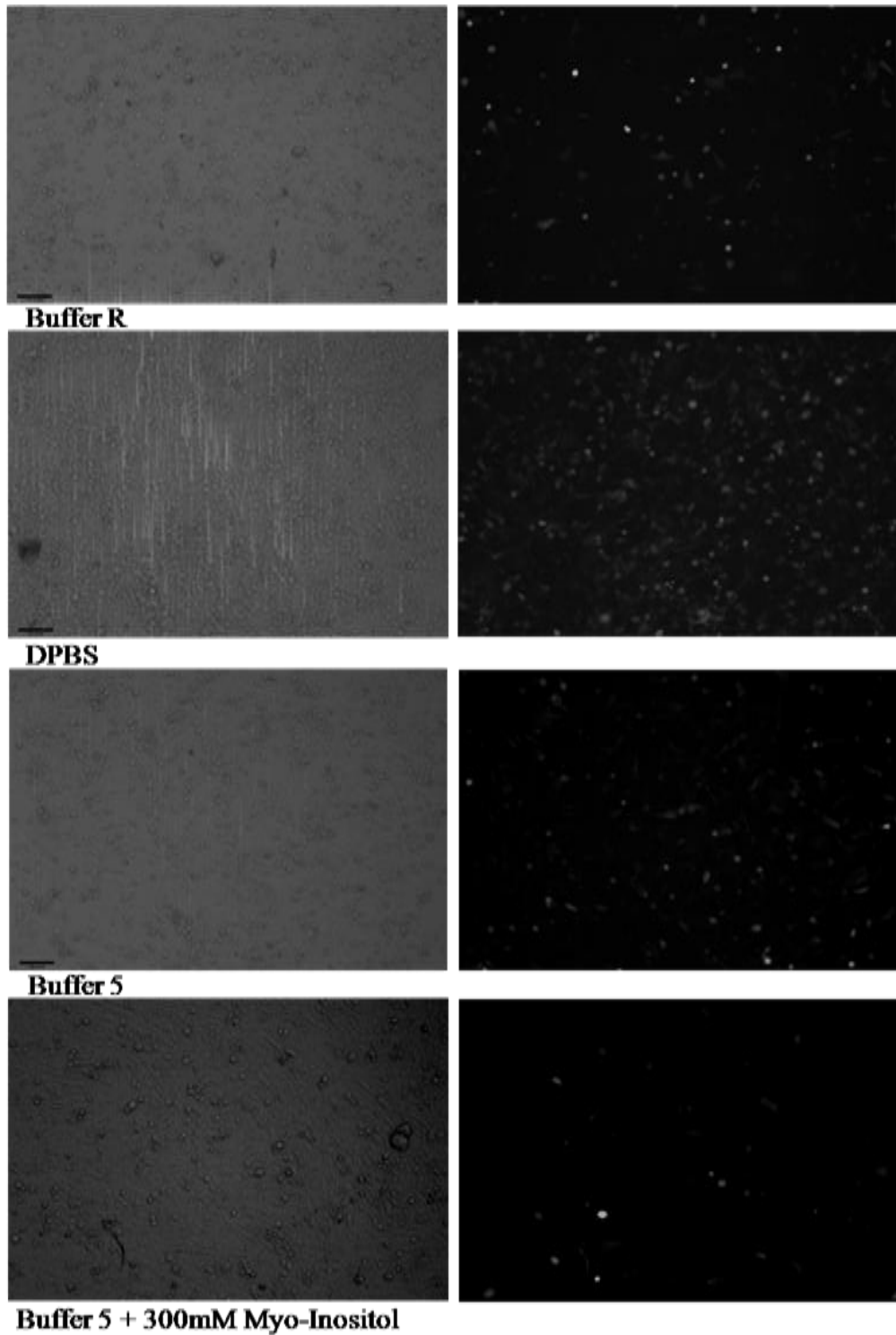
Buffer 5	PBS + Glucose
250mM Trehalose	1x PBS (see Materials and Methods)
5mM Potassium Phosphate	200mM Glucose
25mM HEPES	
5mM MgCl ₂	
2mM EDTA	
pH 7.2-7.5	

Observation of the electrotransfection apparatus during transfection appeared to indicate a difference in the conductivity of the buffer solutions, as when Buffer R was used, small bubbles of gas due to decomposition of water were emitted from the apparatus, but this did not occur with the other buffer solutions. Measurement of the conductivity of Buffer R with a conductivity meter gave 14.71 mS/cm, similar to Dulbecco's PBS, from which the buffer is derived (Kim, Cho et al. 2008) Addition of myo-inositol as recommended in the Eppendorf multiporator manual did not improve transfection efficiency over Buffer 5 alone (see Figure 4.2. 8)

Table 4.2. 5 - Conductivities of Electrotransfection Buffers

Buffer	Conductivity (mS/cm)
Buffer R	14.71
DPBS	14.00
Buffer 5	3.09
Buffer 5 + 300mM Myo-inositol	3.30

Figure 4.2. 8 - Transfection efficiency with electrotransfection buffers. Left-hand panels show visible light microscopy and right-hand GFP fluorescence with UV light. DPBS-based buffers exhibit high efficiency of transfection, as opposed to experimental buffers.

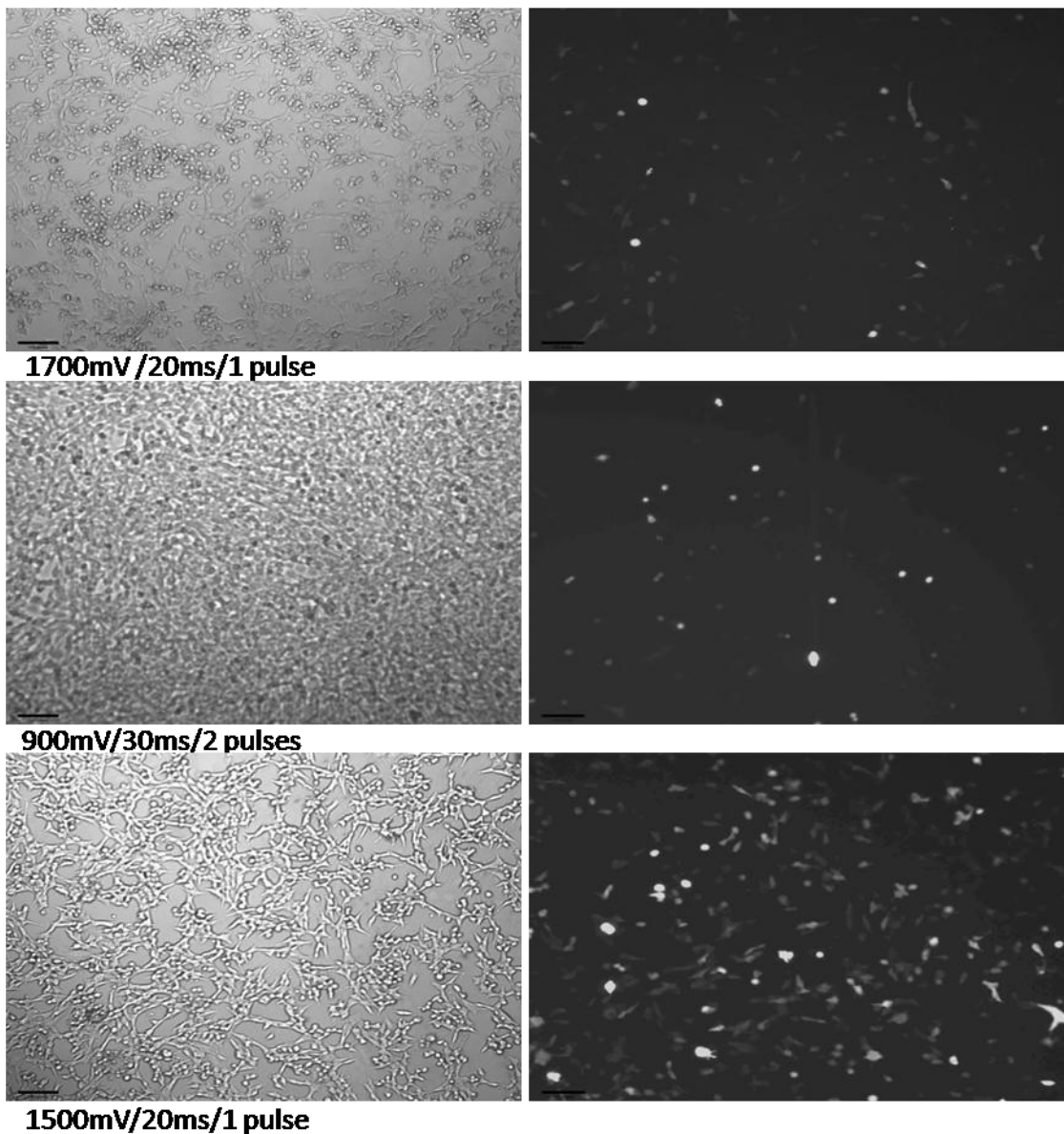


Preliminary experiments comparing buffers from the patent/literature to Buffer R using the standard conditions used for Buffer R did not produce an improvement in viability or transfection – therefore it was determined to perform the optimisation for transfection conditions using the methodology as listed in the microporator manual using Buffer 5 which appeared to produce the most fluorescence. The electrotransfection was repeated as above with Buffer 5, but the electrotransfection parameters were altered as in Table 4.2. 6. Conditions producing a viability and transfection efficiency equivalent to that of Buffer R were achieved (see Figure 4.2. 9) were no better than Buffer R and therefore did not contribute to improved RNA or protein yields (see later chapters).

Table 4.2. 6 - Optimisation of Electrotransfection Buffer

Pulse Voltage (mV)	Pulse Width (ms)	Number of pulses	Transfection efficiency	Viability
1400	20	1	80%	60%
1500	20	1	80%	60%
1600	20	1	80%	50%
1700	20	1	80%	50%
1100	30	1	60%	80%
1200	30	1	40%	50%
1300	30	1	40%	40%
1400	30	1	50%	30%
1000	40	1	30%	70%
1100	40	1	40%	60%
1200	40	1	30%	50%
1100	20	2	50%	90%
1200	20	2	50%	70%
1300	20	2	20%	80%
1400	20	2	10%	60%
900	30	2	20%	100%
1000	30	2	10%	90%
1100	30	2	40%	80%
1200	30	2	30%	50%
1300	10	3	10%	40%
1400	10	3	20%	30%
1500	10	3	10%	30%
1600	10	3	30%	20%

Figure 4.2. 9 - Buffer 5 Optimisation. Left-hand panels show visible light microscopy and right-hand GFP fluorescence with UV light. Upper panels represent previous optimized transfection conditions with Buffer R. Middle panels show a low voltage with low transfection efficiency. Lowest panels represent optimum conditions for Buffer 5, indicating this buffer requires a higher voltage.



4.2.10 Summary

From the outset, viability issues with MEFs after IRE1 plasmid transfection impeded analysis after transfection. Reduction in transfection plasmid concentration did improve viability, but not to any useful extent and transfection efficiency was sacrificed as a result. Use of alternative buffers/transfection conditions did not improve viability in any way which was not again a tradeoff against transfection efficiency. As plasmid expression did not appear to occur until eight hours after transfection, it was not possible to use an earlier timepoint in order to catch cells before they had completed apoptosis. The mechanism of IRE1 plasmid transfection-induced cell death is unclear – transfection alone was not the cause, as the use of a GFP expressing plasmid did not kill the cells to the same extent. Apoptosis induced via the IRE1-TRAF2 arm was unlikely, as cells without TRAF2 also suffered cell death from transfection. This left the possibility that overexpression of the IRE1 protein was causing lethal ER stress, therefore IRE1 constructs were produced with a low-copy thymidine kinase promoter. These constructs did not produce any improvement in viability over the stronger promoters.

4.3 Testing of IRE1 α constructs in IRE1 α ^{-/-}MEFs by transient transfection

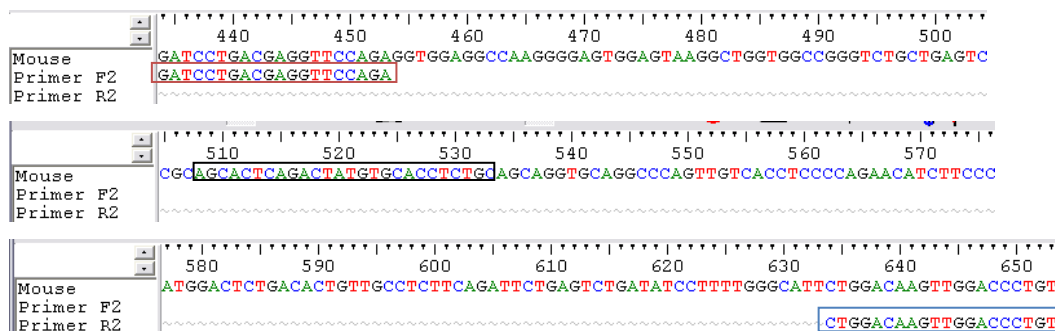
4.3.1 Rationale

Before it was discovered that viability loss due to IRE1 transfection would severely impede the harvesting of sufficient RNA to allow reliable and repeatable analysis of XBP-1 splicing (Chapter 4.2), the transient transfection was thought to be a suitable method for testing the IRE1 wild type and mutant constructs for activity, as it allows for relatively simply performed, short-term expression of plasmid constructs, and should have provided usable results indicating IRE1 kinase and RNase function without the long complex procedures required to produce stable cell lines, and allow the testing of antibodies against IRE1 and JNK to permit examination of expression levels of IRE1 and activation of apoptosis.

4.3.2 D711A mutant exhibits XBP-1 Splicing In MEFs Transiently Transfected with Mutant IRE1 α

In order to assess the effectiveness of the IRE1 expressing wild type and mutant plasmids in producing functional IRE1, splicing of the bZIP transcription factor XBP-1 in response to ER stress was used as a marker for function of IRE1's RNase activity and therefore activation of a properly folded and functional protein. Proportional spliced/unspliced XBP-1 was assessed by harvesting RNA from IRE1 transfected MEFs. RNA harvesting was performed according to the protocols in Materials and Methods "RNA isolation". RNA thus harvested was analysed using the Molecular Devices Spectramax Spectrophotometer for RNA concentration. Total RNA was then reverse transcribed into DNA (see Materials and Methods – RNA - "cDNA Production from RNA") and PCR was performed using primers flanking the splicing excision site (Figure 4.3. 1) in order to obtain products that would differ detectably when run on a 2% electrophoresis gel (see Materials and Methods – RNA - "Reverse transcription (RT)-PCR Assay for Actin/XBP-1 splicing/IRE1 α "). Products from unspliced XBP-1 run at 219bp, spliced at 193bp.

Figure 4.3. 1 - Sequence section from murine XBP-1. Red box – Forward primer flanking splicing excision site. Black box – 26 base pairs excised in spliced XBP-1. Blue box – Reverse primer flanking splicing excision site.

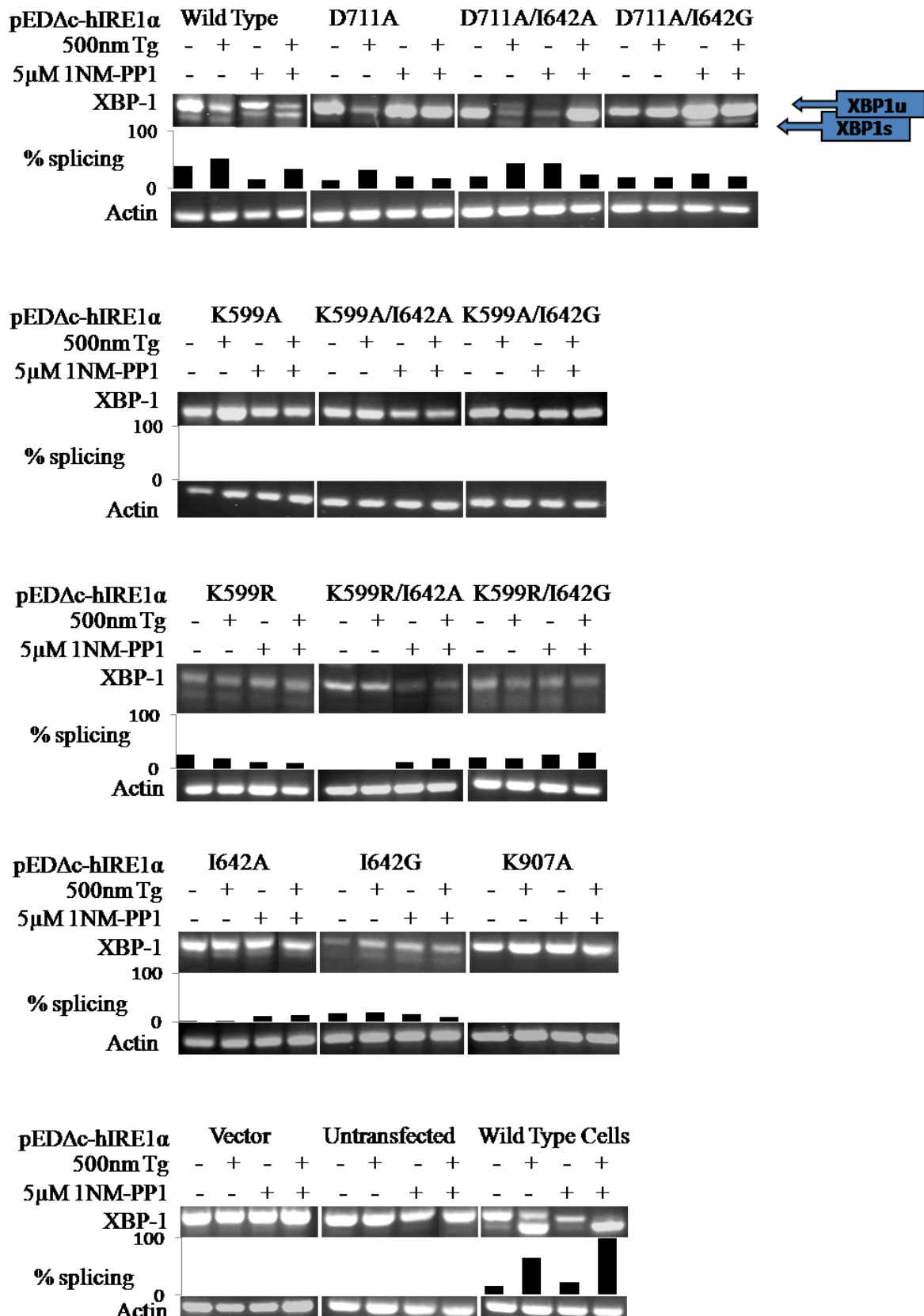


As was explained in Section 4.2, it proved difficult to reliably produce viable transfected cells. Therefore several repeats of each XBP-1 splicing assay were required to produce sufficient data. *ire1 α* ^{-/-} MEFS were transfected with 2 μ g of each pED Δ c-hIRE1 α plasmid and grown for 24 hours. Those undergoing ER stress induction were then treated for two hours with 500nM thapsigargin (Tg). Both stressed and unstressed cells were also treated with 5 μ M 1NM-PP1 for two hours to attempt to induce splicing bypassing the kinase pocket in analogue-sensitised I642A/G mutants. After treatment cells were harvested for RNA. Total RNA was reverse transcribed and Touchdown RT-PCR performed as described the Materials and Methods (“Touchdown RT-PCR for mouse XBP-1/Actin“) to obtain XBP-1 splicing PCR products. As a negative control, *ire1 α* ^{-/-} cells untransfected were used and as a positive wild type cells (wild type mouse embryonic fibroblasts, see Materials and Methods – “Cell Lines”) with or without 500nM thapsigargin treatment.

In Figure 4.3. 2, although splicing can be seen in the wild-type IRE1 α transient transfection, the level of splicing does not fully recapitulate to the splicing in wild type cells. Low levels of splicing can be seen in D711A, K599R and I642A/G mutants. As would be expected with the analogue sensitised mutant, this splicing was only clearly inducible by 1NM-PP1 in the case of the D711A/I642G mutant. No splicing could be seen in any of the K599A mutants, potentially because this is the least conservative mutation of K599 over the K599R. In this system no 1NM-PP1 induction was seen in the analogue sensitised mutants as in (Papa2003). As expected, no splicing can be seen in the K907A, untransfected and empty vector transfected samples. These data indicated a possible bypassing of the need for kinase function

of IRE1, but did not give clear or reliable results due to the irregular amounts of RNA obtained because of the viability issues. For this reason, the main methodology for obtaining material for assessing IRE1 function was changed to production of a stable cell line expressing the mutant constructs.

Figure 4.3. 2 – *XBP-1* splicing in IRE1-construct expressing cells with/without ER stress induction/1NM-PP1 treatment. XBP1u – unspliced bands, XBP1s – spliced bands.



4.3.3 Conclusion

It was possible using these experiments to verify that the D711A and D711A double mutants, and to some extent the I642A and I642G mutants were capable of producing a low level of XBP-1 splicing and useful for further investigation. Whether this is a true reflection remained to be confirmed by a more appropriate method. However, low viability lead to a low concentration of cells harvested after transfection and thus a low RNA yield, RNA being required for the XBP-1 splicing assay that is the standard marker of IRE1 activation.

Optimisation of cDNA production by use of gene-specific primers, and of the PCR reaction by use of touchdown PCR and hot start polymerases gave some improvement in results (data not shown), but in some cases the starting concentration of RNA was too low for use in PCR detection. It was determined part way through the attempts at producing sufficient RNA that an alternative strategy to transient transfection of IRE1 plasmids would be to construct a stable cell line of MEFs into which the IRE1 constructs could be stably transfected, thus allowing as much cell mass to be grown as was required for sufficient RNA. Attempts were also made to gain enough protein to test the transient system for JNK activation/phosphorylation and IRE1 expression by Western blotting, but this did not prove possible. With hindsight, the stable tranfection strategy would have been better started earlier and given greater priority as it was time-consuming, but ultimately successful, and completed earlier would have allowed more study of the resulting cell lines (see later).

Difficulties in harvesting sufficient protein and RNA from transient transfection of IRE1 α constructs precipitated the production of the stable cell lines as described in chapter 4. As XBP-1 splicing was successfully tested with sufficient RNA yield to give clear results in the *ire1 α ^{-/-}* MEF cell lines thus constructed, this method can be considered a success. The D711A mutant has also been confirmed to be capable of splicing as was seen in the yeast model in our hands and in (Chawla, Chakrabarti et al. 2011) – based on this information it was determined to continue and test this mutant in the CHO system, as will be detailed in the following chapters. However, although it was possible to test the apoptotic responses of the stable cell lines examined here, it was not possible due to issues with the phospho-IRE1 α antibody to reliably confirm that differences in cell viability or JNK activation/expression were attributable to IRE1 α phosphorylation and activation and not due to some other effect of the mutant, and that the D711A mutant had any impairment in IRE1 α phosphorylation. If

more time were available, trying an alternative antibody, assay by immunoprecipitation or radioactive phosphate incorporation assay could be used to verify this. It is also evident from the high baseline XBP-1 splicing that a physiological UPR was not reconstituted by the stable expression system thanks to expression of the constructs occurring even without tetracycline induction. Tetracycline-free serum was obtained to eliminate this problem, but insufficient time was available to test this and ascertain whether it was tetracycline in the medium or leakiness of the construct that was responsible. Due again to shortage of time, it was not possible to test any of the other constructs, - particularly valuable would have been the testing of the D711A/I642G construct with and without 1NM-PP1 to ascertain whether the enlarged kinase pocket could be used to bypass phosphorylation.

4.4 Construction of stable *irea*^{-/-} MEF lines with FRT-IRE1

4.4.1 Rationale

As described in chapters two and three, the transient transfection system used initially proved too detrimental to the viability of the MEF cells to allow sufficient RNA and Protein to be harvested. Therefore, since no prepared stable transfection-competent *irea*^{-/-} cell line existed, it was necessary to produce one from the MEFs used for the transient system. It was determined to use the Invitrogen Flp-In™ Core Kit stable cell line system as this had already been used successfully in our laboratory (see Materials and Methods – Commercially Available Kits).

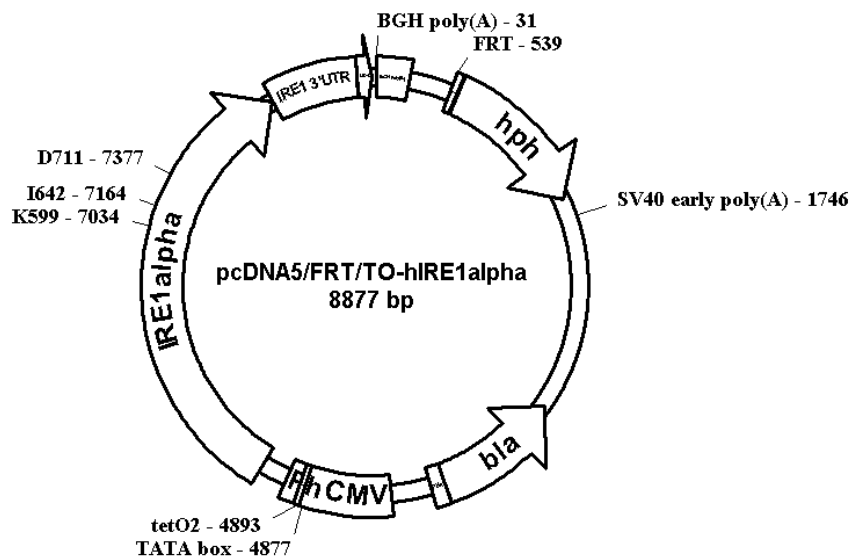
4.4.2 Flp-In™ System

The Flp-In system involves the stable transfection of a number of plasmids containing a system that permits stable, controllable expression of a required construct. First, the pFRT/lacZeo plasmid is transfected into the cell line of interest – this transfection is then screened using a concentration of the antibiotic Zeocin which kills all cells in the cell line within two weeks against which the lacZeo fusion gene confers resistance. Those cells which remain after this time has elapsed have stably integrated the pFRT/lacZeo plasmid into their genome – the function of this plasmid can then be assessed by performing a beta-gal assay for the lac operon. This plasmid renders the cell line competent to accept the content of the pcDNA5™/FRT/TO, which contains a hygromycin resistance gene. The protein of interest is transferred into the pcDNA5™/FRT/TO plasmid – this vector if co-transfected with the pOG44 plasmid, which expresses the Flp recombinase that exchanges the two Flp sites, will transfer the protein sequence of interest into the stable integration site, exchanging zeocin resistance for hygromycin resistance. The third plasmid, which is stably transfected as is the pFRT/lacZeo, is the pcDNA6/TR tet repressor plasmid. This plasmid confers blasticidin resistance on cell lines into which it is stably transfected and is screened for with blasticidin as is the pFRT/lacZeo plasmid. Cells expressing the tet repressor protein from this plasmid suppress expression of the pcDNA5™/FRT/TO product, as this plasmid is preceded by two copies of the tetracycline operator. This allows expression from the pcDNA5™/FRT/TO plasmid to be induced by addition of tetracycline to growth medium/cells. This chapter describes the process of constructing a stable MEF cell line using this methodology.

4.4.3 Construction of pcDNA5/FRT/TO-hIRE1 α and Mutants Thereof

Before transfection, it was necessary to clone the protein of interest, IRE1 and its mutant forms into the pcDNA5/FRT/TO vector. This cloning was performed by our collaborator Sergej Seřtak, Bratislava. Since the D711A/I642A construct did not exhibit clear splicing where the D711A/I642G did, possibly due to the greater difference in the size of the kinase pocket extension, only the I642G double mutants were produced.

Figure 4.4. 1 – Plasmid map of pcDNA5/FRT/TO-hIRE1 α . Plasmid contains the human IRE1 gene in a vector competent for transfer to a stable cell line using the FRT site.

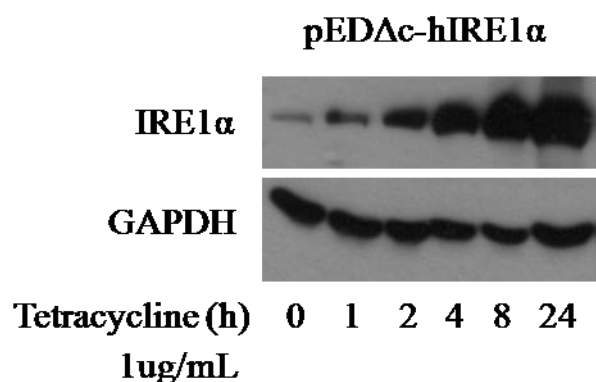


4.4.4 Testing of pcDNA5-FRT-TO-hIRE1 α for successful IRE1 α expression in T-Rex HEK293 Cells

In order to ensure the pcDNA5 constructs containing the IRE1 α for transfer into the stable cell line were expressing IRE1 at detectable levels, they were transfected into T-Rex HEK293 cells (Invitrogen, Glasgow, UK) which stably express the tet repressor required to control IRE1 expression from the pcDNA5/FRT/TO construct. 1×10^6 T-Rex HEK293 cells were transiently transfected using the Jetprime Method (see Materials and Methods “Transfection – JetPrime”), as this was the method optimised for this cell type in our laboratory, with 2 μ g of pcDNA5-FRT-TO-hIRE1 α and grown for 24 hours before treatment for a timecourse of 1,2,4,8 or 24 hours with 1 μ g/mL of tetracycline to induce

expression of IRE1 α . After the required amount of time, the medium was removed and the cells lysed *in situ* with RIPA buffer (see Materials and Methods, Solutions for Protein Work) and harvested for protein. Protein levels were quantified using the DC protein assay on the Molecular Devices Spectramax. 50 μ g of protein was then run on an SDS-PAGE gel and a Western blot performed for IRE1 α as described in Materials and Methods – Western Blotting (Figure 4.4. 2).

Figure 4.4. 2 – Western blot for IRE1 α in HEK293 Cells transiently transfected with pcDNA5-FRT-TO-hIRE1 α construct and induced with tetracycline.



Clear induction can be seen with the wild-type construct along with a consistent GAPDH control. However, induction is not as obvious in the mutant construct transfections, and the GAPDH result was missing or inconsistent in other samples, making it difficult to draw any conclusions about induction. IRE1 expression also occurs at 0 hours without tetracycline treatment – this may be due to either leakiness of the construct, tetracycline in the fetal calf serum used for tissue culture, or the HEK293's own endogenous IRE1 expression – the Cell Signalling IRE1 α antibody reliably hybridises with human IRE1 in our hands, but does not detect MEF or CHO endogenous IRE1 α in cell lines. All constructs successfully expressed IRE1 in the T-Rex HEK293 cells.

4.4.5 Stable Transfection with pFRT/lac/Zeo

In order to produce stable transfection competent *ire1 α* ^{-/-} cells, it was necessary to stably transfect the pFRT/lac/Zeo plasmid into the cells in order to render the cell line competent to accept the IRE1 α

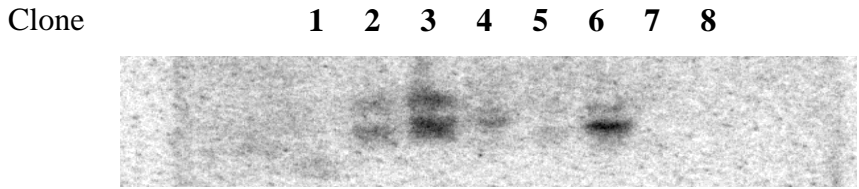
constructs from the pcDNA5 plasmid. In order to perform the selection procedure, as recommended in the Flp-In manual, the tolerance of the MEF cells for the antibiotic was ascertained (see Materials and Methods – Antibiotic Tolerance). The concentration 100 μ g/mL of Zeocin was chosen as suitable for the selection process, as the lowest concentration which caused total viability loss within seven days. Transfection was then performed according to the protocol in Materials and Methods – “Transfection with pFRT/lac/Zeo” and stably transfected clones selected by limited dilution cloning. Three stocks of each of the clones grown from a single cell were frozen as described above. In order to ensure the pFRT/lac/Zeo plasmid had been integrated, the clones were first analysed for β -gal activity as described in Materials and Methods “Beta Gal Assay for pcDNA integration”. Results of this analysis are given in (Table 4.4. 1) below. Clones 3 and 7 exhibited no or negligible β -gal activity, and were not considered suitable for progression in the stable cell line generation.

Table 4.4. 1 – Beta-galactosidase activity in *ire1* -/- MEF clones stably transfected with pFRT/lac/Zeo

Clone	β -gal activity(munits/50 μ l)	
	10x Dilution	2x Dilution
1	5.88	6.735
2	10.455	8.959
3	-0.833	0.767
4	14.148	10.774
5	12.798	10.428
6	5.021	4.068
7	-1.577	0.071
8	6.72	7.219

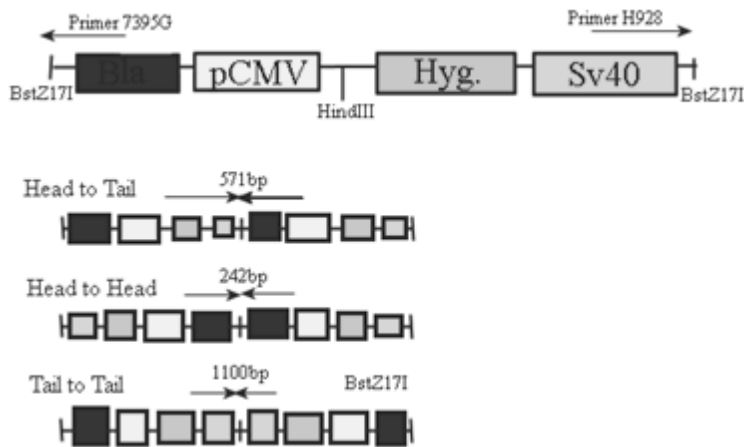
To confirm the presence of the pFRT/lac/Zeo in the clones, Southern Blotting was performed using a primer pair against the lacZ gene in the plasmid. Cells from each clone were harvested and the genomic DNA extracted using the EZ RNA kit according to the protocol (Geneflow Ltd, Staffordshire, UK), digested with the restriction enzyme *HindIII*, run on a 1% agarose gel and Southern blotted as described in Materials and Methods – Southern Blotting (Figure 4.4. 3). Clones 1,7 and 8 did not contain a sequence that hybridised to the primer product and were not considered suitable for progression – clones 2 and 3 exhibit two bands and may indicate extra copies of the insert. Clones 4 and 5 exhibited faint bands, and Clone 6 a clear single band.

Figure 4.4. 3 – Phosphoimage of Southern Blot for pFRT/lac/Zeo site. Lanes represent radioactive signal from Clones 1-8.



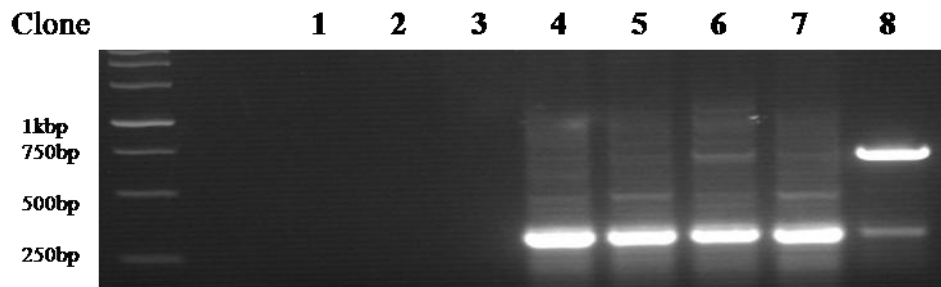
Since it was still possible that multiple copies of the insert had integrated at the same site and this would not appear as a distinct band in the Southern blot, a PCR reaction was performed on the *HindIII* digested DNA prepared for the Southern blot using primers against the pFRT/lac/Zeo insert – if multiple copies of the insert had been integrated, the following size products would be produced see Figure 4.4. 4. Clones 1-3 did not successfully produce PCR products.

Figure 4.4. 4 – Potential multiple insertions of the pFRT/lac/Zeo



As no bands could be seen at 1100, 571 or 242 base pairs, there is no evidence to suggest that clones 4-8 had multiple insertions of the pFRT/lac/Zeo sequence (Figure 4.4. 5).

Figure 4.4. 5 - PCR for multiple insertions of pcDNA site



Based upon the results of the beta-gal assay, the southern blot and the PCR for insertion sites, Clones 4,5 and 6 were selected for further analysis as the most likely clones to contain a single, functional pFRT/lac/Zeo insertion. Upon revival, however, clone 6 did not grow sufficiently and was not used in the following assays.

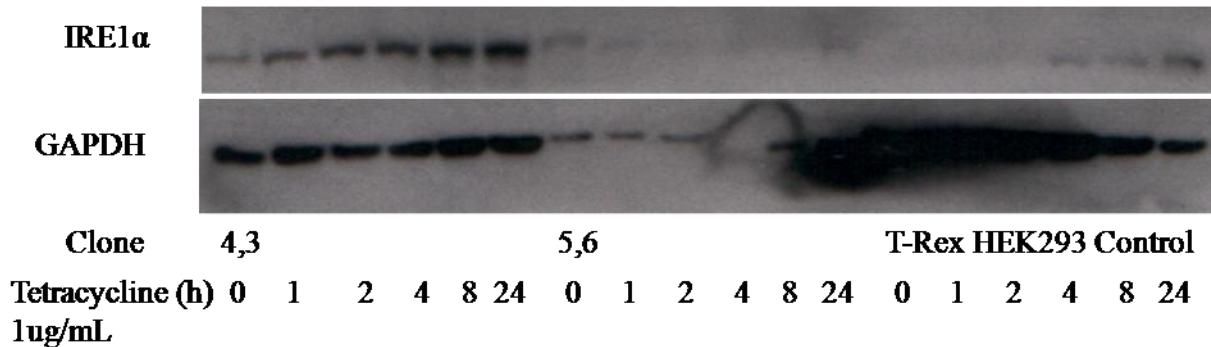
4.4.6 Stable Transfection with Tet Repressor Plasmid pcDNA6/TR

In order to produce stable transfection competent *ire1 α* ^{-/-} cells, it was necessary to stably transfect a plasmid expressing the Tet Repressor, pcDNA6/TR (supplied with the Flp-In system). This plasmid was linearised and transfected into the cells and stable transfectants selected with blasticidin. In order to perform the selection procedure, as recommended in the Flp-In manual, the tolerance of the MEF cells for the antibiotic was ascertained (see Materials and Methods – Antibiotic Tolerance). A blasticidin concentration of 10 μ g/mL, which resulted in 100% loss by 10 days, was used for future selection. Transfection was then performed according to the protocol in Materials and Methods – “Transfection with pFRT/lac/Zeo” and stably transfected clones selected by limited dilution cloning.

Three stocks of each of the clones obtained from a single cell were frozen as described above and tested for Tet repressor function. Those clones which had grown up fastest and exhibiting healthy morphology were chosen for further testing. This testing was performed by the transfection of an Fv2e-IRE1 α construct produced by David Cox, University of Durham which contained a tet-inducible HA-tagged form of IRE1 which only dimerised/activated in the presence of the chemical AP20187. 2 μ g of this plasmid was transfected by electroporation into two of the clones produced and the cells harvested for protein, run on an SDS page gel and a Western blot performed for the HA tag at a concentration of 1:1000 as recommended by the manufacturer (Sigma, Gillingham, UK) (Figure 4.4. 6). Clone 4,3 produced a visible induction of the IRE1 product, indicating a functional tet-repressor in this clone. Clone 5,6 gave very low levels of induction, but also appeared to have a low GAPDH control, possibly indicating low protein levels in the sample. T-Rex HEK293 cells were used as a

positive control for Tet repressor function as these were used when testing the pcDNA5 constructs above, but only showed a low level of induction despite strong GAPDH signal.

Figure 4.4. 6 - Transient transfection with FV2e-IRE1 for tetracycline induction



4.4.7 Stable Transfection/Replacement with pcDNA5-FRT-TO-hIRE1α

ire1α^{-/-} cells rendered competent to produce the tet repressor and shown to contain the FRT site, were next required to be transfected with the pcDNA5-FRT-TO-hIRE1α, which contained the hygromycin resistance site. Therefore, as above it was necessary to perform an antibiotic tolerance assay. In addition, as the cells had now been through several passages and procedures, a second β-Galactosidase assay was also performed to ensure the pFRT/Lac/Zeo site was still present in the cell line. Once this was verified, the clone selected for the final cell production was co-transfected with pcDNA5-FRT-TO-hIRE1α and pOG44 as described in Materials and Methods – “Co-Transfection with pcDNA5-FRT-TO-hIRE1α/ pOG44”.

4.4.8 Summary

Using the methodology above, it proved possible to successfully produce a cell line competent for stable transfection of the IRE1 α constructs, and to stably transfect those constructs to successfully produce the required cell lines. Certain aspects of the procedure could have been improved, for example, a repeat of the Southern blot to produce better confirmation of the presence of the FRT site, better blots for inducibility of the pcDNA5 IRE1 constructs, but otherwise the production process was satisfactory. Note: The recommended methodology for assessment of tet repressor function in the Flp-In manual is transfection of a plasmid providing tetracycline-induced expression of chloramphenicol acetyl transferase (CAT) – in our hands this assay could not be made to function, therefore the Fv2e IRE1 construct was used instead.

4.5 Viability and unfolded protein response activation of stably transfected *ire1 α* ^{-/-} MEF lines with FRT-IRE1 α

4.5.1 Rationale

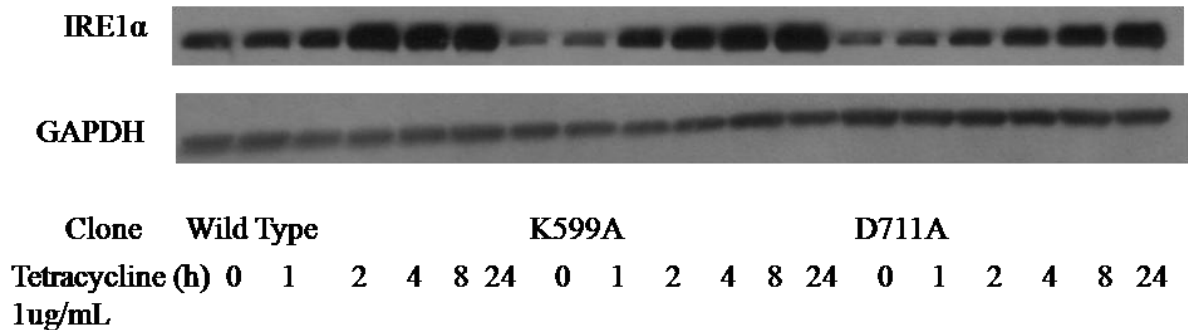
The IRE1 constructs having been stably integrated into the genome of the *ire1 α* ^{-/-} MEFs, and integrated into a site which permitted sufficient growth, the issues which made transient transfection unsuitable for characterising the mutant constructs (lack of viability, and concomitant insufficiencies in cell mass and therefore RNA and protein yields). Whereas previously the maximum cell limits of the transfection system constrained the amount of cell mass that could be obtained, larger 75cm² plates could be used for the assay. Most further analyses in this chapter were performed at this scale of growth, and initially using the stably transfected cell lines expressing wild type, the kinase-dead K599A mutant and the D711A mutant which was of interest having exhibited splicing previously in our laboratory and in (Chawla, Chakrabarti et al. 2011), where it was proposed in yeast to be competent for splicing induction but not for the attenuation of the unfolded protein response. This being the case in the mammalian system it would be expected that there would be a difference or prolonged duration of splicing in cells expressing the D711A mutant.

4.5.2 Verification of IRE1 α expression in Stably Transfected IRE1 Reconstituted MEFS

Successful transfection of the pcDNA5 IRE1 constructs was indicated in Chapter 4 by resistance to hygromycin, however, the expression of the IRE1 constructs under the control of the tet repressor required testing in order to verify the presence of a functional IRE1 and ensure consistent expression across different cell lines. 2x10⁶ cells of each cell line expressing the constructs were seeded into a 75cm² tissue culture plate (Sarstedt, Leicester, UK) and grown for 24 hours until the plates reached 50-70% confluency to allow for the longest (24 hour) induction with tetracycline without the plates becoming overconfluent. Cells were then treated with 1 μ g/mL tetracycline for 1,2,4,8 or 24 hours before the medium was removed, the cells were washed with PBS and lysed directly in the culture plate with RIPA buffer, and then harvested for protein as described in the Materials and Methods. After

quantification by DC Protein Assay on the Molecular Devices Spectrophotometer, the protein lysate was run on an SDS-PAGE gel and blotted as described in Materials and Methods – “Western Blotting”, for IRE1 α and GAPDH at 5% (w/v) casein (see Materials and Methods – Chemicals).

Figure 4.5. 1 - IRE1 expression in Stably Transfected IRE1Reconstituted MEFS



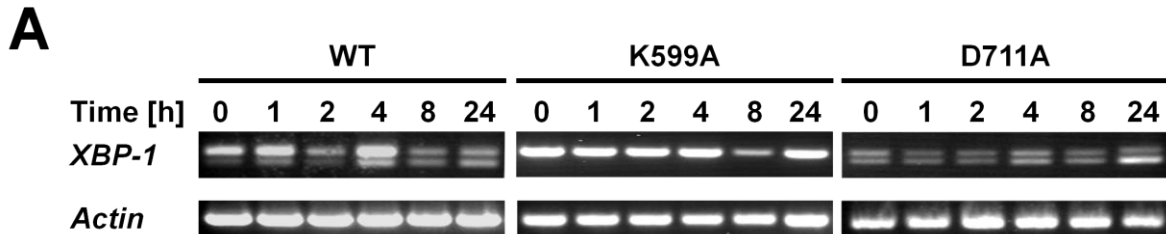
Stable and inducible expression of IRE1 α can be seen in the Western blot indicating a functional tet repressor producing similar levels of expression across the different cell lines, and when compared to GAPDH as a housekeeping gene. As when the pcDNA constructs were tested in Chapter 4.4, there was some background IRE1 expression at 0 hours (no tetracycline treatment) indicating either leakiness/improper regulation of the construct or potentially expression due to tetracycline in the foetal calf serum used in the growth medium.

4.5.3 D711A Mutant exhibits *XBP-1* splicing in Stably Transfected *ire1 α ^{-/-}* MEFS

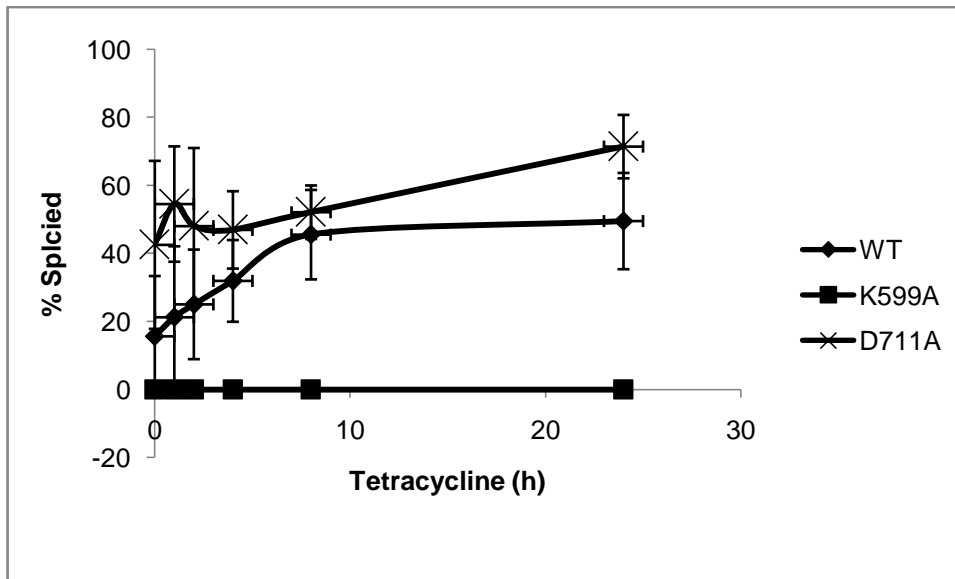
Having verified the expression of IRE1 α in the stably transfected cell lines, it was then determined to examine XBP-1 splicing in the cell lines to confirm the presence of splicing in the D711A mutant already seen in the transient system. As above, 2×10^6 cells of each cell line expressing the constructs was seeded into a 75cm^2 tissue culture plate (Sarstedt, Leicester, UK). Cells were then treated with $1\mu\text{g/mL}$ tetracycline for 0,1,2,4,8 or 24 h before the medium was removed, the cells were washed with PBS. Cells were lysed directly in the dish using Solution A of the EZ-RNA kit (Geneflow, Staffordshire, UK). The cells were prepared for RNA using the kit, and $5\mu\text{g}$ of the harvested RNA used to produce cDNA as described in Materials and Methods – cDNA production from RNA. RT PCR was performed on the cDNA thus produced as described in Materials and Methods - “RT-PCR for Mouse

XBP-1/Actin". Reactions were run on a 2% agarose gel and representative gels and graphs of averages of three biological repeats are shown in Figure 4.5. 2

Figure 4.5. 2 – Tetracycline induction of *XBP-1* splicing in IRE1 stably transfected *ire1α*^{-/-} MEFs.



B

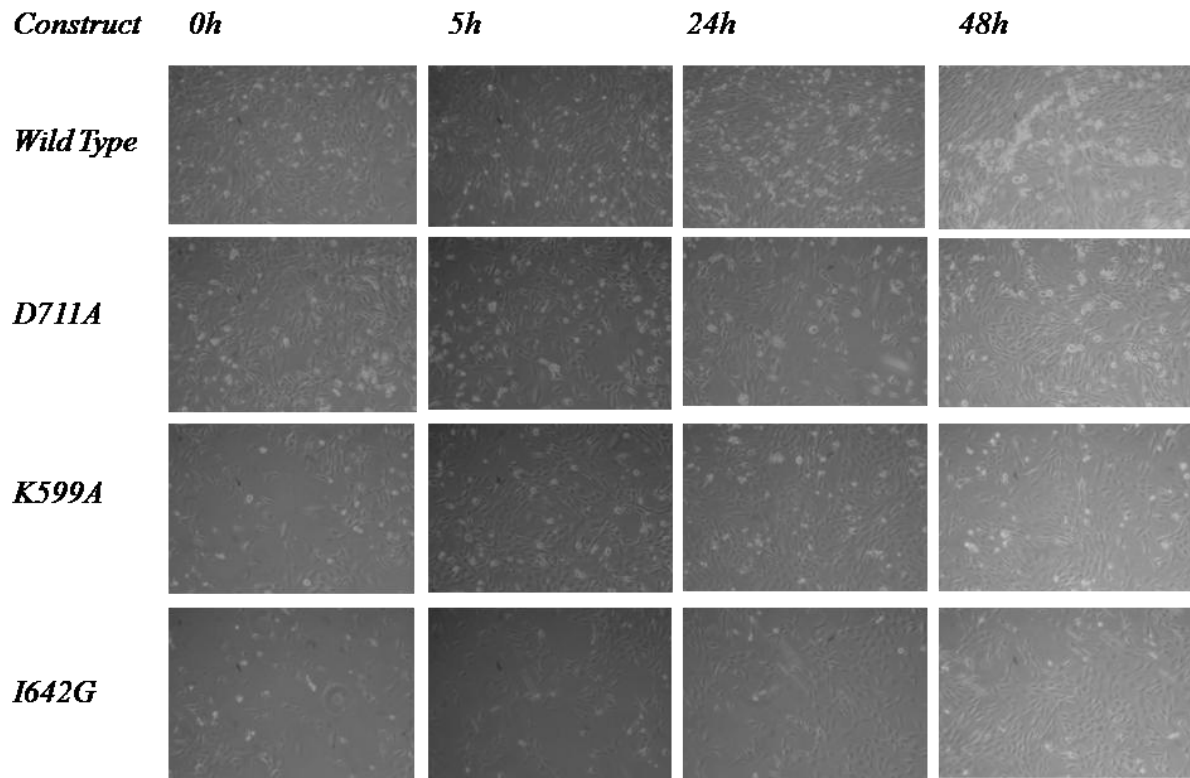


As expected, the wild-type transfected cell line produced a clear induction of splicing in response to tetracycline induction of expression – this effect was also seen in response to overexpression in the transient system. The K599A did not induce splicing which is consistent with previous results in the transient system and the published literature (Tirasophon, Welihinda et al. 1998). The D711A mutant appeared to exhibit strong splicing (Figure 4.5. 2A), but upon analysis of replicates, the splicing was not shown to be different from the wild type (Figure 4.5. 2B).

4.5.4 D711A mutant exhibits similar growth characteristics to wild type IRE1 α in stably transfected *ire1 α ^{-/-}* mouse embryonic fibroblasts.

Once expression and XBP-1 splicing had been established in the stably transfected cell lines, basic investigations were made into their growth and cell death characteristics and how these were affected by the particular mutant. Potentially, those mutants which did not possess kinase function, or which had a reduced kinase function could exhibit lower levels of cell death due to the inactivation of the TRAF2 arm, but equally the lack of XBP-1 splicing could be severely detrimental to the cell viability overall if it prevented the cell from dealing with high loads of unfolded protein. As a basic indicator of cell viability, a visual inspection of adherent versus floating cells was used. As above, 2×10^6 cells of each cell line expressing the constructs was seeded into a 75cm^2 tissue culture plate and grown for 24 hours until the plates reached 50-70% confluency. As can be seen in Figure 4.5. 3, initial growth of the K599A and I642G mutants was slower than that of the wild-type and D711A mutants, suggesting these mutants are detrimental to the cell lines. As a result, the Wild Type and D711A mutants reached confluency faster and began to die off as can be seen in the 48 hour images which exhibit many floating cells.

Figure 4.5. 3 – Viability of *ire1 α ^{-/-}* cells stably transfected with IRE1 constructs after 0-48 h tetracycline induction.

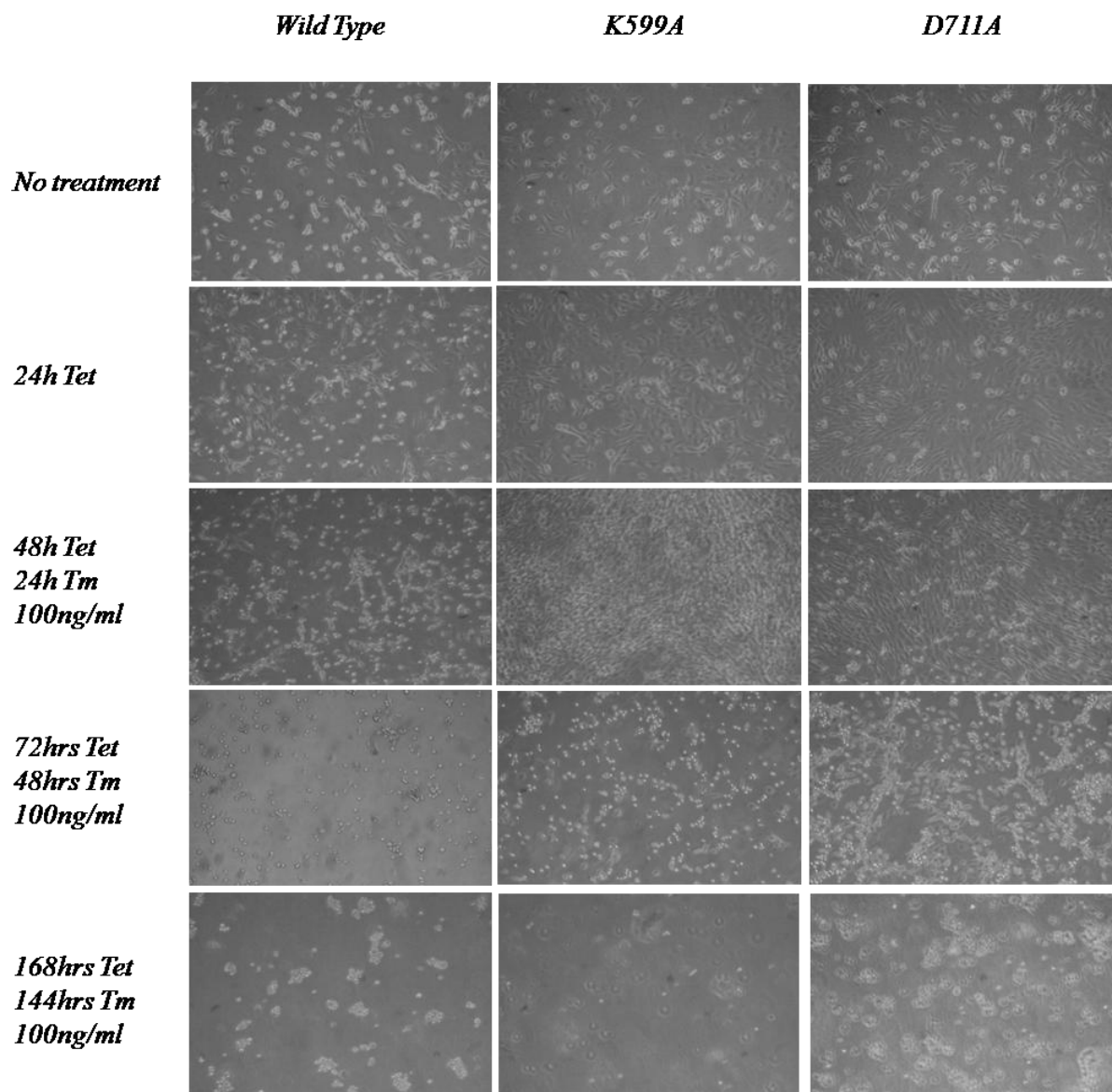


4.5.5 D711A mutant improves survival of tunicamycin/thapsigargin-induced unfolded protein stress in stably transfected *ire1 α ^{-/-}* MEFS

Having established the base growth characteristics of the stably transfected cell lines, next they were exposed to varying concentrations of the ER stressors thapsigargin (an inhibitor of the SERCA pump which perturbs ER calcium homeostasis) and tunicamycin (an inhibitor of GlcNAc phosphotransferase which prevents the synthesis of N-linked glycoproteins). As above, 2×10^6 of each cell line expressing the constructs was seeded into a 75cm^2 tissue culture plate and grown for 24 hours until the plates reached 50-70% confluency. The K599A and I642G mutants appeared to exhibit slower growth characteristics than the Wild Type and D711A. Having established a baseline of growth, an experiment was set up with a low dose of tunicamycin (100ng/ml). As above, 2×10^6 of each cell line expressing the constructs were seeded into a 75cm^2 tissue culture plate and grown for 24 h until the plates reached 50-70% confluency. The K599A mutant did not appear to suffer from the low growth characteristics in this experiment, although the reason for this is unknown. Plates were first treated for 24 h with tetracycline to ensure strong expression of the IRE1 construct, and then treated with

100ng/ml tunicamycin and photographed at 24, 48, and 144h after treatment to examine the long term effects of low-level ER stress on the cell lines.

Figure 4.5. 4 - Viability of *ire1α*^{-/-} cells stably transfected with IRE1α constructs and treated with 100ng/ml tunicamycin – longer timecourse.



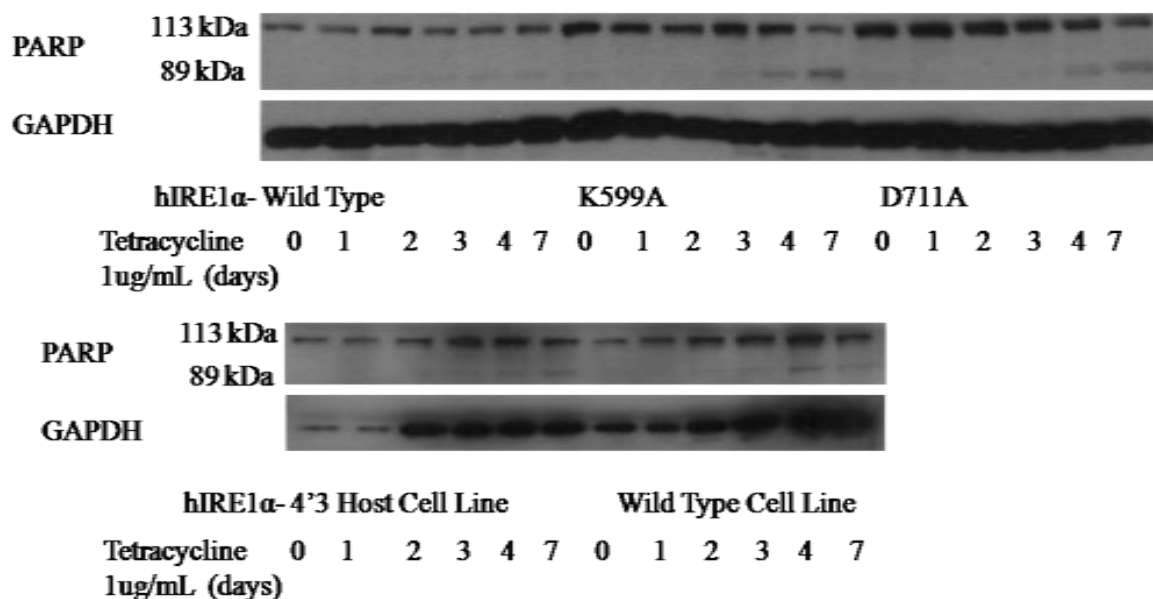
Some differences could be seen between the growth and death characteristics of the mutants and the wild type transfected cells. Both the kinase-impaired mutants appeared to initially exhibit stronger growth up to 24h of tunicamycin treatment, whereas the wild type suffered a

gradual deterioration over time under unfolded protein stress, indicating a lack of cell death induction due to IRE1 α in the kinase impaired mutants. After 48h of tunicamycin treatment, the K599A mutant began to suffer cell death more extensively than the D711A and by 144 hours the cell death in these plates matched those in the wild type, whereas the D711A mutant cells died off more slowly. Whether this is due to the extent of the effect on kinase activity of the D711A mutant versus the K599A, or due to the splicing activity of the D711A mutant is unclear without kinase activity data, but the potential improvement in survival is promising for industrial cell productivity.

4.5.6 K599A and D711A mutants exhibit increased PARP cleavage in Stably Transfected *ire1 α ^{-/-}* MEFS

Cleavage and inactivation of Poly ADP ribose polymerase (PARP), a DNA repair enzyme, by caspases into a 24kDa and 89kDa fragments occurs as part of apoptotic programmed cell death and is therefore a marker of the induction of the apoptotic programme (Oliver, de la Rubia et al. 1998). To investigate the induction of cell death in the IRE1 α transfected cell lines, PARP cleavage over time was assessed as a marker of apoptotic induction. 0.5×10^6 cells from each cell line expressing the constructs was seeded into a 75cm^2 tissue culture plate. The lower cell density allowed for longer growth in the plates. Cells were then treated with $1\mu\text{g/ml}$ tetracycline for 0,1,2,3,4 or 7 days before the medium was removed, the cells were washed with PBS and lysed directly in the culture plate with RIPA buffer, and then harvested for protein as described in the Materials and Methods. After quantification by DC Protein Assay on the Molecular Devices Spectrophotometer, the protein lysate was run an SDS-PAGE gel (Bio-Rad, Hemel Hempstead, UK) and blotted as described in Materials and Methods – “Western Blotting”, using the antibodies and conditions described in Materials and Methods – “Antibodies” for PARP and GAPDH.

Figure 4.5. 5 – PARP Cleavage in IRE1 α stably transfected *ire1 α ^{-/-}* MEFs

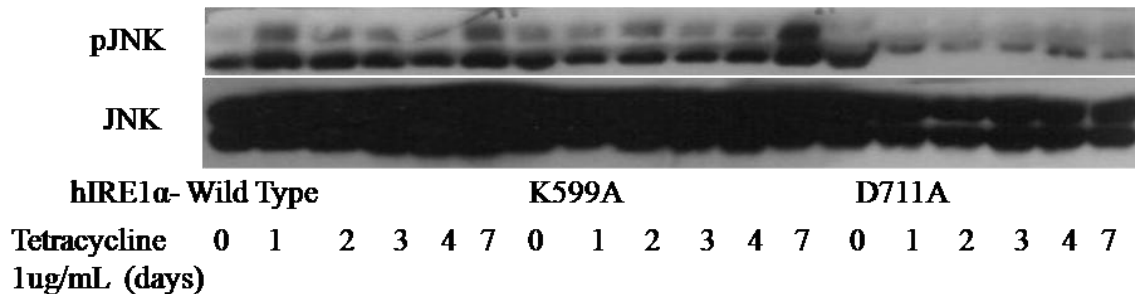


Seeded plates began to approach confluency at Day 4 and were overconfluent and therefore likely to be inducing apoptosis at Day 7. The untransfected host cell line was used as a negative control for the effect of IRE1 α and the wild type cell line as a positive. Both these cell lines began to exhibit cleavage of PARP at confluency as would be expected. The wild type-transfected cell line appeared to exhibit similar levels of cleavage to controls, whereas the kinase-impaired K599A mutant showed slightly stronger 89kDa bands and reduced 113kDa, suggesting it was more vulnerable to apoptosis, although it is difficult to verify this as general levels of PARP appeared to be lower in the wild type and controls (see below). The D711A mutant exhibited levels between the wild type and the K599A which is consistent with the results of Figure 4.5. 4 where the D711A phenotype appeared to have similar effects to the K599A but with a greater viability at higher cell density, a potentially useful effect for industrial biosynthesis where high biomass is required. Both kinase-impaired mutants appeared to have slight increases in PARP expression, although GAPDH control levels are similar – this could potentially indicate a response to an increase in DNA damage due to oxidative stress from poorly-controlled protein folding.

4.5.7 D711A Mutant appears to exhibit decreased JNK expression in Stably Transfected *ire1α*^{-/-} MEFs

As the PARP assay had indicated a potential difference in apoptotic responses between the mutant and the wild-type transfected cells, further investigation was made into markers of the apoptotic arm of the downstream effects of IRE1 α activation. Protein obtained from the cells harvested for the PARP assay above was used to Western blot for both JNK phosphorylation and phospho-IRE1 α (see next section). Although in the transient transfection system the phospho-JNK/JNK results were unsuitable for analysis, this may have been due to low protein yields, therefore these assays were retried with the stable cell protein lysates (data not shown). Lysate was run on an SDS-PAGE gel (Bio-Rad, Hemel Hempstead, UK) and blotted as described in Materials and Methods – “Western Blotting”, using the antibodies described in Materials and Methods – “Antibodies” for phospho JNK and total JNK.

Figure 4.5. 6 – JNK Activation in IRE1 α stably transfected *ire1α*^{-/-} MEFs



JNK activation in the experiment appeared to indicate an increase in JNK phosphorylation at the seven day mark when similar increases in PARP had indicated apoptosis due to overconfluence. No similar increase could be seen in the D711A mutant, however this may be due to a lower JNK concentration in these samples, as the total JNK result in these samples was also lower, where the GAPDH result was not altered (see Figure 4.5. 5 above), and the levels of total JNK were generally high – even a very short exposure (5 seconds) gave an overexposed signal. This may indicate some alteration of regulation of JNK itself in the D711A cells which could be contributing the lower cell death in Figure 4.5. 4.

4.5.8 IRE1 α phosphorylation in Stably Transfected *ire1 α ^{-/-}* MEFS

Although the Abcam phospho-IRE1 α had not given detectable results in the transient transfection system, and the phospho-JNK/JNK results were unsuitable for analysis, this may have been due to low protein yields, therefore these assays were retried with the stable cell protein lysates (data not shown). Disappointingly although a larger quantity of protein was used, the results for phospho-IRE1 α remained inconclusive – no clear induction of phospho-IRE1 α could be seen over time, potentially due to non-specificity of the antibody. As a result it was not possible to directly confirm activation of the kinase domain of IRE1 α .

4.5.9 Summary

Difficulties in harvesting sufficient protein and RNA from transient transfection of IRE1 α constructs precipitated the production of the stable cell lines as described in chapter 4. As XBP-1 splicing was successfully tested with sufficient RNA yield to give clear results in the *ire1^{-/-}* MEF cell lines thus constructed, this method can be considered a success. The D711A mutant has also been confirmed to be capable of splicing as was seen in the yeast model in our hands and in (Chawla, Chakrabarti et al. 2011) – based on this information it was determined to continue and test this mutant in the CHO system, as will be detailed in the following chapters. However, although it was possible to test the apoptotic responses of the stable cell lines examined here, it was not possible due to issues with the phospho-IRE1 α antibody to reliably confirm that differences in cell viability or JNK activation/expression were attributable to IRE1 phosphorylation and activation and not due to some other effect of the mutant, and that the D711A mutant had any impairment in IRE1 phosphorylation. If more time were available, trying an alternative antibody, assay by immunoprecipitation or radioactive phosphate incorporation assay could be used to verify this, but there was insufficient time for these analyses in this study. It is also evident from the high baseline XBP-1 splicing that a physiological UPR was not reconstituted by the stable expression system thanks to expression of the constructs occurring even without tetracycline induction. Tetracycline-free serum was obtained to eliminate this problem, but insufficient time was available to test this and ascertain whether it was tetracycline in the medium or leakiness of the construct that was responsible. Due again to shortage of time, it was not possible to test any of the other constructs, - particularly valuable would have been the testing of the

D711A/I642G construct with and without 1NM-PP1 to ascertain whether the enlarged kinase pocket could be used to bypass phosphorylation.

4.6 Cloning of CHO IRE1 α

4.6.1 Rationale

Having seen in the analyses in the previous chapter that the D711A mutant exhibited XBP-1 splicing and improvements in viability, this mutant was considered suitable to be brought forward into analysis on the working, industrial cell line, CHO (Chinese hamster ovary). As detailed in the introduction to this thesis, the CHO cell line is used for production of biopharmaceuticals, in particular the CHOK1 lines used by our industrial collaborator (de la Cruz Edmonds, Tellers et al. 2006). However, unlike the MEF line used in the earlier chapters of this thesis, no CHO *ire1 α* ^{-/-} cell line was available without its own endogenous IRE1 α . Studies that have been performed using cell lines with their own IRE1 α and transient transfection of mutant constructs appear to produce expression from the mutants so much greater than that of the endogenous IRE1 α that it is sufficient to titrate out the effects of the endogenous and cause for example, the K599A mutant to have a dominant negative effect (e.g. Zhang 2005, Lipson 2008), and so this approach was also tested (see Chapter 4.10). However, this is not an ideal approach, as it is impossible to completely rule out the effects of a small but physiological level of wild-type IRE1 α forming heterodimers with the mutant constructs. Therefore concurrently to the titration strategy, it was determined to attempt to produce a transient knockdown by siRNA of the endogenous CHO IRE1 α protein. Although currently there is a collaborative initiative to sequence the CHO genome, at the time of this work the genome was not available publicly. Therefore, in order to produce sequence to target the siRNA against, it was necessary to clone at least part of the sequence of the CHO IRE1 α gene. Since the IRE1 α protein sequences of other organisms (*H. sapiens*, *M. musculus* and *R. norvegicus*) are known, these were used as templates for a degenerate primer strategy.

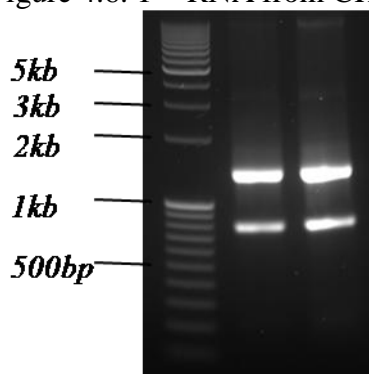
4.6.2 Degenerate primer design for CHO IRE1 α

Degenerate primers intended for use against the CHO IRE1 α sequence were derived by inserting the protein sequences listed in Genbank for *R. norvegicus* (XP_573211) *M. Musculus* (NP_076402) and *H. sapiens* (NP_001424) (aligned in Appendix 1) into the iCODEHOP program (<http://dbmi-icode-01.dbmi.pitt.edu/i-codehop-context/Welcome>) and selecting degenerate primers spanning approximately every 150 nucleotides/50 amino acids along the length of the sequence where there was good homology (primers listed in Materials and Methods – Primers – CHO IRE1 α sequencing). See Appendix 1 for protein sequence alignment, iCODEHOP readout and primers selected.

4.6.3 Harvesting of RNA from CHOK1SV Host Cells

In order to produce cDNA for sequencing of CHO IRE1 α , 1×10^7 cells from a culture of CHOK1SV donated by Lonza Biologics, Slough were harvested for RNA using the RNA Easy Mini Kit according to the kit protocol listed in Materials and Methods – Commercially Available Kits. RNA concentration was measured by spectrophotometer: concentrations of 0.9 and 1.4 $\mu\text{g}/\mu\text{l}$ were obtained. To verify this 1 μL of each sample were run on a 0.9% agarose gel (Figure 4.6. 1). Clear, even bands on the electrophoresis gel indicated good quality RNA and therefore this RNA was used in further analysis.

Figure 4.6. 1 - RNA from CHOK1SV host cell line.



4.6.4 Cloning Methods and RACE

Initial cloning for CHO IRE1 α sequences was performed using the FirstChoice $^{\text{®}}$ RLM-RACE Kit, which uses a version of the Rapid Amplification of cDNA Ends methodology (Maruyama1994 Shaefer1995). Initially, 3' RACE was performed on the RNA according to

the protocol version listed in Materials and Methods – Commercially Available Kits. 1µg total RNA was used in the reaction with murine moloney leukaemia virus reverse transcriptase and the 3' RACE adaptor from the kit incubated at 42°C for 1h to produce cDNA which was used in sequencing reactions.

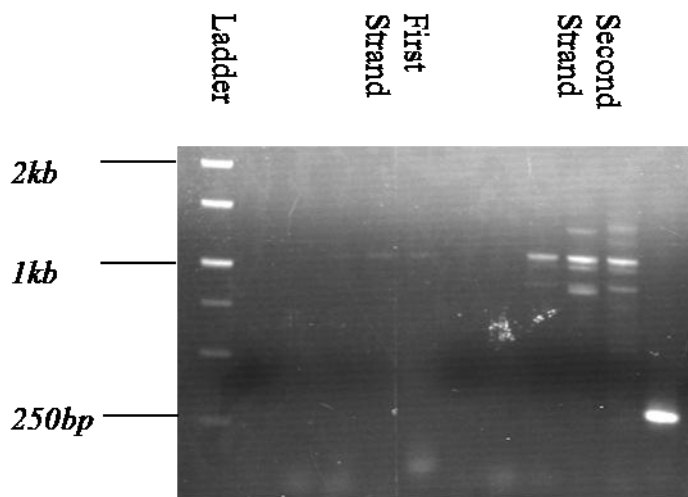
The initial conditions used for RACE PCR did not appear to be sufficient to produce IRE1 α sequence. The RLM-RACE manual recommended 60°C as an initial temperature, but that optimisation would be required. Therefore, a touchdown PCR method was used as with the XBP-1 splicing assay. The reaction was repeated as listed above, but the cycling altered as below, with an initial low and potentially non-selective temperature of 50°C to ensure any possible products were visible. As predicted, due to the lower annealing temperature, a number of unselective bands were produced. It did not prove possible to selectively PCR any IRE1 α products using a single degenerate primer, and therefore it was determined to attempt to increase selectivity by using two degenerate primers against IRE1 α instead of the single primer and general 3' RACE primer. This approach yielded single products of which two were the correct length for the primer positions in the IRE1 α sequence, A49+A173 (~500bp) and B61+B161 (~600bp). Both products were TOPO vector cloned into competent cells and screened by colony PCR before sending those of the correct length A49+A173 (Clone 1) and B61+B161 (Clone 2) to be sequenced. Both products when run on the NCBI BLAST server had >90% homology with *M. musculus* IRE1 α /ERN1 (NM_023913.2). The A49+A173 matched base pairs 775-1403 and B61+B161 base pairs 2125- 2708 of this sequence. See Appendix 2 for full sequences from successful PCRs.

4.6.5 T-RACE Methodology

It did not prove possible in this study to successfully perform the RLM-RACE for 5' and 3' ends even with specific primers, an alternative methodology was tried, Targeted Rapid Amplification of cDNA Ends (Bower2010). This method involves A) Using a poly-A tail primer with an additional sequence to B) Using murine moloney leukaemia virus reverse transcriptase's ability to add 2-4 cytosines to the 5' cap end of the cDNA and a cap finder primer (See Materials and Methods – T-RACE Primers) to place an additional sequence on the 5' end and C) Then using the two extended ends for firstly a second-strand synthesis to increase the amount of cDNA and then as the non-specific primer binding site for amplification of cDNA ends. Asymmetric PCR is then performed using a gene-specific

primer, producing a sequence of unspecified length from the target gene. The first and second strand synthesis are performed with dUTP in excess over dTTP, allowing these cDNAs to be digested with uracil DNA glycosylase leaving only the dTTP-only asymmetric PCR products. Normal PCR is then performed with a nested gene specific primer and a T-RACE primer against one of the 3' or 5' end caps. When this methodology was used with gene specific primers against the CHO sequence, no products were obtained in the final reaction. To isolate where the issue was, a selection of primers known to have given products already in PCR reactions were used to PCR cDNAs from each stage of the process. As can be seen in Figure 4.6. 2, both the first and second strand synthesis had produced cDNA and the second strand synthesis had produced an increased level, indicating that the 5' and 3' caps had attached and this synthesis was successful. However, after the asymmetric PCR and UDG digestion stage no products were obtained, most likely indicating the asymmetric PCR was unsuccessful in yielding products. However, as the second strand synthesis had resulted in a better cDNA yield, this method was used in later experiments.

Figure 4.6. 2 - T-RACE Synthesis



4.6.6 Primers Designed using provided Assembly Sequences

By this point in the study, early work had been done on a collaborative project from which our industrial sponsor, Lonza Biologics had obtained and donated to us a set of sequences from the CHO assembly. These sequences were aligned with those already obtained and used to design more gene specific primers at approx 500bp intervals which were used in PCRs as

above (in “PCR using standard primers designed from sequence”) to fill in any missing sequence and attempt to obtain the 3’ end and if this proved possible, the 5’ end. Although the sequences obtained from the 3’ end primers did not have any homology with IRE1 α when investigated, the products from the 3000-3500 were successfully cloned. Products from these primers were sent off for sequencing and yielded sequences matching 2963 – 3264 and 3472-3868 of the *M. musculus* ERN1.

4.6.7 Final CHO IRE1 α assembly

When sequences produced in this study were combined with those donated from the CHO assembly by Lonza, all but a predicted 29bp of the 3’ end and 179 bp of the coding 5’ end were sequenced. The full sequence aligned against *M. musculus* and *H.sapiens* ERN1 sequence and annotated with domains follows.

Table 4.6. 1 – Final CHO IRE1 α assembly.

H. sapiens (DNA)	GCCTAGTCAGTTCTGCGTCCGCTGAGGCTCGGTCACCGCCTCGCTGTCGTCGCGGCGCCCC
M. musculus (DNA)	----- CCGTGTCCACCGATCCTCCGCCGGTGCCGCGCTGTCGTTGCCGGCGCCCC
C. griseus (DNA)	-----
M. musculus (pro)	
C. griseus (pro)	
Annotations	[5’ UTR
H. sapiens (DNA)	CGCCCCGTCTCTGTCCG-----T-----ACCGCC-----
M. musculus (DNA)	CCGGCGTCCAGCCCTCTGTTTCGCGCGGGCTCCAGAACC GGCCGGGCGGGCCCCGG
C. griseus (DNA)	
M. musculus (pro)	
C. griseus (pro)	
Annotations	
H. sapiens (DNA)	AGCCAGGGCCGAGTCTCGCCATGCCGGCCCGGCGGCTGCTGCTGCTGCT
M. musculus (DNA)	AGTCAGGGCCACGTCTGCC-ATGCCGGCCCGGTGGCTGTTGCTCCTGCT
C. griseus (DNA)	-----
M. musculus (pro)	M P A R W L L L L L
C. griseus (pro)	
Annotations	5’ UTR][Signal peptide -----

H. sapiens (DNA)	GACGCTGCTGCT-----GCCCGGCTCGGGATTTTGGGAAGTACCAGCAC
M. musculus (DNA)	GACGCTGCTGCTACCGCCGCCCGGGCCCCGGGAGTTTGGGAAGAACCAGCAC
C. griseus (DNA)	-----GAGTTTTGGGAAGTGCCAGCAC
M. musculus (pro)	A L L L P P P G P G S F G R T S T
C. griseus (pro)	S F G S A S T
Annotations	-----] [Luminal domain
H. sapiens (DNA)	AGTGACGCTTCTGAAACCTTGTGTTTGTGTCAACGCTGGATGGAAGTT
M. musculus (DNA)	AGTTACTACTGCCTGAGACCTTGTGTTTGTCTCGACCCTGGATGGAAGCT
C. griseus (DNA)	AGTAACACTGCCTGAAACCTGTTGTTTGTTC AACCTGGATGGAAGTT
M. musculus (pro)	V T L P E T L L F V S T L D G S L
C. griseus (pro)	V T L P E T L L F V S T L D G S L
Annotations	
H. sapiens (DNA)	TGCATGCTGTCAGCAAGAGGACAGGCTCAATCAAATGGACTTTAAAAGAA
M. musculus (DNA)	TGCATGCTGTTAGCAAGAGGACGGGCTCCATCAAGTGGACTTTAAAAGAA
C. griseus (DNA)	TGCATGCTGTCAGCAAGAGGACAGGCTCGATCAAATGGACTTTAAAAGAA
M. musculus (pro)	H A V S K R T G S I K W T L K E
C. griseus (pro)	H A V S K R T G S I K W T L K E
Annotations	
H. sapiens (DNA)	GATCCAGTCCTGCAGGTCCCAACACATGTGGAAGAGCCTGCCTTCTCCC
M. musculus (DNA)	GATCCAGTCCTGCAGGTCCCAACACACGTGGAAGAGCCGGCTTCTCCC
C. griseus (DNA)	GATCCAGTCCTGCAGGTCCCAACACACGTGGAAGAGCCTGCCTTCTCCC
M. musculus (pro)	D P V L Q V P T H V E E P A F L P
C. griseus (pro)	D P V L Q V P T H V E E P A F L P
Annotations	
H. sapiens (DNA)	AGATCCCTAATGATGGCAGCCTGTATACGCTTGGGAAGCAAGAATAATGAAG
M. musculus (DNA)	AGATCCCAATGATGGCAGTCTGTACACACTTGGAGGCAAGAACAACGAAG
C. griseus (DNA)	AGATCCCAATGATGGCAGTCTGTACACACTTGGAGGCAAAAACAACGAAG
M. musculus (pro)	D P N D G S L Y T L G G K N N E G
C. griseus (pro)	D P N D G S L Y T L G G K N N E G
Annotations	
H. sapiens (DNA)	GCCTGACGAAACTTCCTTTTACCATCCCAGAATTGGTGCAGGCATCCCCA
M. musculus (DNA)	GCCTGACGAAACTTCCTTTTACCATCCCAGAATTGGTTCAGGCCTCCCCA
C. griseus (DNA)	GCCTGACGAAACTTCCTTTTACCATCCCAGAATTAGTCCAAGCATCTCCA
M. musculus (pro)	L T K L P F T I P E L V Q A S P
C. griseus (pro)	L T K L P F T I P E L V Q A S P
Annotations	

H. sapiens (DNA)	TGCCGAAGTTCAGATGGAATCCTCTACATGGGTAAAAAGCAGGACATCTG
M. musculus (DNA)	TGCCGAAGTTCAGATGGAATCCTCTACATGGGTAAAAAGCAAGATATTTG
C. griseus (DNA)	TGCCGAAGTTCAGATGGAATCCTCTACATGGGTAAAAAGCAGGACATCTG
M. musculus (pro)	C R S S D G I L Y M G K K Q D I W
C. griseus (pro)	C R S G D G I L Y M G K K Q D I W
Annotations	
H. sapiens (DNA)	GTATGTTATTGACCTCCTGACCGGAGAGAAGCAGCAGACTTTGTCATCGG
M. musculus (DNA)	GTATGTTATCGACCTCCTGACTGGCGAGAAGCAGCAGACTTTGTCATCGG
C. griseus (DNA)	GTATGTTATCGACCTCCTGACTGGAGAGAAGCAGCAGACTTTGTCATCGG
M. musculus (pro)	Y V I D L L T G E K Q Q T L S S A
C. griseus (pro)	Y V I D L L T G E K Q Q T L S S A
Annotations	
H. sapiens (DNA)	CCTTTGCAGATAGTCTCTGCCCATCAACCTCTCTTGTATCTTGGGCGA
M. musculus (DNA)	CCTTTGCTGATAGTCTCTGCCCATCAACTTCCCTTCTATATCTTGGACGG
C. griseus (DNA)	CCTTTGCAGATAGTCTCTGCCCATCAACTTCCCTGCTGTATCTTGGACGG
M. musculus (pro)	F A D S L C P S T S L L Y L G R
C. griseus (pro)	F A D S L C P S T S L L Y L G R
Annotations	
H. sapiens (DNA)	ACAGAATACACCATCACCATGTACGACACCAAAACCCGAAAGCTCCGGTG
M. musculus (DNA)	ACAGAATACACCATCACCATGTATGACACCAAGACCCGGGAGCTCCGCTG
C. griseus (DNA)	ACAGAATATACCATCACTATGTATGACACCAAGACCCGAGAACTTCGTTG
M. musculus (pro)	T E Y T I T M Y D T K T R E L R W
C. griseus (pro)	T E Y T I T M Y D T K T R E L R W
Annotations	
H. sapiens (DNA)	GAATGCCACCTACTTTGACTATGCGGCTCACTGCCTGAGGACGACGTGG
M. musculus (DNA)	GAATGCCACCTATTTTACTATGCAGCCTCACTGCCGGAAGACGACGTGG
C. griseus (DNA)	GAACGCCACCTATTTTACTATGCAGCCTCACTGCCCGAGGATGATGTGG
M. musculus (pro)	N A T Y F D Y A A S L P E D D V D
C. griseus (pro)	N A T Y F D Y A A S L P E D D V D
Annotations	
H. sapiens (DNA)	ACTACAAGATGTCCCACTTTGTGTCCAATGGTGATGGGCTGGTGGTGACT
M. musculus (DNA)	ACTACAAGATGTCCCACTTTGTGTCCAATGGCGATGGACTGGTGGTAACT
C. griseus (DNA)	ACTACAAGATGTCCCACTTTGTGTCCAATGGCGATGGACTAGTGGTAACT
M. musculus (pro)	Y K M S H F V S N G D G L V V T
C. griseus (pro)	Y K M S H F V S N G D G L V V T
Annotations	

H. sapiens (DNA)	GTGGACAGTGAATCTGGGGACGTCCTGTGGATCCAAAACCTACGCCTCCCC
M. musculus (DNA)	GTGGACAGTGAATCTGGGGATGTCCTGTGGATCCAAAACCTATGCCTCTCC
C. griseus (DNA)	GTGGACAGTGATTCTGGGGATGTCTTGTGGATCCAAAACCTATGCCTCTCC
M. musculus (pro)	V D S E S G D V L W I Q N Y A S P
C. griseus (pro)	V D S D S G D V L W I Q N Y A S P
Annotations	
H. sapiens (DNA)	TGTGGTGGCCTTTTATGTCTGGCAGCGGGAGGGTCTGAGGAAGGTGATGC
M. musculus (DNA)	TGTGGTGGCCTTCTACGTCTGGCAGGGGGAGGGTCTGAGAAAGGTGGTGC
C. griseus (DNA)	TGTGGTAGCCTTCTATGTCTGGCAGCGGGAGGGCCTGAGAAAGGTGATGC
M. musculus (pro)	V V A F Y V W Q G E V L R K V V H
C. griseus (pro)	V V A F Y V W Q R E G L R K V M H
Annotations	
H. sapiens (DNA)	ACATCAATGTCGCTGTGGAGACCCTGCGCTATCTGACCTTCATGTCTGGG
M. musculus (DNA)	ACATCAACGTTGCTGTGGAGACTCTACGCTACTTGACCTTCATGTCTGGG
C. griseus (DNA)	ACATCAACGTCGCTGTGGAGACTCTCCGCTACCTGACCTTCATGTCTGGG
M. musculus (pro)	I N V A V E T L R Y L T F M S G
C. griseus (pro)	I N V A V E T L R Y L T F M S G
Annotations	
H. sapiens (DNA)	GAGGTGGGGCGCATCACAAAGTGAAGTACCCGTTCCCAAGGAGACAGA
M. musculus (DNA)	GAAGTGGGGCGCATCACCAAGTGAAGTATCCATTCCCAAGGAGACAGA
C. griseus (DNA)	GAAGTGGGGCGCATCACCAAGT~~AAGTATCCGTTTC~CCAAGGAGACAGA
M. musculus (pro)	E V G R I T K W K Y P F P K E T E
C. griseus (pro)	E V G R I T K - K Y P F - K E T E
Annotations	
H. sapiens (DNA)	GGCCAAGAGCAAGCTGACGCCACTCTGTATGTTGGGAAATACTCTACCA
M. musculus (DNA)	GGCCAAGAGCAAGCTAACGCCTACTCTGTATGTTGGGAAGTATTCACCA
C. griseus (DNA)	GGCCAAGAGCAAGCTGACGCCTACCCTGTACGTTGGGAAGTACTCAACCA
M. musculus (pro)	A K S K L T P T L Y V G K Y S T S
C. griseus (pro)	A K S K L T P T L Y V G K Y S T S
Annotations	
H. sapiens (DNA)	GCCTCTATGCCTCTCCCTCAATGGTACACGAGGGGGTTGCTGTCGTGCC
M. musculus (DNA)	GCCTCTATGCCTCTCCCTCAATGGTGCATGAGGGGGTTGCTGTCGTGCCT
C. griseus (DNA)	GCCTCTATGCCTCTCCATCAATGGTGCACGAGGGGGTTGCTGTAGTGCC
M. musculus (pro)	L Y A S P S M V H E G V A V V P
C. griseus (pro)	L Y A S P S M V H E G V A V V P
Annotations	Luminal domain][Linker domain

H. sapiens (DNA)	CGCGGCAGCACACTTCCTTTGCTGGAAGGGCCCCAGACTGATGGCGTCAC
M. musculus (DNA)	CGAGGCAGCACTCTTCCTTTGCTGGAAGGGCCCCAGACAGATGGCGTCAC
C. griseus (DNA)	CGAGGAAGCACTCTTCCTTTGCTGGAAGGTCCCCAGACAGATGGTGTTCAC
M. musculus (pro)	R G S T L P L L E G P Q T D G V T
C. griseus (pro)	R G S T L P L L E G P Q T D G V T
Annotations	
H. sapiens (DNA)	CATTGGGGACAAGGGGGAGTGTGTGATCACGCCACGACGGACGTCAAGT
M. musculus (DNA)	CATTGGAGACAAAGGAGAGTGTGTGATCACTCCCAGCACAGACCTCAAGT
C. griseus (DNA)	CATTGAAGACAAAGGAGAGTGTGTGATCACCCCCAGCACAGACCTCAAGT
M. musculus (pro)	I G D K G E C V I T P S T D L K F
C. griseus (pro)	I E D K G E C V I T P S T D L K F
Annotations	
H. sapiens (DNA)	TTGATCCCGGACTCAAAGCAAGAACAAGCTCAACTACTTGAGGAATTAC
M. musculus (DNA)	TTGACCCTGGACTCAAAGGGAAGAGCAAGCTGAACTACTTGAGGAATTAC
C. griseus (DNA)	TTGACCCTGGACTCAAAGGGAAGAGCAAGCTGAACTACTTGAGGAATTAC
M. musculus (pro)	D P G L K G K S K L N Y L R N Y
C. griseus (pro)	D P G L K G K S K L N Y L R N Y
Annotations	
H. sapiens (DNA)	TGGCTTCTGATAGGACACCATGAAACCCCACTGTCTGCGTCTACCAAGAT
M. musculus (DNA)	TGGCTTCTCATAGGACACCATGAAACTCCTCTGTCTGCATCCACCAAGAT
C. griseus (DNA)	TGGCTTCTCATAGGACACCATGAAACTCCTCTGTCTGCATCTACCAAGAT
M. musculus (pro)	W L L I G H H E T P L S A S T K M
C. griseus (pro)	W L L I G H H E T P L S A S T K M
Annotations	
H. sapiens (DNA)	GCTGGAGAGATTTCCCAACAATCTACCCAAACATCGGGAAAATGTGATTC
M. musculus (DNA)	GCTGGAGAGATTTCCCTAACCAACCTGCCCAAACATCGAGAAAATGTGATTC
C. griseus (DNA)	GCTGGAGAGATTTCCCAACAACCTGCCCAAACATCGGGAAAATGTGATTC
M. musculus (pro)	L E R F P N N L P K H R E N V I P
C. griseus (pro)	L E R F P N N L P K H R E N V I P
Annotations	
H. sapiens (DNA)	CTGCTGATTCAGAGAAAAAGAGCTTTGAGGAAGTTATCAACCTGGTTGAC
M. musculus (DNA)	CTGCTGATTCAGAAAAAGGAGCTTTGAGGAAGTTATCAACATAGTTGGC
C. griseus (DNA)	CTGCTGATTCGGAAAAAGGAGCTTTGAGAAAGTTATCAACATGGTTGAC
M. musculus (pro)	A D S E K R S F E E V I N I V G
C. griseus (pro)	A D S E K R S F E K V I N M V D
Annotations	

H. sapiens (DNA)	CAGACTTCAGAAAACGCACCTACCACCGTGTCTCGGGATGTGGAGGAGAA
M. musculus (DNA)	CAGACTTCAGACAACACACCGACCACCGTATCTCAGGATGTGGAGGAGAA
C. griseus (DNA)	CAGACTTCAGAAAACACACCCATCCACTGTGTCTCAGGCCGTGGAAGAGAA
M. musculus (pro)	Q T S D N T P T T V S Q D V E E K
C. griseus (pro)	Q T S E N T P S T V S Q A V E E K
Annotations	
H. sapiens (DNA)	GCCCGCCCAT GCCCCTGCCC GGCCCGAGGC CCCCGTGGAC TCCATGCTTA
M. musculus (DNA)	GCTCGCTCGC GCCCCTGCCA AGCCTGAGGC CCCCGTGGAC TCCATGCTCA
C. griseus (DNA)	GCTGGTCCAT GCCCCCGCCA AGCCTGAGGC CCCCGTTGAC TCCATGCTCA
M. musculus (pro)	L A R A P A K P E A P V D S M L K
C. griseus (pro)	L V H A P A K P E A P V D S M L K
Annotations	
H. sapiens (DNA)	AGGACATGGCTACCATCATCCTGAGCACCTTCCTGCTGATTGGCTGGGTG
M. musculus (DNA)	AGGACATGGCTACCATTATCCTGAGCACCTTCCTGCTGGTTGGATGGGTG
C. griseus (DNA)	AGGACATGGCTACTATTATCCTGAGCACCTTCCTGCTGGTTGGATGGGTG
M. musculus (pro)	D M A T I I L S T F L L V G W V
C. griseus (pro)	D M A T I I L S T F L L V G W V
Annotations	Linker domain][Transmembrane domain
H. sapiens (DNA)	GCCTTCATCATCACCTATCCCCTGAGCATGCATCAGCAGCAGCTCCA
M. musculus (DNA)	GCGTTCATCATCACTTACCCCCTGAGCGTGCATCAGCAGCGTCAGCTCCA
C. griseus (DNA)	GCCTTCATCATCACTTACCCCCTGAGCATGCATCAGCAGCGCCAGCTCCA
M. musculus (pro)	A F I I T Y P L S V H Q Q R Q L Q
C. griseus (pro)	A F I I T Y P L S M H Q Q R Q L Q
Annotations	transmembrane domain][Poly Q region
H. sapiens (DNA)	GCACCAGCAGTTCAGAAAGAACTGGAGAAGATTCAGCTCCTGCAGCAGC
M. musculus (DNA)	GCACCAACAGTTCAGAAAGAGCTGGAGAAGATTCAGCTCCTGCAGCAGC
C. griseus (DNA)	GCACCAGCAGTTCAGAAAGAACTGGAGAAAATTCAGCTCCTGCAGCAGC
M. musculus (pro)	H Q Q F Q K E L E K I Q L L Q Q Q
C. griseus (pro)	H Q Q F Q K E L E K I Q L L Q Q Q
Annotations	
H. sapiens (DNA)	AGCAGCAGCAGCTGCCCTTCCACCCACCTGGAGACACGGCTCAGGACGGCGAGCTC
M. musculus (DNA)	AGCAG-----CTGCCCTTCCACCCACACGGAGACCTTACCCAGGACCTTGAGTTC
C. griseus (DNA)	AGCAG-----CTGCCCTTCCACCCACATGGAGACCTTACTCAGGACCCCGAGTTT
M. musculus (pro)	Q L P F H P H G D L T Q D P E F
C. griseus (pro)	Q Q Q L P F H P H G D L T Q D P E F
Annotations	Poly Q]

H. sapiens (DNA)	CTGGACACGTCTGGCCCGTACTCAGAGAGCTCGGGCACCAGCAGCCCCAG
M. musculus (DNA)	CTGGATTCATCTGGCCCTTCTCAGAGAGCTCTGGCACCAGCAGCCCCAG
C. griseus (DNA)	CTGGATTCATCTGGTC~CTTCTCAGAGAGCTCAGGCACCAGCAGCTCCAG
M. musculus (pro)	L D S S G P F S E S S G T S S P S
C. griseus (pro)	L D S S G X F S E S S G T S S S S
Annotations	
H. sapiens (DNA)	CACGTCCCCCAGGGCCTCCAACCACTCGCTCTGCTCCGGCAGCTCTGCCT----
M. musculus (DNA)	CCCATCCCCCAGAGCCTCCAACCACTCCCTCCACCCAGCAGCTCTGCCT----
C. griseus (DNA)	CCCATCCCCCAGAGCCTCCAACCACTCACTCCACTCCAGCAGCTCTGCCTCCAA
M. musculus (pro)	P S P R A S N H S L H P S S S A S -
C. griseus (pro)	P S P R A S N H S L H S S S S A S N
Annotations	
H. sapiens (DNA)	CCAAGGCTGGCAGCAGCCCTCCCTGGAACAAGACGATGGAGATGAGGAA---
M. musculus (DNA)	CCAGGGCCGGCACCAGCCCTCTCTGGAGCAGGATGATGAGGATGAGGAA---
C. griseus (DNA)	CCAAGACTGGCACCAACCTTCCCTGGAACAAGACGATGGAGATGAGGAACT
M. musculus (pro)	R A G T S P S L E Q D D E D E E -
C. griseus (pro)	Q T G T N P S L E Q D D E D E E T
Annotations	
H. sapiens (DNA)	ACCAGCGTGGTGATAGTTGGGAAAATTTCTTCTGTCCCAAGGATGTCCT
M. musculus (DNA)	ACCAGAATGGTGATTGTTGGGAAAATTTCACTTCTGCCCCAAGGATGTCCT
C. griseus (DNA)	ACTAGAATGGTGATTGTTGGGAAAATTTCACTTCTGCCCCAAGGATGTCCT
M. musculus (pro)	T R M V I V G K I S F C P K D V L
C. griseus (pro)	T R M V I V G K I S F C P K D V L
Annotations	[Kinase domain]
H. sapiens (DNA)	GGGCCATGGAGCTGAGGGCACAATTGTGTACCGGGGCATGTTTGACAACC
M. musculus (DNA)	GGGTCATGGAGCTGAGGGCACAATTGTATACAAAGGTATGTTTGACAACC
C. griseus (DNA)	GGGCCATGGAGCTGAGGGCACAATTGTATACAAAGGCATGTTTGACAACC
M. musculus (pro)	G H G A E G T I V Y K G M F D N R
C. griseus (pro)	G H G A E G T I V Y K G M F D N R
Annotations	
H. sapiens (DNA)	GCGACGTGGCCGTGAAGAGGATCCTCCCCGAGTGTTTTAGCTTCGCAGAC
M. musculus (DNA)	GAGATGTGGCCGTGAAGAGGATCCTCCCTGAGTGTTTTAGCTTTGCCGAC
C. griseus (DNA)	GTGATGTGGCAGTGAAGAGGATCCTCCCTGAGTGTTTTAGCTTTGCAGAC
M. musculus (pro)	D V A V K R I L P E C F S F A D
C. griseus (pro)	D V A V K R I L P E C F S F A D
Annotations	K599

H. sapiens (DNA)	CGTGAGGTCCAGCTGTTGCGAGAATCGGATGAGCACCCGAACGTGATCCG1951
M. musculus (DNA)	CGTGAGGTCCAGCTGCTTCGAGAATCAGACGAGCACCCAAATGTGATCCG
C. griseus (DNA)	CGTGAGGTCCAGCTGCTTCGAGAATCAGACGAGCATCCAAACGTGATCCG
M. musculus (pro)	R E V Q L L R E S D E H P N V I R
C. griseus (pro)	R E V Q L L R E S D E H P N V I R
Annotations	
H. sapiens (DNA)	CTACTTCTGCACGGAGAAGGACCGGCAATTCCAGTACATTGCCATCGAGC
M. musculus (DNA)	CTACTTTTGCACAGAGAAGGACCGGCAGTTCAGTACATTGCTATCGAGC
C. griseus (DNA)	CTACTTTTGCACAGAGAAGGACCGGCAGTTCCTAATACATTGCTATTGAAT
M. musculus (pro)	Y F C T E K D R Q F Q Y I A I E L
C. griseus (pro)	Y F C T E K D R Q F Q Y I A I E L
Annotations	I642
H. sapiens (DNA)	TGTGTGCAGCCACCCTGCAAGAGTATGTGGAGCAGAAGGACTTTGCGCAT
M. musculus (DNA)	TGTGTGCAGCCACCCTACAAGAGTATGTGGAGCAGAAGGACTTTGCCAC
C. griseus (DNA)	TGTGTGCAGCCACTCTGCAAGAGTATGTGGAGCAGAAGGACTTTGCCAC
M. musculus (pro)	C A A T L Q E Y V E Q K D F A H
C. griseus (pro)	C A A T L Q E Y V E Q K D F A H
Annotations	
H. sapiens (DNA)	CTCGGCCTGGAGCCCATCACCTTGCTGCAGCAGACCACCTCGGGCCTGGC
M. musculus (DNA)	CTTGGCCTCGAGCCCATCACCTTGCTTCATCAGACCACCTCAGGCCTGGC
C. griseus (DNA)	CTTGGCCTGGAGCCCATCACCTTGCTTCAGCAGACCACCTCAGGCCTGGC
M. musculus (pro)	L G L E P I T L L H Q T T S G L A
C. griseus (pro)	L G L E P I T L L Q Q T T S G L A
Annotations	
H. sapiens (DNA)	CCACCTCCACTCCCTCAACATCGTTTCACAGAGACCTAAAGCCACACAACA
M. musculus (DNA)	ACACCTGCATTCTCTCAACATTGTTTCACAGAGACCTGAAGCCCCACAACA
C. griseus (DNA)	ACACCTGCACTCTCTCAACATAGTTTCACAGAGACCTGAAACCCCAACA
M. musculus (pro)	H L H S L N I V H R D L K P H N I
C. griseus (pro)	H L H S L N I V H R D L K P H N I
Annotations	
H. sapiens (DNA)	GACTTTGGCCTCTGCAAGAAGCTGGCAGTGGGCAGACACAGTTTCAGCCG
M. musculus (DNA)	GACTTTGGCCTCTGCAAGAAGCTGGCAGTGGGCAGGCACAGTTTCAGCCG
C. griseus (DNA)	GACTTTGGCCTCTGCAAGAAGCTGGCAGTGGGTAGGCACAGTTTCAGCCG
M. musculus (pro)	D F G L C K K L A V G R H S F S R
C. griseus (pro)	D F G L C K K L A V G R H S F S R
Annotations	D711 < Activation loop S1 S2

H. sapiens (DNA)	TCCTCATATCCATGCCCAATGCACACGGCAAGATCAAGGCCATGATCTCC
M. musculus (DNA)	TTCTCCTCTCCATGCCCAACGCACATGGCAGGATCAAGGCGATGATCTCT
C. griseus (DNA)	TTCTCCTCTCCATGCCCAACGCACATGGCAAGATCAAGGCCATGATCTCT
M. musculus (pro)	L L S M P N A H G R I K A M I S
C. griseus (pro)	L L S M P N A H G K I K A M I S
Annotations	
H. sapiens (DNA)	CCGATCTGGGGTGCCTGGCACAGAAGGCTGGATCGCTCCAGAGATGCTGA
M. musculus (DNA)	CCGTTTCAGGGGTACCTGGCACTGAAGGGTGGATCGCCCCAGAGATGCTGA
C. griseus (DNA)	TCGTTTCAGGGGTACCTGGCACTGAAGGCTGGATCGCCCCAGAGATGTTGA
M. musculus (pro)	R S G V P G T E G W I A P E M L S
C. griseus (pro)	R S G V P G T E G W I A P E M L S
Annotations	S3 >
H. sapiens (DNA)	GCGAAGACTGTAAGGAGAACCCTACCTACACGGTGGACATCTTTTCTGCA
M. musculus (DNA)	GTGAAGACTGTAAGGACAACCCTACCTACACGGTGGACATCTTTTCTGCA
C. griseus (DNA)	GTGAAGACTGCAAGGAAAACCCTACCTACACAGTGGACATCTTCTCTGCA
M. musculus (pro)	E D C K D N P T Y T V D I F S A
C. griseus (pro)	E D C K E N P T Y T V D I F S A
Annotations	
H. sapiens (DNA)	GGCTGCGTCTTTTACTACGTAATCTCTGAGGGCAGCCACCCTTTTGGCAA
M. musculus (DNA)	GGCTGTGTCTTTTACTATGTTCATCTCTGAGGGCAACCATCCTTTTGGCAA
C. griseus (DNA)	GGCTGTGTTTTTTACTATGTTCATCTCTGAGGGCAACCATCCTTTTGGCAA
M. musculus (pro)	G C V F Y Y V I S E G N H P F G K
C. griseus (pro)	G C V F Y Y V I S E G N H P F G K
Annotations	
H. sapiens (DNA)	GTCCCTGCAGCGGCAGGCCAACATCCTCCTGGGTGCCTGCAGCCTTGACT
M. musculus (DNA)	ATCCTTGCAGCGGCAGGCCAACATCCTCCTGGGCGCCTGCAACCTTGACT
C. griseus (DNA)	GTCCTTGCAGCGGCAGGCCAACATCCTCCTGGGCGCCTGCAGCCTTGACT
M. musculus (pro)	S L Q R Q A N I L L G A C N L D
C. griseus (pro)	S L Q R Q A N I L L G A C S L D
Annotations	
H. sapiens (DNA)	GCTTGCACCCAGAGAAGCACGAAGACGTCATTGCACGTGAATTGATAGAG
M. musculus (DNA)	GTTTCCACTCAGACAAGCATGAGGACGTCATTGCTCGTGAATTGATAGAG
C. griseus (DNA)	GCTTCCACTCAGACAAGCATGAGGACGTCATTGCTCGTGAATTGATAGAG
M. musculus (pro)	C F H S D K H E D V I A R E L I E
C. griseus (pro)	C F H S D K H E D V I A R E L I E
Annotations	

H. sapiens (DNA)	AAGATGATTGCGATGGATCCTCAGAAACGCCCTCAGCGAAGCATGTGCT
M. musculus (DNA)	AAAATGATTGCTATGGATCCCCAGCAGCGTCCCTCTGCAAAGCACGTGCT
C. griseus (DNA)	AAGATGATTGCTATGGATCCCCAGCAACGGCCCTCTGCAAAGCATGTGCT
M. musculus (pro)	K M I A M D P Q Q R P S A K H V L
C. griseus (pro)	K M I A M D P Q Q R P S A K H V L
Annotations	
H. sapiens (DNA)	CAAACACCCGTTCTTCTGGAGCCTAGAGAAGCAGCTCCAGTTCTTCCAGG
M. musculus (DNA)	GAAACACCCCTTCTTCTGGAGCCTGGAGAAGCAGCTCCAGTTTTTCCAGG
C. griseus (DNA)	AAAACACCCATTCTTCTGGAGCCTGGAAAAGCAGCTCCAGTTTTTCCAGG
M. musculus (pro)	K H P F F W S L E K Q L Q F F Q D
C. griseus (pro)	K H P F F W S L E K Q L Q F F Q D
Annotations	Kinase domain][RNase domain
H. sapiens (DNA)	ACGTGAGCGACAGAATAGAAAAGGAATCCCTGGATGGCCCGATCGTGAAG
M. musculus (DNA)	ATGTAAGTGACCGAATAGAAAAGGAGGCCTTGGACGGTCCAATCGTACGG
C. griseus (DNA)	ATGTGAGTGACCGAATAGAAAAGGAGTCCTTGGATGGCCCGATAGTAAGA
M. musculus (pro)	V S D R I E K E A L D G P I V R
C. griseus (pro)	V S D R I E K E S L D G P I V R
Annotations	
H. sapiens (DNA)	CAGTTAGAGAGAGGCGGGAGAGCCGTGGTGAAGATGGACTGGCGGGAGAA
M. musculus (DNA)	CAGTTGGAGAGAGGCGGGAGAGCTGTGGTCAAGATGGACTGGCGGGAGAA
C. griseus (DNA)	CAGTTGGAGAGAGGCGGGAGAGCCGTGGTGAAGATGGACTGGCGGGAGAA
M. musculus (pro)	Q L E R G G R A V V K M D W R E N
C. griseus (pro)	Q L E R G G R A V V K M D W R E -
Annotations	
H. sapiens (DNA)	CATCACTGTCCCCCTCCAGACAGACCTGCGTAAATTCAGGACCTATAAAG
M. musculus (DNA)	CATCACTGTCCCCCTGCAGACAGATCTGCGCAAATTCAGAACCTACAAAG
C. griseus (DNA)	~~~~~CAGAACCTACAAAG
M. musculus (pro)	I T V P L Q T D L R K F R T Y K G
C. griseus (pro)	- - - - - - - - - - R T Y K G
Annotations	
H. sapiens (DNA)	GTGGTTCTGTGAGAGATCTCCTCCGAGCCATGAGAAAATAAGAAGCACCAC
M. musculus (DNA)	GTGGCTCTGTGAGAGACCTCCTCCGAGCCATGAGAAAACAAGAAACACCAC
C. griseus (DNA)	GTGGCT~~~~~AGAAACACCAC
M. musculus (pro)	G S V R D L L R A M R N K K H H
C. griseus (pro)	G - - - - - - - - - - K H H
Annotations	K907

H. sapiens (DNA)	TACCGGGAGCTGCCTGCAGAGGTGCGGGAGACGCTGGGGTCCCTCCCCGA
M. musculus (DNA)	TACCGGGAGCTCCCCGTGGAGGTTTCAGGAGACGCTGGGGCTCCATCCCCGA
C. griseus (DNA)	TACCGAGAGCTCCCCATGGAGGTTTCAGGAGACGCTGGGGCTCCATCCCCGA
M. musculus (pro)	Y R E L P V E V Q E T L G S I P D
C. griseus (pro)	Y R E L P M E V Q E T L G S I P D
Annotations	
H. sapiens (DNA)	Cgacttcgtgtgctacttcacatctcgcttccccacctcctcgcacaca
M. musculus (DNA)	TGACTTTGTGCGCTACTTCACTTCCCCGCTTCCCCACCTCCTCTCTCACA
C. griseus (DNA)	Tgactttgtgcgctatttcacatcacgcttcccctacctcctctcacaca
M. musculus (pro)	D F V R Y F T S R F P H L L S H T
C. griseus (pro)	D F V R Y F T S R F P Y L L S H T
Annotations	
H. sapiens (DNA)	CCTACCGGGCCATGGAGCTGTGCAGCCACGAGAGACTCTTCCAGCCCTAC
M. musculus (DNA)	CCTACCAAGCCATGGAGCTGTGCAGACATGAGAGACTCTTTCAGACCTAC
C. griseus (DNA)	CCTACCGAGCCATGGAGCTCTGCAGACATGAGAGACTCTTCCAGACCTAC
M. musculus (pro)	Y Q A M E L C R H E R L F Q T Y
C. griseus (pro)	Y R A M E L C R H E R L F Q T Y
Annotations	
H. sapiens (DNA)	TACTTCCACGAGCCCCAGAGCCCCAGCCCCAGTGACTCCAGACGCCCT
M. musculus (DNA)	TACTGGCACGAGCCCACAGAACCCAGCCTCCAGTGATTCCATATGCCCT
C. griseus (DNA)	TACTTGCACGAGCCCACAGAACCCAGCCTCCAGTGACTCCAGATGCGCT
M. musculus (pro)	Y W H E P T E P Q P P V I P Y A L
C. griseus (pro)	Y L H E P T E P Q P P V T P D A L
Annotations	
H. sapiens (DNA)	CTGAGCGAGGGCGGCCCTCTGTTCTGGTGGCCCCAGCTGT----GACTGAGGGC
M. musculus (DNA)	CTGAGCTAGGGCAGCCC-TCTGGTCTGGTGGCCCCA----ATAATGACCATGGGC
C. griseus (DNA)	CTGAGCCATGGCAGCCC-TCTAGTCTGGTGGCCCCAGCAGAGATTG~~CA~~GGC
M. musculus (pro)	*
C. griseus (pro)	*
Annotations	RNase domain][3' UTR
H. sapiens (DNA)	CTGGTCACCACAATT-AGAGCTTGATGCCTCCCGCTTTGCAGGGAGACCA
M. musculus (DNA)	CCGATCTCTGCAGTC-ATAGTTTGTTCCTCTGGGATTAGCAGGAAGACTA
C. griseus (DNA)	CCAATCTCTGCAGTCTGTAGCTTGCTGCCTCTGGGATTAGCAGGAAGACTA
M. musculus (pro)	
C. griseus (pro)	
Annotations	

H. sapiens (DNA)	TGGGA-CAGCTAGGCTGAGATGCACCAAGTACAGCCTTCACTGG-AGACCGGA
M. musculus (DNA)	TGGAAGCAGCCTGGTTGGGGTATTGCATGTGCAGCCT---CTGATAGAAATGG
C. griseus (DNA)	----AGCAGCCTGGCTGGGGTGCAGCAAGAGCACCT---CTGCTAGAAATGG
M. musculus (pro)	
C. griseus (pro)	
Annotations	
H. sapiens (DNA)	ATTGAGAGGTGGGGGATG--
M. musculus (DNA)	CTGAGGAGGGGGAGGACGGAGTTCAGAGGGTGTTCGTCCTGCAGTG
C. griseus (DNA)	TTTGAGAGATGTGGGGTG--CTAAGGAAG---AG-ATG-TTCAGAGG-TGT-----
M. musculus (pro)	TGCCATG
C. griseus (pro)	TTTTTGAGAAGTACAGTGTGCTCAGGAAG---AG-GGC-TGCAGAAG-TGT-----
Annotations	TGTCCTG
H. sapiens (DNA)	TGAGATTTCTCATTGATCACAGATGTGCCCAGAGTA
M. musculus (DNA)	GG-----GAT---AGGAG-GCACC---T-
C. griseus (DNA)	GA-----GAC---AGGAG-GCGCC---T-
M. musculus (pro)	
C. griseus (pro)	
Annotations	
H. sapiens (DNA)	GCCCAGGTCACTGTAACTAGTGT---CTGCAGAGGCAG
M. musculus (DNA)	CCAAGTTACTGATA-GCCCGTGTG-CCTCAT---GCAG
C. griseus (DNA)	CCAAGTTACTGGCA-GCCTGTGTG-CCTTGT---GCA-
M. musculus (pro)	
C. griseus (pro)	
Annotations	
H. sapiens (DNA)	CAGGAGCCATGAGCATGAGGTGTGGCATTAGGG----
M. musculus (DNA)	ACTGGTCAGCTATGCATGCTGGCAGGT
C. griseus (DNA)	CA-AGTTGTGAGAGTGGGTTGTGG-----AG-----ACTCGTTAGCAATGC-
M. musculus (pro)	TGTGGACA-CT
C. griseus (pro)	CA-AGTTGTGAGTGTGGAGCATGG-----
Annotations	AGTTAAAGACTGGTTAGCCATGCATCTGGACAAC
H. sapiens (DNA)	GGGGTTGTGTCTGCAGGTCTCAG-AAATGAAGAGGCTGCTCTGTTCTGGAGGC
M. musculus (DNA)	GACAT-GTG-CT-GTGGGTCTGGAAGATGAAGCAGACACTCAGTTCTGGATGT
C. griseus (DNA)	GAGGT-ATA-TCTGTGGGAAAGA~AAATGAAAAGGACA~TCAGTTCTGGGTGT
M. musculus (pro)	
C. griseus (pro)	
Annotations	

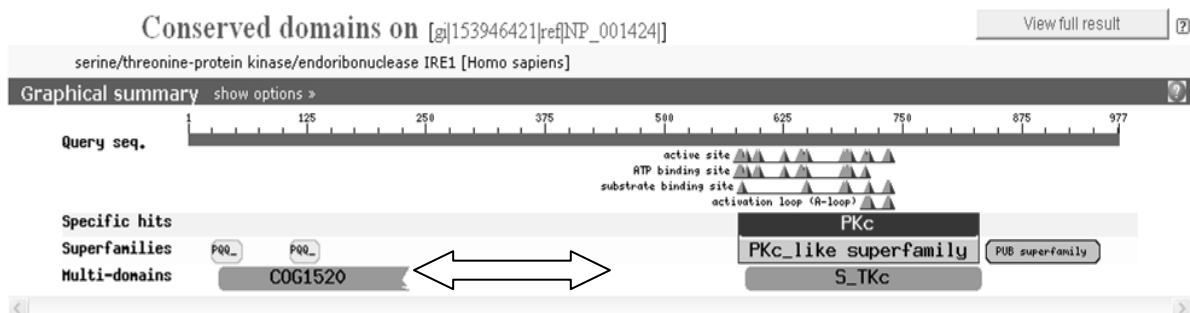
H. sapiens (DNA)	AGCCGTGGCCCAGTGCCAGTGCCAGAACAGTGGCCTTTGGTGGGTGTGTC
M. musculus (DNA)	GGTGCTGGCCCAGCACAGTGG-CCTAAATAGTGGCCCCTGATAGGTTGAAT
C. griseus (DNA)	GGTGCTGGCCCAACACAAGTGGCCTAAATAGTGGCCCCTGATAGACTGAAT
M. musculus (pro)	
C. griseus (pro)	
Annotations	
H. sapiens (DNA)	CCGGGCCATCTCGGGGTGGTGTCTCAGGAGCGCCTGGGGCAAGAGGTAAA
M. musculus (DNA)	CCTGGCTAT-----GTGG-----GCC-----AGAGAT---
C. griseus (DNA)	CCTGGCCAT-----GTGA-----GCC-----AGAGAT---
M. musculus (pro)	
C. griseus (pro)	
Annotations	
H. sapiens (DNA)	GAGTTCCTGGCCTTCAAGGAGAGCAGCGA
M. musculus (DNA)	GAGTTCCTGGCCACCAG-GTG-GCAGCTA
C. griseus (DNA)	AAAGAGTTCCTGACCAA-GAAGGCAGCTA
M. musculus (pro)	
C. griseus (pro)	
Annotations	
H. sapiens (DNA)	AGACCCAGACAGGGGC-----CAGCCT-TCAGGACCAGAGGGAGCCGCCGA
M. musculus (DNA)	AGACC-AGACAGGGACAGAGACAGATTGTCAGGGCCAGAGAGGCAACTA
C. griseus (DNA)	AGACC-AGACAGGGACAGAGACAGGTATTTCAGGGCCAGAGGGGAGCAGCTA
M. musculus (pro)	
C. griseus (pro)	
Annotations	
H. sapiens (DNA)	ATGGGACCCTCCTGGTCAACCAGGAGAAAGCCCTGGGCCAGCGAGTAGGC-AGTCA
M. musculus (DNA)	GAGGGAGCTTCCCAGTCACTCAAAGATGC---TAAG--AACTAGAAGGTGAGTGA
C. griseus (DNA)	GAGGGAACCTCCCAGTCA TGTGGAGAGGC---TCAG-AACCAGA-AGGTAAGTGA
M. musculus (pro)	
C. griseus (pro)	
Annotations	
H. sapiens (DNA)	AAC--TCCTTCGTCCCCA- AGGCCGGTGGAAACAAGAGGCT
M. musculus (DNA)	TATGGTCCCTCTACCCCAGAGGCCAGCAGATTAGCGCATA
C. griseus (DNA)	TAGGGCCCCTCTGCCCCAGAGGC-----
M. musculus (pro)	
C. griseus (pro)	
Annotations	

H. sapiens (DNA)	-----
M. musculus (DNA)	GATTATGAATCAAGGCCCTGGGGGTAGAGAGCCAAG
C. griseus (DNA)	-----
M. musculus (pro)	
C. griseus (pro)	
Annotations	3' UTR]

4.6.8 Summary

The primary aim of this section of work was to produce sufficient sequence to design siRNA sequences targeted against CHO IRE1 α (which will be discussed in chapter 4.8). The sequence obtained from this section was more than adequate for this – indeed the sequence obtained from one of the 900bp fragments was considered particularly suitable for the targeting of the siRNAs, as when the IRE1 α sequence was subjected to a conserved domain search on the NCBI website (<http://www.ncbi.nlm.nih.gov/Structure/cdd/cdd.shtml>) the area upstream of the kinase domain was found to have no significant homology with other proteins (marked with an arrow on Figure 4.6. 3), making it a far better target for specific siRNAs than, for example, the highly conserved kinase domain. It is not surprising that this area was also the easiest section to sequence given again, the low homology with other sequences.

Figure 4.6. 3 – Conserved domain analysis of H. sapiens ERN1/IRE1 α .



The secondary outcome of this section was the production of a CHO IRE1 α sequence for deposit in NCBI and general scientific use – this was for the main part successful, although unfortunately the most difficult 3' and 5' ends could not be sequenced due to non-specificity of primers. Sequences were returned to Lonza with annotations to be combined with assemblies from their project. If time had allowed, further work could have been attempted to clone these ends using nested primer combinations to reduce the non-specificity.

A major impedance in this work was equipment contamination – upon sequencing of one of the constructs in the area of the kinase domain, human sequence was found instead of CHO (sequence was identical to human whereas previously CHO sequences had understandably better homology with mouse sequences). One of the cDNA samples had become contaminated with human IRE1 α from one of the other constructs used in this thesis and needed to be discarded. All equipment used was thoroughly decontaminated and fresh cDNA produced, and all further sequences produced were found to be CHO.

4.7 Production of Lonza vector pEE12.4-derived silencing vectors.

4.7.1 Rationale

RNA interference (RNAi) is a method of silencing genes by using the RNA-induced silencing complex and the enzyme Dicer. This pathway is used in the cell to destroy double-stranded RNA from viruses and prevent their genes from being expressed – however, it can also be utilised to silence genes by inserting double-stranded RNA matching their sequence into the cell (Fire, Xu et al. 1998). RNAi delivery of siRNAs into the cell can be performed by simply inserting the siRNA sequences themselves directly into the cell, or by inserting a plasmid expressing a short hairpin RNA (shRNA) or a micro-RNA (miRNA) into the cell. These latter strategies gives a longer-lasting effect than the former (Fewell and Schmitt 2006). The structures of the si/shRNAs used in this thesis will be discussed in greater detail in Chapter 4.8 – this chapter discusses the delivery vector plasmid developed for the shRNA.

Certain criteria needed to be met by the delivery vector for potential future uses.

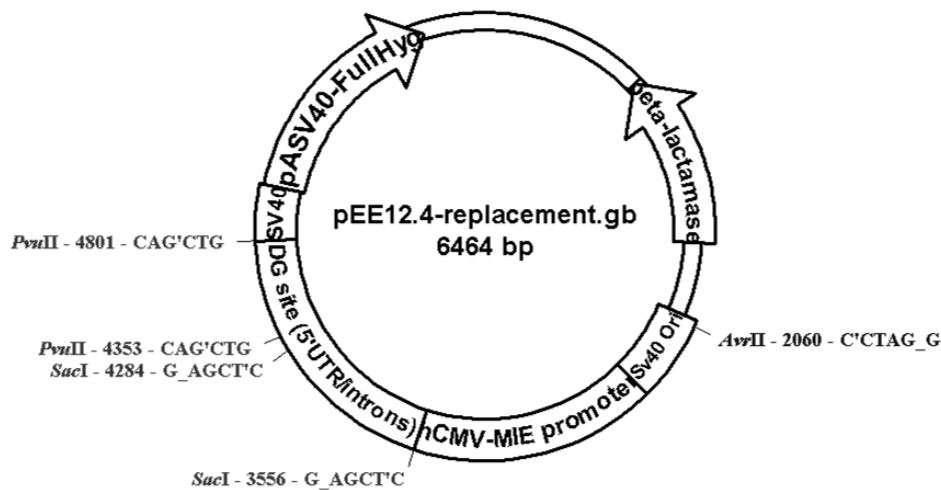
1) That it contain a suitable promoter to drive shRNA expression, such as U6, CMV or H1.

- 2) That it be based on a Lonza-owned vector to avoid potential intellectual property conflicts (see below) and
- 3) That it be competent for later addition of IRE1 α constructs in order to co-express the shRNA and these constructs and perform knockdown in combination with expression. This combination of shRNA and cDNA was successfully used in (Li and Mahato 2009) by the insertion of an internal ribosome entry site (IRES) between the shRNA and the cDNA. In the following sections, the construction of this vector is described.

4.7.2 Cloning Strategy – shRNA Polylinker

The Lonza vector pEE12.4 was used to derive the shRNA vectors. This vector contains sequences in addition to the normal apparatus for selection and replication in *E. coli* which made it fit for purpose and for potential later applications: a CMV promoter which was used to drive the double gene expression the vector was designed for, which could be used to drive expression of the shRNA and the hygromycin resistance gene which would permit screening for potential. A U6 promoter driven vector was also designed in order that two vectors would be available, one RNA polymerase II dependent (CMV) and one RNA polymerase III dependent (U6), both of which have been used to drive shRNA production (Zhou, Xia et al. 2005). The pEE12.4 vector contained suitable restriction enzyme sites (Figure 4.7. 1) to excise only the double gene insert (*SacI/PvuII*) or the double gene insert and the CMV promoter (*AvrII/PvuII*) to allow replacement with the U6 promoter.

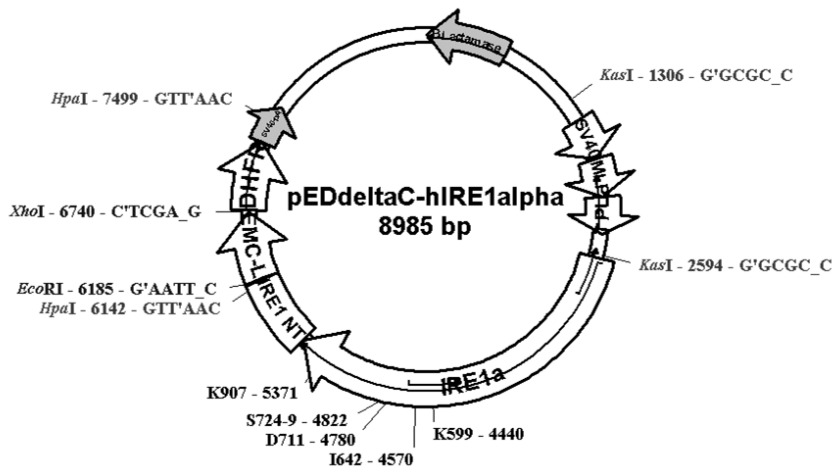
Figure 4.7. 1 – Lonza pEE12.4 vector backbone.



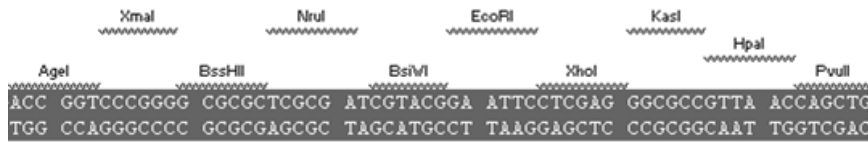
A polylinker was also designed to be cloned into the vector after either the CMV or U6 promoter (Figure 4.7. 2B). The polylinker contains an *EcoRI* and an *XhoI* site to allow later cloning of the EMC-Leader/internal ribosome entry site already available in the pED Δ c-hIRE1 α plasmid, and a *KasI* and a *HpaI* site to allow cloning of the IRE1 α sequence, also from this plasmid (Figure 4.7. 2A). Upstream of these cloning sites in the polylinker were several restriction enzyme sites that did not already exist in the pEE12.4 vector which permitted cloning in of the shRNA sequence itself (*AgeI*, *XmaI*, *BssHIII*, *NruI* and *BsiWI*). The polylinker was designed with a *PvuII* site to permit ligation to the *PvuII* site at bp 4801 in pEE12.4 (Figure 4.7. 1) and the appropriate restriction enzyme site (*AvrII/SacI*) for the CMV/U6 vector. However, as it did not prove possible to clone the CMV vector successfully, the following sections describe the cloning of the U6 promoter-driven vector.

Figure 4.7. 2 - Multicloning site insert.

A



B

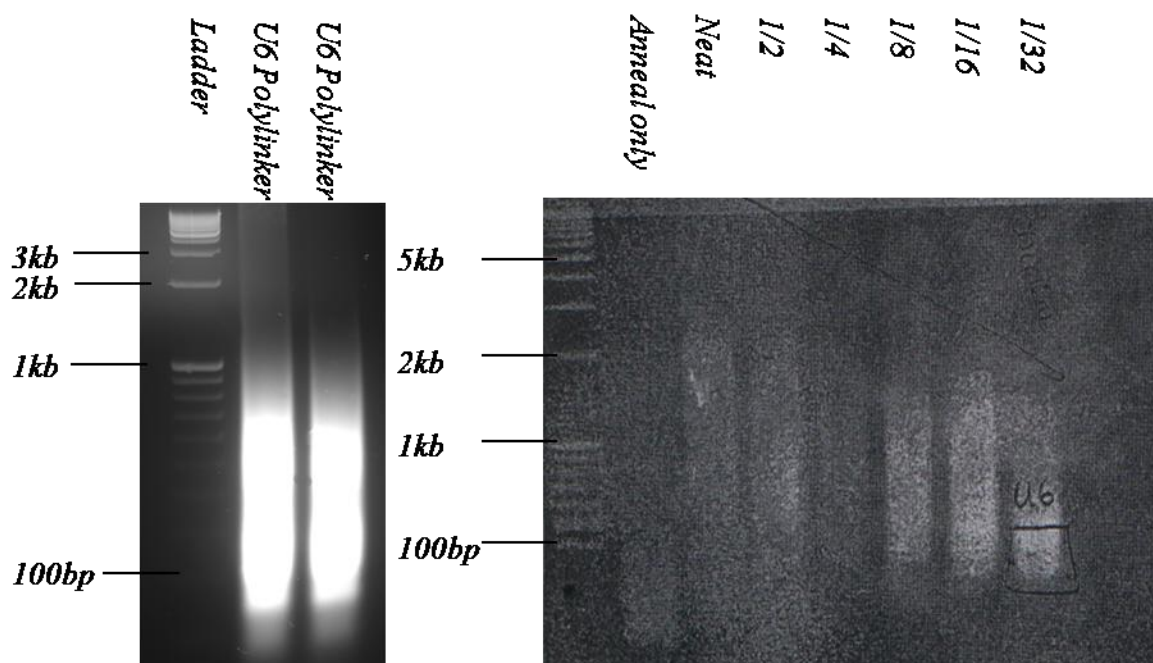


4.7.3 Cloning Strategy – U6 Promoter vector

The U6 promoter drives the transcription of small nuclear RNA molecules (snRNA) in vertebrates. It consists of a TATA box (TATATA) and upstream of it a proximal sequence element, or PSE. Specificity of the sequence for RNA polymerase II or III is dependent upon the distances between the PSE and the TATA box (Goomer and Kunkel 1992). Sequences coding for the wild type human U6 promoter were taken from (Lin, Yang et al. 2004) and a polylinker consisting of the restriction enzyme site *AvrII*, followed by the U6 promoter (see Figure 4.7. 3), followed by the multicloning site designed above (Figure 4.7. 2) with sufficient gap (~29bp) between the TATA box and the multicloning site to cause the promoter to begin transcribing at the start of the shRNA once it was cloned in. This sequence was too long to order as a single primer pair, unlike the multicloning site alone, and therefore was ordered as four primer pairs.

The ligation mixture was incubated overnight at 16°C to ligate and run on a 0.9% gel to check the length of the product. However, it appeared that multiple copies of the product had ligated together causing a range of different length constructs (Figure 4.7. 4, left panel). To attempt to ligate a single copy of the completed insert, a range of dilutions of the T4 ligase from 1:2 to 1:32 were used to perform the ligation reaction (Figure 4.7. 4, right panel) and products run on a gel as above. The lowest concentration produced inserts of the correct length (160bp), which were excised and purified from the gel.

Figure 4.7. 4 - U6 Polylinker Annealing

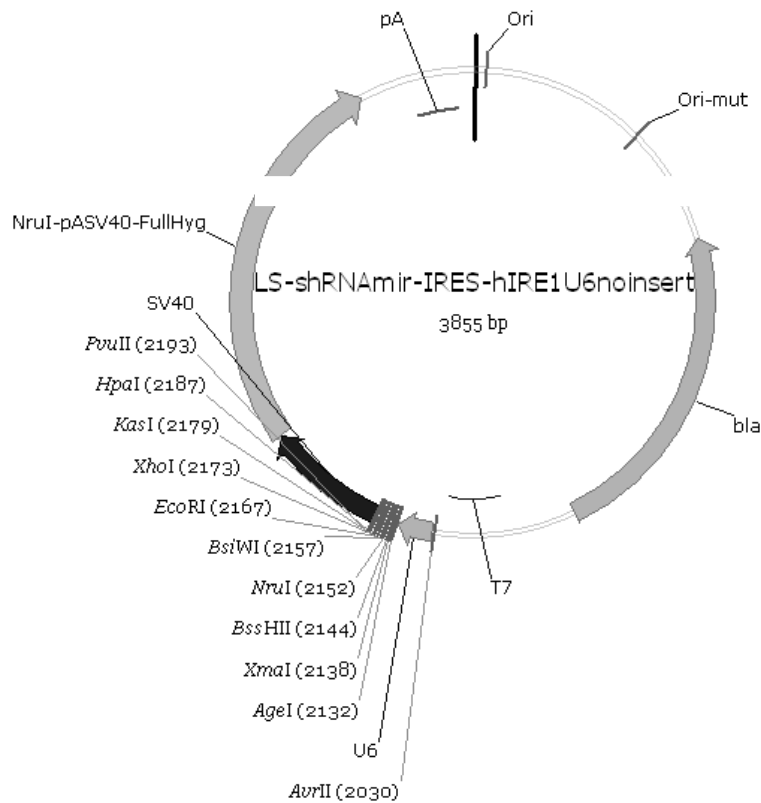


4.7.5 Ligation and Screening of vector with polylinker

To produce the vector backbone for cloning in the insert produced above, pEE12.4 was digested with *AvrII* and *PvuII* in a standard 10µl reaction as described in Materials and Methods – Restriction Enzyme digestion. Ligation of the U6 polylinker insert to the *AvrII*-*PvuII* fragment of was performed as described in Materials and Methods - DNA Ligation with T4 DNA ligase and the ligation reaction was chemically transformed and the clones plated out. Four clones were screened by digestion with a selection of enzymes both within the multicloning site (e.g. *AgeI*) and within the vector backbone (e.g. *PvuI*). Digestions did not

appear to run to completion, however, a significant amount of linearization occurred with the *HpaI* enzyme, which only appeared in the multicloning site, indicating at least one copy of this site had been cloned in. PCR was performed on the clone using primers flanking the multicloning insertion site (Materials and Methods – Primers “MC Site II” and “Avr to MC Site”) and the product sequenced – sequencing revealed a single copy of the multicloning/U6 construct in the correct site. The final pEE12.4-U6 vector is shown in Figure 4.7. 5.

Figure 4.7. 5 – U6 Promoter Vector (pEE12.4-U6)



4.7.6 Summary

With some adjustments to the cloning methods it was possible to produce a U6 promoter-driven vector competent for the introduction of the required shRNA sequences, and this vector was used to clone the shRNA sequences (See Chapter 4.8). This vector may be a useful tool for future shRNA studies. However, due potentially to improper digestion of the vector and to difficulties with PCR and sequencing, it was not possible to produce the CMV promoter-driven vector or to confirm whether it had been produced. What sequence could be gained by directly sequencing the clones gave confusing results, likely due to multiple CMV promoter sequences in the vector. Although it would have been useful to have this vector

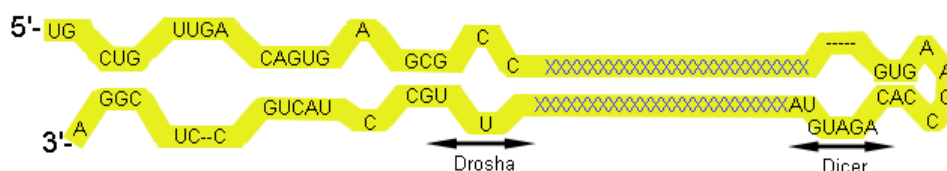
available, as long as one vector existed that could be used, this was sufficient. Had more time been available, diagnostic digests could have been performed to ascertain whether *SacI* and *PvuII* had star activity under these conditions and this was the cause of the extra bands at ~3500 and ~1800 or whether some sort of improper digest had occurred/extra enzyme site was present.

4.8 Production of shRNA against CHO IRE1 α

4.8.1 Rationale

As described in Chapter 4.7, RNAi Delivery of siRNAs into the cell can be performed by inserting a plasmid expressing a short hairpin RNA (shRNA) or a micro-RNA (miRNA) from a plasmid expressing in the cell. micro-RNAs utilise the microRNA pathway, an endogenous pathway to achieve gene silencing. The micro-RNA pathway begins with a primary miRNA transcript which is cleaved by the enzyme Drosha in the nucleus to create an intermediate, which is then transported into the cytoplasm where it is processed by the enzyme Dicer into siRNA sequences and activates the RNA induced silencing complex to silence the complementary gene (Fewell and Schmitt 2006). The mir-30 human miRNA construct has been used to successfully knock down HIV-1 (Boden, Pusch et al. 2004). The mir-30 scaffold is given below (Figure 4.8. 1), showing the hairpin structure of the short hairpin RNA, and the Drosha and Dicer processing sites. In the final construct, the area marked with “X”s is replaced with the passenger complementary (upper section) and siRNA sequence (lower section).

Figure 4.8. 1 – miRNA scaffold – after (Chang, Elledge et al. 2006)



4.8.2 Design of shRNAs against choIRE1 α

In chapter 4.6 of this thesis, the sequencing of CHO IRE1 α was described, and reference was made to the section upstream of the kinase domain which did not possess any significant homology to any other domain when subject to a conserved domain search on NCBI. Given this information, it was logical then to target any shRNAs to this section of the IRE1 α sequence as this low homology to other sequences should also reduce the likelihood of off-target effects of the shRNA. A number of studies exist in which an siRNA knockdown of IRE1 α was performed (Hu, Han et al. 2006; Lipson, Fonseca et al. 2006; Rahmani, Davis et al. 2007; Hollien, Lin et al. 2009; Sha, He et al. 2009; Rahmani, Mayo et al.). Of these, the sequence #4 used in (Sha, He et al. 2009), which resulted in a reduction to <10% of control levels of IRE1 α protein when stably transfected into 3T3-L1 cells was not only targeted against this area, but also had an identical sequence in CHO to the mouse sequence making it suitable as a candidate. Two more new shRNAs were designed by putting the low homology section's sequence into the invitrogen RNAi designer (<http://rnaidesigner.invitrogen.com/rnaiexpress/>) and an eGFP sequence was used as an IRE1 α negative shRNA. Sequences of siRNAs are listed in Table 4.8. 1, along with GC content of sequences as high GC content negatively correlates with shRNA efficiency of knockdown (Chan, Carmack et al. 2009).

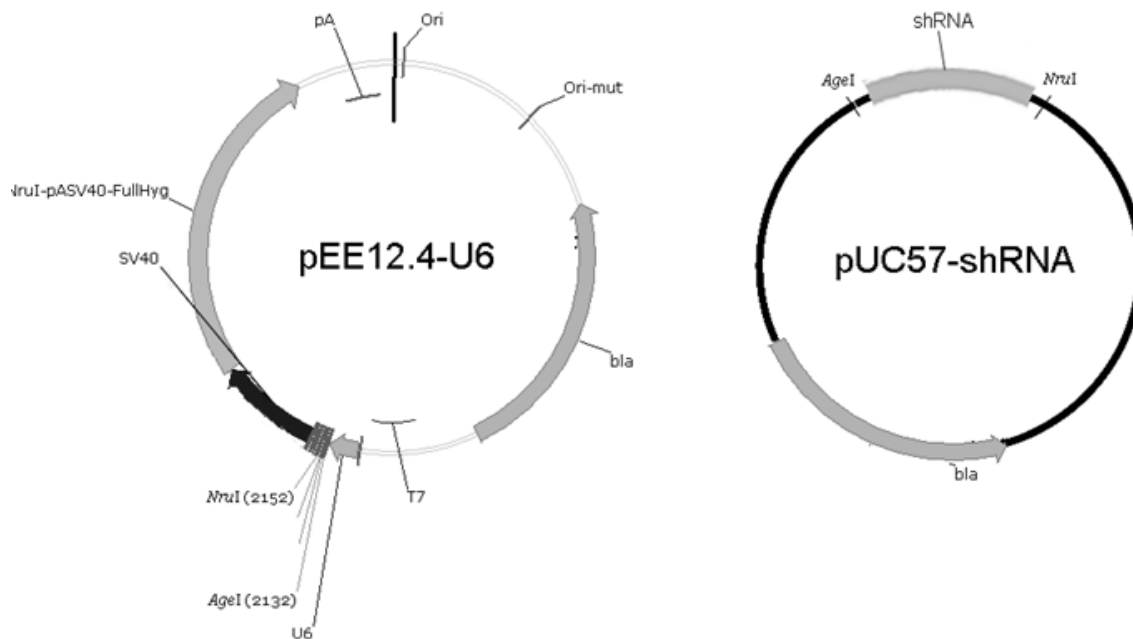
Table 4.8. 1 – Anti-CHO IRE1 α shRNAs

Name	Source	G/C Content	Sequences
U6-IRE1 α (-) ⁴	(Sha, He et al. 2009)	50%	Passenger – 5' GGA AGA GCA AGC TGA ACT AC 3' siRNA - 3' CCT TCT CGT TCG ACT TGA TG 5'
choIRE1 α -sh-01	Designed from cloned sequence	47.62%	Passenger – 5' GCTCAAGGACATGGCTACTAT 3' siRNA - 3' CGAGTTCCTGTACCGATGATA 5'
choIRE1 α -sh-02	Designed from cloned sequence	47.62%	Passenger – 5' GGTGGCCTTCATCATCACTTA 3' siRNA - 3' CCACCGGAAGTAGTAGTGAAT 5'
anti-eGFP	Sigma (Dorset, UK)	50%	Passenger – 5' GCAAGCTGACCCTGAAGTTCAT 3' siRNA - 3' CGTTCGACTGGGACTTCAAGTA 5'

4.8.3 Cloning of shRNAs into U6 Vector

Since it was not possible to clone the CMV driven vector within the time available for this study, the U6 vector constructed in Chapter 4.7 was used as the delivery system for the shRNA sequences. The shRNA sequences designed above, flanked by the restriction enzyme sites *AgeI* and *NruI* present in the multicloning site in the U6 were ordered from Eurogentec's (Eurogentec, Southampton, UK) Custom Genes service in a puc57 vector ready for cloning into the pEE12.4 vector (Figure 4.8. 2).

Figure 4.8. 2 - Cloning of shRNAs into U6 Promoter Vector



4.8.4 Cloning into pEE12.4-U6

The custom gene insert site in the puc57 vector was flanked by two M13 priming sites, which could be used to clone a larger amount of the ~100bp shRNA inserts from the vector. PCR was performed using a proofreading polymerase to reduce the amount of inserted errors, according to the protocol in Materials and Methods – “Polymerase Chain Reaction (PCR) for insert construction” and the products run on a 1% agarose gel and purified. ShRNA inserts were then ligated into the 3827bp backbone from the pEE12.4-U6 vector using T4 ligase according to the protocol in “DNA Ligation with T4 DNA ligase” and chemically transformed. A selection of clones were screened by digestion with *NruI* to ensure proper ligation of the shRNA insert. To confirm, a single clone of each construct that gave a band closest to 4kbp was sent for sequencing using the AvrII to MC Site Primer (Materials and Methods – Primers) as for the pEE12.4-U6 construction. The U6-IRE1 α (-)₄, sh01 and egfp sequences all showed correct integration into the pEE12.4-U6, whereas the clones with the sh02 insert had not been ligated correctly in any of these – all were religated vector. Attempts to retry this cloning were unfortunately unsuccessful within the time allocated for this study and only the

U6-IRE1 α (-)⁴, sh01 and egfp were used in further applications. Clones of these were frozen down and retained for further use.

4.8.5 Transient Transfection of shRNA Sequences into Cell Line 42 (High Producer) to produce cDNA for RT-PCR and qPCR knockdown analysis

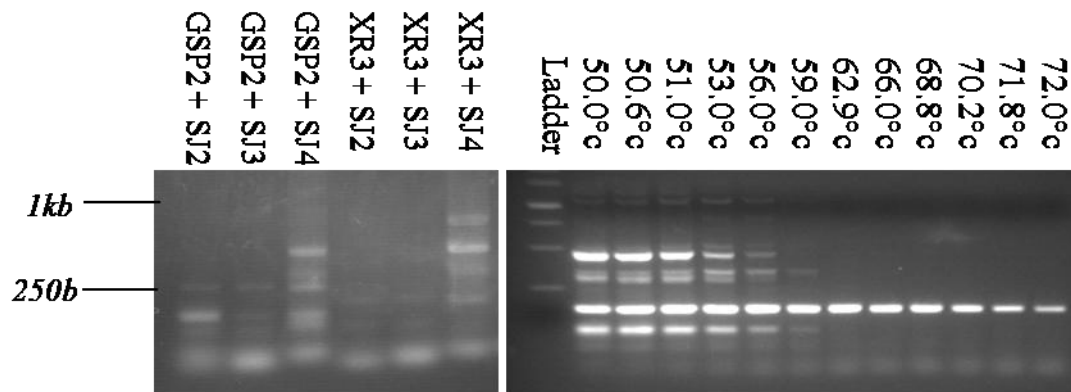
Once the shRNA vectors had been produced they were maxipreped from the retained clones using an endotoxin-free maxiprep kit suitable for mammalian transfection. Several CHOK1 cell lines expressing a range of different yields of monoclonal antibody (see Chapters 4.9 and 4.10) were donated by Lonza and the highest producer of these, Line 42, was selected for this experiment, as it would most likely be the line subjected to the most stress due to high protein throughput. Three 75cm² plates for each vector were grown to 60-80% confluence and 2 μ g of each shRNA vector was transfected into the cells using the Lipofectamine method recommended by Lonza (see Materials and Methods - Transfection – Lipofectamine). Controls were also run – transfection only, 10mM DTT treatment to induce XBP-1 splicing and no transfection. After 24 hours, the cells were harvested and RNA extracted using the EZ RNA kit as with the MEF system. Yields of RNA were 1-2 μ g/ μ l and therefore suitable for use in RT-PCR.

4.8.6 qPCR for XBP-1, Actin

In order to perform qPCR for XBP, it was first necessary to isolate suitable primers for this analysis. The actin primers donated by Lonza had already been used successfully in qPCR by Lonza. The XBP-1 splicing primers used for RT-PCR for CHO XBP-1 were unsuitable for qPCR as they did not give a single product – these primers span the site that is excised by IRE1 α and therefore give two lengths of product to determine spliced vs unspliced XBP-1. Therefore, to gauge the amount of spliced XBP-1, primers were designed against the site formed when the intron is removed and religated, which would therefore only prime against spliced XBP-1. Several primers were ordered and tested with two available primers from the 3' end already used in RT-PCR (Figure 4.8. 3, LH panel) using the protocol as in Materials and Methods – “RT-PCR for CHO XBP-1/Actin using Promega Taq” but with a lower annealing temperature of 52°C. The primer combination of Splice Junction Primer 2 (SJ2 below) and Gene Specific Primer 2 (GSP2 below) was found to give the clearest band at the correct length (~130bp). A temperature optimisation with variable annealing temperatures

was performed (RH panel) and 66°C was chosen as this temperature suffered no reduction in product and no non-specific banding.

Figure 4.8. 3 - Splice junction primer test.



qPCR was performed using the the Qiagen/Corbett Research Rotorgene 3000 qPCR machine as described in Materials and Methods – “qPCR assay for XBP-1/IRE1 α /Actin”. qPCR efficiency of spliced XBP-1 and Actin calculated from controls can be seen in Figure 4.8. 5 and Figure 4.8. 6. Despite multiple repeats a better qPCR efficiency than 0.9 for XBP-1 and 0.83 for Actin could not be achieved.

Figure 4.8. 4 - Actin qPCR Efficiency

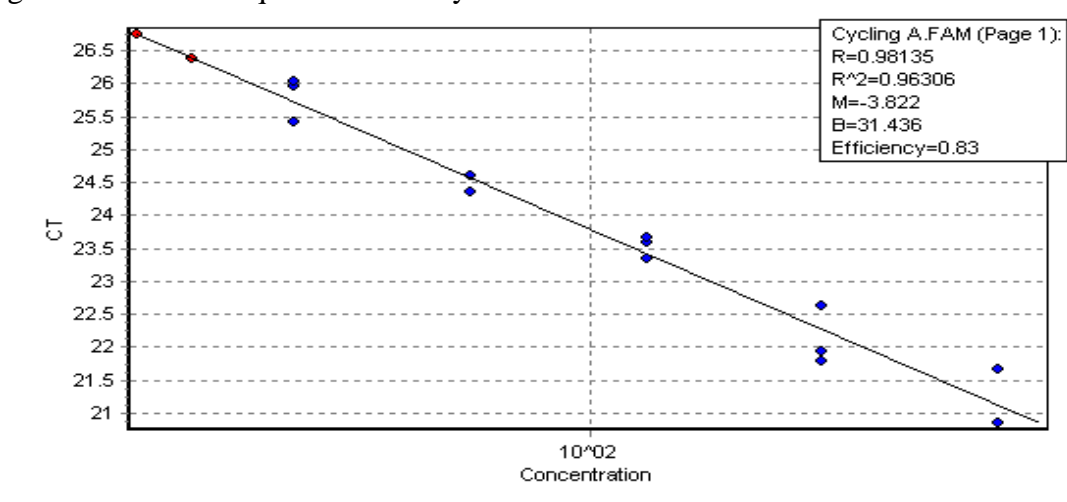
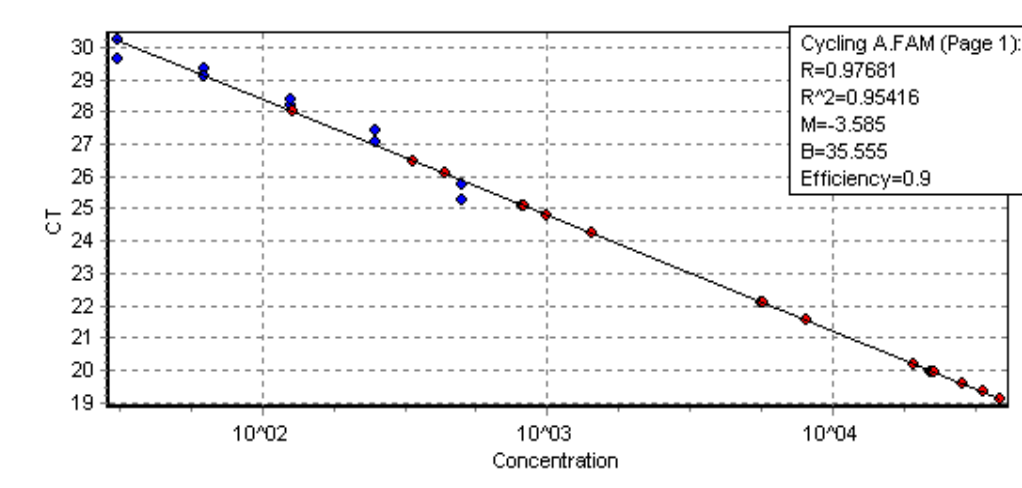


Figure 4.8. 5 – Spliced XBP-1 qPCR Efficiency



Data derived from these analyses can be seen in Figure 4.8. 6 and Table 4.8. 2. The normalisation was done using the Pfaffl method (Equation 1) using actin as the housekeeping gene and normalising to the “no transfection control”. No significant up or downregulation could be seen with the shRNAs, which when taken with the RT-PCR results above indicated that the shRNAs did not produce knockdown.

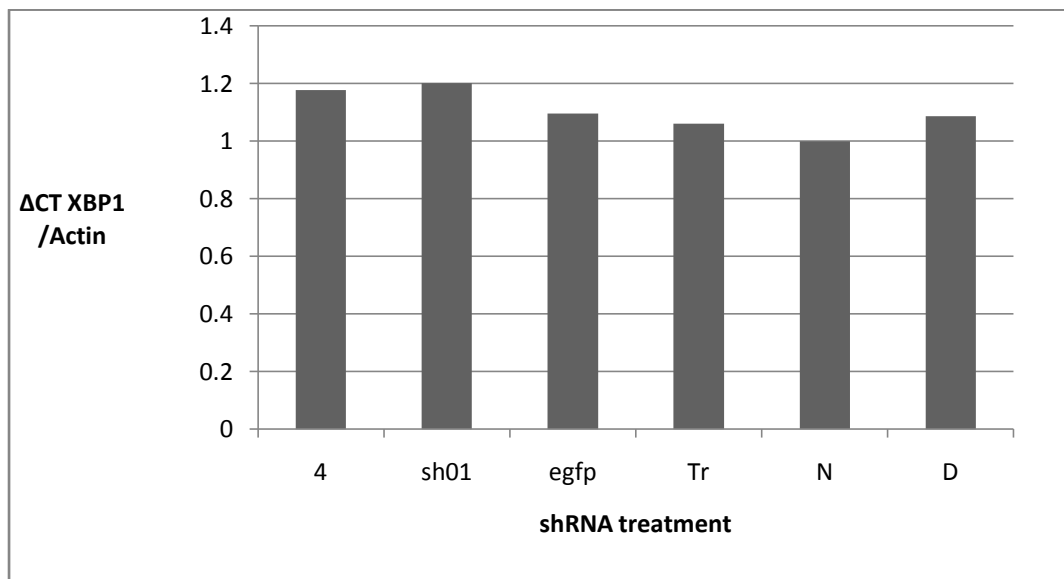
Equation 1 – Pfaffl Method (Pfaffl 2001).

$$\text{ratio} = \frac{(E_{\text{target}})^{\Delta\text{Ct target (control-treated)}}}{(E_{\text{ref}})^{\Delta\text{Ct ref (control-treated)}}$$

Table 4.8. 2 – CT values from qPCR Analysis

<i>shRNA Vector/Treatment</i>	<i>XBP-1</i>	<i>Actin</i>
U6-IRE1 α (-) ⁴	26.57	19.1
choIRE1a-sh-01	21.78	16
anti-eGFP	25.7	17.19
Transfection only	20.19	13.11
No transfection	22.14	13.61
10mM DTT	19.87	13.2

Figure 4.8. 6 - qPCR for IRE1 α knockdown



4.8.7 Summary

Although it was possible to successfully clone the shRNA sequences into the pEE12.4-U6 vector, upon examination by RT-PCR and qPCR, the shRNA vectors did not appear to be producing knockdown. However, it is uncertain whether the samples used were suitable, as there was no increase in XBP-1 splicing with DTT as would have been expected. Were further time available, it would be advisable to repeat the transfection experiment. Given that it was not possible to tell whether the lack of knockdown was due to a non-functional shRNA or due to the shRNA vectors not functioning properly, it would be useful to either test the shRNAs by producing simple siRNA sequences and testing them transiently, or by cloning a known sequence which had produced knockdown previously in CHO cells into the shRNA vector and assessing the level of knockdown when expression was driven by the U6

promoter. RT-PCR primers were ordered which spanned at least one of the sites in IRE1 α (U6-IRE1 α (-4)) as this had already been shown to work in *M. musculus* cells in (Sha, He et al. 2009). However, there was insufficient time to test these primers.

4.9 Characterisation of the UPR and its correlation with mAb Production in CHOK1SV

4.9.1 Rationale

One of the principles of this thesis is that an improved or adjusted function of the unfolded protein response could potentially increase throughput of proteins in the secretory pathway and therefore increase biopharmaceutical yields. This is indicated by the fact that increases in gene copy number, mRNA and intracellular protein concentration do not improve the productivities of individual cells (Schroder 2008) – most improvements in biopharmaceutical production titres have been due to increases in viable cell mass. It is therefore possible that cell lines used for industrial biomanufacture may suffer from chronic or abnormal unfolded protein response activation. To examine the role of the unfolded protein response in cell lines used for industrial biomanufacture, several different cell lines from a panel of stable transformants donated by Lonza producing a range of different titres of the assembled monoclonal antibody cB72.3 were analysed, along with host/null cells expressing no antibody. Actual values of productivity in batch culture were not provided for all cell lines, but were calculated by Lonza according to their industrial criteria.

Table 4.9. 1 - Cell line specific productivities of lines used in this thesis (donated by Lonza)

Cell Line	Productivity in Batch Culture
33	Low
41	Low
137	Medium
159	Medium
42	High

4.9.2 Spliced and unspliced XBP-1 levels are not significantly different between cell lines of differing mAb production capacity

XBP-1 splicing in cB72.3 monoclonal antibody-producing cells was assessed by RT-PCR as in the MEF and CHO shRNA studies. As this assay was being run at the same time as the shRNA studies in Chapter 4.8, initially primers were designed using the sequences from same locus as those used in the MEF system (labelled in Materials and Methods – Primers as “CHO XBP-1 Forward 1” and “CHO XBP-1 Reverse 1”, “CHO Actin Forward”, “CHO Actin Reverse”). CHO cells producing different levels of antibody were grown to stationary phase, as this was when harvesting of product would normally occur, and one flask for each of the cell lines studied was treated by the addition of 10mM DTT (which induces the unfolded protein response by preventing proper formation of disulphide bonds during folding) two hours before harvesting by centrifugation. Harvested cells were prepared for RNA and cDNA produced as described in the materials and methods. RT PCR was performed on the cDNA as in “RT-PCR for CHO XBP-1/Actin using Promega Taq”. Three replicates each of all five available cell lines were subjected to the same growth and DTT treatment as above. All samples from each cell line seemed to have a low level of splicing under non-stressed conditions (Figure 4.9. 1), unlike the MEF system, indicating that none of the cell lines, of any level of production were splicing XBP-1 to maximum capacity, and therefore there was potential for further activation of the unfolded protein response. However, there was no significant difference that could be detected between the levels of splicing in different producers, when the samples were quantified and analysed by ANOVA, indicating potentially a low level of splicing is sufficient for output in these cells (Figure 4.9. 2).

Figure 4.9. 1 - RT-PCR for XBP-1 Splicing in producer cell lines after optimisation.

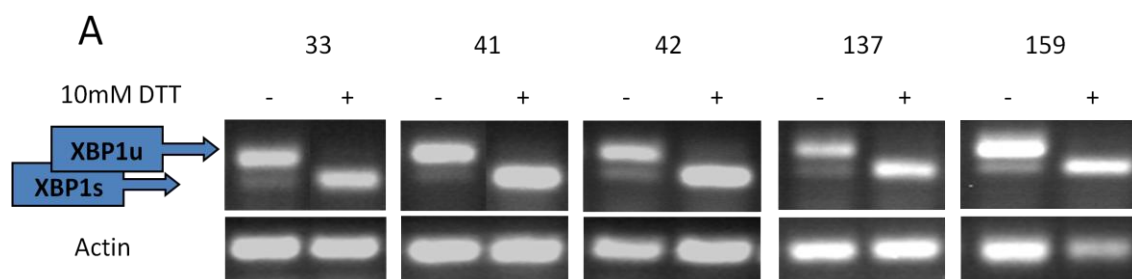
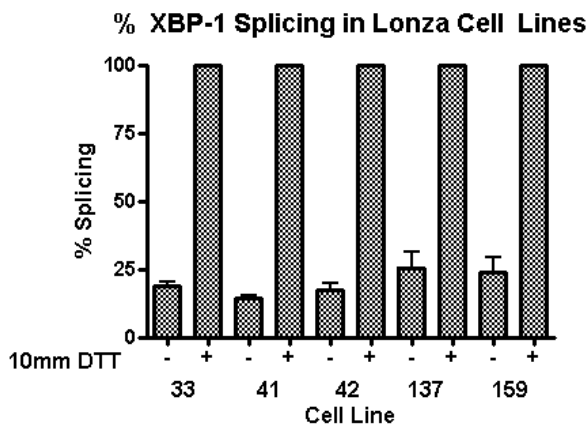


Figure 4.9. 2 - Quantification and statistical analysis of XBP-1 Splicing in producer cell lines after optimization.



No significant differences by one way ANOVA between no DTT treatments. $P > 0.05$

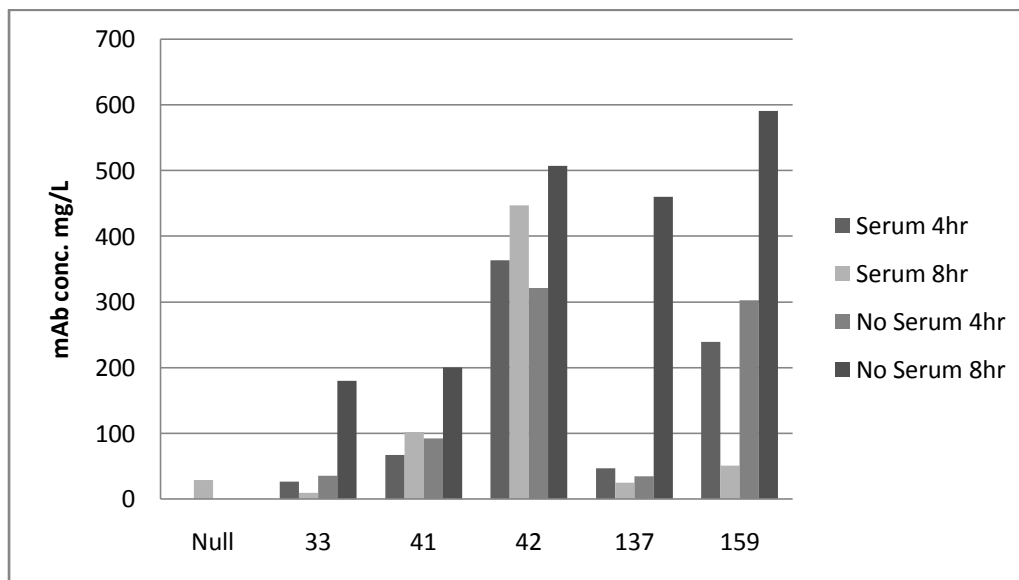
4.9.3 Addition of serum to culture medium alters mAb Production and XBP-1 splicing in different levels of mAb Producer

As examination of the levels of XBP-1 splicing in the different cell lines in a single incidence after treatment with DTT having produced no clear differences, it was determined to investigate differences between cB72.3 mAb output of the varied cell lines in the laboratory conditions, and how this correlated with XBP-1 splicing both in the adherent, serum fed state used in the lab and the serum-starved suspension growth (as required by animal-component free biomanufacture) used at Lonza. cB72.3 analysis required the setup of the Lonza Sandwich ELISA (see Materials and Methods – “Sandwich ELISA for assembled IgG cB72.3” for full details).

A null cell line without the monoclonal antibody was used as a control. Cells were seeded at 0.2×10^6 cells in 2.5mLs of either CD-CHO or Dulbecco’s Modified Eagle’s Medium without pyruvate in 6cm cell culture dishes and grown for 8 days, with one set of cells harvested at 4 days, during growth phase, and one at 8 days (normal harvesting time in batch culture). Cells were collected, and a sample stained 1:2 with trypan blue (Sigma, Dorset) and counted with an Improved Neubauer haemocytometer. Remaining cell samples were centrifuged to collect cells for RNA/RT-PCR and to clarify the medium to analyse for assembled cB72.3 antibody.

Using the samples of medium taken from the Day 4 and Day 8 samples above, the levels of assembled cB72.3 monoclonal antibody were assessed using the Sandwich ELISA for assembled IgG cB72.3 listed in Materials and Methods (Figure 4.9. 3). Cell line 42 seems to have performed consistently, if not necessarily as the highest expressing of the cell lines. The low expressing lines produced consistently low levels. However, the medium expressors exhibited a differing profile, giving higher expression later on rather than consistently.

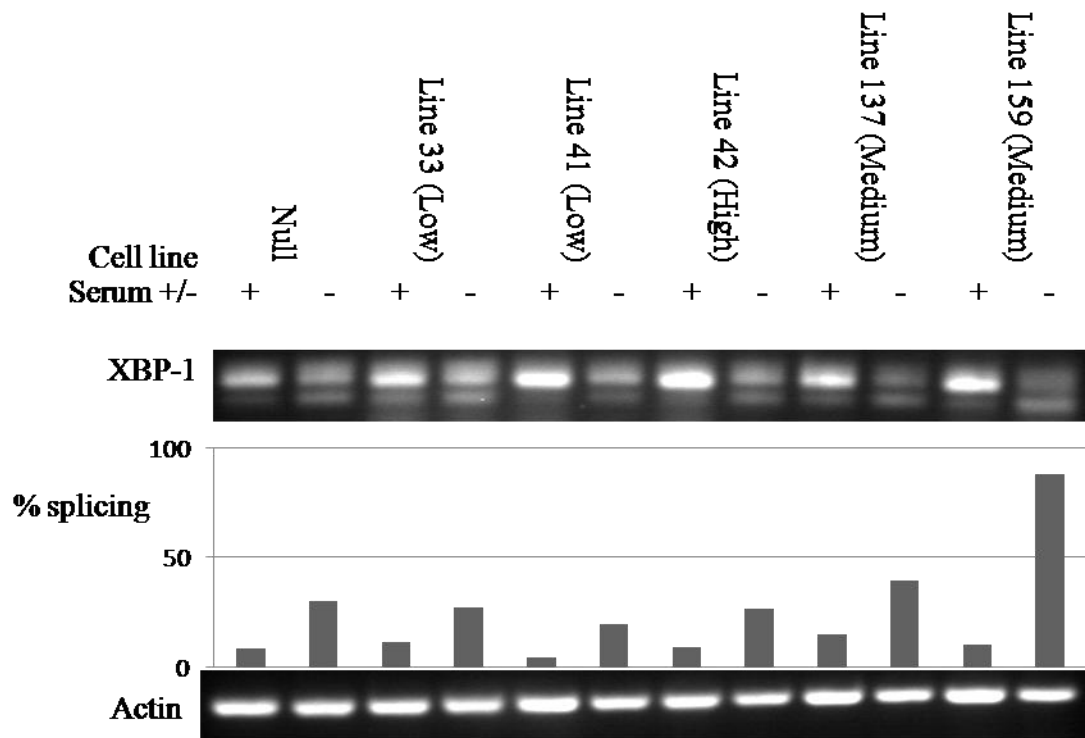
Figure 4.9. 3 - Monoclonal antibody expression during cell viability time course.



Finally, RT-PCR was performed using the protocol listed in the materials and methods “CHO XBP-1 and Actin” to compare Day 4 samples with and without serum (Figure 4.9. 4). A clear difference can be seen between cells grown with serum and without, even in the null cell line indicating that cells grown in serum-starved conditions are undergoing higher levels of ER stress. This is consistent with the idea that nutrient starvation induces ER stress, particularly in nutrient starved tumour cells (Wang, Hua et al. 2008). The null and cell line 42 samples at the earlier Day 4 timepoint appear to show a lower level of XBP-1 splicing in the serum treated samples, and the low producer 33 slightly more, although as shown previously in the single timepoint samples there is no clear difference between the non-serum grown cells, apart from the medium producer cell line 159, which appears to have a slightly stronger spliced band than unspliced. This may indicate that the high producer cell line induced less unfolded protein response than the other cell lines. The stronger splicing in the 159 line correlates with the high production of antibody in the 4hr no serum result. Taken together,

these results may indicate adaptations by producer cell lines in their unfolded protein response that permit them to deal with fluctuations in viability caused by unfolded protein stress and to control XBP-1 splicing in response to unfolded protein stress, although further investigation and repeats would be required to verify this conclusion.

Figure 4.9. 4 - RT-PCR for XBP-1 splicing during cell viability time course.



4.9.4 Summary

Analysing the production characteristics and XBP-1 splicing in several producer cell lines indicates two things – That growth in serum-free medium appears to induce XBP-1 splicing and potentially ER stress, and that there is no clear correlation between productivity and increased XBP-1 splicing. Unfortunately there was insufficient time in this study to perform any further examinations – a full time course correlating product, XBP-1 splicing and viability would have been useful, as would other investigations into the unfolded protein response such as peIF2 α levels. Time could have been saved in these assays by switching to new primers for XBP-1 earlier on in the investigations, as with the shRNA analysis. Furthermore, cell counting by the Neubauer haemocytometer counting method while useful

for transfection was insufficiently accurate to allow correlation of monoclonal antibody output with viable cell density. It would be have been preferable to perform these counts with the ViCell counter used at Lonza, but this was not available during the later work.

4.10 Effect of IRE1 α mutant constructs on viability and productivity in CHOK1SV industrial cell lines.

4.10.1 Rationale

Having examined the correlations between product yield, and XBP-1 splicing, next it was determined to ascertain the effect of the IRE1 α mutants on these parameters in industrial cell lines. Constructs used for transfection were pED Δ c-hIRE1 α with wild type IRE1 α , kinase dead K599A, RNase dead K907A and the D711A and D711A/I642A mutants which had exhibited splicing in transient and stable transfection respectively. These constructs were selected in order to test a range of IRE1 α responses in a normal state, in wild type states and in states predicted to be without kinase or RNase activity (K599A), with only kinase activity (K907A), or with only RNase activity (D711A) and therefore provide information on the effect of each function of IRE1 α on parameters affecting industrial biomanufacture. Although it was not proven possible to knock down CHO IRE1 α during the time allotted to this study, there is evidence that a transfection of mutant IRE1 α is dominant negative over the endogenous (Zhang, Kenski et al. 2005; Lipson, Ghosh et al. 2008) and therefore transient transfection of mutant constructs could give some information as to the effect of the mutants.

4.10.1 Transient Transfection of kinase deficient IRE1 α plasmids reduces viability in CHOK1SIV cells

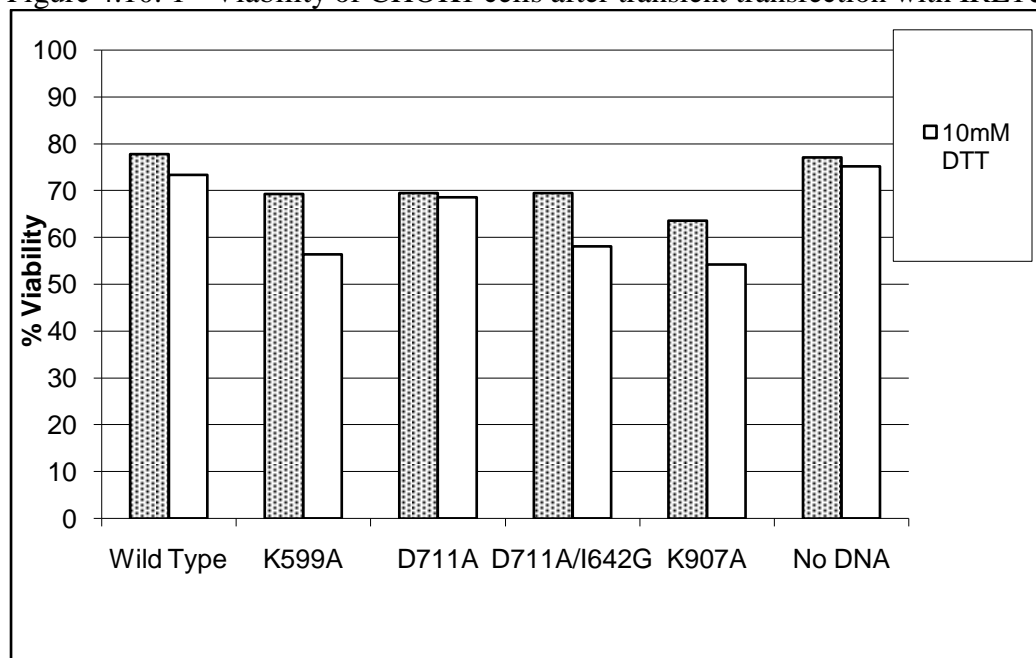
In order to test the usefulness of the mutant constructs in improving protein throughput it was determined to assess the effect of the constructs on the unfolded protein response/XBP-1 splicing, viability and product yield as markers for potential use in improving product throughput. Transfection was performed with IRE1 α plasmids as described in the Materials and Methods – “Transfection – Lipofectamine”. After 24 hours, the cells were harvested and RNA extracted using the RNA easy kit (Promega, Southampton). cDNA was synthesised and RT-PCR performed as described in Materials and Methods. Although RNA was of a reasonable quality and concentration, it was not possible to achieve clear XBP-1 splicing results within the time allocated to this study – an expanded experiment that was attempted using tunicamycin, thapsigargin and DTT yielded even less RNA than the smaller one (data not shown). Given the similar issues in the MEF system that had necessitated the production

of a stable cell line, and the irregular transient IRE1 α expression shown in the Western blot above, it was determined not to investigate the XBP-1 splicing any further in the transient transfection, and proceed directly to producing a stable CHO cell line if possible as it was unlikely that better quality results would be obtained (see later). However, it was possible to quantify the viability of transfectants using the Beckman Coulter Vi-Cell counter available at Lonza, which automates the standard Trypan Blue assay by taking an average of 50 images of stained cells to calculate the average viability. Cell samples from the transfections above were counted with the Vi-Cell counter. Although there is not a great deal of difference between viabilities, it is notable that the mutant transfected samples suffer apparent drops in viability, particularly when stressed with DTT and that the largest reductions are in the K907A mutant, concomitant with the possible dysregulation of IRE1 α expression. This effect is potentially detrimental, and appears to contradict the findings in Chapter 4.5 where the D711A improved viability of the cells. However, it is not clear whether this effect is due to the confounding effects of the wild type endogenous CHO IRE1 α .

Table 4.10. 1 – Viabilities of Mutant Transfected CHOK1SV (by ViCell count)

DNA	10mM DTT	Viability
pED Δ c-hIRE1 α	Y	73.3
	N	77.8
pED Δ c-hIRE1 α -K599A	Y	56.4
	N	69.3
pED Δ c-hIRE1 α -D711A	Y	68.6
	N	69.5
pED Δ c-hIRE1 α -D711A/I642A	Y	58.1
	N	69.5
pED Δ c-hIRE1 α -K907A	Y	54.2
	N	63.6
No transfection	Y	75.2
	N	77.1

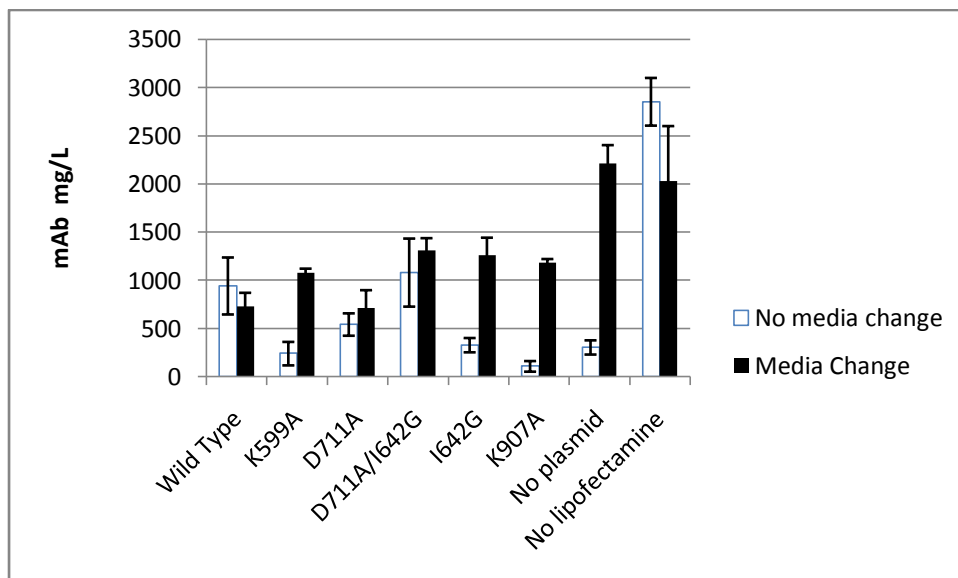
Figure 4.10. 1 - Viability of CHOK1 cells after transient transfection with IRE1 α plasmids



4.10.2 Transient transfection with D711A mutant improves mAb yield in CHOK1SV cells

Having investigated the effect of the mutant constructs on viability, as in the previous section, the effect on product output of the cell lines was next examined. CHOK1SV cells (three replicates for each transfection) were grown for 24 hours before transfection as described in Materials and Methods “Transfection – Lipofectamine”. Medium was harvested after 48 hours and assayed by ELISA for assembled IgG cB72.3. Normally after eight hours Lipofectamine + Optimem medium was replaced with DMEM growth medium for further cell growth, however to do this discarded much of the antibody produced during this time, and therefore samples were taken with and without this replacement of medium. Results can be seen in Figure 4.10. 2. Differences between transfectants and untransfected controls are clearer in those samples which retain their medium from the earliest time points post transfection. As would be expected, the wild type transfection is the same with or without medium change as the wild type is expressing at all time points, whereas it would be expected that there would be less expression of the mutant plasmids over time as the plasmid was rejected by the cells. Without medium replacement, the D711A and D711A/I642G mutants appeared to have similar levels of production to the wild type, whereas the K599A, I642G and K907A had reduced production. However, the no plasmid control also had similar low production, possibly indicating this was not a significant difference despite the statistics.

Figure 4.10. 2 - Monoclonal Antibody Production in High Producer Cell transiently transfected with human IRE1 α mutants – cumulative production vs production with medium change. Error bars represent +/- SEM.



In Figure 4.10. 3, the experiment was repeated with a time course of four hours, eight hours and 48 hours (after medium change) to compare the results from the same biological set of transfections. However, in the pre-medium change samples there is significant difference between the D711A and wild type samples, but none between the K599A and D711A or wild type samples. Results from D711A/I642G, I642G and K907A samples are mainly lower than D711A in the earlier samples before the plasmid would have been removed from the cells. Again, there is less difference after the medium change, and results for no plasmid and no transfection controls indicate that the differences between transfected samples may not be significant. Figure 4.10. 4 shows a Western blot against human IRE1 α . As seen in transient transfection of this mutant in the MEF system and previous CHO transfections (data not shown) K907A expression is greater, potentially due to self-dysregulation of IRE1 α , but generally when compared to GAPDH expression, expression of the IRE1 α constructs is consistent, ruling out the possibility of varied IRE1 α expression being the cause of any differences in product yield.

Figure 4.10. 3 - Monoclonal Antibody Production in High Producer Cell transiently transfected with human IRE1 α mutants at timecourse after transfection.

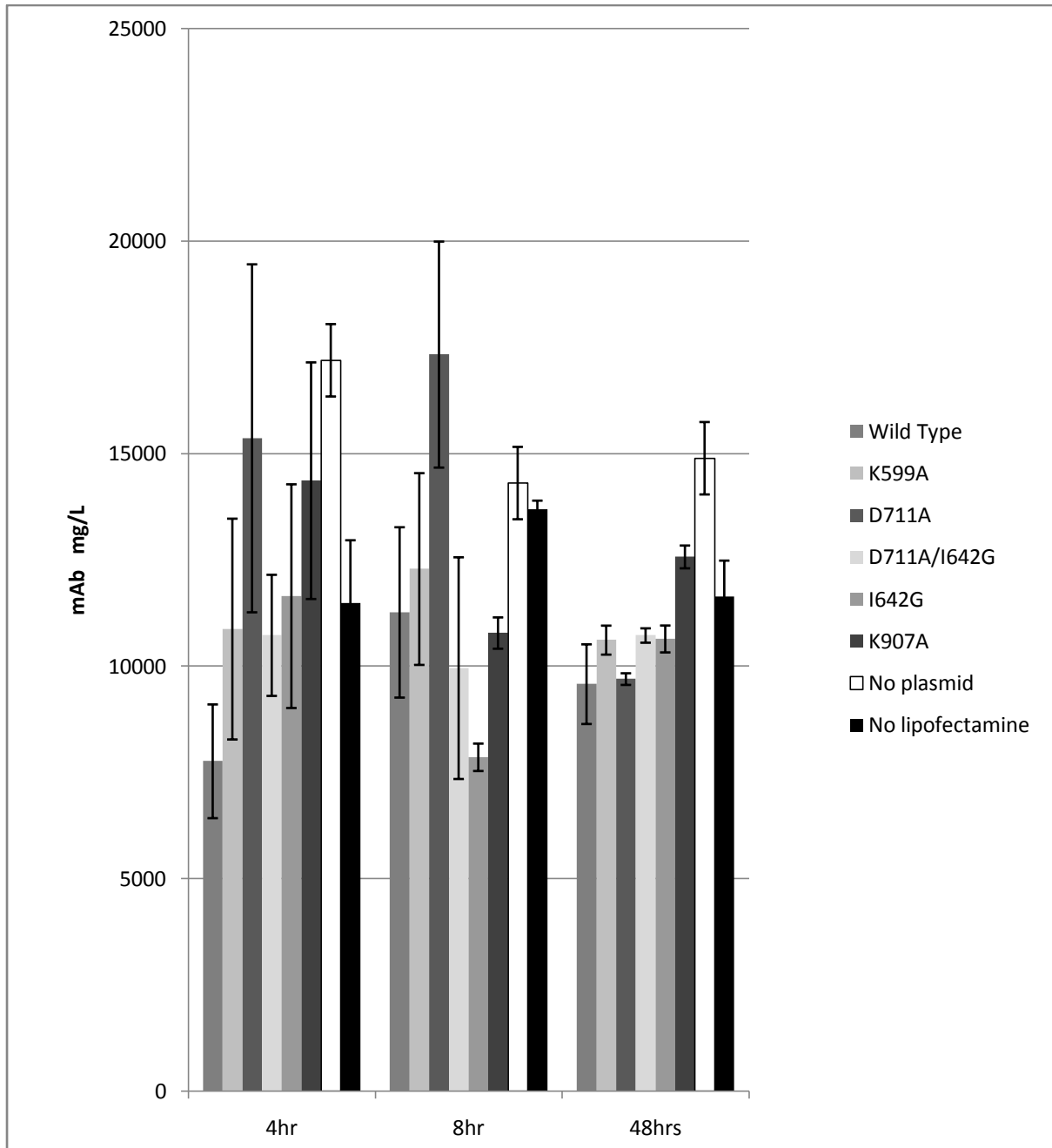
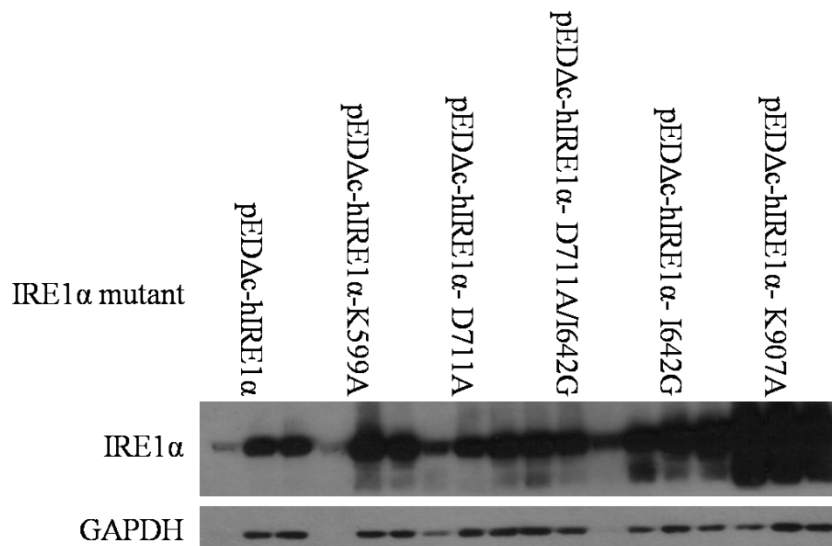


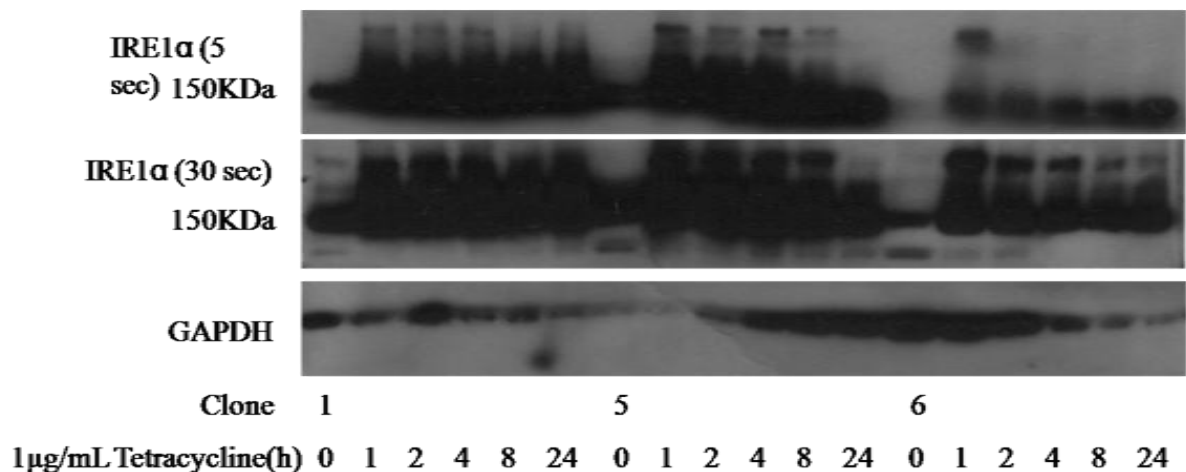
Figure 4.10. 4 – IRE1 α expression after transient transfection. Each marked lane is three biological replicates.



4.10.3 Construction of stable CHO cell line

Given the issues with harvesting enough RNA for XBP-1 splicing analysis in the transient transfections, work was begun on an additional CHO cell line that could be stably transfected with IRE1 α constructs as the MEF line was. Lonza provided an Invitrogen FLP-CHO cell line in which the pFRT/lac/Zeo site was already present, but still required the insertion of the pcDNA6/TR tet repressor plasmid. A blasticidin tolerance curve was performed for the FLP-CHO cells as described in the Materials and Methods – “Antibiotic Tolerance” and “Transfection with pcDNA6/TR”. Three stocks of each of the clones obtained from the transfection were frozen as described above and tested for tet repressor function as in the MEF system in chapter 4.5, using a tet-inducible HA-tagged form of IRE1 α which only dimerised/activated in the presence of the chemical AP20187. 2 μ g of this plasmid was transfected by Lipofectamine methodology into three of the clones produced and the cells harvested for protein, run on an SDS page gel and Western blots performed for the HA tag.

Figure 4.10. 5- Transient transfection of FV2e-IRE1 α to verify presence of tet repressor.



The fastest growing clones 1,5 and 6 all gave strong bands at the appropriate length, which increased in strength upon addition of 1 μ g/mL tetracycline, however induction of Fv2e-IRE1 α was not as clear-cut as in the MEF system most likely because expression was so strong, (even a low exposure resulted in strong bands). Had there been sufficient time, this experiment would have been repeated with a lower strength detection reagent. Unfortunately there was insufficient time to perform the transfection/replacement with pcDNA5-FRT-TO-hIRE1 α plasmids or stable transfection of the plasmid expressing the assembled IgG cB72.3 and examine XBP-1 splicing in CHO cells. However, this cell line may now be used with tet-inducible promoters and will provide a tool for future examination of industrial bioproduction.

4.10.4 Summary

From the results of the above experiments, it would be possible to draw the conclusion that the D711A mutant improves monoclonal antibody output in CHOK1SV cells whilst reducing their viability. However, it is potentially possible that the K599A, D711A and other mutants may simply have dysregulated IRE1 α 's control over protein synthesis (which would be consistent with(Rubio, Pincus et al. 2011)) and this may account for either the extra production or lower production dependent on experiment as protein production either continues uncontrolled or quickly results in the induction of other control mechanisms. From these results it is difficult to ascertain whether, however, given the additional evidence for a

reduction in viability, it is probable that dysregulation of IRE1 α by mutation may cost more in cells lost to apoptosis than would be gained in product output. This is consistent with the necessity in (Becker, Florin et al. 2009) to combine a suppressor of apoptosis with overexpression of spliced XBP-1 to prevent viability loss, which would be a potential strategy if this investigation were to be continued. Once again, transient transfection of IRE1 α plasmids did not yield sufficient quality of RNA for analysis of XBP-1, although curiously there was no difference between the wild type and untransfected viabilities when counted with the Vicell counter, in sharp contrast to the MEF system where the wild type transfection resulted in more cell death – this is likely attributable to the CHO cells still possessing their own endogenous IRE1 α . Work on a stable cell line for CHO cells was begun to overcome the viability issue in a similar manner to the MEF but there was insufficient time to complete it. It was, however, possible to transfect and detect the mutant plasmids in the CHO system and examine their effect on viability and product output.

5. DISCUSSION

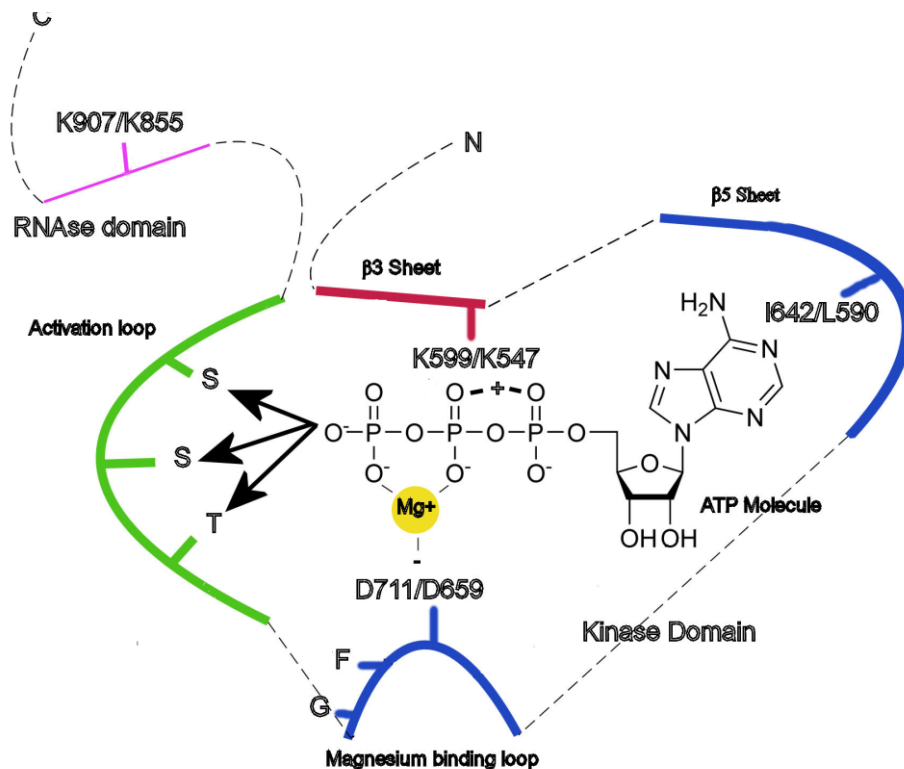
5.1 IRE1 α mechanisms and outputs

Any strategy that can combine both control of apoptosis and improvement in cell-specific productivity is potentially useful for improving overall biopharmaceutical yield, and reducing input and cost of product appropriately – in this thesis it was attempted to use the dual outputs of IRE1 α to produce a strategy that, via engineering of IRE1 α structure, combined the upregulation of biopharmaceutical expression seen with increases in spliced XBP-1 expression with reduction in IRE1 α induced apoptosis. IRE1 α is an ER transmembrane protein with both a serine/threonine kinase domain and an RNase domain (Tirasophon, Welihinda et al. 1998). Activation of IRE1 α in response to unfolded protein induces trans-autophosphorylation (Shamu and Walter 1996). The activated RNase domain removes a 26bp intron from XBP-1 mRNA producing a longer spliced isoform of XBP-1 which functions as a transcription factor to upregulate unfolded protein response genes which help the cell deal with unfolded protein stress (Calton, Zeng et al. 2002). The kinase domain is thought to be responsible for inducing apoptosis by binding to TRAF2. This pathway results in JNK activation by an unknown mechanism and activates the p38 apoptotic signalling cascade to upregulate apoptotic genes (Urano, Bertolotti et al. 2000). Together, these dual functions are thought to control the switch between survival and apoptosis in response to unfolded protein stress (Jager, Bertrand et al. 2012). Although the mechanisms of this switch are not fully understood, it was proven possible, in yeast, to activate the RNase domain without autophosphorylation by mutation of the conserved residue Leu⁷⁴⁵ to alanine or glycine. Normally these mutations would result in a loss of activity, but in the presence of the kinase pocket binding compound 1NM-PP1, function was rescued (Papa, C. et al. 2003). This thesis attempted to elucidate further the role of the kinase and RNase activities in mammalian cells by studying the mutations in the kinase and RNase domains and the effect of these mutations on IRE1 α function and product yield.

In order to fulfil this outcome the following mutants were chosen for investigation:

D711A - Mutation of the aspartic acid in the conserved DFG motif in the activation loop of IRE1 α produces a form of kinase pocket that cannot chelate the magnesium ion for MgATP (Hubbard, Mohammadi et al. 1998). The yeast orthologue of this mutant (D828A) possessed 4% of wild type activity in a reporter assay (Mori, Ma et al. 1993) and is capable of binding

Figure 5. 1 – IRE1 kinase pocket, see Fig 1.8 for original.



nucleotide (Chawla, Chakrabarti et al. 2011). Chawla et al found that this mutant appeared to be capable of activating but incapable of inactivating the unfolded protein response, which impaired survival under Tunicamycin ER stress. This mutant could resemble an active conformation for splicing, altering the alignment of the kinase's activation loop to match or partially match that of a phosphorylated and active IRE1α – functionally a constitutively active form, and was therefore potentially a useful tool for improving protein throughput.

- K599A - Mutation of the lysine residue that aligns the α and β phosphates of ATP in the kinase pocket to alanine – this produces a completely kinase-defective IRE1 α (Tirasophon, Welihinda et al. 1998). This mutant has been used in many studies as a trans-dominant negative control capable of repressing endogenous IRE1 α activity, as it cannot be phosphorylated or activated, and does not splice *XBP-1* mRNA (Tirasophon 2000; Urano, Bertolotti et al. 2000; Lee, Tirasophon et al. 2002; Kaneko, Niinuma et al. 2003; Zhou, Liu et al. 2006; Imagawa, Hosoda et al. 2008; Han, Lerner et al. 2009; Lin, Li et al. 2009; Oikawa, Kimata et al. 2009; Uemura, Oku et al. 2009; Nakamura, Tsuru et al. 2010; Mao, Shao et al. 2011; Kato, Nakajima et al.).

- I642A/G - The analogue sensitized mutant I642A/G confers an enlarged kinase pocket on the IRE1 α protein into which an enlarged ATP analogue such as 1NM-PP1 can fit. In yeast, mutation of L745 to a smaller residue results in a 40% loss of activity in L745A and a 90% loss in L745G. This loss can be rescued by addition of 1NM-PP1. Stable transfection of the I642G mutants into HEK293 cells did not impair IRE1 α function, but did permit induction of XBP-1 splicing by the addition of 1NM-PP1, without ER stress as in the yeast analogue (Lin, Li et al. 2007). No JNK activation was observed with this 1NM-PP1 only induction, indicating activation of the RNase domain only, and these mutants have a defect in autophosphorylation to the same level as the K599A (Han, Lerner et al. 2009). Addition of 1NM-PP1 to I642G expressing cells also enhanced survival (Lin, Li et al. 2009). This mutant represented a pharmacological way of bypassing the kinase function of IRE1 α to potentially improve viability
- K907A - an RNase defective control – this mutant does not splice XBP-1 or exhibit RNase activity (Tirasophon 2000). The IRE1 β form, K855A also exhibited no XBP-1 splicing in HeLa cells (Imagawa, Hosoda et al. 2008).

5.2 Observed effects of IRE1 α mutants

D711A

In our laboratory the D828A mutant was also found to retain HAC1 splicing activity whilst remaining unphosphorylated (Sestak et al, unpublished). In this thesis, in the stable transfection of the *ire1 α ^{-/-}* MEFs the D711A had ~60% of the splicing activity of the wild type and also exhibited the same increase in viability as the K599A (Fig 4, Chapter 4.5). The results in this work agree with the possibility of a D828A/D711A as a constitutively active form – XBP-1 splicing results in Chapter 4.5 show a gradual increase in splicing with induction of the D711A mutant (Fig 2, Chapter 4.5), but do not agree with the viability loss resulting from it (Fig 4, Chapter 4.5). These differences may be accounted for by the mammalian versus yeast systems – other mechanisms such as PERK and ATF6 are available

in the mammalian system to modulate unfolded protein stress and these may adjust the life/death balance in such a way as to either compensate for IRE1 α , or directly alter the active/inactive IRE1 α equilibrium, particularly in cells that have already adapted to a lack of IRE1 α such as the *ire1 α ^{-/-}* MEFs.

K599A

In transient transfections in COS-1 cells, the K599A was found to express at a higher level than the endogenous (Tirasophon, Welihinda et al. 1998) – this did not occur in the stable MEF line created in this study (Figure 4.5. 1, Chapter 4.5). It was found not to induce XBP-1 splicing or to restore it in *ire1 α ^{-/-}* MEFs (Zhou, Liu et al. 2006) – a finding which again was replicated in this thesis in the stable MEF cell line, indicating that at least this lysine residue is required for RNase domain activation. Given the K599A mutant is both kinase-inactive with or without unfolded protein stress (Tirasophon 2000) and RNase-inactive it follows that it should also be incapable of inducing downstream apoptotic effects – this does appear to be the case, as cells stably expressing K599A had lower expression of CHOP and lower ER stress-induced NF κ B activation, although there are conflicting accounts whether K599A mutant IRE1 α does (Urano, Bertolotti et al. 2000) or does not (Kaneko, Niinuma et al. 2003) co-immunoprecipitate with TRAF2 and the requirements for kinase activity to induce this. In Figure 4.5. 4, *ire1 α ^{-/-}* MEFs stably transfected with the K599A mutant exhibited stronger growth early in ER stress induction than the wild-type transfected, and longer lasting viability, as well as a slight reduction in early JNK activation, although in the transient CHO model they suffered the opposite - some loss of viability, which may be an artefact of the difference between endogenous IRE1 α expression in the CHO and stably transfected in the MEF. Interestingly there was also slight upregulation of PARP in this mutant's stable transfection (Figure 4.5. 5) - potentially indicating a response to increased reactive oxygen species from improper protein folding. It was unfortunately not possible within the time allotted to directly confirm kinase activity in the K599A stably transfected cells, although the evidence above indicates a reduction.

I642A/G

In the transient MEF system in this work, low levels of splicing could be seen (0-20%) in cells transiently transfected with these mutants, (Figure 4.3. 2) but possibly due to

the limitations of the transient system, no increase in splicing could be seen with the addition of 1NM-PP1 – had there been sufficient time, this assay would have been repeated with the stably transfected cells.

K907A

In this work in both the transient MEF and transient CHO systems K907A mutants synthesized at much higher levels than the wild type - this could also be seen in Tirasophon (2000) (Tirasophon 2000) and may be due to impairment of IRE1 α self-regulation. K907A in this thesis also resulted in no splicing (Figure 4.3. 2). K907A was capable of phosphorylating K599A, indicating a functional kinase domain. However, in INS-1 cells, interestingly this mutant does not induce apoptosis (Han, Lerner et al. 2009). This is consistent with the idea that XBP-1 splicing has some role in the apoptotic responses as well as the protective as indicated by (Becker, Florin et al. 2009), and that a functional kinase and a functional RNase domain may be required for this response.

Returning to the original aims, it was possible to fulfil the first two – to produce analogue sensitized and kinase mutants in both isoforms of IRE1, however, it was not possible to test both isoforms, only the IRE1 α . Transfection into *ire1*^{-/-} cells was not successful, and instead a stable cell line was produced which allowed assessment of expression, by Western blot and analysis of XBP-1 splicing and JNK activation and additionally analysis of visible cell death by loss of adherence and apoptosis by PARP cleavage. Analysis of kinase activity was not successful in this study, but the data produced from the *XBP-1* splicing activity and the analysis of cell death by the above methods suggested that the D711A mutant was the most suitable for further investigation in industrial cell lines, exhibiting reduced cell death characteristics whilst retaining *XBP-1* splicing.

5.3 Improvements in industrial biopharmaceutical synthesis.

Yield in industrial synthesis of biopharmaceuticals is dependent upon a combination of cell-specific productivity and viable cell density. Mammalian cells are used for industrial biosynthesis because these cells are more likely to produce the correct post-translational modifications which affect the activity and immunogenicity of biopharmaceuticals (Wurm 2004; Jones, Nivitchanyong et al. 2005). Because of the requirements for proper folding,

disulphide bond formation and post-translational modification of protein biopharmaceuticals such as monoclonal antibodies industrial synthesis of biopharmaceuticals is thought to have among its rate-limiting steps exit of the correctly folded polypeptide chain from the ER (Schroder 2008) – the final stages of which are regulated by the unfolded protein response. A number of methods of improving cell-specific biopharmaceutical production have been attempted using unfolded protein response components and chaperones – overexpression of the chaperone Hsp70 improved monoclonal antibody production in NS0 hybridomas (Lasunskaja, Fridlianskaia et al. 2003), and constitutive expression or overexpression of the spliced and active version of the bZip transcription factor XBP-1 in CHO cells improved production of secreted digestive enzymes (Tigges and Fussenegger 2006), and expression of erythropoietin in CHO and NS0 cells (Ku, Ng et al. 2008). While these strategies can be used to improve cell-specific productivity, they can potentially be detrimental to the viable cell density component of biopharmaceutical synthesis, reducing survival over time (Becker, Florin et al. 2008) and necessitating additional control of apoptosis (Becker, Florin et al. 2009). Improvement in biopharmaceutical cell mass can also be achieved by control of apoptosis, for example the use of anti-apoptotic supplements and peptides (Sunstrom, Gay et al. 2000; Zanghi, Renner et al. 2000; Jones, Nivitchanyong et al. 2005), nutrient control (Sanfeliu and Stephanopoulos 1999; deZengotita, Abston et al. 2002; Lengwehasatit and Dickson 2002; Mendonca, Arrozio et al. 2002), anti-apoptotic Bcl family proteins and homologues (Mastrangelo, Hardwick et al. 2000; Jung, Cote et al. 2002; Boya, Roumier et al. 2003; Figueroa, Sauerwald et al. 2003; Arden and Betenbaugh 2004) and caspases (Sauerwald, Betenbaugh et al. 2002; Sauerwald, Oyler et al. 2003).

5.4 Effects of IRE1 α mutants on monoclonal antibody productivity of CHOK1SV cells

The second main aim of this study was to assess the effect of a mutant IRE1 construct produced with increased protective signaling and reduced apoptotic signalling on industrial protein yields. Although it is was not possible to produce a suitable knockdown of endogenous CHO IRE1 α to remove this factor, or stable cell lines similar to those in the MEF system, results from the transient transfection of the D711A mutant into the CHO system agree with the “constitutively active mutant concept” of (Chawla, Chakrabarti et al. 2011) – a small potential increase in output due to an increase in folding capacity from the constitutively active IRE1 α coupled with a viability loss, as in the yeast system. In the CHO

cells transiently transfected with mutants known to be kinase deficient - D711A, K599A, K907A, viability was 5-10% lower than wild type or no DNA control (Figure 4.10. 1), in contrast to the MEF system where the D711A mutant exhibited better survival (chapter 4.5) potentially indicating some sort of detrimental effect on IRE1 α regulation or alteration to the life/death switch. This effect may also be due, as stated above, to the presence of endogenous IRE1 α in the CHO cells as opposed to the *ire1 α ^{-/-}* MEFs.

Overall, based on the data from the stable transfection it can be said that the K599A mutant would be unsuitable for increasing the output or viability in industrial biopharmaceutical manufacture, whereas the D711A mutant's increases in viability in the MEF data and the improvements to monoclonal antibody yields in the CHO system indicate that it is worthy of further investigation both to characterize the effect on the unfolded protein response and to potentially produce an applied improvement in protein throughput and biopharmaceutical output.

5.5 Methodologies

Given differences in viability found between the results in the stable MEF transfections and the transient MEF and CHO transfections, coupled with the potential increase it seems as if either the presence of an endogenous IRE1 α or the transfection itself renders the cell line used vulnerable to ER stress when transiently transfected with a mutant – an adapted stable cell line does not suffer the same issues as can be seen in the MEF system. It would have been preferable then to examine an *ire1 α ^{-/-}* CHO cell line with stably transfected monoclonal antibody product and a D711A mutant, potentially adapted to ER stress from a lack of IRE1 α to the point where the mutant can only improve its growth characteristics, and with a deregulated IRE1 α constitutively activating the unfolded protein response - unfortunately there was insufficient time for this, and it would be difficult to anticipate the extent XBP-1s apparent apoptotic effect would affect it.

The methodologies used for this thesis were of mixed provenance. A great deal of time was expended attempting to optimise the transient system in the MEFs (Chapter 4.2, 4.3) when the viability issues were too severe and it would have been advisable from the outset to begin stable cell line production – this method progressed smoothly and what results were obtainable from it were of generally good quality (Figure 4.5. 1-Figure 4.5. 5). With more time having produced them earlier it might have been possible to characterise all the

mutants and examine the effect of 1NM-PP1 on those with the I642A analogue sensitised mutation. The CHO system suffered less from detriments due to transient transfection but did exhibit some of the flaws – low RNA concentrations, irregular expression of the IRE1 α construct (Chapter 4.10, “*Transient Transfection of kinase deficient IRE1 α plasmids reduces viability in CHOK1SIV cells*“ and also seen in (Tirasophon 2000)) making it difficult to draw conclusions about either the apparently detrimental effects of the mutants on viability or the positive effects, despite their agreeing with the results of other studies that used this arm of the UPR for industrial bio-output improvements (Becker, Florin et al. 2008; Becker, Florin et al. 2009). Production of the shRNA against IRE1 α would have benefited from a multiple methodology strategy to verify why it did not function – transient knockdown with siRNA sequences could have been compared to control shRNAs to verify whether it was the vector design or the siRNA which was not functional (Chapter 4.9).

6. CONTINUATION OF WORK

Most importantly for the continuation of this work, for completion of the results from the MEF system, it would definitely be necessary to produce some clear evidence of the presence or absence of kinase activity in at least the wild type, K599A and D711A mutants . Several strategies could be tried for this: alternative antibodies would be the simplest method. Failing this, radioactive phosphate incorporation could be tried. After this, the testing of the remaining mutants and the effect of 1NM-PP1 on those with analogue sensitization and the effect of this on XBP-1 splicing, viability and phosphorylation could be completed.

In the CHO system as described above, the ideal line for testing of the mutants would be an *ire1 α ^{-/-}* CHO cell line with stably transfected monoclonal antibody product. This would require either a functional knockdown or a knockout, neither of which are currently available and one of which would require animal work. The shRNA vector knockdown with controls for siRNA and vector function would need to be completed as described above.

REFERENCES

- Abcouwer, S. F., C. Schwarz, et al. (1999). "Glutamine deprivation induces the expression of GADD45 and GADD153 primarily by mRNA stabilization." *J Biol Chem* **274**(40): 28645-51.
- Adams, J. A. (2001). "Kinetic and catalytic mechanisms of protein kinases." *Chem Rev* **101**(8): 2271-90.
- Adams, J. M. and S. Cory (2002). "Apoptosomes: engines for caspase activation." *Curr Opin Cell Biol* **14**(6): 715-20.
- Ali, M. M., T. Bagratuni, et al. (2011). "Structure of the Ire1 autophosphorylation complex and implications for the unfolded protein response." *EMBO J* **30**(5): 894-905.
- Allen, N., Cran, DG., Barton, SC., Hettle, S., Reik, W., Surani, MA. (1988). "Transgenes as probes for active chromosomal domains in mouse development." *Nature* **333**: 852 - 855.
- Andersen, D. C. and C. F. Goochee (1994). "The effect of cell-culture conditions on the oligosaccharide structures of secreted glycoproteins." *Curr Opin Biotechnol* **5**(5): 546-9.
- Aragon, T., E. van Anken, et al. (2009). "Messenger RNA targeting to endoplasmic reticulum stress signalling sites." *Nature* **457**(7230): 736-40.
- Arden, N. and M. J. Betenbaugh (2004). "Life and death in mammalian cell culture: strategies for apoptosis inhibition." *Trends Biotechnol* **22**(4): 174-80.
- Ashkenazi, A. (2002). "Targeting death and decoy receptors of the tumour-necrosis factor superfamily." *Nat Rev Cancer* **2**(6): 420-30.
- Bailey, D., C. Barreca, et al. (2007). "Trafficking of the bZIP transmembrane transcription factor CREB-H into alternate pathways of ERAD and stress-regulated intramembrane proteolysis." *Traffic* **8**(12): 1796-814.
- Baker, K. N., M. H. Rendall, et al. (2001). "Metabolic control of recombinant protein N-glycan processing in NS0 and CHO cells." *Biotechnol Bioeng* **73**(3): 188-202.
- Baldi, L., D. L. Hacker, et al. (2007). "Recombinant protein production by large-scale transient gene expression in mammalian cells: state of the art and future perspectives." *Biotechnol Lett* **29**(5): 677-84.
- Barber, G. N., M. Wambach, et al. (1993). "Translational regulation by the interferon-induced double-stranded-RNA-activated 68-kDa protein kinase." *Proc Natl Acad Sci U S A* **90**(10): 4621-5.
- Barr, F. A. (2002). "Inheritance of the endoplasmic reticulum and Golgi apparatus." *Curr Opin Cell Biol* **14**(4): 496-9.
- Bebbington, C. R., G. Renner, et al. (1992). "High-level expression of a recombinant antibody from myeloma cells using a glutamine synthetase gene as an amplifiable selectable marker." *Biotechnology (N Y)* **10**(2): 169-75.
- Becker, E., L. Florin, et al. (2008). "An XBP-1 dependent bottle-neck in production of IgG subtype antibodies in chemically defined serum-free Chinese hamster ovary (CHO) fed-batch processes." *J Biotechnol* **135**(2): 217-23.
- Becker, E., L. Florin, et al. (2009). "Evaluation of a combinatorial cell engineering approach to overcome apoptotic effects in XBP-1(s) expressing cells." *J Biotechnol* **146**(4): 198-206.

- Ben-David, Y., K. Letwin, et al. (1991). "A mammalian protein kinase with potential for serine/threonine and tyrosine phosphorylation is related to cell cycle regulators." *EMBO J* **10**(2): 317-25.
- Bertolotti, A., Wang, X., Novoa, I., Jungreis, R., Schlessinger, K., Cho, JH., West, AB., Ron, D. (2001). "Increased sensitivity to dextran sodium sulfate colitis in IRE1beta-deficient mice." *J Clin Invest*. **107**(5): 585-93.
- Bertolotti, A., Zhang, Y., Hendershot, L. M., Harding, H. P., and Ron, D. (2000). "Dynamic interaction of BiP and ER stress transducers in the unfolded-protein response." *Nat. Cell Biol.* **2**: 326-32.
- Bisbal, C. and R. H. Silverman (2007). "Diverse functions of RNase L and implications in pathology." *Biochimie* **89**(6-7): 789-98.
- Bishop, A. C., J. A. Ubersax, et al. (2000). "A chemical switch for inhibitor-sensitive alleles of any protein kinase." *Nature* **407**(6802): 395-401.
- Blais, J. D., V. Filipenko, et al. (2004). "Activating transcription factor 4 is translationally regulated by hypoxic stress." *Mol Cell Biol* **24**(17): 7469-82.
- Boden, D., O. Pusch, et al. (2004). "Enhanced gene silencing of HIV-1 specific siRNA using microRNA designed hairpins." *Nucleic Acids Res* **32**(3): 1154-8.
- Borth, N., D. Mattanovich, et al. (2005). "Effect of increased expression of protein disulfide isomerase and heavy chain binding protein on antibody secretion in a recombinant CHO cell line." *Biotechnol Prog* **21**(1): 106-11.
- Borys, M. C., D. I. Linzer, et al. (1993). "Culture pH affects expression rates and glycosylation of recombinant mouse placental lactogen proteins by Chinese hamster ovary (CHO) cells." *Biotechnology (N Y)* **11**(6): 720-4.
- Bower, N. I. and I. A. Johnston (2010). "Targeted rapid amplification of cDNA ends (T-RACE)--an improved RACE reaction through degradation of non-target sequences." *Nucleic Acids Res* **38**(21): e194.
- Boya, P., T. Roumier, et al. (2003). "Mitochondrion-targeted apoptosis regulators of viral origin." *Biochem Biophys Res Commun* **304**(3): 575-81.
- Butler, M. (2005). "Animal cell cultures: recent achievements and perspectives in the production of biopharmaceuticals." *Appl Microbiol Biotechnol* **68**(3): 283-91.
- Calfon, M., H. Zeng, et al. (2002). "IRE1 couples endoplasmic reticulum load to secretory capacity by processing the XBP-1 mRNA." *Nature*. **415**(6867): 92-6.
- Carlson, S., T. Fawcett, et al. (1993). "Regulation of the C/EBP-related gene, gadd153, by glucose deprivation." *Mol. Cell. Biol.* **13**(4736-4744.).
- Carrera, A. C., K. Alexandrov, et al. (1993). "The conserved lysine of the catalytic domain of protein kinases is actively involved in the phosphotransfer reaction and not required for anchoring ATP." *Proc Natl Acad Sci U S A* **90**(2): 442-6.
- Casagrande, R., P. Stern, et al. (2000). "Degradation of proteins from the ER of *S. cerevisiae* requires an intact unfolded protein response pathway." *Mol Cell* **5**(4): 729-35.
- Chan, C. Y., C. S. Carmack, et al. (2009). "A structural interpretation of the effect of GC-content on efficiency of RNA interference." *BMC Bioinformatics* **10 Suppl 1**: S33.
- Chandler, J. M., G. M. Cohen, et al. (1998). "Different subcellular distribution of caspase-3 and caspase-7 following Fas-induced apoptosis in mouse liver." *J Biol Chem* **273**(18): 10815-8.
- Chang, K., S. J. Elledge, et al. (2006). "Lessons from Nature: microRNA-based shRNA libraries." *Nat Methods* **3**(9): 707-14.
- Chang, L., S.-H. Chiang, et al. (2004). "Insulin Signaling and the Regulation of Glucose Transport." *Mol Med.* **10**(7-12): 65-71.
- Chawla, A., S. Chakrabarti, et al. (2011). "Attenuation of yeast UPR is essential for survival and is mediated by IRE1 kinase." *J Cell Biol* **193**(1): 41-50.

- Chen, J. J. and I. M. London (1995). "Regulation of protein synthesis by heme-regulated eIF-2 alpha kinase." Trends Biochem Sci **20**(3): 105-8.
- Coller, H. A. and B. S. Coller (1986). "Poisson statistical analysis of repetitive subcloning by the limiting dilution technique as a way of assessing hybridoma monoclonality." Methods Enzymol **121**: 412-7.
- Cox, J. and P. Walter (1996). "A novel mechanism for regulating activity of a transcription factor that controls the unfolded protein response." Cell **87**: 394-404.
- Cox, J. S., R. E. Chapman, et al. (1997). "The unfolded protein response coordinates the production of endoplasmic reticulum protein and endoplasmic reticulum membrane." Mol Biol Cell **8**(9): 1805-14.
- Cox, J. S., C. E. Shamu, et al. (1993). "Transcriptional induction of genes encoding endoplasmic reticulum resident proteins requires a transmembrane protein kinase." Cell **73**(6): 1197-206.
- Credle, J., J. Finer-Moore, et al. (2005). "Inaugural Article: On the mechanism of sensing unfolded protein in the endoplasmic reticulum." Proc. Natl. Acad. Sci. U S A **102**: 18773-84.
- Cullinan, S. B., D. Zhang, et al. (2003). "Nrf2 is a direct PERK substrate and effector of PERK-dependent cell survival." Mol Cell Biol **23**(20): 7198-209.
- de Haro, C., R. Mendez, et al. (1996). "The eIF-2a kinases and the control of protein synthesis." FASEB J. **10**(1378-1388).
- de la Cruz Edmonds, M. C., M. Tellers, et al. (2006). "Development of transfection and high-producer screening protocols for the CHOK1SV cell system." Mol Biotechnol **34**(2): 179-90.
- deZengotita, V. M., L. R. Abston, et al. (2002). "Selected amino acids protect hybridoma and CHO cells from elevated carbon dioxide and osmolality." Biotechnol Bioeng **78**(7): 741-52.
- Dinnis, D. M. and D. C. James (2005). "Engineering mammalian cell factories for improved recombinant monoclonal antibody production: lessons from nature?" Biotechnol Bioeng **91**(2): 180-9.
- Doerks, T., R. R. Copley, et al. (2002). "Systematic identification of novel protein domain families associated with nuclear functions." Genome Res **12**(1): 47-56.
- Dong, B. and R. H. Silverman (1995). "2-5A-dependent RNase molecules dimerize during activation by 2-5A." J Biol Chem **270**(8): 4133-7.
- Dong, B., L. Xu, et al. (1994). "Intrinsic molecular activities of the interferon-induced 2-5A-dependent RNase." J Biol Chem **269**(19): 14153-8.
- Dorner, A. J., M. G. Krane, et al. (1988). "Reduction of endogenous GRP78 levels improves secretion of a heterologous protein in CHO cells." Mol Cell Biol **8**(10): 4063-70.
- Du, Y., M. Pypaert, et al. (2001). "Aux1p/Swa2p is required for cortical endoplasmic reticulum inheritance in *Saccharomyces cerevisiae*." Mol Biol Cell **12**(9): 2614-28.
- Dulbecco, R. and G. Freeman (1959). "Plaque production by the polyoma virus." Virology **8**(3): 396-7.
- Eagle, H. (1959). "Amino acid metabolism in mammalian cell cultures." Science **130**(3373): 432-7.
- Elphick, L., S. Lee, et al. (2007). "Using chemical genetics and ATP analogues to dissect protein kinase function." ACS Chem Biol **2**(5): 299-314.
- Fewell, G. D. and K. Schmitt (2006). "Vector-based RNAi approaches for stable, inducible and genome-wide screens." Drug Discov Today **11**(21-22): 975-82.
- Figuroa, B., Jr., T. M. Sauerwald, et al. (2003). "A comparison of the properties of a Bcl-xL variant to the wild-type anti-apoptosis inhibitor in mammalian cell cultures." Metab Eng **5**(4): 230-45.

- Fike, R., B. Dadey, et al. (2001). "Advanced Granulation Technology (AGT(TM)). An alternate format for serum-free, chemically-defined and protein-free cell culture media." Cytotechnology **36**(1-3): 33-9.
- Fire, A., S. Xu, et al. (1998). "Potent and specific genetic interference by double-stranded RNA in *Caenorhabditis elegans*." Nature **391**(6669): 806-11.
- Floyd-Smith, G., E. Slattery, et al. (1981). "Interferon action: RNA cleavage pattern of a (2'-5')oligoadenylate--dependent endonuclease." Science **212**(4498): 1030-2.
- Follstad, B. D., D. I. Wang, et al. (2002). "Mitochondrial membrane potential selects hybridomas yielding high viability in fed-batch cultures." Biotechnol Prog **18**(1): 1-5.
- Gardner, B. M. and P. Walter (2011). "Unfolded proteins are Ire1-activating ligands that directly induce the unfolded protein response." Science **333**(6051): 1891-4.
- Gasser, C. S., C. C. Simonsen, et al. (1982). "Expression of abbreviated mouse dihydrofolate reductase genes in cultured hamster cells." Proc Natl Acad Sci U S A **79**(21): 6522-6.
- Gibbs, C. S. and M. J. Zoller (1991). "Rational scanning mutagenesis of a protein kinase identifies functional regions involved in catalysis and substrate interactions." J Biol Chem **266**(14): 8923-31.
- Gonzalez, T., C. Sidrauski, et al. (1999). "Mechanism of non-spliceosomal mRNA splicing in the unfolded protein response pathway." EMBO J., **18**(11): 3119-32.
- Goomer, R. S. and G. R. Kunkel (1992). "The transcriptional start site for a human U6 small nuclear RNA gene is dictated by a compound promoter element consisting of the PSE and the TATA box." Nucleic Acids Res **20**(18): 4903-12.
- Gorfien, S., J. Dzimian, et al. (1998). "Recombinant protein production by CHO cells cultured in a chemically defined medium." Animal Cell Technology: Basic and Applied Aspects **9**(247-252).
- Guan, D., H. Wang, et al. (2009). "N-glycosylation of ATF6beta is essential for its proteolytic cleavage and transcriptional repressor function to ATF6alpha." J Cell Biochem **108**(4): 825-31.
- Guerfal, M., S. Ryckaert, et al. (2010). "The HAC1 gene from *Pichia pastoris*: characterization and effect of its overexpression on the production of secreted, surface displayed and membrane proteins." Microb Cell Fact **9**: 49.
- Guo, B., D. Zhai, et al. (2003). "Humanin peptide suppresses apoptosis by interfering with Bax activation." Nature **423**(6938): 456-61.
- Han, D., A. G. Lerner, et al. (2009). "IRE1alpha kinase activation modes control alternate endoribonuclease outputs to determine divergent cell fates." Cell **138**(3): 562-75.
- Han, D., J. P. Upton, et al. (2008). "A kinase inhibitor activates the IRE1alpha RNase to confer cytoprotection against ER stress." Biochem Biophys Res Commun **365**(4): 777-83.
- Hanks, S. K. and T. Hunter (1995). "Protein kinases 6. The eukaryotic protein kinase superfamily: kinase (catalytic) domain structure and classification." FASEB J **9**(8): 576-96.
- Hanks, S. K., A. M. Quinn, et al. (1988). "The protein kinase family: conserved features and deduced phylogeny of the catalytic domains." Science **241**(4861): 42-52.
- Harding, H. P., I. Novoa, et al. (2000). "Regulated translation initiation controls stress-induced gene expression in mammalian cells." Mol Cell **6**(5): 1099-108.
- Harding, H. P., Y. Zhang, et al. (1999). "Protein translation and folding are coupled by an endoplasmic-reticulum-resident kinase." Nature **397**(6716): 271-4.
- Harris, M. H. and C. B. Thompson (2000). "The role of the Bcl-2 family in the regulation of outer mitochondrial membrane permeability." Cell Death Differ **7**(12): 1182-91.

- Hayes, J. D., S. A. Chanas, et al. (2000). "The Nrf2 transcription factor contributes both to the basal expression of glutathione S-transferases in mouse liver and to their induction by the chemopreventive synthetic antioxidants, butylated hydroxyanisole and ethoxyquin." *Biochem Soc Trans* **28**(2): 33-41.
- Haze, K., T. Okada, et al. (2001). "Identification of the G13 (cAMP-response-element-binding protein-related protein) gene product related to activating transcription factor 6 as a transcriptional activator of the mammalian unfolded protein response." *Biochem J* **355**(Pt 1): 19-28.
- Haze, K., H. Yoshida, et al. (1999). "Mammalian transcription factor ATF6 is synthesized as a transmembrane protein and activated by proteolysis in response to endoplasmic reticulum stress." *Mol Biol Cell* **10**(11): 3787-99.
- He, C. H., P. Gong, et al. (2001). "Identification of activating transcription factor 4 (ATF4) as an Nrf2-interacting protein. Implication for heme oxygenase-1 gene regulation." *J Biol Chem* **276**(24): 20858-65.
- Hetz, C., Bernasconi, P., Fisher, J., Lee, AH., Bassik, MC., Antonsson, B., Brandt, GS., Iwakoshi, NN., Schinzel, A., Glimcher, LH. and Korsmeyer, SJ. (2006). "Proapoptotic BAX and BAK modulate the unfolded protein response by a direct interaction with IRE1alpha." *Science* **312**: 572-576.
- Hirosumi, J., G. Tuncman, et al. (2002). "A central role for JNK in obesity and insulin resistance." *Cell* **111**(6): 333-336.
- Hodgson, D. R. and M. Schroder (2011). "Chemical approaches towards unravelling kinase-mediated signalling pathways." *Chem Soc Rev* **40**(3): 1211-23.
- Hollien, J., J. H. Lin, et al. (2009). "Regulated Ire1-dependent decay of messenger RNAs in mammalian cells." *J Cell Biol* **186**(3): 323-31.
- Hollien, J. and J. S. Weissman (2006). "Decay of endoplasmic reticulum-localized mRNAs during the unfolded protein response." *Science* **313**(5783): 104-7.
- Hu, P., Z. Han, et al. (2006). "Autocrine tumor necrosis factor alpha links endoplasmic reticulum stress to the membrane death receptor pathway through IRE1alpha-mediated NF-kappaB activation and down-regulation of TRAF2 expression." *Mol Cell Biol* **26**(8): 3071-84.
- Hubbard, S. R. (1997). "Crystal structure of the activated insulin receptor tyrosine kinase in complex with peptide substrate and ATP analog." *EMBO J* **16**(18): 5572-81.
- Hubbard, S. R., M. Mohammadi, et al. (1998). "Autoregulatory mechanisms in protein-tyrosine kinases." *J Biol Chem* **273**(20): 11987-90.
- Hubbard, S. R., L. Wei, et al. (1994). "Crystal structure of the tyrosine kinase domain of the human insulin receptor." *Nature* **372**(6508): 746-54.
- Huse, M. and J. Kuriyan (2002). "The conformational plasticity of protein kinases." *Cell* **110**(3): 275-82.
- Imagawa, Y., A. Hosoda, et al. (2008). "RNase domains determine the functional difference between IRE1a and IRE1b." *FEBS Lett* **582**(5): 656-60.
- Iqbal, J., K. Dai, et al. (2008). "IRE1beta inhibits chylomicron production by selectively degrading MTP mRNA." *Cell Metab* **7**(5): 445-55.
- Iwakoshi, N. N., A. H. Lee, et al. (2003). "The X-box binding protein-1 transcription factor is required for plasma cell differentiation and the unfolded protein response." *Immunol Rev* **194**: 29-38.
- Iwawaki, T., A. Hosoda, et al. (2001). "Translational control by the ER transmembrane kinase/ribonuclease IRE1 under ER stress." *Nature Cell Biology* **3**: 158 - 164.
- Jager, R., M. J. Bertrand, et al. (2012). "The unfolded protein response at the crossroads of cellular life and death during ER stress." *Biol Cell*.

- Jenkins, N., R. B. Parekh, et al. (1996). "Getting the glycosylation right: implications for the biotechnology industry." Nat Biotechnol **14**(8): 975-81.
- Jones, J., T. Nivitchanyong, et al. (2005). "Optimization of tetracycline-responsive recombinant protein production and effect on cell growth and ER stress in mammalian cells." Biotechnol Bioeng **91**(6): 722-32.
- Jung, D., S. Cote, et al. (2002). "Inducible expression of Bcl-XL restricts apoptosis resistance to the antibody secretion phase in hybridoma cultures." Biotechnol Bioeng **79**(2): 180-7.
- Kaneko, M., Y. Niinuma, et al. (2003). "Activation signal of nuclear factor-kappa B in response to endoplasmic reticulum stress is transduced via IRE1 and tumor necrosis factor receptor-associated factor 2." Biol Pharm Bull **26**(7): 931-5.
- Kato, H., S. Nakajima, et al. (2012). "mTORC1 serves ER stress-triggered apoptosis via selective activation of the IRE1-JNK pathway." Cell Death Differ **19**(2): 310-20.
- Kaufman, R., M. Davies, et al. (1991). "Improved vectors for stable expression of foreign genes in mammalian cells by use of the untranslated leader sequence from EMC virus." Nucleic Acids Research, **19**(16): 4485-4490.
- Kaufman, R. J. (2002). "Orchestrating the unfolded protein response in health and disease." J Clin Invest **110**(10): 1389-98.
- Kim, J. A., K. Cho, et al. (2008). "A novel electroporation method using a capillary and wire-type electrode." Biosens Bioelectron **23**(9): 1353-60.
- Kim, J. M., J. S. Kim, et al. (2004). "Improved recombinant gene expression in CHO cells using matrix attachment regions." J Biotechnol **107**(2): 95-105.
- Kimata, Y., Y. Ishiwata-Kimata, et al. (2007). "Two regulatory steps of ER-stress sensor Ire1 involving its cluster formation and interaction with unfolded proteins." J Cell Biol, **179**(1): 75-86. .
- Kimata, Y., D. Oikawa, et al. (2004). "A role for BiP as an adjustor for the endoplasmic reticulum stress-sensing protein Ire1." J Cell Biol **167**(3): 445-56.
- Kimball, S. R. (1999). "Eukaryotic initiation factor eIF2." Int J Biochem Cell Biol **31**(1): 25-9.
- Kincaid, M. M. and A. Cooper (2007). "ERADicate ER Stress or Die Trying." Antioxidants & Redox Signaling, **9**(12): 2373-2387.
- Kohno, K. (2010). "Stress-sensing mechanisms in the unfolded protein response: similarities and differences between yeast and mammals." J Biochem **147**(1): 27-33.
- Kohno, K., K. Normington, et al. (1993). "The promoter region of the yeast KAR2 (BiP) gene contains a regulatory domain that responds to the presence of unfolded proteins in the endoplasmic reticulum." Mol Cell Biol **13**(2): 877-90.
- Kojima, E., A. Takeuchi, et al. (2003). "The function of GADD34 is a recovery from a shutoff of protein synthesis induced by ER stress: elucidation by GADD34-deficient mice." FASEB J **17**(11): 1573-5.
- Kokame, K., H. Kato, et al. (2001). "Identification of ERSE-II, a new cis-acting element responsible for the ATF6-dependent mammalian unfolded protein response." J Biol Chem **276**(12): 9199-205.
- Koning, A. J., L. L. Larson, et al. (2002). "Mutations that affect vacuole biogenesis inhibit proliferation of the endoplasmic reticulum in *Saccharomyces cerevisiae*." Genetics **160**(4): 1335-52.
- Korenykh, A., P. Egea, et al. (2009). "The unfolded protein response signals through high-order assembly of Ire1." Nature Cell Biology **457**: 687-693.
- Koumenis, C., C. Naczki, et al. (2002). "Regulation of protein synthesis by hypoxia via activation of the endoplasmic reticulum kinase PERK and phosphorylation of the translation initiation factor eIF2alpha." Mol Cell Biol **22**(21): 7405-16.

- Kozutsumi, Y., M. Segal, et al. (1988). "The presence of malfolded proteins in the endoplasmic reticulum signals the induction of glucose-regulated proteins." Nature **332**(6163): 462-4.
- Ku, S., D. Ng, et al. (2008). " Effects of overexpression of X-box binding protein 1 on recombinant protein production in Chinese hamster ovary and NS0 myeloma cells." Biotechnol Bioeng. **99**(1): 155-64.
- Lasunskaja, E., I. Fridlianskaia, et al. (2003). "Transfection of NS0 myeloma fusion partner cells with HSP70 gene results in higher hybridoma yield by improving cellular resistance to apoptosis." Biotechnol Bioeng **81**(4): 496-504.
- Lee, A.-H., N. Iwakoshi, et al. (2003). "XBP-1 regulates a subset of endoplasmic reticulum resident chaperone genes in the unfolded protein response." Molecular and Cellular Biology, **23**(21): 7448-7459.
- Lee, A. H., E. F. Scapa, et al. (2008). "Regulation of hepatic lipogenesis by the transcription factor XBP1." Science **320**(5882): 1492-6.
- Lee, K., Dey. M., Neculai D, Cao C, Dever TE, Sicheri F., (2008). "Structure of the Dual Enzyme Ire1 Reveals the Basis for Catalysis and Regulation in Nonconventional RNA Splicing ." Cell **132**(1): 89-100.
- Lee, K., W. Tirasophon, et al. (2002). "IRE1-mediated unconventional mRNA splicing and S2P-mediated ATF6 cleavage merge to regulate XBP1 in signaling the unfolded protein response." Genes Dev, **16**(4): 452-66.
- Lefkovits, I. (1979). Limiting dilution analysis. Immunological Methods. I. Lefkovits and B. Pernis. New York,, Academic Press. **1**: pp. 355-370.
- Lei, K. and R. J. Davis (2003). "JNK phosphorylation of Bim-related members of the Bcl2 family induces Bax-dependent apoptosis." Proc Natl Acad Sci U S A **100**(5): 2432-7.
- Lengwehasatit, I. and A. J. Dickson (2002). "Analysis of the role of GADD153 in the control of apoptosis in NS0 myeloma cells." Biotechnol Bioeng **80**(7): 719-30.
- Li, F. and R. I. Mahato (2009). "Bipartite vectors for co-expression of a growth factor cDNA and short hairpin RNA against an apoptotic gene." J Gene Med **11**(9): 764-71.
- Li, H., A. V. Korennykh, et al. (2010). "Mammalian endoplasmic reticulum stress sensor IRE1 signals by dynamic clustering." Proc Natl Acad Sci U S A **107**(37): 16113-8.
- Li, M., P. Baumeister, et al. (2000). "ATF6 as a transcription activator of the endoplasmic reticulum stress element: thapsigargin stress-induced changes and synergistic interactions with NF-Y and YY1." Mol Cell Biol **20**(14): 5096-106.
- Lin, J., H. Li, et al. (2007). "IRE1 Signaling Affects Cell Fate During the Unfolded Protein Response." Science **318**: 944-9.
- Lin, J. H., H. Li, et al. (2009). "Divergent effects of PERK and IRE1 signaling on cell viability." PLoS One **4**(1): e4170.
- Lin, X., J. Yang, et al. (2004). "Development of a tightly regulated U6 promoter for shRNA expression." FEBS Lett **577**(3): 376-80.
- Liou, H., M. Boothby, et al. (1990). "A new member of the leucine zipper class of proteins that binds to the HLA DR alpha promoter." Science **247**(4950): 1581-4.
- Lipson, K. L., S. G. Fonseca, et al. (2006). "Regulation of insulin biosynthesis in pancreatic beta cells by an endoplasmic reticulum-resident protein kinase IRE1." Cell Metab **4**(3): 245-54.
- Lipson, K. L., R. Ghosh, et al. (2008). "The role of IRE1alpha in the degradation of insulin mRNA in pancreatic beta-cells." PLoS One **3**(2): e1648.
- Lisbona, F., D. Rojas-Rivera, et al. (2009). "BAX inhibitor-1 is a negative regulator of the ER stress sensor IRE1alpha." Mol Cell **33**(6): 679-91.

- Liu, C. Y., M. Schroder, et al. (2000). "Ligand-independent dimerization activates the stress response kinases IRE1 and PERK in the lumen of the endoplasmic reticulum." J Biol Chem **275**(32): 24881-5.
- Liu, M., Y. Li, et al. (2005). "Proinsulin disulfide maturation and misfolding in the endoplasmic reticulum." J Biol Chem **280**(14): 13209-12.
- Maiuolo, J., S. Bulotta, et al. (2011). "Selective activation of the transcription factor ATF6 mediates endoplasmic reticulum proliferation triggered by a membrane protein." Proc Natl Acad Sci U S A **108**(19): 7832-7.
- Mao, T., M. Shao, et al. (2011). "PKA phosphorylation couples hepatic inositol-requiring enzyme 1{alpha} to glucagon signaling in glucose metabolism." Proc Natl Acad Sci U S A **108**(38): 15852-7.
- Mastrangelo, A. J. and M. J. Betenbaugh (1998). "Overcoming apoptosis: new methods for improving protein-expression systems." Trends Biotechnol **16**(2): 88-95.
- Mastrangelo, A. J., J. M. Hardwick, et al. (2000). "Part I. Bcl-2 and Bcl-x(L) limit apoptosis upon infection with alphavirus vectors." Biotechnol Bioeng **67**(5): 544-54.
- Meissner, P., H. Pick, et al. (2001). "Transient gene expression: recombinant protein production with suspension-adapted HEK293-EBNA cells." Biotechnol Bioeng **75**(2): 197-203.
- Mellman, I. and G. Warren (2000). "The Road Taken: Past and Future Foundations of Membrane Traffic." Cell **100**(1): 99-112.
- Mendonca, R. Z., S. J. Arrozio, et al. (2002). "Metabolic active-high density VERO cell cultures on microcarriers following apoptosis prevention by galactose/glutamine feeding." J Biotechnol **97**(1): 13-22.
- Menzel, R., F. Vogel, et al. (1997). "Inducible membranes in yeast: relation to the unfolded-protein-response pathway." Yeast **13**(13): 1211-29.
- Mohammadi, M., G. McMahon, et al. (1997). "Structures of the tyrosine kinase domain of fibroblast growth factor receptor in complex with inhibitors." Science **276**(5314): 955-60.
- Mori, K. (2000). "Tripartite Management of Unfolded Proteins in the Endoplasmic Reticulum." Cell **101**(5): 451-454.
- Mori, K., T. Kawahara, et al. (1996). "Signalling from endoplasmic reticulum to nucleus: transcription factor with a basic-leucine zipper motif is required for the unfolded protein-response pathway." Genes Cells **1**(9): 803-17.
- Mori, K., W. Ma, et al. (1993). "A transmembrane protein with a cdc2+/CDC28-related kinase activity is required for signaling from the ER to the nucleus." Cell. **74**(4): 743-56.
- Mori, K., A. Sant, et al. (1992). "A 22-bp cis-acting element is necessary and sufficient for the induction of the yeast KAR2 (BiP) gene by unfolded proteins." EMBO J., **11**: 2583-2593.
- Morton, H. J. (1970). "A survey of commercially available tissue culture media." In Vitro **6**(2): 89-108.
- Nakamura, D., A. Tsuru, et al. (2010). "Mammalian ER stress sensor IRE1beta specifically down-regulates the synthesis of secretory pathway proteins." FEBS Lett **585**(1): 133-8.
- Nakamura, S., S. Watanabe, et al. (2008). "Cre-loxP system as a versatile tool for conferring increased levels of tissue-specific gene expression from a weak promoter." Mol Reprod Dev. **75**(6): 1085-93.
- Nikawa, J. and S. Yamashita (1992). "IRE1 encodes a putative protein kinase containing a membrane-spanning domain and is required for inositol phototrophy in *Saccharomyces cerevisiae*." Mol Microbiol **6**(11): 1441-6.

- Nolen, B., S. Taylor, et al. (2004). "Regulation of Protein Kinases: Review Controlling Activity through Activation Segment Conformation." *Molecular Cell* **15**: 661-75.
- Ogata, M., S. Hino, et al. (2006). "Autophagy is activated for cell survival after endoplasmic reticulum stress." *Mol Cell Biol* **26**(24): 9220-31.
- Oikawa, D., Y. Kimata, et al. (2009). "Activation of mammalian IRE1alpha upon ER stress depends on dissociation of BiP rather than on direct interaction with unfolded proteins." *Exp Cell Res* **315**(15): 2496-504.
- Oikawa, D., Y. Kimata, et al. (2005). "An essential dimer-forming subregion of the endoplasmic reticulum stress sensor Ire1." *Biochem J* **391**(Pt 1): 135-42.
- Oikawa, D., M. Tokuda, et al. (2007). "Site-specific cleavage of CD59 mRNA by endoplasmic reticulum-localized ribonuclease, IRE1." *Biochem Biophys Res Commun* **360**(1): 122-7.
- Okamura, K., Y. Kimata, et al. (2000). "Dissociation of Kar2p/BiP from an ER sensory molecule, Ire1p, triggers the unfolded protein response in yeast." *Biochem Biophys Res Commun* **279**(2): 445-50.
- Oliver, F. J., G. de la Rubia, et al. (1998). "Importance of poly(ADP-ribose) polymerase and its cleavage in apoptosis. Lesson from an uncleavable mutant." *J Biol Chem* **273**(50): 33533-9.
- Oyadomari, S., A. Koizumi, et al. (2002). "Targeted disruption of the Chop gene delays endoplasmic reticulum stress-mediated diabetes." *J Clin Invest* **109**(4): 525-32.
- Ozcan, U., Q. Cao, et al. (2004). "Endoplasmic Reticulum Stress Links Obesity, Insulin Action, and Type 2 Diabetes." *Science* **306**(5695): 457 - 461.
- Papa, F. R., Z. C., et al. (2003). "Bypassing a kinase activity with an ATP-competitive drug." *Science* **302**: 1533-1537.
- Pincus, D., M. W. Chevalier, et al. (2010). "BiP binding to the ER-stress sensor Ire1 tunes the homeostatic behavior of the unfolded protein response." *PLoS Biol* **8**(7): e1000415.
- Porter, A. J., A. J. Racher, et al. (2010). "Strategies for selecting recombinant CHO cell lines for cGMP manufacturing: improving the efficiency of cell line generation." *Biotechnol Prog* **26**(5): 1455-64.
- Rahmani, M., E. M. Davis, et al. (2007). "The kinase inhibitor sorafenib induces cell death through a process involving induction of endoplasmic reticulum stress." *Mol Cell Biol* **27**(15): 5499-513.
- Rahmani, M., M. Mayo, et al. (2010). "Melanoma differentiation associated gene-7/interleukin-24 potently induces apoptosis in human myeloid leukemia cells through a process regulated by endoplasmic reticulum stress." *Mol Pharmacol* **78**(6): 1096-104.
- Robinson, M. J., P. C. Harkins, et al. (1996). "Mutation of position 52 in ERK2 creates a nonproductive binding mode for adenosine 5'-triphosphate." *Biochemistry* **35**(18): 5641-6.
- Ron, D. and P. Walter (2007). "Signal integration in the endoplasmic reticulum unfolded protein response." *Nat Rev Mol Cell Biol* **8**(7): 519-29.
- Rossomando, A. J., J. Wu, et al. (1992). "Identification of Tyr-185 as the site of tyrosine autophosphorylation of recombinant mitogen-activated protein kinase p42mapk." *Proc Natl Acad Sci U S A* **89**(13): 5779-83.
- Roy, B. and A. S. Lee (1995). "Transduction of calcium stress through interaction of the human transcription factor CBF with the proximal CCAAT regulatory element of the grp78/BiP promoter." *Mol Cell Biol* **15**(4): 2263-74.
- Roy, B., W. W. Li, et al. (1996). "Calcium-sensitive transcriptional activation of the proximal CCAAT regulatory element of the grp78/BiP promoter by the human nuclear factor CBF/NF-Y." *J Biol Chem* **271**(46): 28995-9002.

- Rubin, G. M., M. D. Yandell, et al. (2000). "Comparative genomics of the eukaryotes." Science **287**(5461): 2204-15.
- Rubio, C., D. Pincus, et al. (2011). "Homeostatic adaptation to endoplasmic reticulum stress depends on Ire1 kinase activity." J Cell Biol **193**(1): 171-84.
- Rubio, T. and J. Terefe (2008). High Efficiency Electroporation Buffer. W. I. P. Organization. USA.
- Ruegsegger, U., J. H. Leber, et al. (2001). "Block of HAC1 mRNA translation by long-range base pairing is released by cytoplasmic splicing upon induction of the unfolded protein response." Cell **107**(1): 103-14.
- Rutkowski, D. T. and R. J. Kaufman (2004). "A trip to the ER: coping with stress." Trends Cell Biol **14**(1): 20-8.
- Sakai, J., E. A. Duncan, et al. (1996). "Sterol-regulated release of SREBP-2 from cell membranes requires two sequential cleavages, one within a transmembrane segment." Cell **85**(7): 1037-46.
- Saloheimo, M., M. Valkonen, et al. (2003). "Activation mechanisms of the HAC1-mediated unfolded protein response in filamentous fungi." Mol Microbiol **47**(4): 1149-61.
- Sambrook, J., E. F. Fritsch, et al. (1989). Molecular cloning : a laboratory manual. Cold Spring Harbor, N.Y., Cold Spring Harbor Laboratory.
- Sanfeliu, A. and G. Stephanopoulos (1999). "Effect of glutamine limitation on the death of attached Chinese hamster ovary cells." Biotechnol Bioeng **64**(1): 46-53.
- Sato, M., K. Sato, et al. (2002). "Evidence for the intimate relationship between vesicle budding from the ER and the unfolded protein response." Biochem Biophys Res Commun **296**(3): 560-7.
- Sauerwald, T. M., M. J. Betenbaugh, et al. (2002). "Inhibiting apoptosis in mammalian cell culture using the caspase inhibitor XIAP and deletion mutants." Biotechnol Bioeng **77**(6): 704-16.
- Sauerwald, T. M., G. A. Oyler, et al. (2003). "Study of caspase inhibitors for limiting death in mammalian cell culture." Biotechnol Bioeng **81**(3): 329-40.
- Schroder, M. (2008). "Engineering eukaryotic protein factories." Biotechnol Lett **30**(2): 187-96.
- Schröder, M. (2010). Molecular Chaperones of the Endoplasmic Reticulum, Nova Science Publishers Inc.
- Schroeder, M. (2008). "Endoplasmic reticulum stress responses." Cell. Mol. Life Sci **65**: 862 – 894.
- Schuck, S., W. A. Prinz, et al. (2009). "Membrane expansion alleviates endoplasmic reticulum stress independently of the unfolded protein response." J Cell Biol **187**(4): 525-36.
- Sha, H., Y. He, et al. (2009). "The IRE1alpha-XBP1 pathway of the unfolded protein response is required for adipogenesis." Cell Metab **9**(6): 556-64.
- Shah, K., Y. Liu, et al. (1997). "Engineering unnatural nucleotide specificity for Rous sarcoma virus tyrosine kinase to uniquely label its direct substrates." Proc Natl Acad Sci U S A **94**(8): 3565-70.
- Shamu, C. and P. Walter (1996). "Oligomerization and phosphorylation of the Ire1p kinase during intracellular signaling from the endoplasmic reticulum to the nucleus." EMBO J. **15**: 3028-3039.
- Shen, J., X. Chen, et al. (2002). "ER stress regulation of ATF6 localization by dissociation of BiP/GRP78 binding and unmasking of Golgi localization signals." Dev Cell **3**(1): 99-111.
- Shen, X., R. E. Ellis, et al. (2001). "Complementary signaling pathways regulate the unfolded protein response and are required for C. elegans development." Cell **107**(7): 893-903.

- Shen, X., R. E. Ellis, et al. (2005). "Genetic interactions due to constitutive and inducible gene regulation mediated by the unfolded protein response in *C. elegans*." PLoS Genet **1**(3): e37.
- Shi, Y., J. An, et al. (1999). "Characterization of a mutant pancreatic eIF-2alpha kinase, PEK, and co-localization with somatostatin in islet delta cells." J Biol Chem **274**(9): 5723-30.
- Shi, Y., K. M. Vattem, et al. (1998). "Identification and characterization of pancreatic eukaryotic initiation factor 2 alpha-subunit kinase, PEK, involved in translational control." Mol Cell Biol **18**(12): 7499-509.
- Shinkawa, T., K. Nakamura, et al. (2003). "The absence of fucose but not the presence of galactose or bisecting N-acetylglucosamine of human IgG1 complex-type oligosaccharides shows the critical role of enhancing antibody-dependent cellular cytotoxicity." J Biol Chem **278**(5): 3466-73.
- Sidrauski, C. and P. Walter (1997). "The transmembrane kinase Ire1p is a site-specific endonuclease that initiates mRNA splicing in the unfolded protein response." Cell **90**(6): 1031-9.
- Stadler, J., R. Lemmens, et al. (2004). "Plasmid DNA purification." J Gene Med **6 Suppl 1**: S54-66.
- Sung, Y. H., S. W. Lim, et al. (2004). "Yeast hydrolysate as a low-cost additive to serum-free medium for the production of human thrombopoietin in suspension cultures of Chinese hamster ovary cells." Appl Microbiol Biotechnol **63**(5): 527-36.
- Sunstrom, N. A., R. D. Gay, et al. (2000). "Insulin-like growth factor-I and transferrin mediate growth and survival of Chinese hamster ovary cells." Biotechnol Prog **16**(5): 698-702.
- Suzuki, T. and W. J. Lennarz (2003). "Hypothesis: a glycoprotein-degradation complex formed by protein-protein interaction involves cytoplasmic peptide:N-glycanase." Biochem Biophys Res Commun **302**(1): 1-5.
- Tagawa, Y., N. Hiramatsu, et al. (2008). "Induction of apoptosis by cigarette smoke via ROS-dependent endoplasmic reticulum stress and CCAAT/enhancer-binding protein-homologous protein (CHOP)." Free Radic Biol Med **45**(1): 50-9.
- Thomis, D. C. and C. E. Samuel (1992). "Mechanism of interferon action: autoregulation of RNA-dependent P1/eIF-2 alpha protein kinase (PKR) expression in transfected mammalian cells." Proc Natl Acad Sci U S A **89**(22): 10837-41.
- Thuerauf, D. J., L. Morrison, et al. (2004). "Opposing roles for ATF6alpha and ATF6beta in endoplasmic reticulum stress response gene induction." J Biol Chem **279**(20): 21078-84.
- Tigges, M. and M. Fussenegger (2006). "Xbp1-based engineering of secretory capacity enhances the productivity of Chinese hamster ovary cells." Metab Eng.
- Tirasophon, W., Lee.K., Callaghan B, Welihinda A, Kaufman RJ. , (2000). "The endoribonuclease activity of mammalian IRE1 autoregulates its mRNA and is required for the unfolded protein response." Genes Dev. **14**(21): 2725-36.
- Tirasophon, W., A. Welihinda, et al. (1998). "A stress response pathway from the endoplasmic reticulum to the nucleus requires a novel bifunctional protein kinase/endoribonuclease (Ire1p) in mammalian cells." Genes Dev. **12**(12): 1812-24.
- Tjio, J. H. and T. T. Puck (1958). "Genetics of somatic mammalian cells. II. Chromosomal constitution of cells in tissue culture." J Exp Med **108**(2): 259-68.
- Tu, B. P. and J. S. Weissman (2004). "Oxidative protein folding in eukaryotes: mechanisms and consequences." J Cell Biol **164**(3): 341-6.

- Uemura, A., M. Oku, et al. (2009). "Unconventional splicing of XBP1 mRNA occurs in the cytoplasm during the mammalian unfolded protein response." J Cell Sci **122**(Pt 16): 2877-86.
- Urano, F., A. Bertolotti, et al. (2000). "IRE1 and efferent signaling from the endoplasmic reticulum." J. Cell Sci., **113**(21): 3697-3702.
- Urano, F., M. Calton, et al. (2002). "A survival pathway for *Caenorhabditis elegans* with a blocked unfolded protein response." J Cell Biol **158**(4): 639-46.
- Urano, F., Wang, XZ., Bertolotti, A., Zhang, Y., Chung, P., Harding, HP., and Ron, D. (2000). "Coupling of Stress in the ER to Activation of JNK Protein Kinases by Transmembrane Protein Kinase IRE1." Science **287**(28): 664-666.
- Urlaub, G. and L. A. Chasin (1980). "Isolation of Chinese hamster cell mutants deficient in dihydrofolate reductase activity." Proc Natl Acad Sci U S A **77**(7): 4216-20.
- Vashist, S. and D. T. Ng (2004). "Misfolded proteins are sorted by a sequential checkpoint mechanism of ER quality control." J Cell Biol **165**(1): 41-52.
- Venugopal, R. and A. K. Jaiswal (1996). "Nrf1 and Nrf2 positively and c-Fos and Fra1 negatively regulate the human antioxidant response element-mediated expression of NAD(P)H:quinone oxidoreductase1 gene." Proc Natl Acad Sci U S A **93**(25): 14960-5.
- Volkman, K., J. L. Lucas, et al. (2011). "Potent and selective inhibitors of the inositol-requiring enzyme 1 endoribonuclease." J Biol Chem **286**(14): 12743-55.
- Wagner, M. J., J. A. Sharp, et al. (1981). "Nucleotide sequence of the thymidine kinase gene of herpes simplex virus type 1." Proc Natl Acad Sci U S A **78**(3): 1441-5.
- Wajant, H., Pfizenmaier, K., and P Scheurich (2003). "Tumor necrosis factor signaling." Cell Death and Differentiation **10**: 45-65.
- Wang, J., H. Hua, et al. (2008). "Derlin-1 is overexpressed in human breast carcinoma and protects cancer cells from endoplasmic reticulum stress-induced apoptosis." Breast Cancer Res **10**(1): R7.
- Wang, X., H. Harding, et al. (1998). "Cloning of mammalian Ire1 reveals diversity in the ER stress responses." EMBO J., **17**(19): 5708-17.
- Wang, Y., J. Shen, et al. (2000). "Activation of ATF6 and an ATF6 DNA binding site by the endoplasmic reticulum stress response." J. Biol Chem. **275**(35): 27013-20.
- Wei, J. and L. M. Hendershot (1995). "Characterization of the nucleotide binding properties and ATPase activity of recombinant hamster BiP purified from bacteria." J Biol Chem **270**(44): 26670-6.
- Wiseman, R. L., Y. Zhang, et al. (2010). "Flavonol activation defines an unanticipated ligand-binding site in the kinase-RNase domain of IRE1." Mol Cell **38**(2): 291-304.
- Wooden, S. K., L. J. Li, et al. (1991). "Transactivation of the grp78 promoter by malfolded proteins, glycosylation block, and calcium ionophore is mediated through a proximal region containing a CCAAT motif which interacts with CTF/NF-I." Mol Cell Biol **11**(11): 5612-23.
- Wurm, F. (2004). "Production of recombinant protein therapeutics in cultivated mammalian cells." Nat Biotechnol. **22**(11): 1393-8.
- Xu, Q. and J. C. Reed (1998). "Bax inhibitor-1, a mammalian apoptosis suppressor identified by functional screening in yeast." Mol Cell **1**(3): 337-46.
- Yamamoto, K., T. Sato, et al. (2007). "Transcriptional induction of mammalian ER quality control proteins is mediated by single or combined action of ATF6alpha and XBP1." Dev Cell **13**(3): 365-76.
- Yang, M. and M. Butler (2000). "Effects of ammonia on CHO cell growth, erythropoietin production, and glycosylation." Biotechnol Bioeng **68**(4): 370-80.

- Yanisch-Perron, C., J. Vieira, et al. (1985). "Improved M13 phage cloning vectors and host strains: nucleotide sequences of the M13mp18 and pUC19 vectors." *Gene* **33**(1): 103-19.
- Ye, J., R. B. Rawson, et al. (2000). "ER stress induces cleavage of membrane-bound ATF6 by the same proteases that process SREBPs." *Mol Cell* **6**(6): 1355-64.
- Yeh, W., A. Shahinian, et al. (1997). "Early lethality, functional NF-kappaB activation, and increased sensitivity to TNF-induced cell death in TRAF2-deficient mice." *Immunity* **7**: 715-725.
- Yoshida, H., K. Haze, et al. (1998). "Identification of the cis-acting endoplasmic reticulum stress response element responsible for transcriptional induction of mammalian glucose-regulated proteins. Involvement of basic leucine zipper transcription factors." *J Biol Chem* **273**(50): 33741-9.
- Yoshida, H., T. Matsui, et al. (2003). "A Time-Dependent Phase Shift in the Mammalian Unfolded Protein Response ." *Developmental Cell* **4**(2): 265 - 271.
- Yoshida, H., T. Matsui, et al. (2003). "A time-dependent phase shift in the mammalian unfolded protein response." *Dev Cell* **4**(2): 265-71.
- Yoshida, H., T. Matsui, et al. (2001). "XBP1 mRNA is induced by ATF6 and spliced by IRE1 in response to ER stress to produce a highly active transcription factor." *Cell* **107**(7): 881-91.
- Yoshida, H., T. Okada, et al. (2000). "ATF6 activated by proteolysis binds in the presence of NF-Y (CBF) directly to the cis-acting element responsible for the mammalian unfolded protein response." *Mol Cell Biol* **20**(18): 6755-67.
- Yoshida, H., M. Oku, et al. (2006). "pXBP1(U) encoded in XBP1 pre-mRNA negatively regulates unfolded protein response activator pXBP1(S) in mammalian ER stress response." *J Cell Biol* **172**(4): 565-75.
- Yuan, L., Y. Cao, et al. (2008). "IRE1beta is required for mesoderm formation in Xenopus embryos." *Mech Dev* **125**(3-4): 207-22.
- Zanghi, J. A., M. Fussenegger, et al. (1999). "Serum protects protein-free competent Chinese hamster ovary cells against apoptosis induced by nutrient deprivation in batch culture." *Biotechnol Bioeng* **64**(1): 108-19.
- Zanghi, J. A., W. A. Renner, et al. (2000). "The growth factor inhibitor suramin reduces apoptosis and cell aggregation in protein-free CHO cell batch cultures." *Biotechnol Prog* **16**(3): 319-25.
- Zhang, C., D. M. Kenski, et al. (2005). "A second-site suppressor strategy for chemical genetic analysis of diverse protein kinases." *Nat Methods* **2**(6): 435-41.
- Zhou, H., X. G. Xia, et al. (2005). "An RNA polymerase II construct synthesizes short-hairpin RNA with a quantitative indicator and mediates highly efficient RNAi." *Nucleic Acids Res* **33**(6): e62.
- Zhou, J. and J. A. Adams (1997). "Is there a catalytic base in the active site of cAMP-dependent protein kinase?" *Biochemistry* **36**(10): 2977-84.
- Zhou, J., C. Liu, et al. (2006). "The crystal structure of human IRE1 luminal domain reveals a conserved dimerization interface required for activation of the unfolded protein response." *Proc Natl Acad Sci U S A* **103**(39): 14343-8.

APPENDIX 1 – iCODEHOP Results for mammalian IRE1 α alignments

Mammalian protein sequences for *R. norvegicus* (XP_573211), *M. musculus* (NP_076402) and *H. sapiens* (NP_001424) were entered into the iCODEHOP programme, which then produced alignments of the protein sequences and identified suitable sites for degenerate primers.

```

CLUSTAL 2.0.12 multiple sequence alignment

XP_573211      -----MRRNCNDIQSFGRASTVTLPEALLFVSTLDGSLHAVSKRTGSIKWTLKE
NP_076402      MPARWLLLLLALLLPPPGPGSFGRSTVTLPETLLFVSTLDGSLHAVSKRTGSIKWTLKE
NP_001424      --MPARRLLLLLTLPLGLGIFGSTSTVTLPETLLFVSTLDGSLHAVSKRTGSIKWTLKE
                .   ** :*****:*****

XP_573211      DPVLQVPPTHVEEPAFLPDPNDGSLYTLGGKNNEGLTKLPFTIPELVQASPCRSSDGILYM
NP_076402      DPVLQVPPTHVEEPAFLPDPNDGSLYTLGGKNNEGLTKLPFTIPELVQASPCRSSDGILYM
NP_001424      DPVLQVPPTHVEEPAFLPDPNDGSLYTLGSKNNEGLTKLPFTIPELVQASPCRSSDGILYM
                *****.*****

XP_573211      GKKQDIWYVIDLLTGEKQQTLSAFADSLCPSTSLLYLGRTEYITIMYDTKTRELRWNAT
NP_076402      GKKQDIWYVIDLLTGEKQQTLSAFADSLCPSTSLLYLGRTEYITIMYDTKTRELRWNAT
NP_001424      GKKQDIWYVIDLLTGEKQQTLSAFADSLCPSTSLLYLGRTEYITIMYDTKTRELRWNAT
                *****

XP_573211      YFDYAASLPEDDVDYKMSHFVSNGDGLVVTVDSESGDVLWIQNYASPVVAFYIWQREGLR
NP_076402      YFDYAASLPEDDVDYKMSHFVSNGDGLVVTVDSESGDVLWIQNYASPVVAFYVWQGEVLR
NP_001424      YFDYAASLPEDDVDYKMSHFVSNGDGLVVTVDSESGDVLWIQNYASPVVAFYVWQREGLR
                *****:***

XP_573211      KVVHINAVETLRYLTFMSGEVGRITKWKYPPFKETEAKSKLTPTLYVGKYSTSLYASPS
NP_076402      KVVHINAVETLRYLTFMSGEVGRITKWKYPPFKETEAKSKLTPTLYVGKYSTSLYASPS
NP_001424      KVMHINAVETLRYLTFMSGEVGRITKWKYPPFKETEAKSKLTPTLYVGKYSTSLYASPS
                **:*****

XP_573211      MVHEGVAVVPRGSTLPLLEGPQTDGVTIGDKGECVITPSTD LKFDPGLKGSKLNLYLRNY
NP_076402      MVHEGVAVVPRGSTLPLLEGPQTDGVTIGDKGECVITPSTD LKFDPGLKGSKLNLYLRNY
NP_001424      MVHEGVAVVPRGSTLPLLEGPQTDGVTIGDKGECVITPSTD VKFDPGLKSKNKNLYLRNY
                *****.*****.*
    
```

XP_573211 WLLIGHHETPLSASTKMLERFPNNLPKHRENVIPADSEKRSFEEVINLVGQTSENTPTTV
 NP_076402 WLLIGHHETPLSASTKMLERFPNNLPKHRENVIPADSEKRSFEEVINLVGQTSNTPTTV
 NP_001424 WLLIGHHETPLSASTKMLERFPNNLPKHRENVIPADSEKRSFEEVINLVDQTSNAPTTV
 *****:*****:*.***:*.****

XP_573211 SQDVEEKLPRAPAKPEAPVDSMLKDMATIILSTFLLVGWVAFIITYPLSMHQQRQLQHQQ
 NP_076402 SQDVEEKLARAPAKPEAPVDSMLKDMATIILSTFLLVGWVAFIITYPLSVHQQRQLQHQQ
 NP_001424 SRDVEEKPAHAPARPEAPVDSMLKDMATIILSTFLLIGWVAFIITYPLSMHQQQQLQHQQ
 *:***** .:***:*****:*****:***:*****

XP_573211 FQKELEKIQLLQQQQ--LPFHHPGDLTQDPDFLDSSGLFSESSGTSSPSPSPRASNHSLN
 NP_076402 FQKELEKIQLLQQQQ--LPFHHPGDLTQDPEFLDSSGPFSESSGTSSPSPSPRASNHSLH
 NP_001424 FQKELEKIQLLQQQQQLPFHPPGDTAQDGELLDTSGPYSESSGTSSPSTSPRASNHSLC
 ***** ***** ** :* :*:** :***** .*****

XP_573211 SSSSASKAGTSPSLEPDEDEETRMVIVGKISFCPKDVLGHGAEGTIVYKGMFDNRDVAV
 NP_076402 PSSSASRAGTSPSLEQDDEDEETRMVIVGKISFCPKDVLGHGAEGTIVYKGMFDNRDVAV
 NP_001424 SGSSASKAGSSPSLEQDDGDEETSVMVIVGKISFCPKDVLGHGAEGTIVYRGMFDNRDVAV
 ..****:***:***** ** **** :*****:*****

XP_573211 KRILPECFSFADREVQLLRESDEHPNVIRYFCTEKDRQFQYIAIELCAATLQEYVEQKDF
 NP_076402 KRILPECFSFADREVQLLRESDEHPNVIRYFCTEKDRQFQYIAIELCAATLQEYVEQKDF
 NP_001424 KRILPECFSFADREVQLLRESDEHPNVIRYFCTEKDRQFQYIAIELCAATLQEYVEQKDF

XP_573211 AHLGLEPITLLHQTTSGLAHLHSLNIVHRDLKPHNILLSMPNAHGRIKAMISDFGLCKKL
 NP_076402 AHLGLEPITLLHQTTSGLAHLHSLNIVHRDLKPHNILLSMPNAHGRIKAMISDFGLCKKL
 NP_001424 AHLGLEPITLLQQTTSGLAHLHSLNIVHRDLKPHNILISMPNAHGRIKAMISDFGLCKKL
 *****:*****:*****:*****:*****

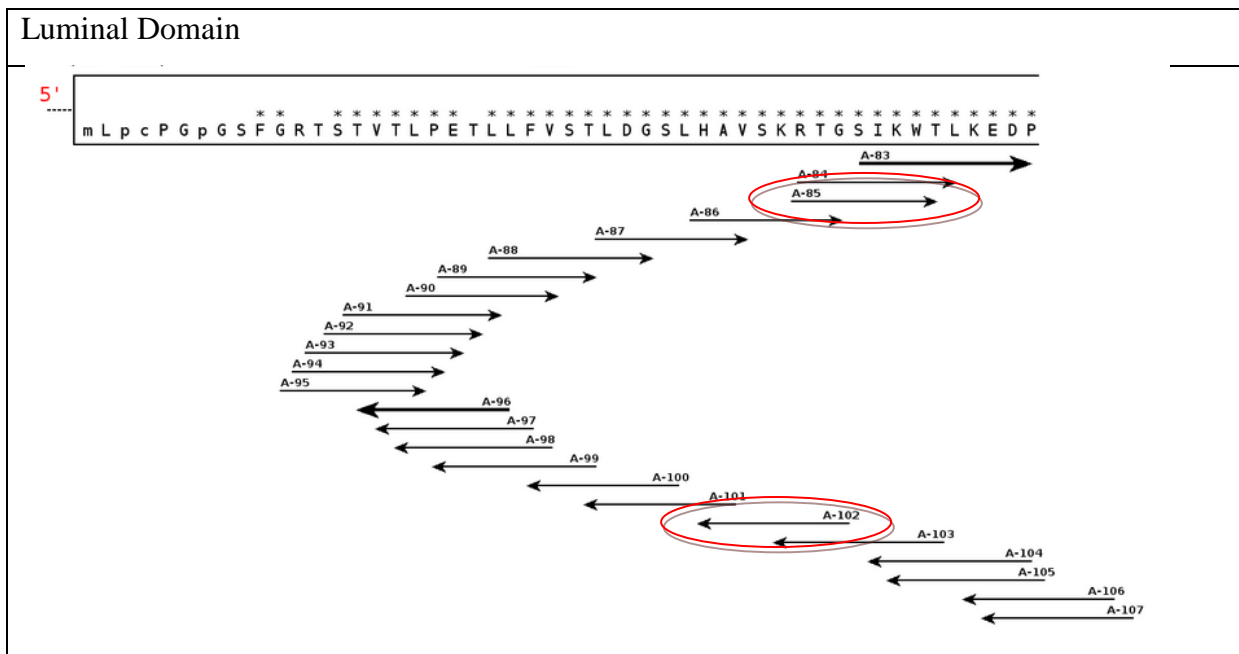
XP_573211 AVGRHSFSRRSGVPGTEGWIAPPEMLSEDCKENPTYTVDIFSAGCVFYYVISEGNHPFGKS
 NP_076402 AVGRHSFSRRSGVPGTEGWIAPPEMLSEDCKDNPTYTVDIFSAGCVFYYVISEGNHPFGKS
 NP_001424 AVGRHSFSRRSGVPGTEGWIAPPEMLSEDCKENPTYTVDIFSAGCVFYYVISEGSHPFKGS
 *****:*****:*****

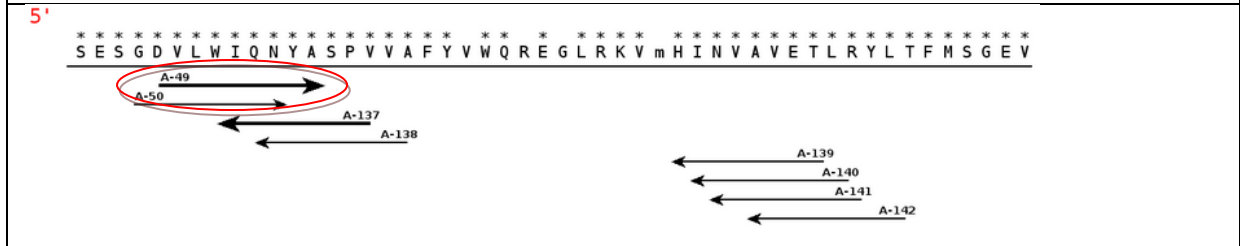
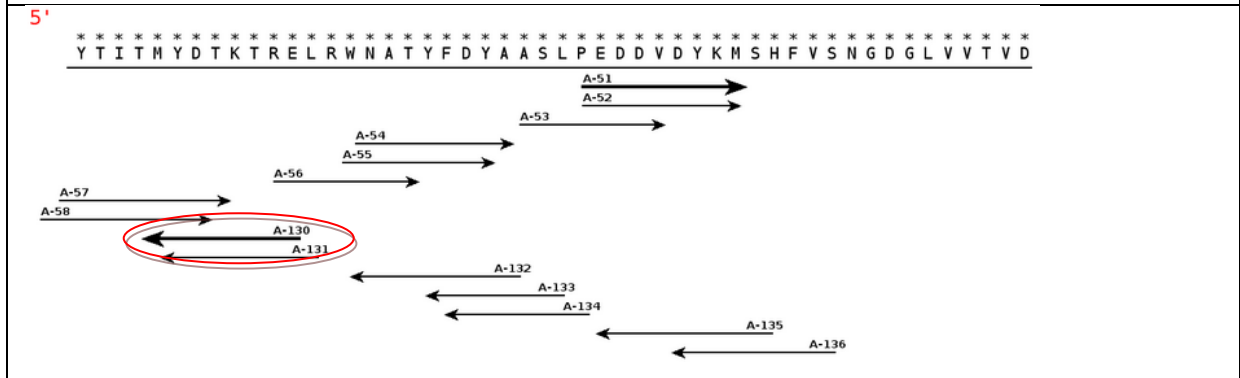
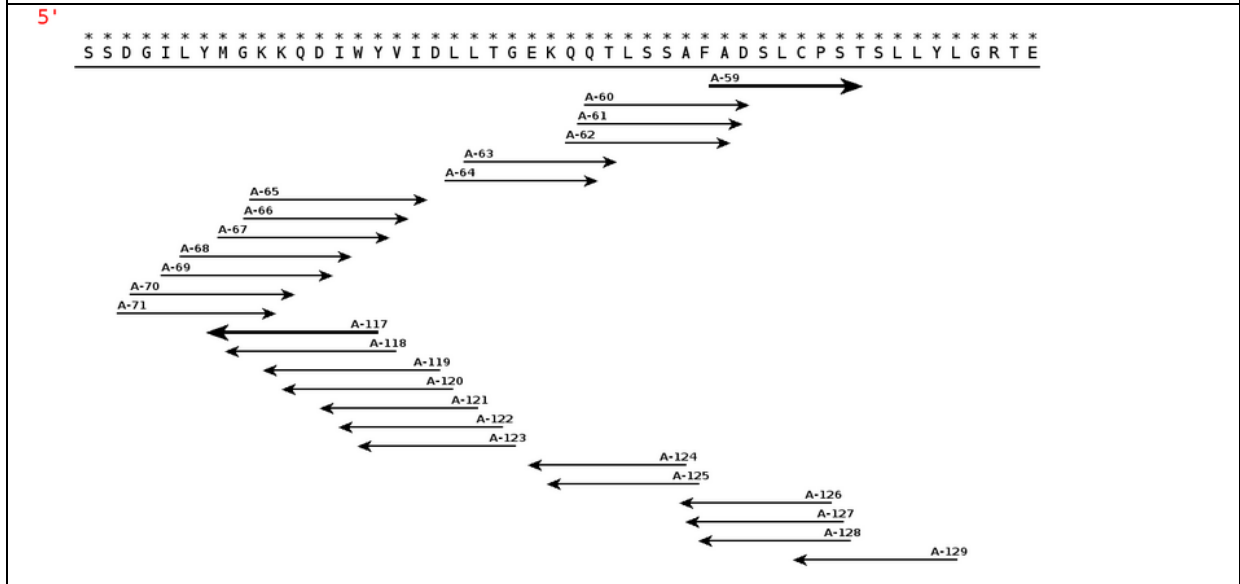
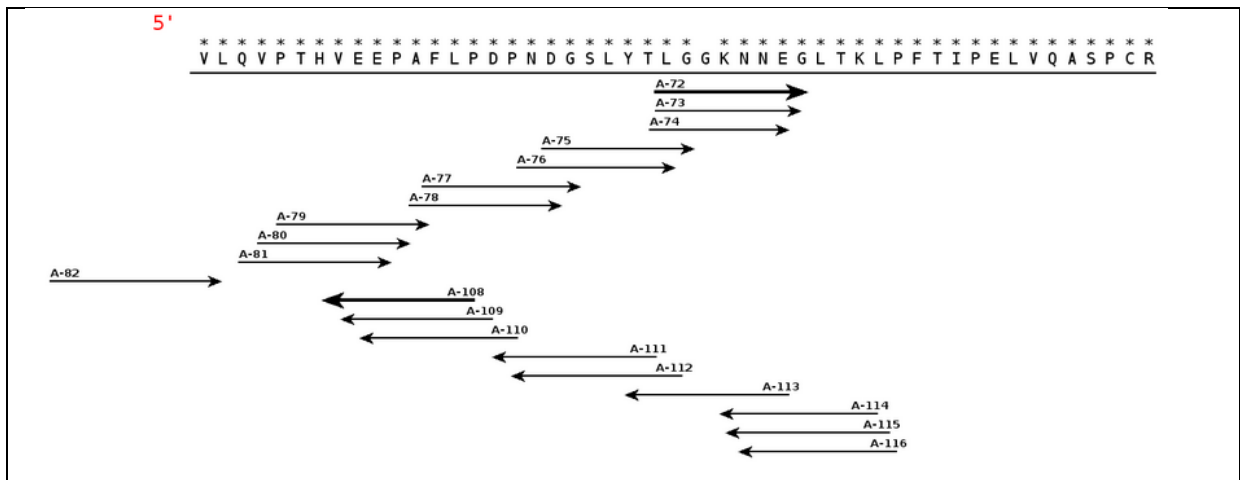
XP_573211 LQRQANILLGACSLDCFHSDKHEDVIARELIEKMIAMDPQQRPSAKHVLKHPFFWSLEKQ
 NP_076402 LQRQANILLGACNLDCFHSDKHEDVIARELIEKMIAMDPQQRPSAKHVLKHPFFWSLEKQ
 NP_001424 LQRQANILLGACSLDCLHPEKHEDVIARELIEKMIAMDPQQRPSAKHVLKHPFFWSLEKQ
 ***** .***:*. :*:*****:*****

XP_573211	LQFFQDVSDRIEKESLDGPIVRQLERGGRAVVKMDWRENITVPLQTDLRKFRTYKGGSVR
NP_076402	LQFFQDVSDRIEKEALDGPIVRQLERGGRAVVKMDWRENITVPLQTDLRKFRTYKGGSVR
NP_001424	LQFFQDVSDRIEKESLDGPIVKQLERGGRAVVKMDWRENITVPLQTDLRKFRTYKGGSVR
	*****:*****:*****
XP_573211	DLLRAMRNKRHHYRELPLEVQETLGSIPDDFVRYFTSRFPHLLSHTYRAMELCRHERLFQ
NP_076402	DLLRAMRNKKHHYRELPEVQETLGSIPDDFVRYFTSRFPHLLSHTYQAMELCRHERLFQ
NP_001424	DLLRAMRNKKHHYRELPAEVRETLSLPPDDFVRYFTSRFPHLLAHTYRAMELCRHERLFQ
	*****:***** **:*****:***** *****:***:***** *****
XP_573211	TYYWHEPTEAQPPGIPDAL
NP_076402	TYYWHEPTEPQPPVIPYAL
NP_001424	PYYFHEPPEPQPPVTPDAL
	.**:***.*.** * **

Protein sequence alignment – IRE1 α

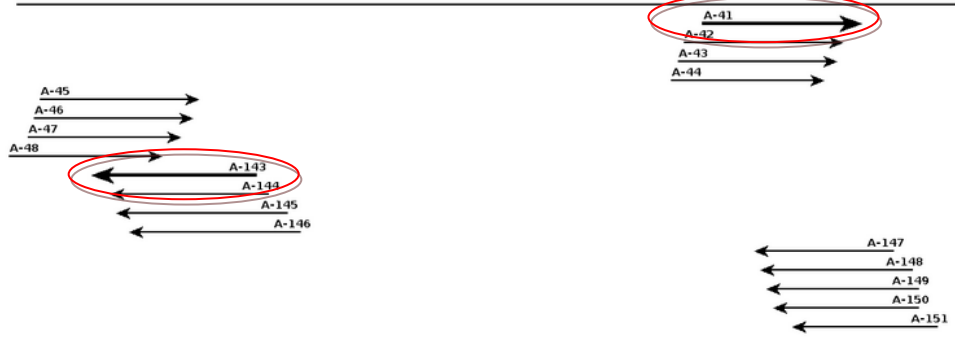
Primers used for sequencing of CHO IRE1 α are circled.





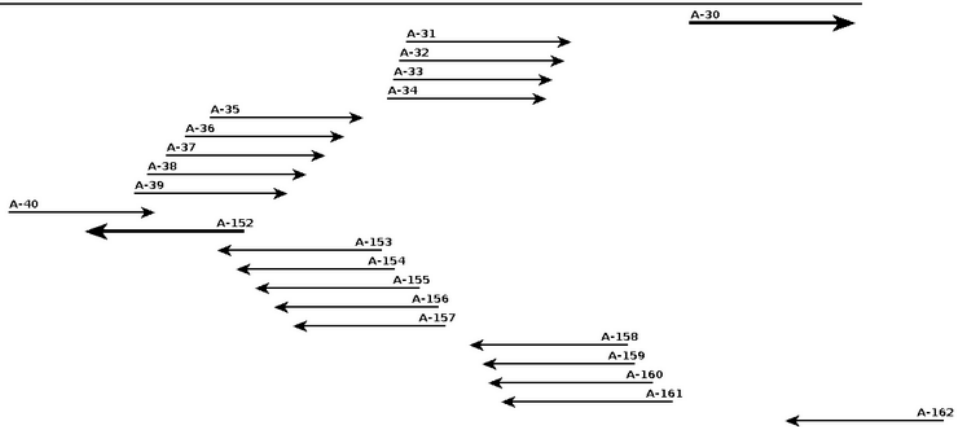
5'

GRITKWKYPFPKETEA KSKLTP TLYV GKYSTSLYASPSMVHEGVAVVPRG



5'

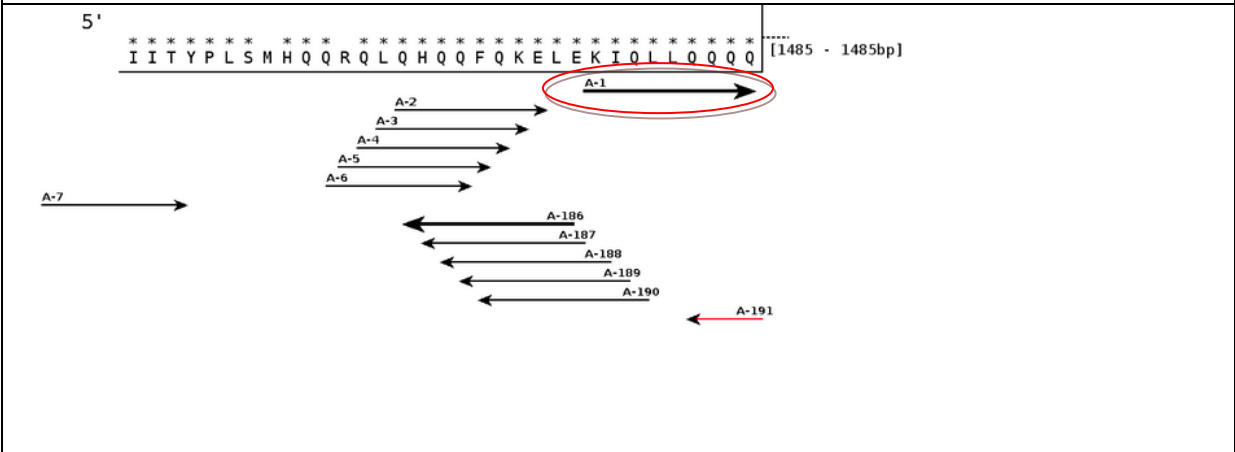
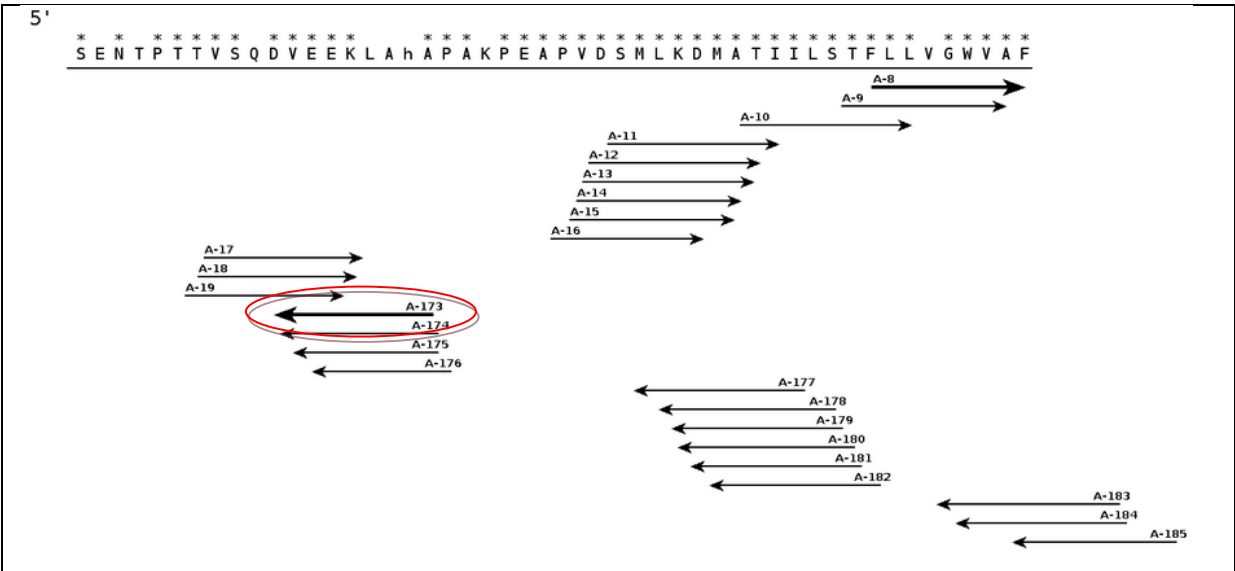
STLPLLEG PQT DGV TIGDKGECVITPSTDLKFD PGLK GKSKLNYLRNYWL



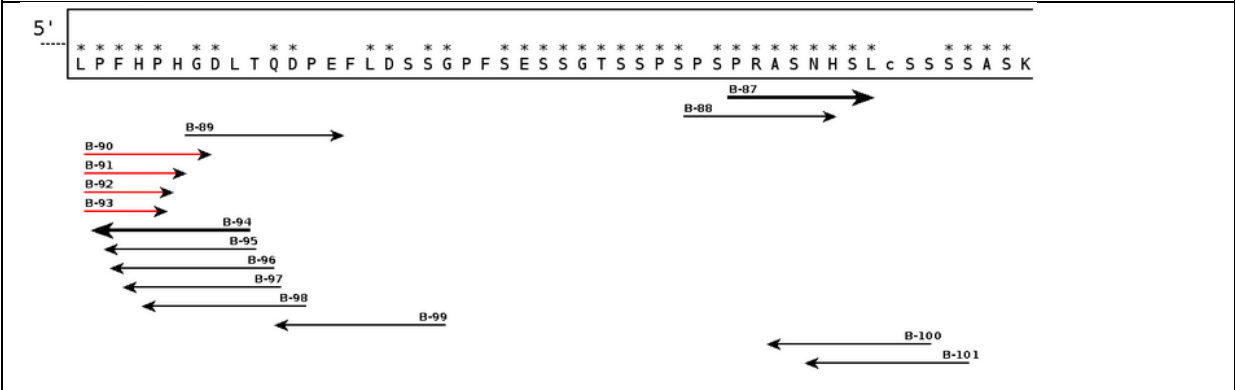
5'

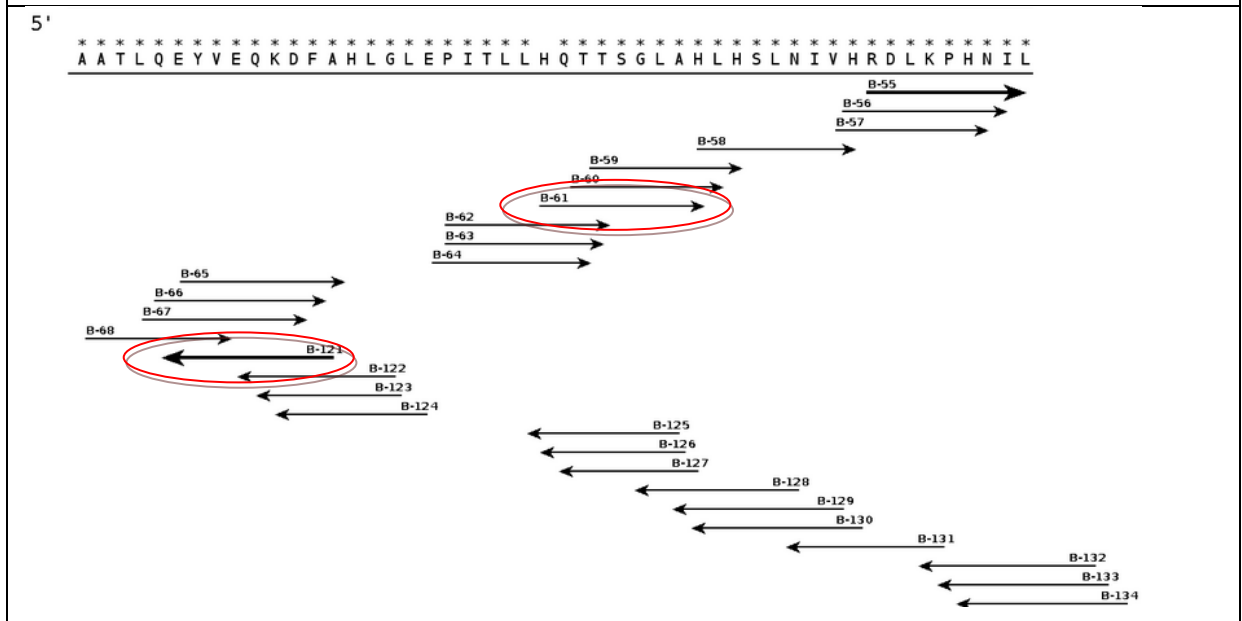
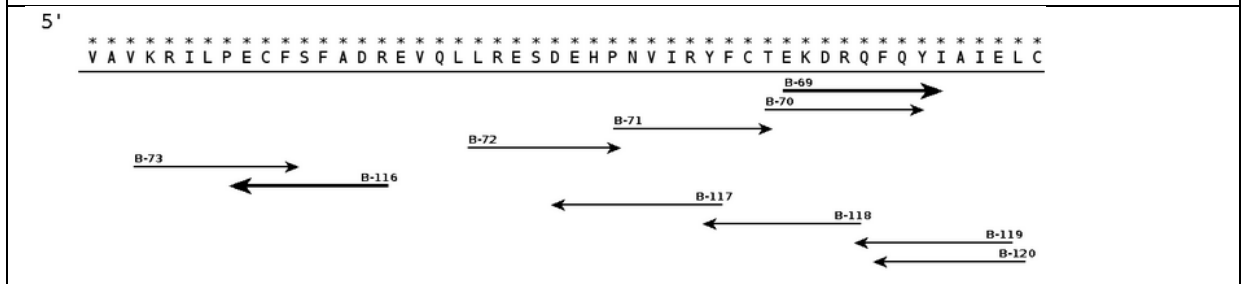
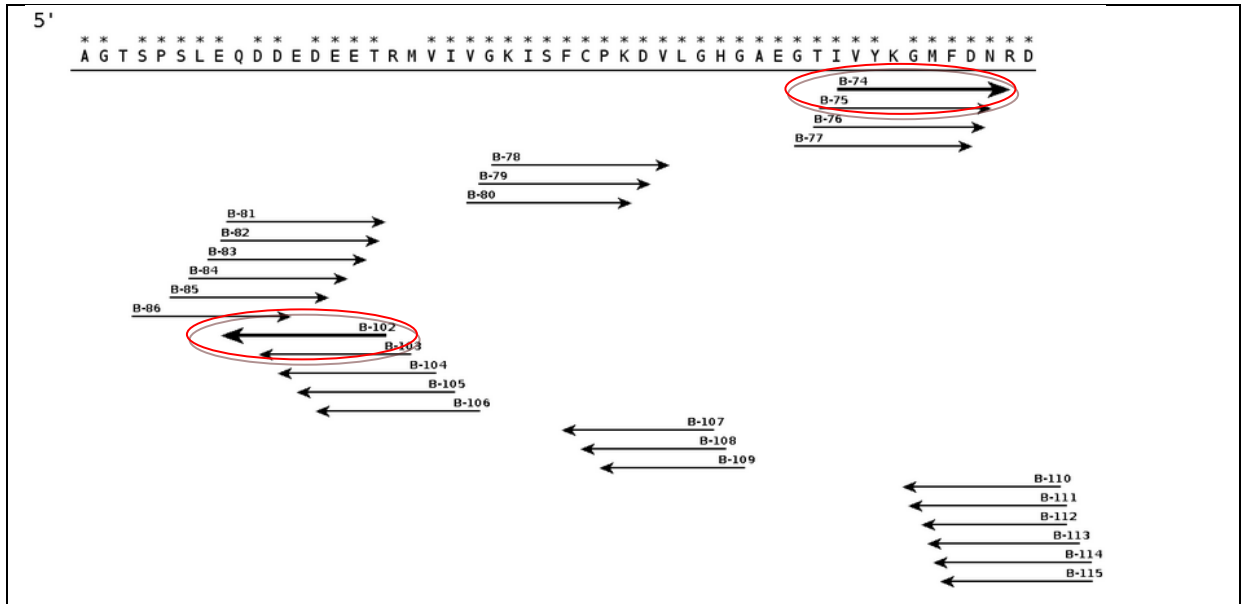
LIGHHETPLSASTKMLERFPNNLPKHRENVIPADSEKRSFEEVINLVGQT

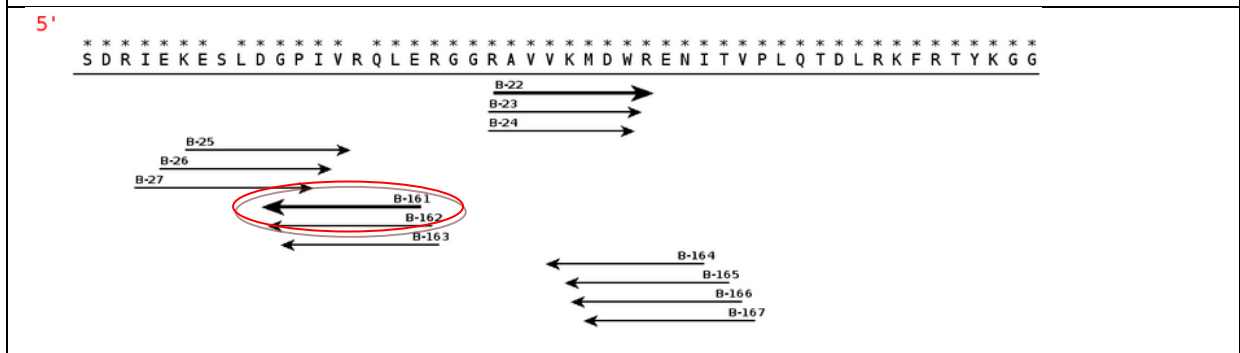
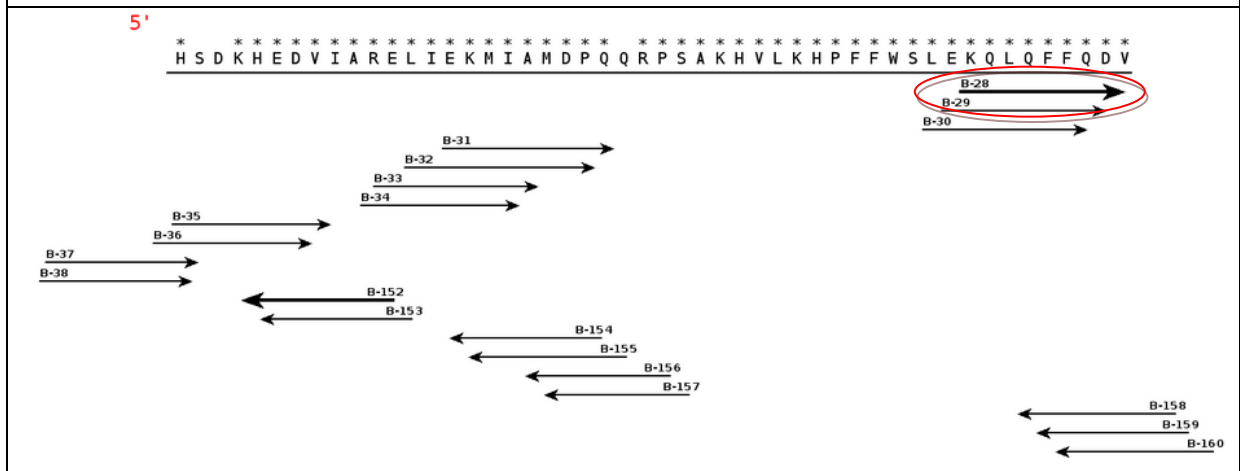
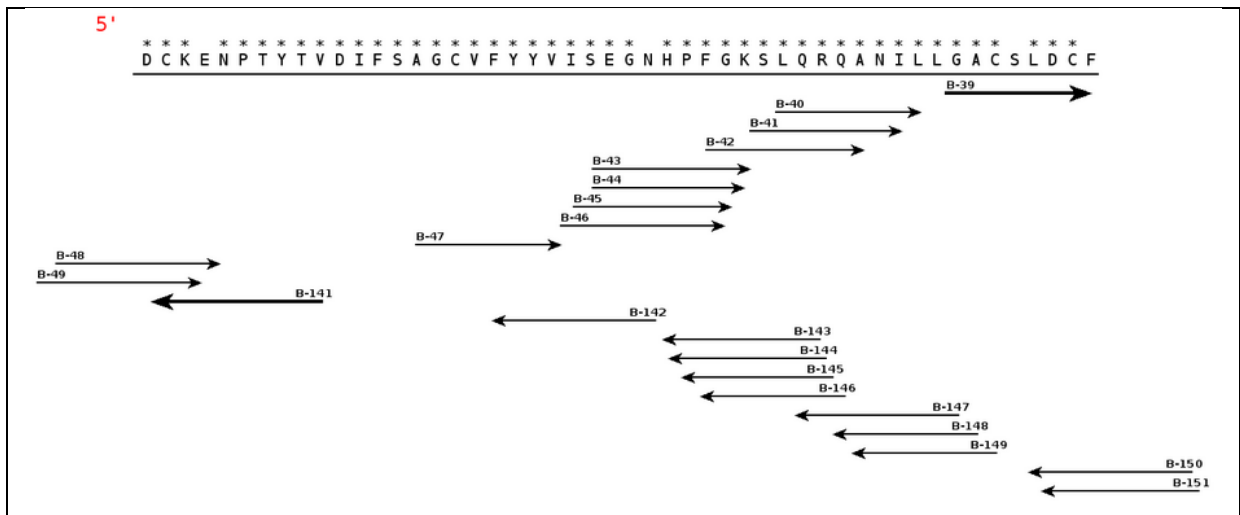




Cytoplasmic Domain

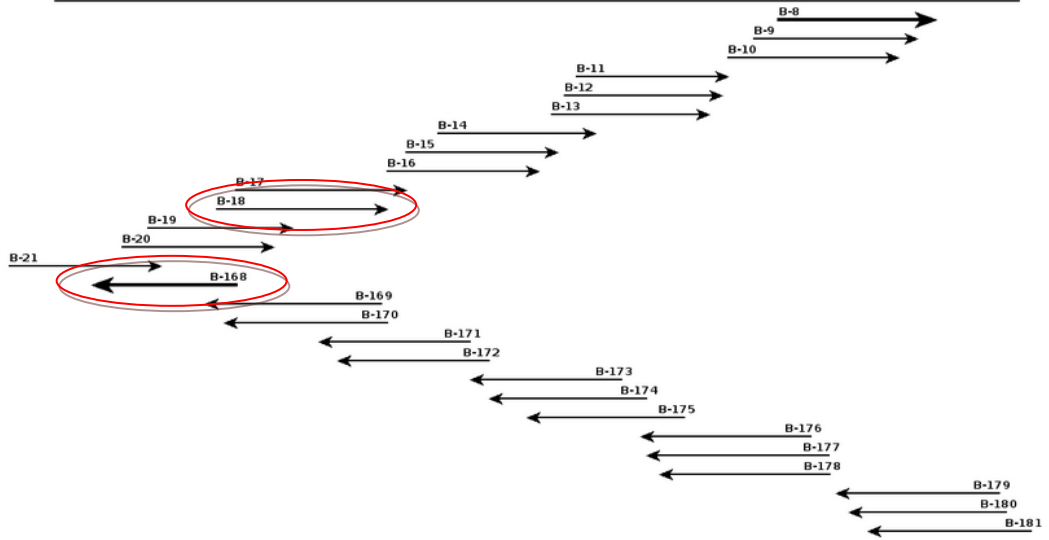






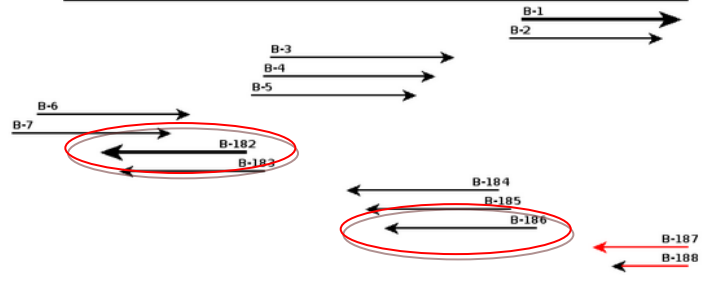
5'

S V R D L L R A M R N K K H H Y R E L P v E V Q E T L G S I P D D F V c Y F T S R F P H L L S H T Y



5'

R A M E L C R H E R L F Q T Y Y W H E P T E P Q P P V I P D A L [2937 - 2937bp]



TTCGGAAAAAAGGAGCTTTGAGAAAGTTATCAACATGGTTGACCAGACTTCAGAAAACACACCATCCACTGTGTCTCAGGCCGTGGA
 AGAGAAGCTGGTCCATGCCCCCGCCAAGCCTGAGGCCCGTTGACTCCATGCTCAAGGACATGGCTACTATTATCCTGAGCACCTT
 CCTGCTGGTTGGATGGGTGGCCTTCATCATCACTTACCCCCTGAGCATGCATCAGCAGCGCCAGCTGGTTGGATGGGTGGCCTTCAT
 CATCACTTACCCCCTGAGCATGCATCAGCAGCGCCAGCTCCAGCACCAGCAGTTCCAGAAGGAACTGGAGAAAATTCAGCTCCTGCA
 GCAGCAGCAGCTGCCCTTCCACCCACATGGAGACCTTACTCAGGACCCCGAGTTTCTGGATTTCATCTGGTCT
 CTTCTCAGAGAGCTCAGGCACCAGCAGCTCCAGCCCATCCCCAGAGCCTCCAACCACTCACTCCACTCCAGCAGCTCTGCCTCCAA
 GACTGGCACCAACCCCTCCCTGGAGCAG

Query	53	CTTCATGTCTGGGGAAGTGGGGCGCATCACCAAGTGGAAAGTATCCGTTCCCCAAGGAGAC	112
Sbjct	888	CTTCATGTCTGGGGAAGTGGGGCGCATCACCAAGTGGAAAGTATCCATTCCCCAAGGAGAC	947
Query	113	AGAGGCCAAGAGCAAGCTGACGCCTACCCTGTACGTTGGGAAGTACTCAACCAGCCTCTA	172
Sbjct	948	AGAGGCCAAGAGCAAGCTAACGCCTACTCTGTATGTTGGGAAGTATTCCACCAGCCTCTA	1007
Query	173	TGCCTCTCCATCAATGGTGCACGAGGGGGTGTGTAGTGCCCCGAGGAAGCACTCTTCC	232
Sbjct	1008	TGCCTCTCCCTCAATGGTGCATGAGGGGGTGTGTCTGCTGCCTCGAGGCAGCACTCTTCC	1067
Query	233	TTTGCTGGAAGGTCCCCAGACAGATGGTGTCCATTGAAGACAAAGGAGAGTGTGTGAT	292
Sbjct	1068	TTTGCTGGAAGGCCCCCAGACAGATGGCGTCCATTGGAGACAAAGGAGAGTGTGTGAT	1127
Query	293	CACCCCCAGCACAGACCTCAAGTTTGACCCTGGACTCAAAGGGAAGAGCAAGCTGAACTA	352
Sbjct	1128	CACTCCAGCACAGACCTCAAGTTTGACCCTGGACTCAAAGGGAAGAGCAAGCTGAACTA	1187
Query	353	CTTGAGGAATTACTGGCTTCTCATAGGACACCATGAAACTCCTCTGTCTGCATCTACCAA	412
Sbjct	1188	CTTGAGGAATTACTGGCTTCTCATAGGACACCATGAAACTCCTCTGTCTGCATCCACCAA	1247
Query	413	GATGCTGGAGAGATTTCCCAACAACCTGCCCAAACATCGGGAAAATGTGATTCTGCTGA	472
Sbjct	1248	GATGCTGGAGAGATTTCCCTAACAACCTGCCCAAACATCGAGAAAATGTGATTCTGCTGA	1307
Query	473	TTCGGAAAAAAGGAGCTTTGAGAAAGTTATCAACATGGTTGACCAGACTTCAGAAAACAC	532
Sbjct	1308	TTCAGAAAAAAGGAGCTTTGAGGAAGTTATCAACATAGTTGGCCAGACTTCAGACAACAC	1367
Query	533	ACCATCCACTGTGTCTCAGGCCGTGGAAGAGAAGCTGGTCCATGCCCCCGCCAAGCCTGA	592
Sbjct	1368	ACCGACCACCGTATCTCAGGATGTGGAGGAGAAGCTCGCTCGCGCCCCTGCCAAGCCTGA	1427
Query	593	GGCCCCCGTTGACTCCATGCTCAAGGACATGGCTACTATTATCCTGAGCACCTTCCTGCT	652
Sbjct	1428	GGCCCCCGTGGACTCCATGCTCAAGGACATGGCTACCATTATCCTGAGCACCTTCCTGCT	1487
Query	653	GGTTGGATGGGTGGCCTTCATCATCACTTACCCCCTGAGCATGCATCAGCAGCGCCAGCT	712
Sbjct	1488	GGTTGGATGGGTGGCCTTCATCATCACTTACCCCCTGAGCGTGCATCAGCAGCGTCAGCT	1547
Query	713	CCAGCACCAGCAGTTCCAGAAGGAACTGGAGAAAATTCAGCTCCTGCAGCAGCAGCAGCT	772
Sbjct	1548	CCAGCACCAACAGTTCCAGAAGGAGCTGGAGAAGATTTCAGCTCCTGCAGCAGCAGCAGCT	1607
Query	773	GCCCTTCCACCCACATGGAGACCTTACTCAGGACCCCGAGTTTCTGGATTTCATCTGGTCT	832
Sbjct	1608	GCCCTTCCACCCACACGGAGACCTTACCAGGACCCTGAGTTCTGGATTTCATCTGGCCC	1667

Sbjct 1681 AGCTCTCTGAGAAGGGGCCAGATGAATCCAGGAACCTCAGGGTCCTGGGTAAGGTCTCCGT 1622

Query 601 GTGGGTGGAAGGGCAGCTGCTGTTGCTGCAGGAGCTGAATTTTCTCCAGTTCCTTCTGGA 660
 ||| |

Sbjct 1621 GTGGGTGGAAGGGCAGCTGCTGCTGCTGCAGGAGCTGAATCTTCTCCAGTTCCTTCTGGA 1562

Query 661 ACTGCTGGTGTGGAGCTGGCGCTGCTGATGCATGCTCAGGGGGTAAGTGATGATGAAGG 720
 ||| |

Sbjct 1561 ACTGTTGGTGTGGAGCTGACGCTGCTGATGCACGCTCAGGGGGTAAGTGATGATGAACG 1502

Query 721 CCACCCATCCAACCAGCANGAAGGTGCTCAGGATAATAGTAGCCATGTCCTTGAGCATGG 780
 ||| |

Sbjct 1501 CCACCCATCCAACCAGCAGGAAGGTGCTCAGGATAATGGTAGCCATGTCCTTGAGCATGG 1442

Query 781 AGTCAACGGGGGCCTCAGGCTTGGCGGGGGCATGGNCCAGCTTCTCTTCCACGGCCTGAG 840
 ||| |

Sbjct 1441 AGTCCACGGGGGCCTCAGGCTTGGCAGGGGCGCAGCGAGCTTCTCTCCACATCCTGAG 1382

Query 841 ACACAGTGGATGGCGTGTTTTCTGAAGTCTGGTCAACCATGTTTGATAACTTTCTCAAAG 900
 | || |

Sbjct 1381 ATACGGTGGTGGTGTGTTGTCTGAAGTCTGGCCAACATATG-TTGATAACTTCTCAAAG 1323

Query 901 CTCNTTTTTTTCCGAATCAGCAG 922
 ||| |

Sbjct 1322 CTCCTTTTTTCTGAATCAGCAG 1301

2125-2665

CTTCACCAGACCACCTCCGGGTGGCCACCTCCACTCCCTCAACATCGTTTCACAGAGACCTAAAGCCACACAACATCCTCATATCC
 ATGCCAATGCACACGGCAAGATCAAGGCCATGATATCCGCCTTTGGCCTCTGCAAGAAGCTGGCAGTGGGCAGACACAGTTTCAGC
 CGCCGATCTGGGGTGCCTGGCACAGAAGGCTGGATCGCTCCAGAGATGCTGAGCGAAGACTGTAAGGAGAACCCTACCTACACGGTG
 GACATCTTTTCTGCAGGCTGCGTCTTTTACTACGTAATCTCTGAGGGCAGCCACCCTTTTGGCAAGTCCCTGCAGCGGCAGGCCAAC
 ATCCTCCTGGGTGCCTGCAGCCTTGACTGCTTGCACCCAGAGAAGCACGAAGACGTCAATTGCACGTGAATTG
 ATAGAGAAGATGATTGCGATGGATCCTCAGAAACGCCCTCAGCGAAGCACGTGCTCAGACACCCGTTCTTCTGGAGCCTAGAGAAG
 CAGCTCCAGTTCTTCCAGGACGTGAGCGACAGAATAGAAAAGGAATCCCTGGACGGCCCGATCGTGAGGCAGCTGGA

Query 41 CTTCACCAGACCACCTCCGGGTGGCCACCTCCACTCCCTCAACATCGTTTCACAGAGAC 100
 ||| |

Sbjct 2125 CTTCATCAGACCACCTCAGGCCTGGCACACCTGCATTCTCTCAACATTGTTTCACAGAGAC 2184

Query 101 CTAAAGCCACACAACATCCTCATATCCATGCCAATGCACACGGCAAGATCAAGGCCATG 160
 || |

Sbjct 2185 CTGAAGCCCCACAACATTCTCCTCTCCATGCCAACGCACATGGCAGGATCAAGGCGATG 2244

Query 161 ATATCCGCCTTTGGCCTCTGCAAGAAGCTGGCAGTGGGCAGACACAGTTTCAGCCGCCGA 220 <
 || || |

Sbjct 2245 ATCTCTGACTTTGGCCTCTGCAAGAAGCTGGCAGTGGGCAGGCACAGTTTCAGCCGCCGT 2304

Query 221 TCTGGGGTGCCTGGCACAGAAGGCTGGATCGCTCCAGAGATGCTGAGCGAAGACTGTAAG 280
 || |

Sbjct 2305 TCAGGGGTACCTGGCACTGAAGGGTGGATCGCCCCAGAGATGCTGAGTGAAGACTGTAAG 2364

Query 281 GAGAACCCTACCTACACGGTGGACATCTTTTCTGCAGGCTGCGTCTTTTACTACGTAATC 340
 || |

Sbjct 2365 GACAACCCTACCTACACGGTGGACATCTTTTCTGCAGGCTGTGTCTTTTACTATGTCATC 2424

Query 341 TCTGAGGGCAGCCACCCTTTTGGCAAGTCCCTGCAGCGGCAGGCCAACATCCTCCTGGGT 400
 ||| |

Sbjct 2425 TCTGAGGGCAACCATCCTTTTGGCAAATCCTTGCAGCGGCAGGCCAACATCCTCCTGGGC 2484

TCAGGACCTATAAAGGTGGTTCTGTCAGAGATCTCCTCCGAGCCATGAGAAATAAGAAGCACCCTACCGGGAGCTGCCTGCAGAGG
TGCGGGAGACGCTGGGGTCCCTCCCCGACGACTTCGTGTGCTACTTCACGTCTCGCTTCCCCCACCTCCTCGCACACACCTACCGGG
CCATGGAGCTGTGCTACTTCACGTCTCGCTTCCCCCACCTCCTCGCACACACCTACCGGGCCATGGAGCTGTGCAGCCACGAGAGAC
TCTTCCAGCCCTACTACTGTCATGANCCACCGAGCCCCAG

Query	7	AAGGATCCCTGGGATGGCCCGATCGTGA-AGCAGTTAGAGAGAGGCGGGAGAGCCGTGGT	65
Sbjct	2671	AAGGAGGCCTTGGACGGTCCAATCGT-ACGGCAGTTGGAGAGAGGCGGGAGAGCTGTGGT	2729
Query	66	GAAGATGGACTGGCGGGAGAACATCACTGTCCCCCTCCAGACAGACCTGCGTAAATTCAG	125
Sbjct	2730	CAAGATGGACTGGCGGGAGAACATCACTGTCCCCCTGCAGACAGATCTGCGCAAATTCAG	2789
Query	126	GACCTATAAAGGTGGTTCTGTCAGAGATCTCCTCCGAGCCATGAGAAATAAGAAGCACCA	185
Sbjct	2790	AACCTACAAAGGTGGCTCTGTGAGAGACCTCCTCCGAGCCATGAGAAACAAGAAACACCA	2849
Query	186	CTACCGGGAGCTGCCTGCAGAGGTGCGGGAGACGCTGGGGTCCCTCCCCGACGACTTCGT	245
Sbjct	2850	CTACCGGGAGCTCCCCGTGGAGGTTTCAGGAGACGCTGGGCTCCATCCCGGATGACTTTGT	2909
Query	246	GTGCTACTTCACGTCTCGCTTCCCCCACCTCCTCGCACACACCTACCGGGCCATGGAGCT	305
Sbjct	2910	GCGCTACTTCACTTCCCGCTTCCCCCACCTCCTCTCTCACACCTACCAAGCCATGGAGCT	2969
Query	306	GTGCAGCCACGAGAGACTCTTCCAGCCCTACTACTGTCATGANCCACCGAGCCCCAG	363
Sbjct	2970	GTGCAGACATGAGAGACTCTTTCAGACCTACTACTGGCACGAGCCCACAGAACCCAG	3027

APPENDIX 3 – Sequencing results from mutagenesis of IRE1 α / β constructs

Sequences show the relevant section of sequences from the IRE1 plasmid constructs where sequencing reactions showed the mutagenesis to have worked correctly and mutagenised both the target amino acids and any additional conservative point mutations required for screening clones. Compare to Table 4.1. 1 and Table 4.1. 2 for appropriate sites.

IRE1 α

Plasmid	Position	K599	I642	D711
L8 pEDcIRE1-P8037		CAAACG-GACGTGGCCGTGAAGAGGATCCTC	GGCAATTCCAGTACATTGCCATGAGCTGTGTGAGCC	AAGATCAAGGCCATGATCTCCGACTTTGG
K599A with H8037 rpt.		CAAACG-GACGTGGCCGTGGCGAGGATCCTC	GGCAATTCCAGTACATTGCCATGAGCTGTGTGAGCC	AAGATCAAGGCCATGATCTCCGACTTTGG
K599A/I642A4 with H8037		CAAACG-GACGTGGCCGTGGCGAGGATCCTC	GGCAATTCCAGTACATTGCCCGGAGAGCTGTGTGAGCC	AAGATCAAGGCCATGATCTCCGACTTTGG
K599A/I642A7 with H8037		CAAACG-GACGTGGCCGTGGCGAGGATCCTC	GGCAATTCCAGTACATTGCCCGGAGAGCTGTGTGAGCC	AAGATCAAGGCCATGATCTCCGACTTTGG
K599A/I642G6 with H8037		CAAACG-GACGTGGCCGTGGCGAGGATCCTC	GGCAATTCCAGTACATTGCCCGGAGAGCTGTGTGAGCC	AAGATCAAGGCCATGATCTCCGACTTTGG
K599R2 with H8037		CAAACG-GACGTGGCCGTGAGGAGAAATCTC	GGCAATTCCAGTACATTGCCATGAGCTGTGTGAGCC	AAGATCAAGGCCATGATCTCCGACTTTGG
K599R/I642A3 with H8037		CAAACG-GACGTGGCCGTGAGGAGAAATCTC	GGCAATTCCAGTACATTGCCCGGAGAGCTGTGTGAGCC	AAGATCAAGGCCATGATCTCCGACTTTGG
K599R/I642A6 with H8037		CAAACG-GACGTGGCCGTGAGGAGAAATCTC	GGCAATTCCAGTACATTGCCCGGAGAGCTGTGTGAGCC	AAGATCAAGGCCATGATCTCCGACTTTGG
K599R/I642G1 with H8037		CAAACG-GACGTGGCCGTGAGGAGAAATCTC	GGCAATTCCAGTACATTGCCCGGAGAGCTGTGTGAGCC	AAGATCAAGGCCATGATCTCCGACTTTGG
K599R/I642G2 with H8037		CAACCG-GACGTGGCCGTGAGGAGAAATCTC	GGCAATTCCAGTACATTGCCCGGAGAGCTGTGTGAGCC	AAGATCAAGGCCATGATCTCCGACTTTGG
D711A7 with H8037		CAAACG-GACGTGGCCGTGAAGAGGATCCTC	GGCAATTCCAGTACATTGCCATGAGCTGTGTGAGCC	AAGATCAAGGCCATGATATCCGACTTTGG
D711A/I642A3 with H8037		CAAACG-GACGTGGCCGTGAAGAGGATCCTC	GGCAATTCCAGTACATTGCCCGGAGAGCTGTGTGAGCC	AAGATCAAGGCCATGATATCCGACTTTGG
D711A/I642G2 with H8037		CAAACG-GACGTGGCCGTGAAGAGGATCCTC	GGCAATTCCAGTACATTGCCCGGAGAGCTGTGTGAGCC	AAGATCAAGGCCATGATATCCGACTTTGG
D711A/I642G3 with H8037		CAAACG-GACGTGGCCGTGAAGAGGATCCTC	GGCAATTCCAGTACATTGCCCGGAGAGCTGTGTGAGCC	AAGATCAAGGCCATGATATCCGACTTTGG
I642A5 with H8037		CAAACG-GACGTGGCCGTGAAGAGGATCCTC	GGCAATTCCAGTACATTGCCCGGAGAGCTGTGTGAGCC	AAGATCAAGGCCATGATCTCCGACTTTGG
I642G5 with H8037		CAAACG-GACGTGGCCGTGAAGAGGATCCTC	GGCAATTCCAGTACATTGCCCGGAGAGCTGTGTGAGCC	AAGATCAAGGCCATGATCTCCGACTTTGG
K907A with H8037		CAAACG-GACGTGGCCGTGAAGAGGATCCTC	GGCAATTCCAGTACATTGCCATGAGCTGTGTGAGCC	AAGATCAAGGCCATGATCTCCGACTTTGG
K907A with H8037 rpt		CAAACG-GACGTGGCCGTGAAGAGGATCCTC	GGCAATTCCAGTACATTGCCATGAGCTGTGTGAGCC	AAGATCAAGGCCATGATCTCCGACTTTGG

